# University of Guelph

School of Engineering
Guelph, Ontario N1G2W1
Phone: 519-824-4120 ext. 52429.
Fax: 519-836-0227
E-Mail: mahassan@uoguelph.ca
Web: http://www.uoguelph.ca/engineering/marwan-hassan-phd-peng

|  |  |
|---|---|
| *Topic:* | **Fluid-Structure Interaction, Dynamics of Tube Bundles** |
| *Title:* | **Investigation of the Fatigue Cracking and Leakage Rate potential of U-Bend Tube Bundles subjected to Flow-Induced Vibrations.** |
| *Date:* | **October 10, 2013** |
| *Revision:* | **Final Report – Revision 2.** |
| *Contract No.:* | **87055-12-0501 - "R554.1"** |
| *Lead Investigator:*<br>*Title:* | **M. A. Hassan, Ph.D., P.Eng.**<br>Associate Professor<br>Fluid-Structure Interaction Lab.<br>University of Guelph |
| *Investigator:*<br>*Title:* | **A. El-Hossainy, M.Sc.**<br>Research Assistant<br>Fluid-Structure Interaction Lab<br>University of Guelph |
| *Investigator:*<br>*Title:* | **S. El Bouzidi, B.Sc.E.**<br>Graduate Research Assistant, Master's candidate<br>Fluid-Structure Interaction Lab<br>University of Guelph |

# 1    Executive Summary

The steam generator (SG) tubes in CANDU comprise most of the reactor primary coolant pressure boundaries. Maintaining the integrity of SG tubes is a major safety issue since they ensure the separation of the two fluids. These devices contain a large number of tubes. A large amount of energy, in the form of high-speed fluid flow, passes around these tubes. Serious problems can arise if a small portion of this energy is converted into mechanical energy. This mechanical energy can cause violent tube vibrations, which in turn can cause failure due to fatigue and/or wear at the support locations. Therefore measures are taken to reduce the fretting wear potential by stiffening the structure and reducing clearances at the support. The fretting wear due to normal operations should be accounted for in the design stage. However, in some situations supports located on the straight part of the tube may deteriorate to the point where extremely large clearances, or even total wastage of the supports, may result. One example of this type of situation is the problem experienced in Bruce Unit 8 where severe degradation of tube support plate occurred. This degradation was revealed by eddy current testing and later confirmed by visual inspection. The finding was described as metal loss, caused by flow-accelerated corrosion of the carbon steel trefoil support plate and varying from minor to complete loss of the ligaments. This loss of TSP ligaments results in lack of support for the adjacent tubes making them more susceptible to fretting-wear damage and fatigue cracking at these locations. In addition, this may affect the rate of wear in the U-bend portion of the tube due to the evolution of unstable modes. The integrity could be seriously breached as result of a potential support loss. Therefore, remedies were proposed and installed. Such remedies include adding flat bars at locations in U-bend as well as the insertion of the so-called comb support at the place of the corroded broached-hole support. Previous investigation by the Fluid-Structure interaction laboratory at the University of Guelph showed that these remedies are effective in reducing the vibration amplitude and the resulting fretting wear damage when all U-bend support clearances are kept under 0.2 mm.

This report presents the finding of a work aimed at investigating the crack fatigue potential caused by such an accident. Numerical simulations were employed for the full U-bend tube subjected to a variable flow field typical of a CANDU steam generator configuration. Both deterministic and probabilistic evaluations have been utilized. It has been shown that the suggested remedies are effective in reducing the damage potential if the radial clearances are kept within 0.2 mm. In addition, the scallop bar supports at the U-bend apex is proven to be critical. Crack propagation for an assumed Surface Circumferential and Through Wall cracks were simulated. In addition, the leakage rate in the through wall crack was also calculated. Charts providing the probability of life and leakage rates exceeding certain thresholds were also presented.

# Table of Contents

# List of Figures

# List of Tables

## 2   Background Research

### 2.1   Tube Cracking

Green and Hetsroni (1995) provided an extensive review of PWR steam generators covering a wide variety of topics including thermal-hydraulic analysis and steam generator problems. An example of the contribution of different mechanisms to the overall plugging incidents is shown in the following figure for 1992. Stress corrosion cracking (SCC) accounts for 52% of the reported numbers of tubes, which have been removed from service per annum worldwide. Fretting wear accounts for 19.6% of the total incidents. Fretting related failures account for 40% of the tube failures that are not corrosion related.

At the microscopic level, materials are not homogeneous and contain discontinuities generated by manufacturing. These discontinuities lead to local stress concentrations that can lead to circumferential cracks when subjected to cyclical stresses. Fatigue failure occurs in three steps, crack initiation, propagation and fracture due to unstable growth. Cracking in all forms tends to occur more commonly in the hot leg of the U tube.
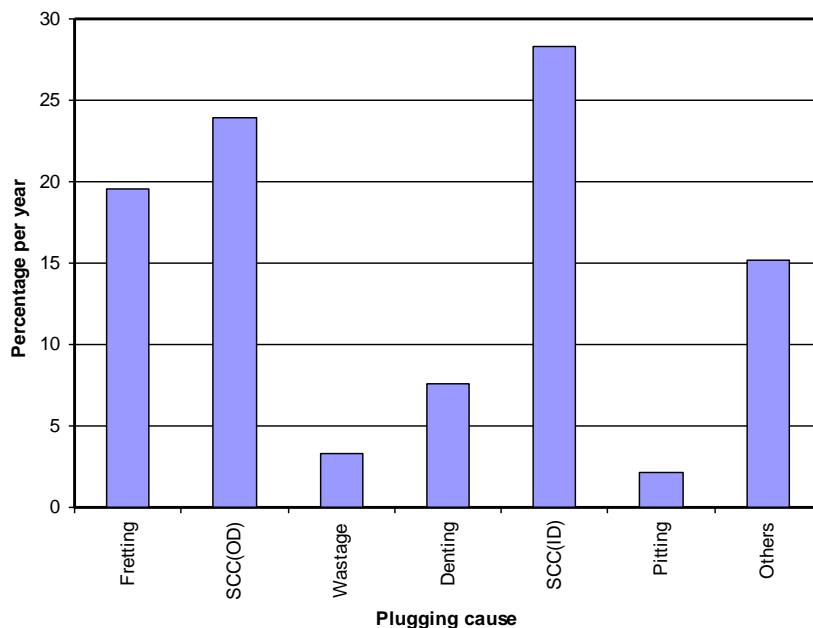


**Figure 1: Classification of Steam Generator Tube Plugging Leading Causes (***data was compiled from*** Green and Hetsroni (1995))**

### 2.2   Cracks Types

Figure 2 shows the various types of potential crack geometries in heat exchanger tubes. These types are listed as follows:
- Through-Wall Circumferential Cracks (TWC) .
- Surface Circumferential Cracks (SCC).

- Through-Wall Axial Cracks (TWA).
- Surface Axial Cracks (SAC).

Surface flaws (cracks) are characterized as semi-elliptical in cross section, located on the inside surface of the pipe. The depth of a surface crack is taken as $a$ with the length given as $2L$. The length of a through-wall crack is $2a$ and the crack opening displacement at the center is given by $\Delta$. The crack geometry for these two types of crack can be seen in Figure 2.
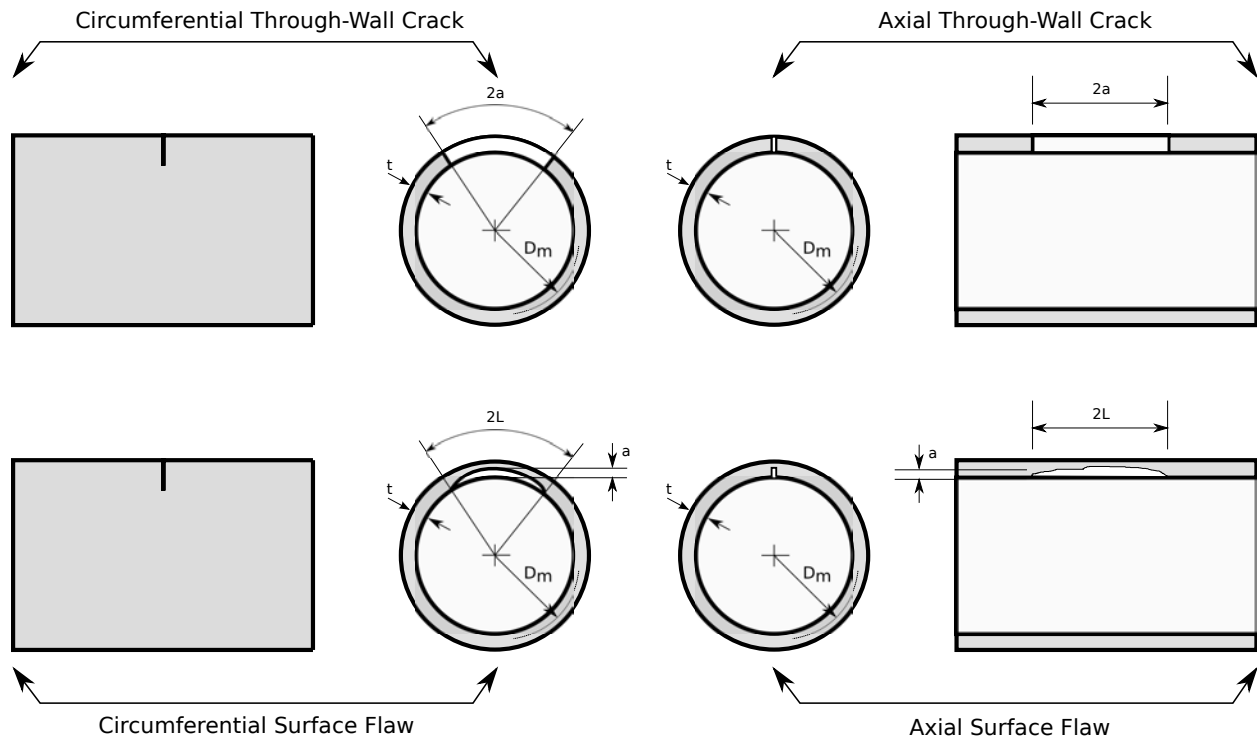


**Figure 2: Geometry of through-wall and surface cracks**

## 2.3 Crack Tip Stress Intensity Factor

Assuming linear elastic fracture mechanics conditions, the growth of fatigue cracks can be estimated from the crack tip stress intensity factor $K_I$:

$$K_I = \sqrt{\pi a}(F_m \sigma_m + F_b \sigma_b)$$

where $\sigma_m$ and $\sigma_b$ represent the membrane and bending stress while $F_m$ and $F_b$ represent crack tip stress intensity geometry factors (Kozluk, 1998).

Given below is a set of equations for circumferential and axial crack tip stress intensity geometry factors for both through-wall and surface flaws (Kozluk, 1998). The equations are curve fits to the data presented by (Kozluk, 1998). The range of applicability for each of the equations is given in Table 1.

**Table 1: Stress intensity factors' applicability range for various flaw models.**

| Flaw Model | Equation | $\dfrac{d_m}{t_w}$ | $\dfrac{2a}{\pi}d_m$ | $\dfrac{2Lc}{a}$ | $\dfrac{a}{t_w}$ |
|:---:|:---:|:---:|:---:|:---:|:---:|
| TWC | Table 2 | $10-40$ | $0.06-0.50$ | - | $1.0$ |
| SCC | Table 2 | $10-40$ | - | $3-12$ | $0.20-0.80$ |
| TWA | Table 2 | $>20$ | $<2.2\left(\dfrac{t}{D}\right)^{0.5}$ | - | $1.0$ |
| SCA | Table 2 | $10-40$ | - | $3-100$ | $0.20-0.80$ |

The values for the $F_m$ and $F_b$ are dependent on the type of crack and are given by Table 2.

**Table 2: Empirical curve fits for $F_m$ and $F_{bm}$ for various crack types.**

| Crack type | $F_m$ and $F_b$ | Stresses |
|:---|:---|:---|
| TWC | $F_m^{TWC} = 1 + \left[3.64 + 0.146\left(\dfrac{d_m}{t_w}\right) - 0.00123\left(\dfrac{d_m}{t_w}\right)^2\right]\left[\left(\dfrac{2a}{\pi d_m}\right)^{1.5} + 3.93\left(\dfrac{2a}{\pi d_m}\right)^{4.5}\right]$ <br><br> $F_b^{TWC} = 1 + \left[2.51 + 0.143\left(\dfrac{d_m}{t_w}\right) - 0.00120\left(\dfrac{d_m}{t_w}\right)^2\right]\left[\left(\dfrac{2a}{\pi d_m}\right)^{1.5} + 0.695\left(\dfrac{2a}{\pi d_m}\right)^{4.5}\right]$ | $\sigma_m = \dfrac{P_i d_m}{4 t_w} + \dfrac{F_x}{\pi d_m t_w}$ <br><br> $\sigma_b = \dfrac{4 M_c}{\pi d_m^2 t_w}$ |
| SCC | $F_m^{SCC} = F_b^{SCC}$ <br><br> $= \dfrac{1 + 0.025\left[1 + 1.90\left(\dfrac{2L_C}{t_w}\right) + 0.10\left(\dfrac{2L_C}{t_w}\right)^2 + 0.10\left(1 + 0.10\left(\dfrac{2L_C}{t_w}\right)\right)\left(\dfrac{d_m}{t_w} - 10\right)\right]}{\sqrt{Q}}$ <br><br> $Q = 1 + 4.595\left(\dfrac{a}{2L_C}\right)^{1.65}$ | |
| TWA | $F_m^{TWA} = F_b^{TWA} = \sqrt{1 + 0.51\left(\dfrac{2a}{d_m t_w}\right)^2}$ | $\sigma_m = \dfrac{P_i d_m}{2 t_w}$ <br><br> $\sigma_b = 0$ |
| SCA | $F_m^{SCA} = F_b^{SCA} = \dfrac{\left[0.209 + \left[0.696\left(\dfrac{2L_C}{a}\right) - 0.632\right]^{N_1}\right]\left[1230 - 15.8\left(\dfrac{d_m}{t_w}\right) + 0.214\left(\dfrac{d_m}{t_w}\right)^2\right]}{1000\sqrt{Q}}$ <br><br> $N_1 = 0.554\left(\dfrac{a}{t_w}\right) - 0.0545$ <br><br> $Q = 1 + 4.595\left(\dfrac{a}{2L_C}\right)^{1.65}$ | |

## 2.4 I600 Crack Growth Model

The model that was selected to predict the crack growth for this project was initially introduced by Kozluk (1998). A series of fatigue tests were performed on I600 (Inconel 600) and I800 test specimens by varying the loading ratio, operating temperature and the environment. The experimental data was then normalized in order to develop a curve fit through the data (Figure 3). It was found that the coefficient $C$ was dependent on the loading ratio and the temperature indirectly through the modulus of elasticity while the exponent $n$ was determined to be a constant. A best-fit curve through the data is given as:

$$\frac{da}{dN} = \frac{2.39}{E^2\sqrt{1-R}}\left[\varDelta K - (25.9\times10^{-6}E)\times(e^{-0.66R})\right]^2$$

where $E$ and $R$ are the modulus of elasticity and the loading ratio. A curve fitted to the upper bound of the data is given as:

$$\frac{da}{dN} = \frac{3.58}{E^2\sqrt{1-R}}\left[\varDelta K - (24.6\times10^{-6}E)\times(e^{-0.66R})\right]^2$$

The threshold stress intensity $\varDelta K_{th}$, which is the minimum $\varDelta K$ for there to be any crack growth, for the best fit curve is given as:

$$\varDelta K_{th} = (25.9\times10^{-6}E)\times(e^{-0.66R})$$

As can be seen the above Equations, $\varDelta K_{th}$ is dependent on the loading ratio $R$ and the temperature indirectly through the modulus of elasticity $E$.
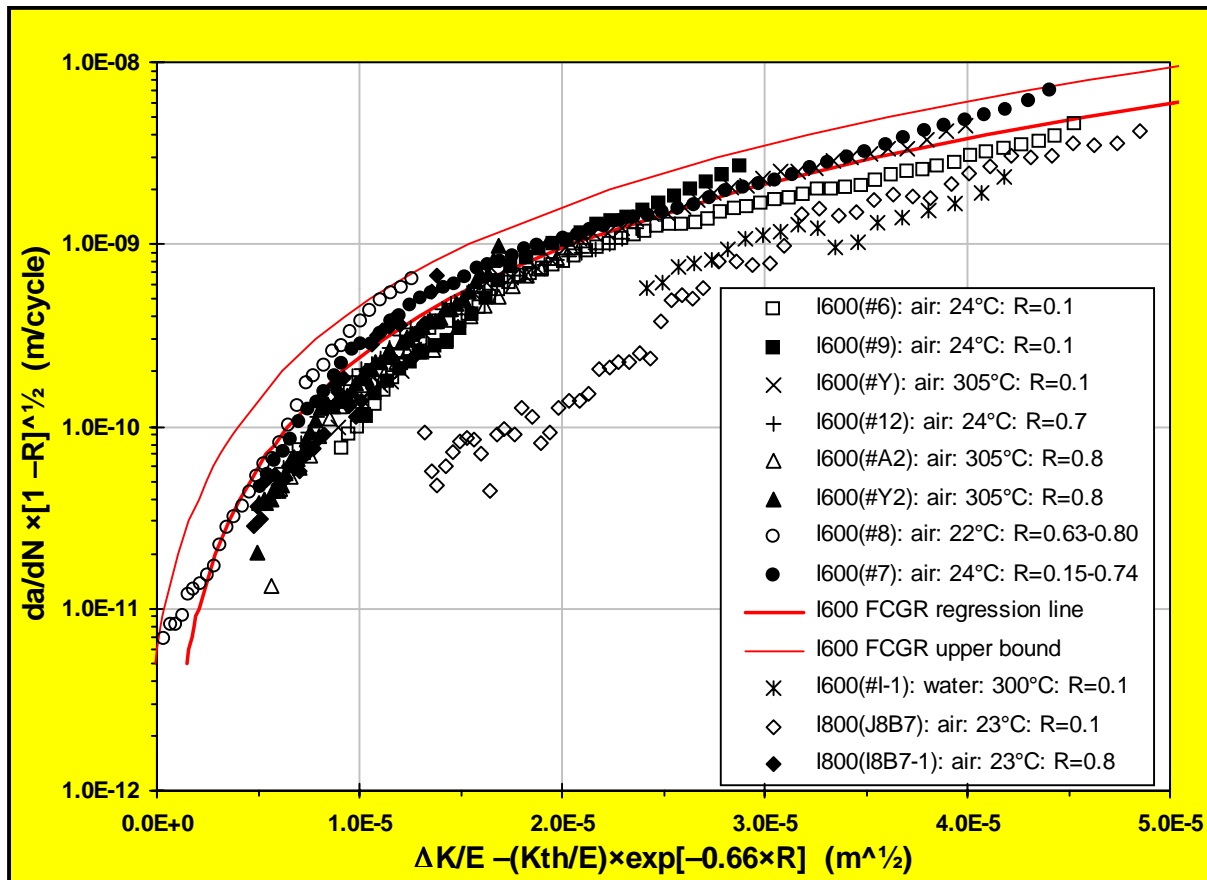


**Figure 3: Crack Growth per Cycle for I600 and I800 alloys for various temperatures and load ratios.**
*Sources:* **Ogundele *et. al.* (1998) and Kozluk's empirical formula (1998)**

## 2.5 Crack Opening Displacement Model Comparison

Prior to choosing the model developed by Zahoor various alternatives were considered, such as the model developed by Paris and Tada (1993). Figure 4 shows the crack opening displacement computed as a function of the bending moment applied while using Paris and Tada's approach,

Zahoor's approach with purely elastic behavior, and Zahoor's approach with both elastic and plastic behavior. It was seen that there is little difference between Paris-Tada and Zahoor's elastic model. Zahoor's elasto-plastic model agrees with the latter two for small bending stresses but shows increased crack opening displacement over higher bending moments. This is consistent with available experimental data. The three predictions agree well with the experimental data for the low range of stresses, which represents the expected bending stress in the tube. Therefore, using of any of these approaches will be suitable for the COD estimation.
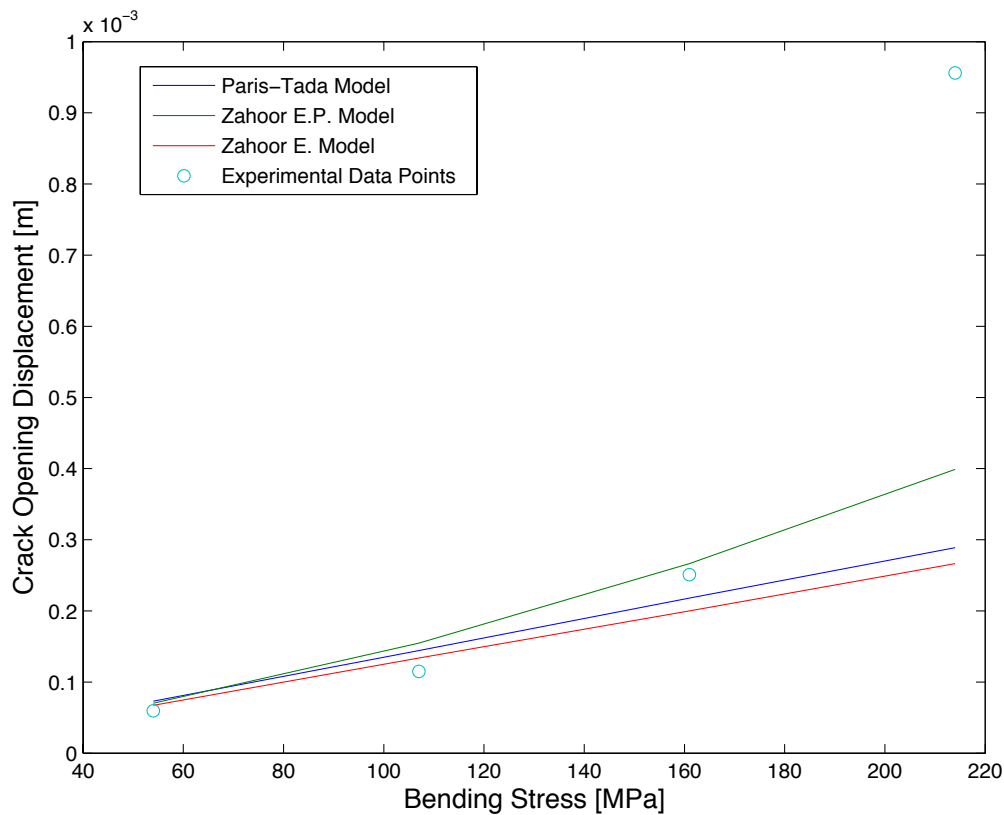


**Figure 4: Comparing the Crack Opening Displacement (COD) for various crack growth models: Paris-Tada, Zahoor elastic-plastic, and Zahoor elastic.**

## 2.6    Variable Amplitude Loading

The problem of predicting fatigue crack growth life becomes more complex when the loading is not of constant amplitude. This is commonly referred to as variable amplitude loading. However, the fatigue crack growth data is measured with test specimens using constant amplitude and frequency loading while most loading seen during operation is random with varying amplitudes and frequencies. Once the loading history is obtained, the first step is to count the number of cycles that occur within a given stress history. ASTM gives several methods for calculating the number of cycles in a loading history. The method that is used for this

research is the Rain-flow Counting method given by Downing (1982). Once the number of cycles is known, two methods for calculating the crack growth rate are given.

## 2.7    Thermal hydraulic analysis

Several flow calculations were performed at AECL with the THIRST (Thermal-Hydraulics In Recirculating STeam generator) code (Heppner et al. 2006). Figure 5 shows the calculated velocity distribution along a CANDU steam generator tube at 100% power. This velocity distribution exhibits a higher velocity on the hot side and in the upper portion of the tube bundle. Mixture density is lower in the hot side and higher in the cold side and the U-portion of the tube bundle. These calculations predict that the U-bend region is subjected to two-phase cross-flows with gap velocities ranging from less than 1 m/s to as high as 11 m/s. Similarly, the flow density ranges from 70 kg/m$^3$ to 800 kg/m$^3$.



(a)                                                          (b)
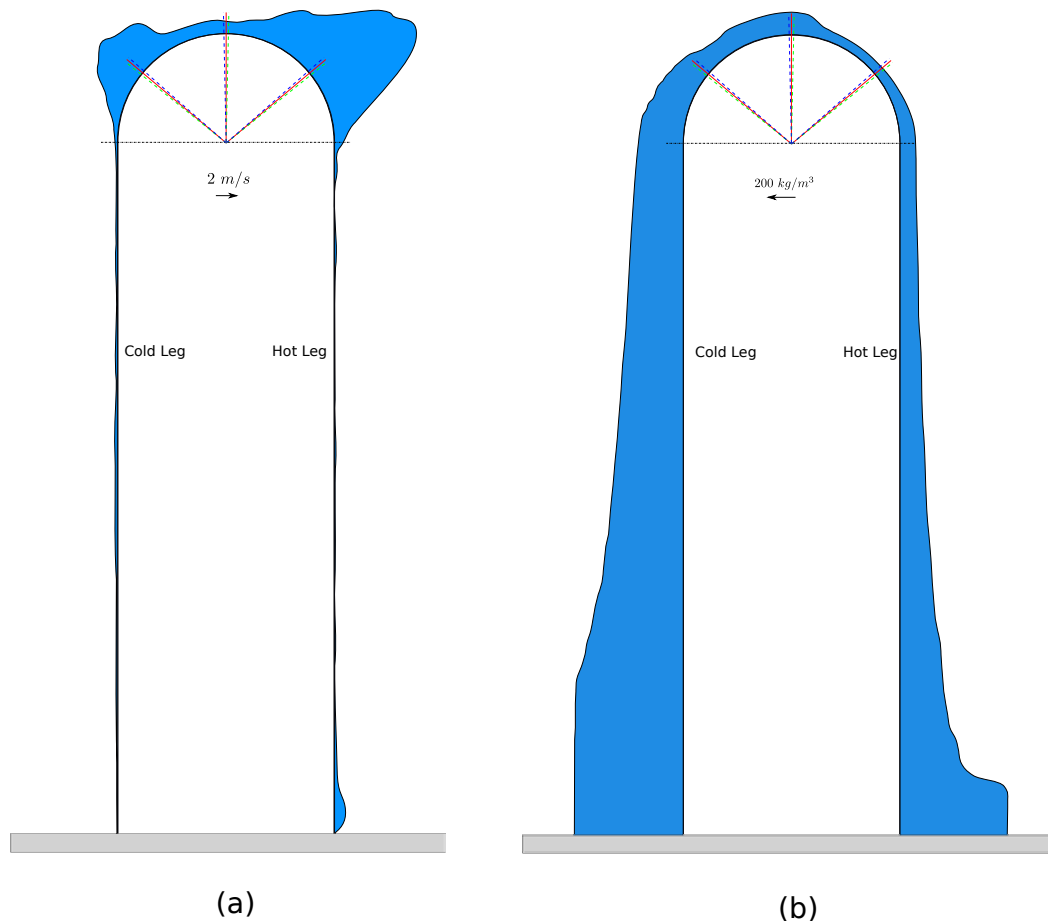
**Figure 5: Flow (a) and density (b) distribution**

## 2.8   Leakage rate

The leakage rate analytical approach followed here is presented in details in the open literature (Matsumoto et al. 1991). For the case of single-phase flow the total pressure drop subdivided into the prediction of the inlet pressure drop, flow resistance, and exit pressure drop.

$$P_i - P_o = \Delta P_f + \Delta P_i + \Delta P_o$$

$$\Delta P_f = \int_{z_i}^{z_o} f(z) \frac{\rho(z)V(z)^2}{2d_h(z)} dz$$

$$\Delta P_i = K_i \frac{\rho_i V_i^2}{2}$$

$$\Delta P_o = K_o \frac{\rho_o V_o^2}{2}$$

$$f = \left[ C_1 log\left(\frac{d_h}{2r_c}\right) + C_2 \right]^{-2}$$

$$\dot{m} = \sqrt{\frac{2\rho\Delta P}{\frac{K_i}{A_i^2} + \frac{K_o}{A_o^2} + \int_i^o f(z) \frac{dz}{d_h A(z)^2}}}$$

For the multi-phase flow model the equilibrium expansion model for the phase change of the fluid in the crack was adapted from the non-equilibrium model discussed in details in Brady *et al.* (2009). The assumption of equilibrium expansion gives a lower bound to the solution. The mass balance equation is:

$$\frac{dV}{dz} - \frac{V}{v_m}\frac{dv_m}{dz} = \frac{-V}{A}\frac{dA}{dz}$$

$$\frac{dP}{dz} + \frac{V}{v_m}\frac{dV}{dz} = \frac{-P_\omega}{A}\tau_\omega$$

$$H^o = h_s + \frac{1}{2}V^2$$

$$\tau_\omega = \frac{\sum_k \frac{P_\omega}{k}\frac{\tau_\omega}{k}}{P_\omega}$$

$$\tau_{liquid=\frac{\Delta PR}{2\Delta L}}$$

$$\Phi_L^2 = (1 - \alpha G)^{-1.75}$$

$$\tau_\omega = \dot{m} f(z) \frac{v_{ls}}{A(x)^2} \Phi_L^2$$

The flow parameters are as follows:
- Internal pressure: 9.31 MPa.
- External pressure: 4.43 MPa.
- Primary fluid temperature: 303.2 C.
- Secondary fluid Temperature: 243.0 C.
- Surface roughness 8.814 µm.

- Entrance loss coefficient: $K_i = 0.35$.
- Exit loss coefficient: $K_o = 0.65$.

# 3   Solution Methodology and Outline

## 3.1   Tube configuration

Figure 6 shows an overall view of the nuclear steam generator under study. The unit has three U-bend supports. The straight portion of the tube is supported by seven tube-support plates (TSP) placed evenly along the tube.
The tubes' geometrical and material properties are listed as follows:

- Outer diameter: 13.02 mm.
- Inner diameter: 10.76 mm.
- Modulus of elasticity: 199.8 GPa.
- Tube density: 8304 kg/m$^3$.

Figure 7 shows the finite element model for a tube. The model contains 97 three-dimensional beam elements each of which has 12 DOFs. The model boundary conditions for the original configuration are listed in Table 3. The broached hole and scallop bar supports are modeled as nonlinear supports in order to account for the effects of tube on support impacts. Table 4 lists the boundary conditions of the remedied configuration. In this case, the support clearances are varied and its effect on crack growth and leakage rates may be observed.

**Table 3: Boundary condition descriptions for the finite element model (Original Configuration).**

| Nodes | Restrain | Restrained DOF |
|---|---|---|
| 1,98 | Fixed support | X, Y, Z, Rx, Ry, Rz |
| 5,9,13,17,21,25,29 | Hot Leg Nonlinear Supports | Broached hole |
| 70,74,78,82,86,90,94 | Cold Leg Nonlinear supports | Broached hole |
| 39,40,49,50,59,60 | U-Bend Nonlinear supports | Scallop bars |

**Table 4: Boundary condition descriptions for the finite element model (Remedied Configuration).**

| Nodes | Restrain | Restrained DOF |
|---|---|---|
| 1,98 | Fixed support | X, Y, Z, Rx, Ry, Rz |
| 5,9,13,17,21,25 | Hot Leg Nonlinear Supports | Broached hole |
| 70,74,78,82,86,90,94 | Cold Leg Nonlinear Supports | Broached hole |
| 39,40,49,50,59,60 | U-Bend Nonlinear Supports | Scallop bars |
| 29 | H07 replacement NL Support | Comb Support |
| 42,57 | U-Bend Nonlinear Support | Flat Bar Support |

Figure 6 shows the structural configurations of the U-bend tube. In the straight portions, the tube is supported by broached hole supports (H01 to H07, and C01 to C07), where the letters C and H refer to the cold leg side and the hot leg side, respectively. In addition, there are three sets of scallop bar supports (S1, S2, S3). Each scallop-bar support set consists of two bars (A and B) each of which contains half-circle drilled-hole support space. Such a configuration (Config01) is shown in Figure 6a, which is the original configuration of Bruce 8. Configuration 2 is shown in Figure 6b. This configuration resembles the full loss of support H07. Configuration 3 is shown in Figure 6c which represents the addition of two flat bar supports (F1 and F2) to remedy the loss of

H07. Additional flat bars at the H07 location (support comb) were also used to remedy the problem of H07 support loss.
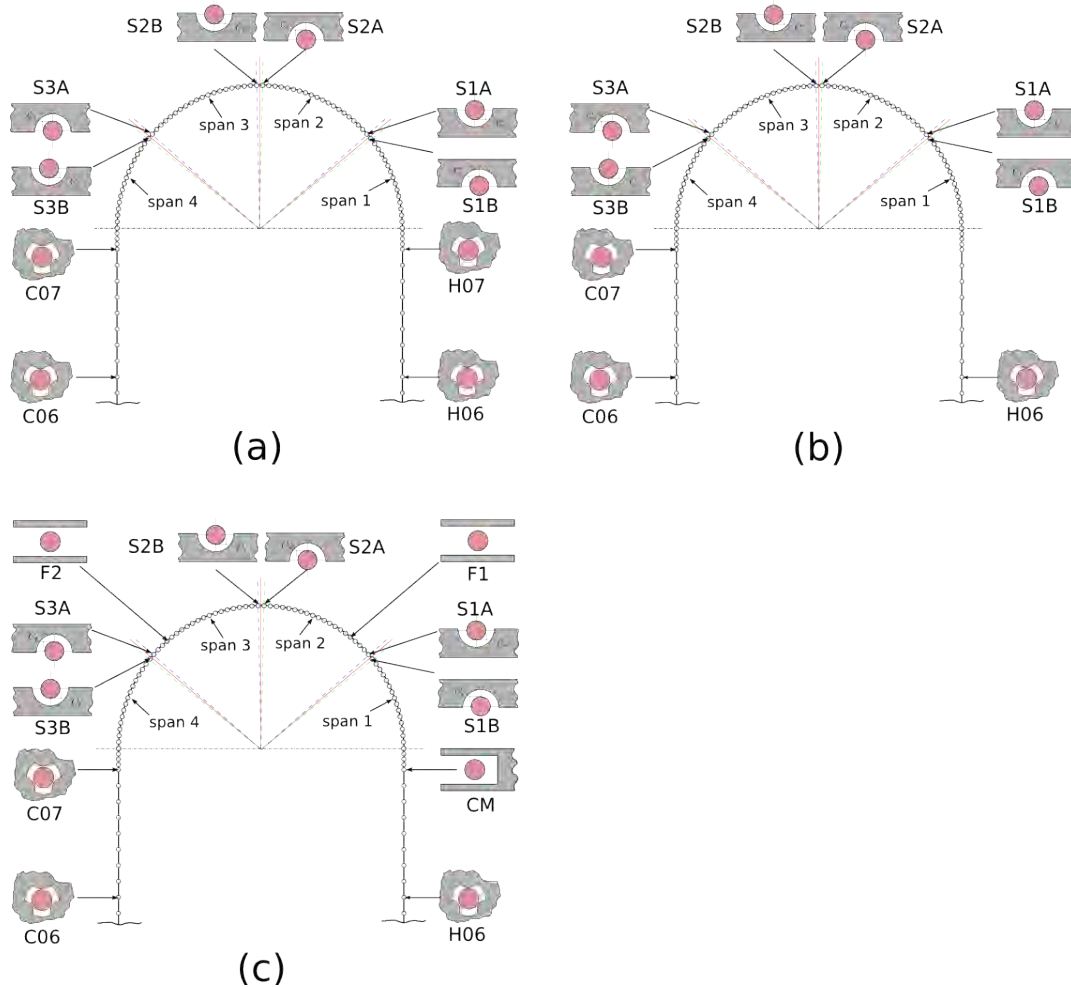


**Figure 6: Support types, locations, and labels for various steam generator configurations.**

**(a) Configuration 1, (b) Configuration 2, (c) Configuration 3.**

Figure 7 shows the location of the supports and their type for configuration 3. It illustrates the situation where two flat bar supports (F1 and F2) along the U-Bend and a comb support (CM) has been placed at the location of H07 in the scenario where a full failure of the support H07 has occurred.

**Table 5: Description of the crack locations considered.**

| Location | Node Number |
|----------|-------------|
| 1 | 29 |
| 2 | 39 |
| 3 | 49 |
| 4 | 59 |
| 5 | 70 |

For surface circumferential cracks, the range of crack ratios studied was 45% to 75% while the aspect ratios considered were from 3 to 12. For through wall cracks, the initial crack size $a_0$ ranged from 1.5 mm to 3.5 mm.
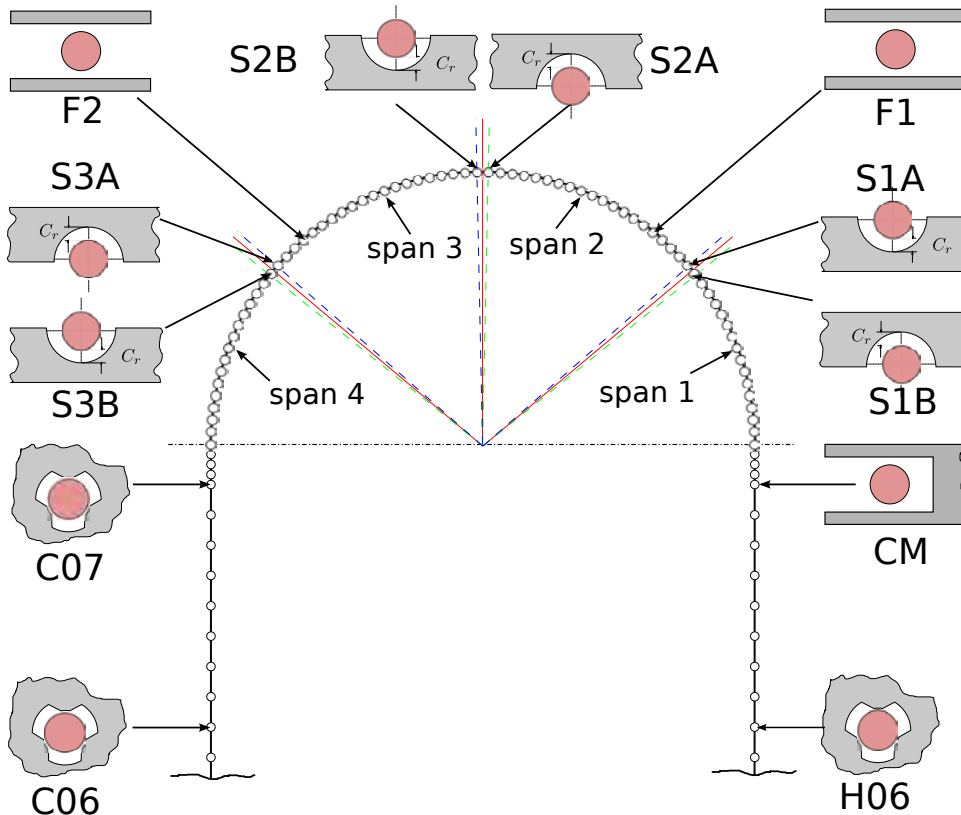


**Figure 7: Remedied configuration (Configuration 03) support types and locations.**

## 3.2 Fluid Excitation

### 3.2.1 Turbulence Loading

Random turbulence excitation is a significant vibration mechanism of tubes subjected to crossflow. The interior tubes within a tube bundle are excited by the turbulence generated within the bundle. In general, fluid excitation due to turbulence is modelled as randomly distributed forces. To implement this approach, the empirically based bounding spectra of turbulence excitation is obtained using the flow velocity, the tube diameter, and the array geometry. Several bounding spectra have been proposed and the one by Oengoren and Ziada (1998) has been utilized in this project. This PSD curve is then transformed into a force–time record using an inverse Fourier transform algorithm. The resulting fluctuating forces are Gaussian in nature with a zero mean value. The power spectral density of the dynamic force is expressed as:

$$S_{FF} = \tilde{S}_{FF}\left(\frac{1}{2}\rho U \Delta L d^2\right)$$

The normalized PSD of the lift $S_{FF_L}$ and drag $S_{FF_D}$ forces is defined by:

$$S_{FF_L} = 4.75 \times 10^{-4} \left( \frac{fd}{U} \right)^{-0.4} \text{ for } \frac{fd}{U} < 0.43$$

$$S_{FF_L} = 1.02 \times 10^{-5} \left( \frac{fd}{U} \right)^{-5} \text{ for } \frac{fd}{U} \geq 0.43$$

$$S_{FF_D} = 7.35 \times 10^{-4} \left( \frac{fd}{U} \right)^{-0.4} \text{ for } \frac{fd}{U} < 0.53$$

$$S_{FF_D} = 3.96 \times 10^{-5} \left( \frac{fd}{U} \right)^{-5} \text{ for } \frac{fd}{U} \geq 0.53$$

The flow was assumed to be uncorrelated along the tube spans. Based on the flow velocity and density for each element, two different force versus time records were created representing the fluid excitation in the drag and lift directions.

### 3.2.2 *Fluidelastic Instability Modelling*

The fluidelastic instability model utilized in this work is the described in detail in a series of papers by Hassan et al. (2008, 2010, and 2011). Briefly, the entire flow inside the tube bundle is divided into a number of layers each of which is associated with a tube finite element. The flow inside each layer can be idealized by a series of flow channels. The area of these flow channels is decomposed into a steady state component and a perturbation component. The area perturbation is set to the tube lift displacement along the tube-flow channel contact length. The response history is required in order to calculate the area perturbation in the channel. Now, the displacement at each element is needed to calculate the area perturbation. The area perturbation at any given location s is equal to the displacement at $t - \tau(s)$. The time lag $\tau(s)$ is calculated using the flow velocity $U_o$, and the location s as $\tau(s) = \dfrac{2s}{U_o}$. Using the unsteady continuity and momentum equations, the flow velocity and pressure can be obtained at any point in the flow channel. The fluidelastic forces per unit length are evaluated by integrating the pressure along the tube/channel interface. The fluid forces are then treated as a distributed pressure, and the consistent load vector $F_f$ is obtained. Now the newly estimated fluidelastic force vector, along with the impact force vector, are added to the global load vector and checked for convergence. The tube response at the support node is used to calculate the impact force. Upon convergence, the updated displacement, fluidelastic forces, and contact forces are stored. This process is repeated at each time step. Calculating the fluidelastic instability forces using this method does not require knowing the instantaneous vibration frequency.

## 3.3 Tube-Support Impact Modelling

The mathematical modelling of the tube/support impact used herein was described in detail and verified by Hassan et al. (2002). Briefly, the tube is discretized into finite beam elements, and the proper boundary conditions are applied. Any loose support configuration can be modelled by a number of massless bars arranged around the tube. Each bar is attached by an equivalent-contact spring and damper. If the normal component of the tube displacement $w_n$ exceeds the radial

support clearance $C_r$, contact takes place. The normal contact forces are calculated in each bar by evaluating the elastic ($K_c$ ($w_n$-$C_r$)) and damping $1.5\beta K_c\left(w_n - C_r\right)\dot{w}_n$ forces in the spring and the damper. $K_c$ and $\beta$ are the spring stiffness and the material damping coefficient, respectively. The force balance friction model was used to compute the shear contact forces. Additional details of the friction procedure were presented by Hassan and Rogers (2005). This technique has been developed, used, and verified for the last four decades. It is thus widely accepted. Interested readers are referred to the works of Rogers & Pick (1977), Sauvé and Teper (1987), and Axisa *et al.* (1988) for detailed description of the technique.

### 3.4    Deterministic Simulations

In order to fully understand the effect of varying clearances at the support on crack growth and leakage rates, three cases are considered: config03a, config03b, and config03c. For all three configurations the hot leg support clearances were maintained constant with an H01 clearance of 0.25 mm linearly increasing to a clearance of 4.15 mm at support H07. This allows consideration of the gradual degradation from the bottom to the top support due to corrosion amongst other factors. Similarly for the cold leg the support clearances were maintained with a clearance of 0.25 mm at support C01 and 0.55 mm at C07. The three configurations differed in the following specific aspects; for config03a 15 sets of simulations, each containing 15 runs, were conducted. For each set the clearance of the scallop bar support SB1 was varied from 0.1 mm to 1.5 mm, whereas scallop bar supports SB2 and SB3 were maintained at a constant value, referred to as base clearance. Each set of runs represents a different base clearance. Config03b and Config03c are similar except that they involve considering SB2 and SB3 as their respective variable clearances and the remaining scallop bar supports as the base clearances. Table 1 summarizes the support clearance conditions for each configuration. All in all, the study consisted in conducting 225 simulations for each configuration. The premise of the crack growth study was to assume the existence of a crack at each of the supports along the U-bend and determine its progress. As such, the evolution of cracks was provided at 5 different locations: Node 29, Node 39, Node 49, Node 59, and Node 70. These will be referred to as locations 1 through 5, respectively, as indicated by table 2.

**Table 6: U-Bend Scallop Bar support clearances for the three configurations investigated (Config03a, Config03b, and Config03c).**

|  | Config03a | Config03b | Config03c |
|---|---|---|---|
| **SB1** | Variable clearance (0.1 mm – 1.5 mm) | Base clearance ($C_{rb}$) | Base clearance ($C_{rb}$) |
| **SB2** | Base clearance ($C_{rb}$) | Variable clearance (0.1 mm – 1.5 mm) | Base clearance ($C_{rb}$) |
| **SB3** | Base clearance ($C_{rb}$) | Base clearance ($C_{rb}$) | Variable clearance (0.1 mm – 1.5 mm) |

## 3.5   Monte Carlo Simulations

In order to conduct this probabilistic assessment, 2000 clearance cases were generated, based on nominal design clearance values, and assuming a normal (Gaussian) distribution of the clearance for all supports. The number of samples was chosen based on previous sensitivity analyses. This assumption is based on previous studies in the literature (Sauvé *et al.*, 1997). For the hot leg, the clearances were linearly increased from a mean of 0.25 mm for H01 to 4.15 mm for H06, due to corrosion of the hot leg. For these supports the standard deviation was taken as 0.1 mm. The resulting normal distribution is shown in figure 8 for H01. Similarly, for the cold leg the mean clearance at C01 was taken as 0.25 mm, and 0.55 mm at C07. For the entire cold leg the standard deviation was taken as 0.1 mm. In this configuration a full loss of the H07 support is assumed. As a result, flat bar supports are considered with a mean value of 0.21 mm and a standard deviation of 0.02 mm, and the distribution for all 2000 cases is shown in figure 9. All scallop bar supports are generated on the basis of an expected clearance value of 0.3 mm and a standard deviation of 0.1 mm as shown in 10. It should be noted that a very small percentage of the clearances has a negative value due to the distribution chosen. This is selected such that it represents a preload applied to the tube at the support location. The maximum preload value was calculated to be 50 N.

Whereas a normal distribution was considered for the support clearances, when randomizing the crack geometry and crack properties, it was seen from various literature sources that properties such as the crack depth for SCC cracks and initial crack length for TWC were truly random, and as a result a uniform distribution was considered. For SCC cracks, the crack ratio (a/t) was randomized over a range between 45% and 75% (figure 11), and the crack aspect ratio (2L/a) was randomized over the range of validity of the model, that is from 3 to 12 (figure 12). For TWC cracks, the initial crack length was randomized between 1.5 mm and 3.5 mm to consider all possible cases (figure 13). Given the 2000 different stress histories of the U-bend to consider the 2000 clearance combination cases discussed earlier a combined 30000 crack growth and leakage rate simulations were conducted. This is due to considering five crack locations for each clearance combination case, as listed in table 2, and considering the result of an existing SCC or TWC crack. The TWC crack requires further investigation to analyze the likelihood and quantify leakage rates based on the techniques outlined in the previous report.
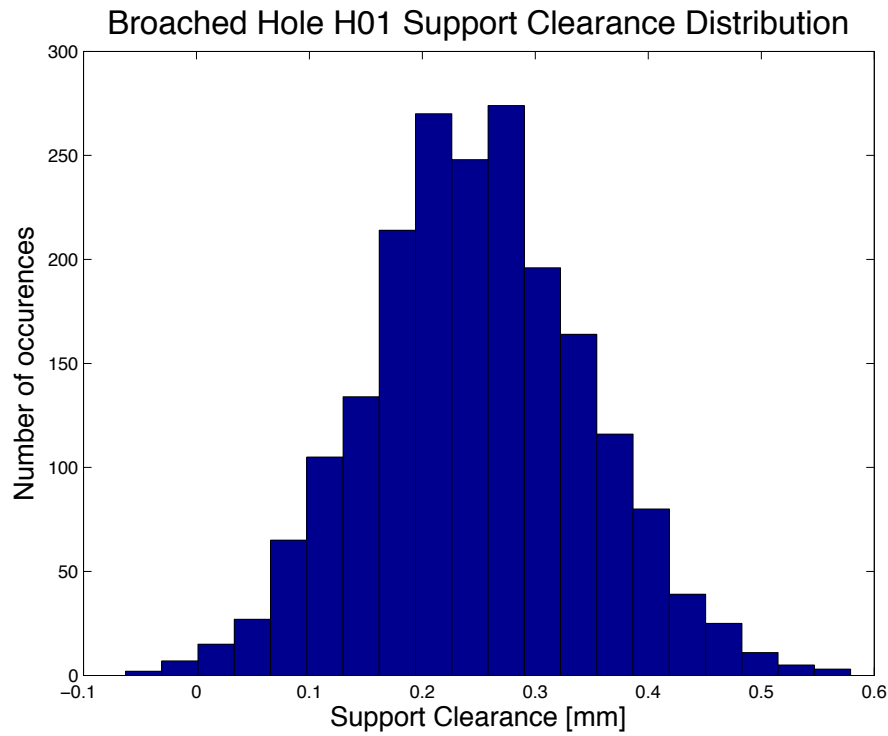
**Figure 8: Support clearance distribution for H01. Mean: 0.25 mm, standard deviation: 0.1 mm**
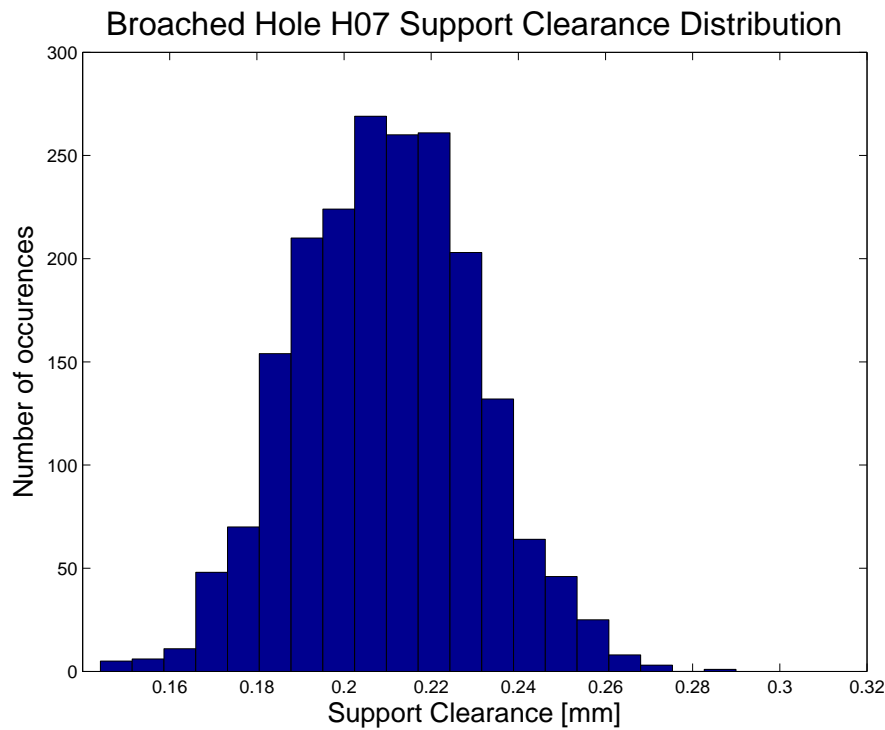


**Figure 9: Support clearance distribution for H07FBS. Mean: 0.21 mm, standard deviation: 0.02 mm**
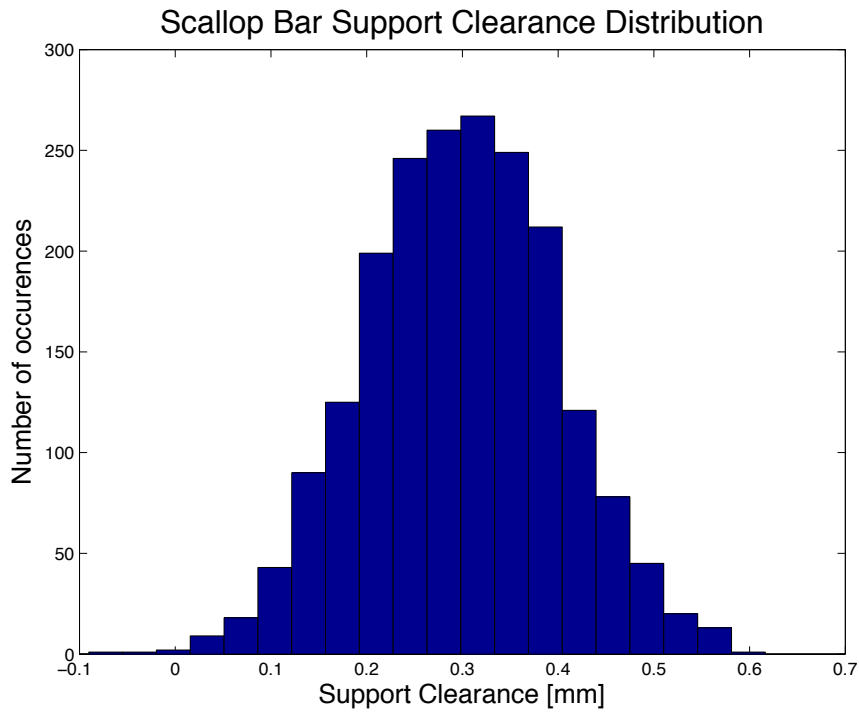
**Figure 10: Support clearance distribution for SB1. Mean: 0.3 mm, standard deviation: 0.1 mm.**
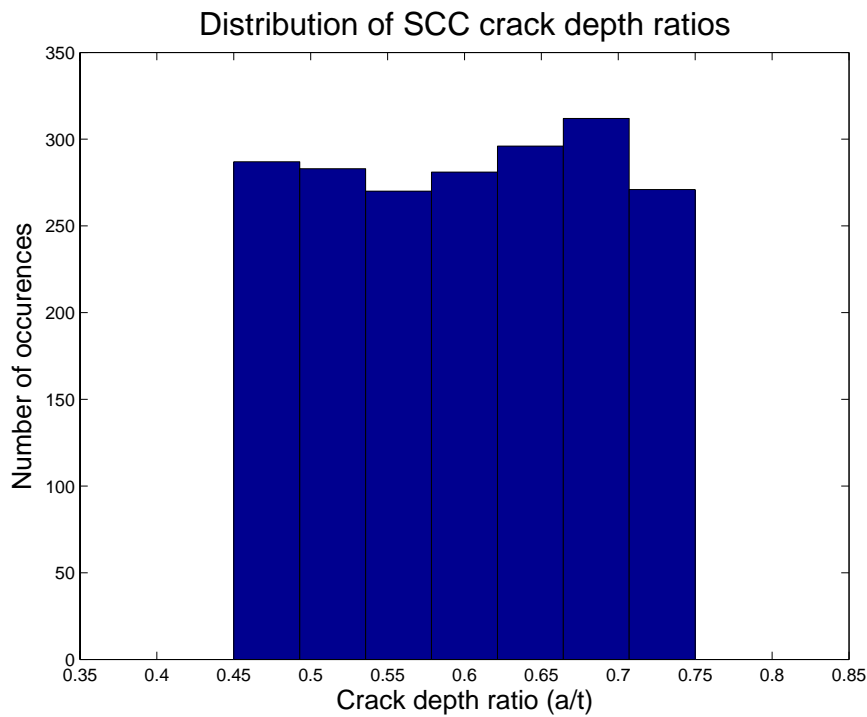


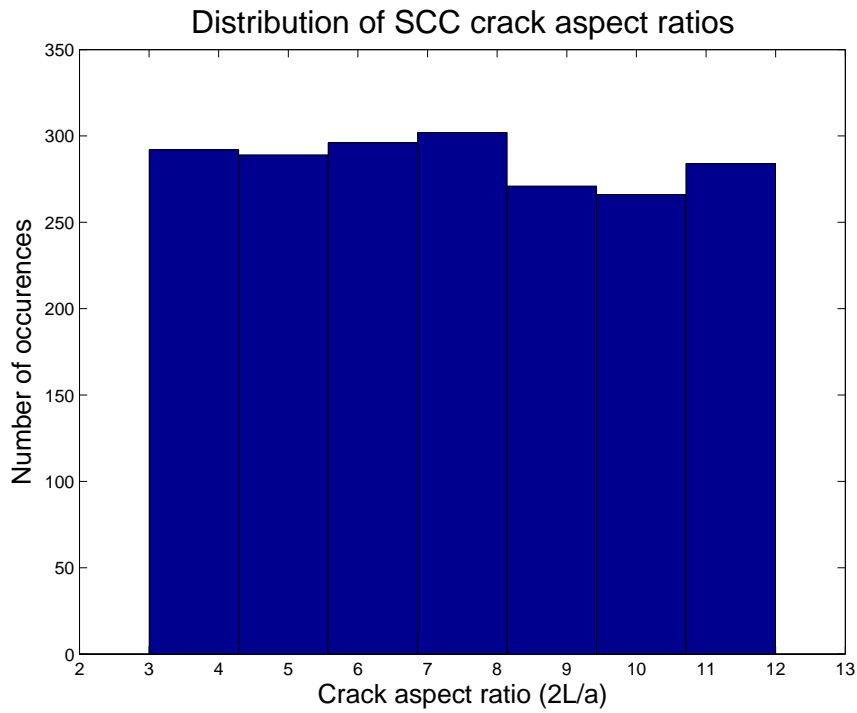**Figure 11: Crack depth ratio distribution for Surface Circumferential Cracks at location 1.**

**Figure 12: Crack aspect ratio distribution for Surface Circumferential Cracks at location 1.**
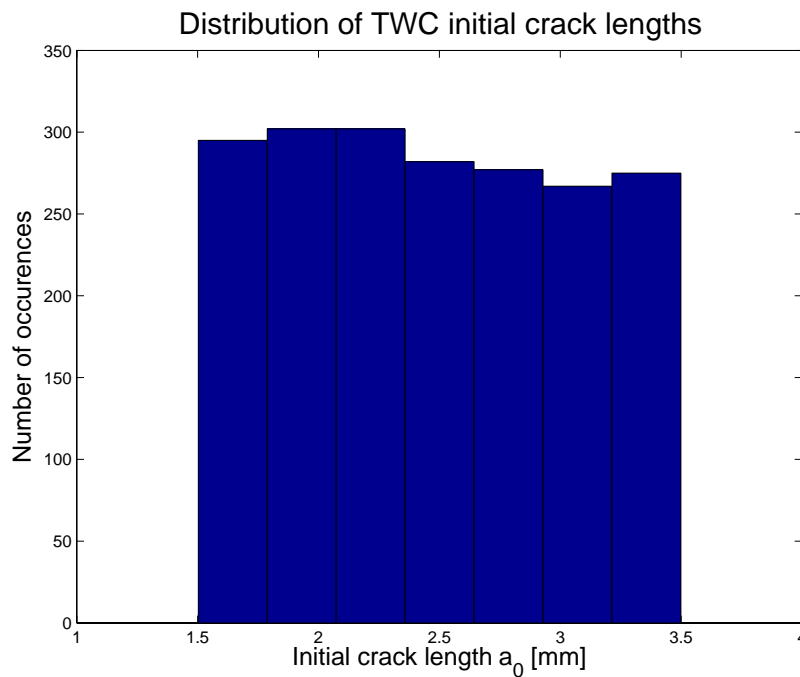


**Figure 13: Initial crack length distribution for Through Wall Cracks at location 1.**

# 4    Results

## 4.1    Deterministic Assessment

### 4.1.1    RMS tube response and bending stress

The RMS resultant responses (in-plane and out-of-plane) are shown in figure 14.  The RMS distribution is shown *vs.* node numbers and is represented for base clearances of 0.2, 0.5, 0.7, 0.9, 1.1, and 1.3mm. For each of these base clearances, the variation of the clearance at support S1 is plotted. As mentioned earlier, nodes 1-19 represents the hot leg part of the tube. It can be seen that the hot leg region shows the highest level of response. This is due to the large clearance values at hot legs supports (H01-H06) as a result of the degradation effect. A secondary region of high displacement level can be seen at the U-bend area.  The level of response in the U-bend region increases as both the support S1 and the base clearance increase.  The response level in the hot lags seems to be affected by the support S1 clearance only.

Figure 14 shows the RMS bending stress along the Configuration 3b tube for various S1 and base clearances.   The U-bend region exhibits the highest level of bending stress with the maximum being in the neighborhood of the apex.  Increasing the S1 clearance from a small value of 0.1 mm to a maximum value of 1.5 mm has a little effect on the overall RMS bending stress. However, the base clearance has a strong effect on the RMS bending stress.  The bending stress increases from a value of 2.6 MPa at $Cr_b$=0.2 mm to 7 MPa for $Cr_b$=1.3mm.

Bending stress levels for Configuration 3c are shown in Figure 15. Similar to the results of Configuration 3a, the peak stresses are observed at the U-bend apex.  However, the increasing the support S2 clearance has a great effect on the RMS stress level. On the other hand, the base clearance has a little effect on the stress level.

### 4.1.2    Crack growth predictions for surface cracks and through wall cracks

Figure 17 shows the evolution of surface circumferential cracks for configuration 3a at location 3 given a crack to tube wall thickness of 45%, at for base clearances of 0.2, 0.5, 1.0, 1.3 mm and for an SB1 clearance ranging between 0.1 mm and 1.5 mm. It is seen that for a base clearance of 0.2 mm, which is a rather tight clearance, the crack's growth is negligible. As the base clearance is increased to 0.5 mm, the crack is shown to propagate, though not reaching a size of 80% of the wall thickness within 12 years. For the 1.0 and 1.3 mm base clearance cases, the crack does propagate to dangerous levels. Note that for those cases as the crack exceeds 0.80 the model goes unstable, as the rate of growth becomes too important. Figure 18 shows similar results for configuration 3b, which is the critical configuration. This is apparent from the fact that there is a potential for the cracks to go unstable even for low base clearances (*i.e.* 0.2 & 0.5 mm), which was not the case for the previous configuration.

### 4.1.3    Tube life summary tables for SCC, TWC and leakage:

Tables 4 to 9 show a summary of the crack growth predictions for configurations 3a, 3b, and 3c, for a crack ratio of 45%. For a given base clearance, if the predicted tube life is greater than 10 years for any $C_r$ between 0.1 mm and 1.5 mm, a dash (-) is shown in the cell. Otherwise, the minimum clearance value that will yield a tube life of less than 10 years is shown.

Table 4 shows that Location 3 (SB2) is the critical location, as it is the first to fail for base clearances as low as 0.3 mm. Starting at a base clearance of 0.5 mm, existing cracks at location 2 will propagate to 80% wall thickness in less than 10 years, if the SB1 clearance exceeds 0.4 mm. This is in addition to the already compromised location 3. The critical region for this configuration appears to be the center of the U-bend, *i.e.* location 3. Similarly, Table 5 shows results for configuration 03b for the same crack aspect ratio of 45%. Configuration 03b is a more dangerous configuration as for SB1 and SB2 clearance of even 0.1 mm that tube's life may be less than 10 years if the SB2 clearance exceeds 0.8 mm. Summary tables for higher crack ratios are included in the appendix, and they show similar trends, in a sense that higher ratios will cause the tube to be susceptible to failure for tighter clearances.

Table 7 looks at through wall crack propagation scenarios for configuration 03a. As previously, these tables provide a summary that lists critical clearances that will yield a tube life of less than 10 years. The initial crack size is set to 1.5 mm, and cracks existing at the center of the U-bend are once again the critical cracks, since for a clearance of 0.4 mm at SB2 and SB3 and a clearance of 0.3 mm at SB1 a crack at SB2 will yield a tube life inferior to 10 years. Table 8 shows the corresponding results for configuration 03b, and it is apparent once again that the top of the U-bend is the critical section of the U-bend, as cracks may propagate to 80% wall thickness in less than 10 years for base clearances of 0.1 mm and a clearance of 0.5 mm at SB2. It is also worth noting for such a configuration cracks are more likely to propagate at multiple locations simultaneously, as it is apparent in table 8. Once again, predictions for larger initial crack sizes show an earlier onset of failure, and the results for those simulations are included in the appendix for initial crack sizes $a_0$ of up to 3.5 mm. All tables show that cracks at location 5 are less likely to propagate than cracks at location 1, even though they are symmetrically located from the U-bend. This is quite likely due to location 1 being on the hot leg whereas location 5 is on the cold leg. This supports the fact that the hot leg is inherently more compromised than the cold leg, due to the worn out supports yielding higher tube displacements and stresses.
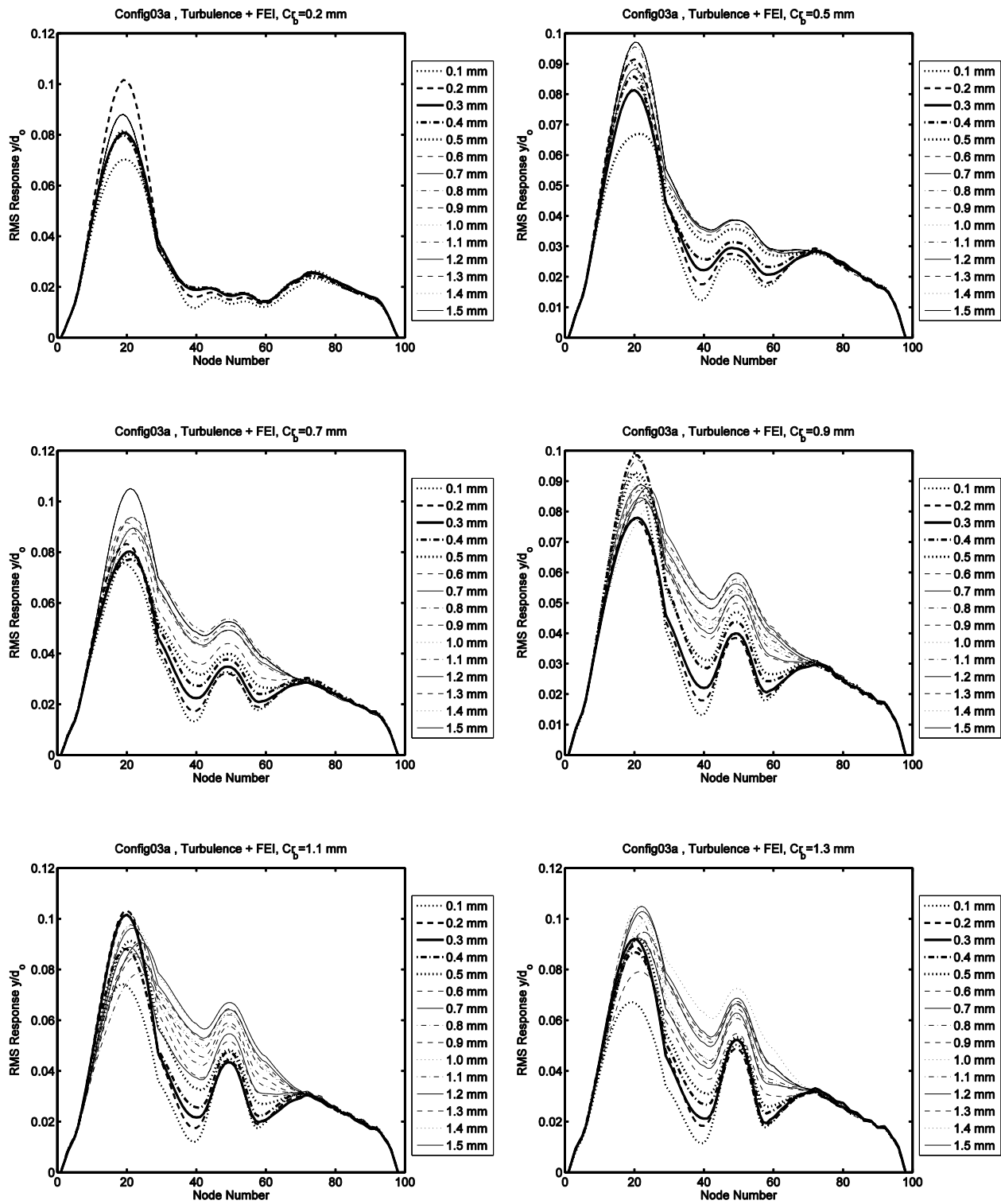
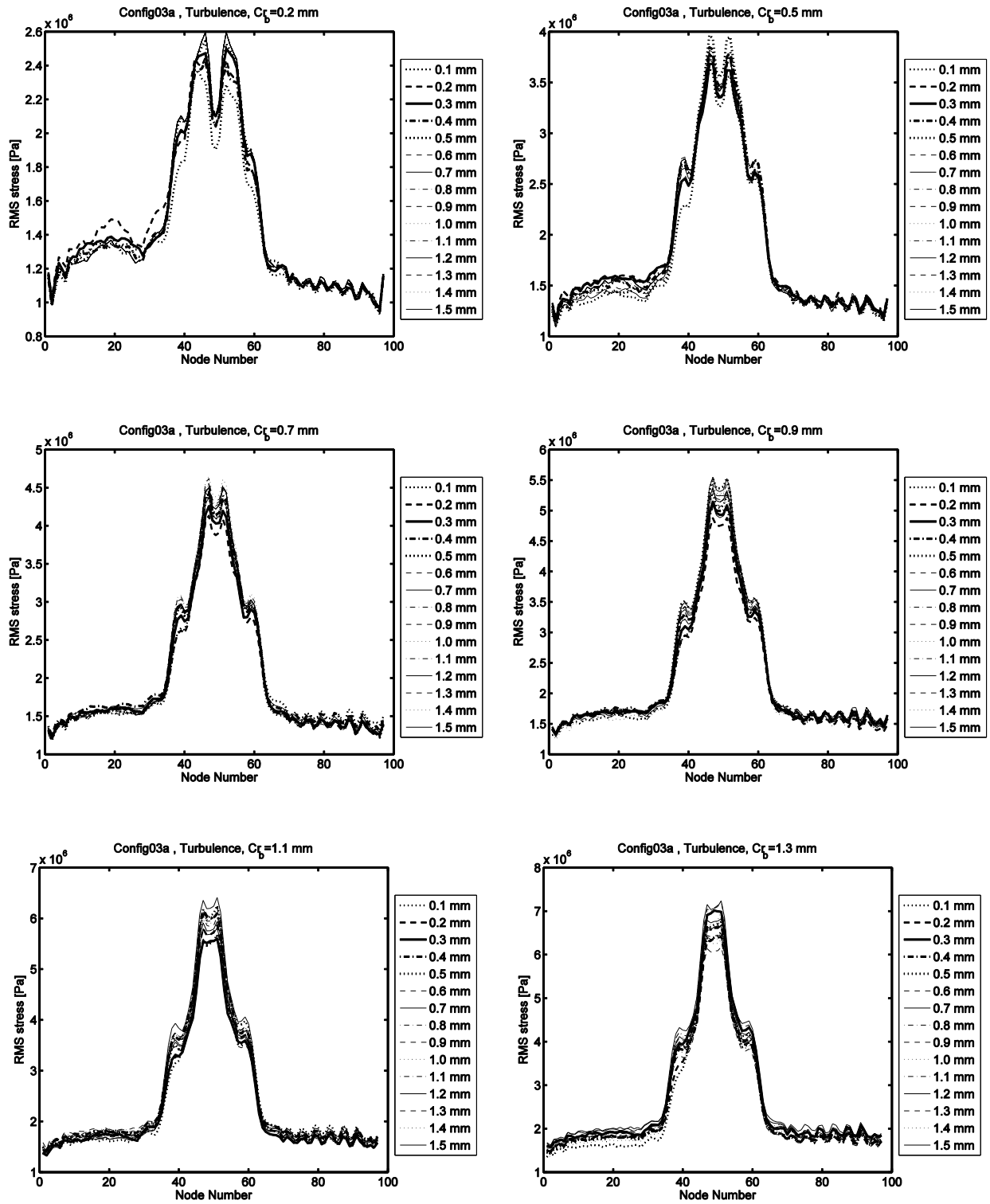**Figure 14: RMS tube displacement for configuration 03a.**

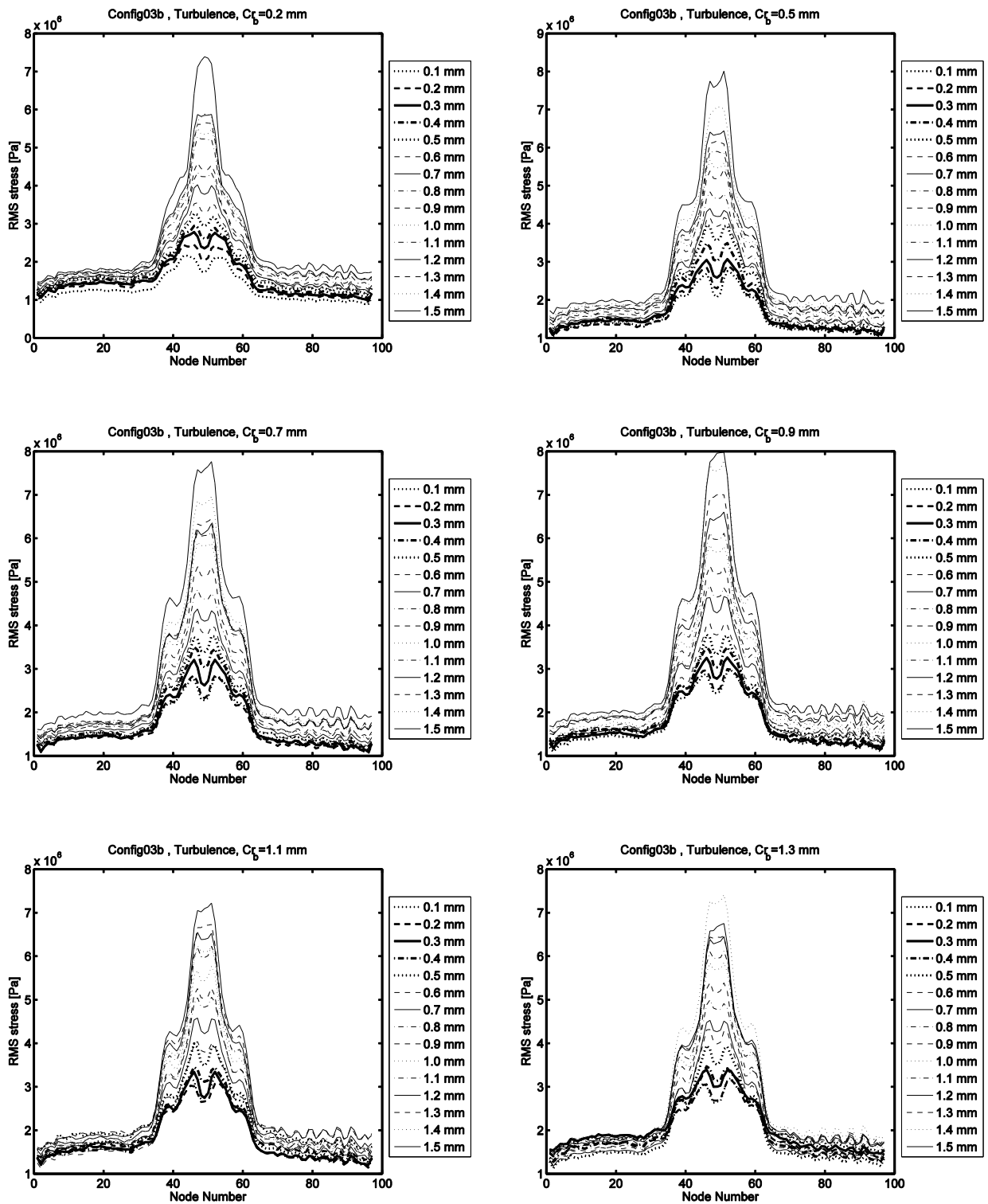**Figure 15: RMS stresses distribution for configuration 03a.**

**Figure 16: RMS stresses distribution for configuration 03b.**

**Table 7: Crack geometry description for surface circumferential crack predictions.**

| Crack ratio (a/t) | Crack size (a) [mm] | Aspect ratio (2L/a) | Crack angle [deg] |
|---|---|---|---|
| 45% | 0.54 | 5.76 | 30 |
| 50% | 0.60 | 5.18 | 30 |
| 55% | 0.66 | 4.71 | 30 |
| 60% | 0.72 | 4.32 | 30 |
| 65% | 0.78 | 3.99 | 30 |
| 70% | 0.84 | 3.70 | 30 |
| 75% | 0.90 | 3.46 | 30 |
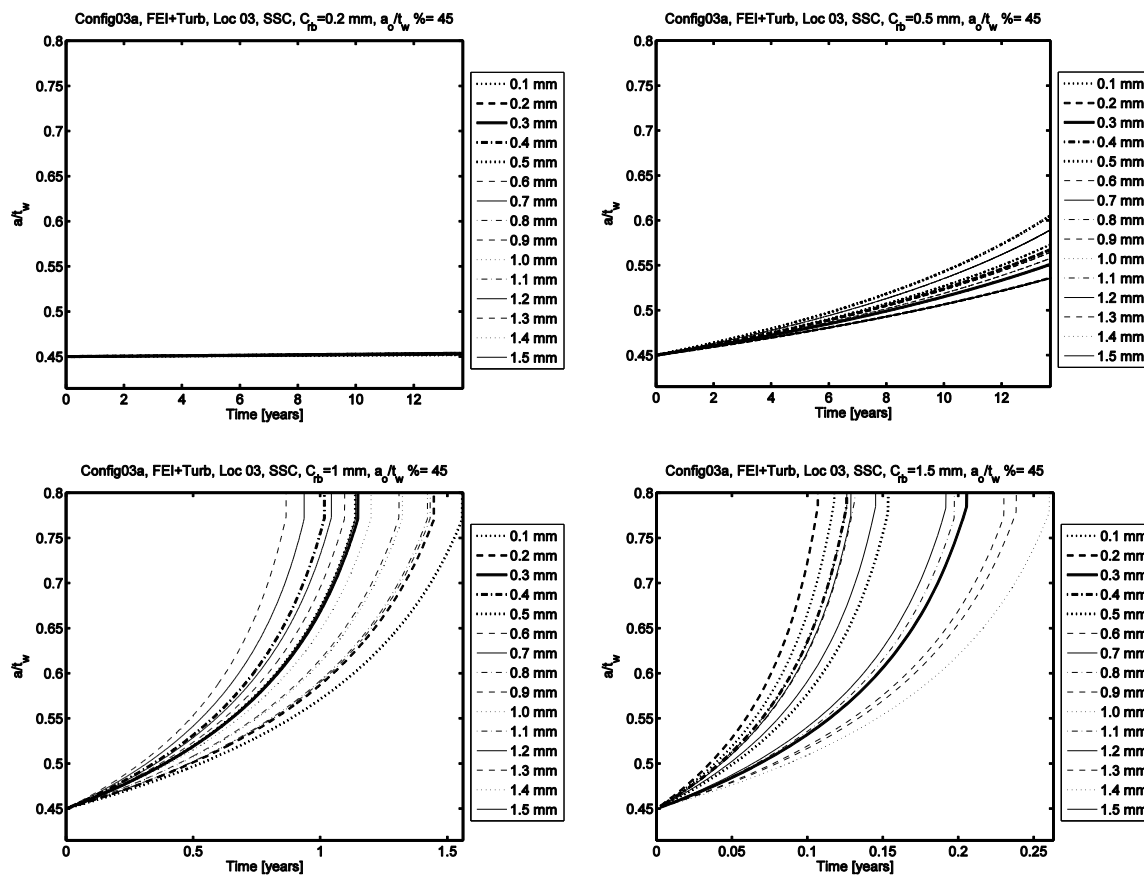


**Figure 17: Surface flaw growth for initial crack size of 45% of the tube wall thickness for configuration 3a**
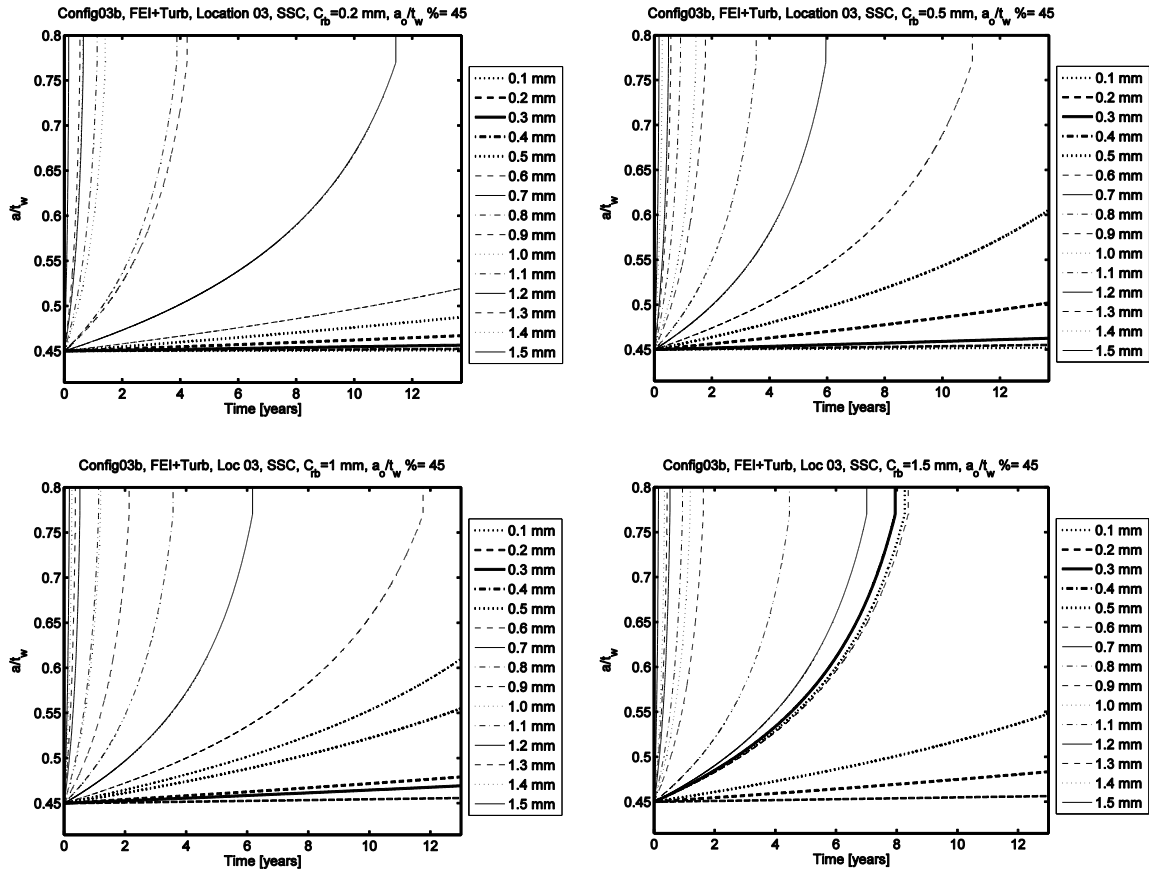
**Figure 18: Surface flaw growth for initial crack size of 45% of the tube wall thickness for configuration 3b.**
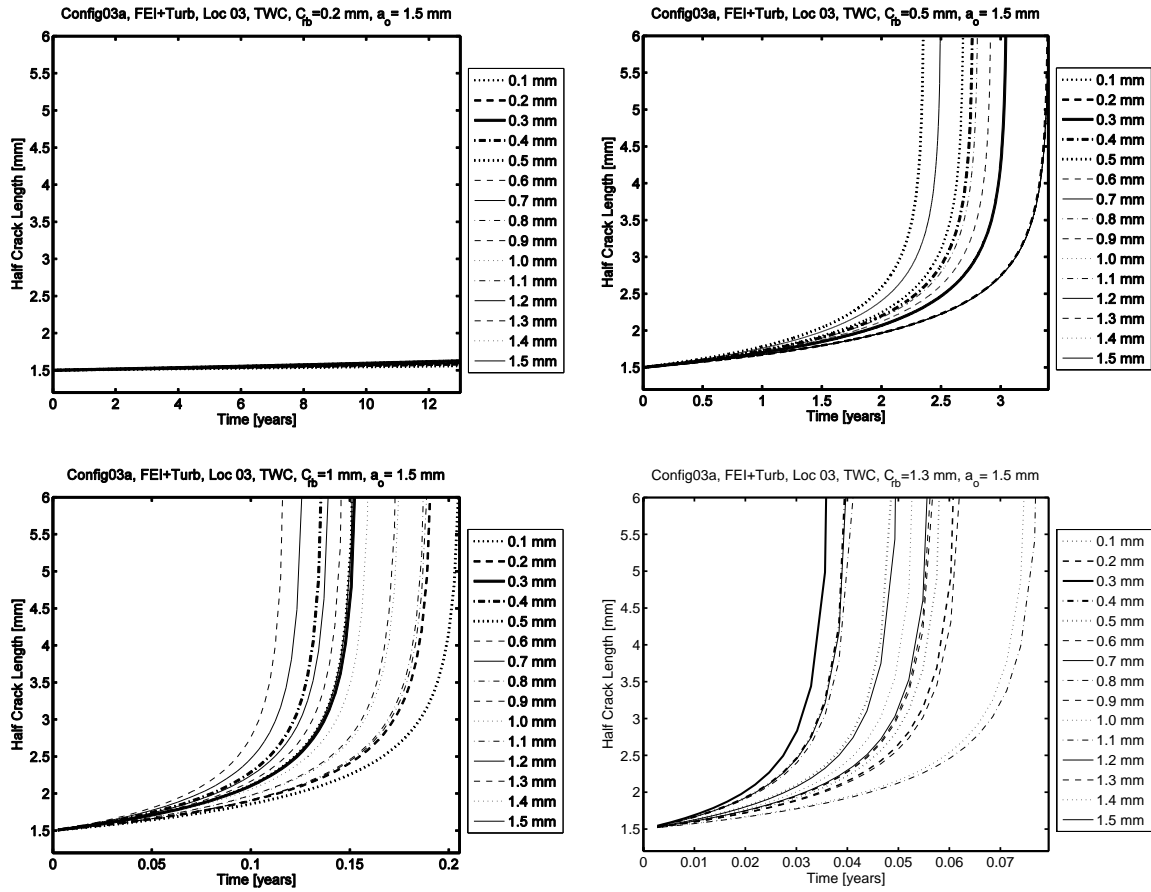
**Figure 19: Circumferential through-wall crack growth for initial crack size $a_o$=1.5 mm, configuration 3a**
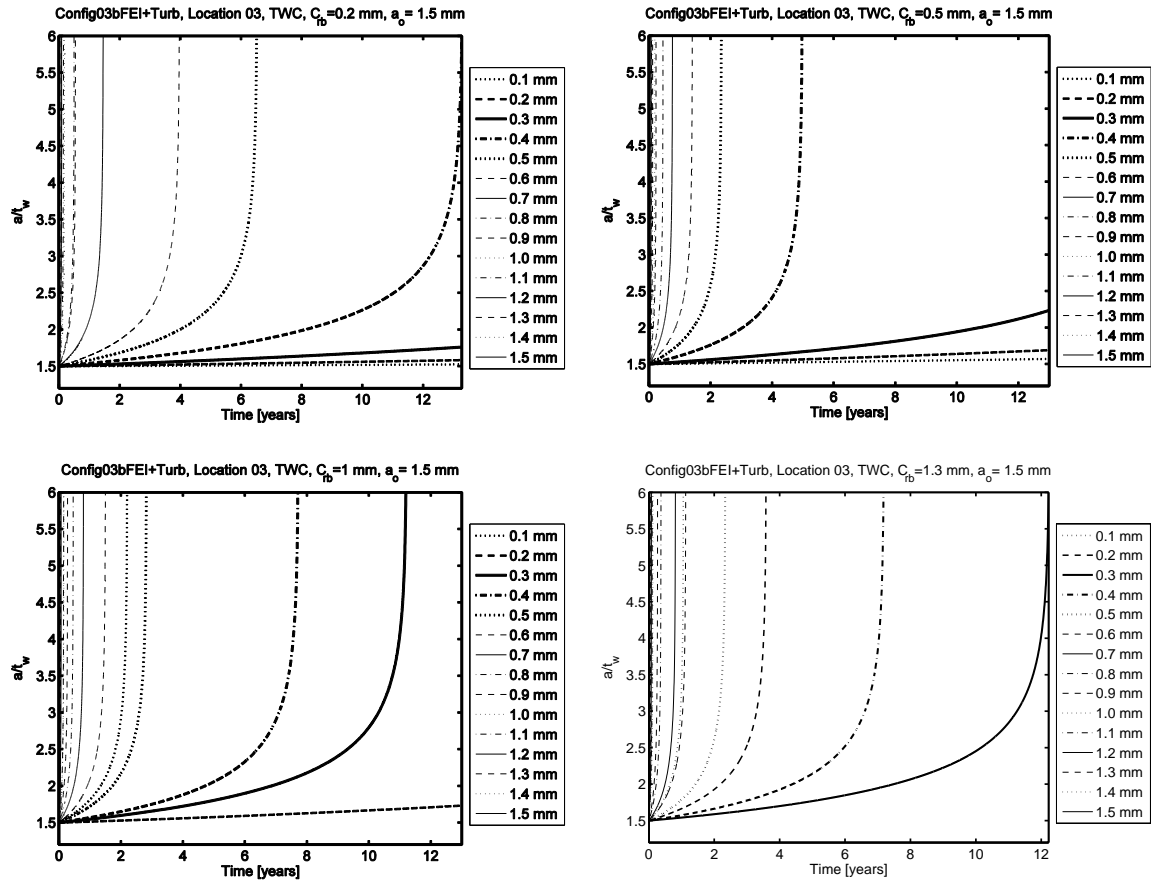
**Figure 20: Circumferential Through-Wall crack growth for initial crack size a$_o$=1.5 mm, configuration 3b**
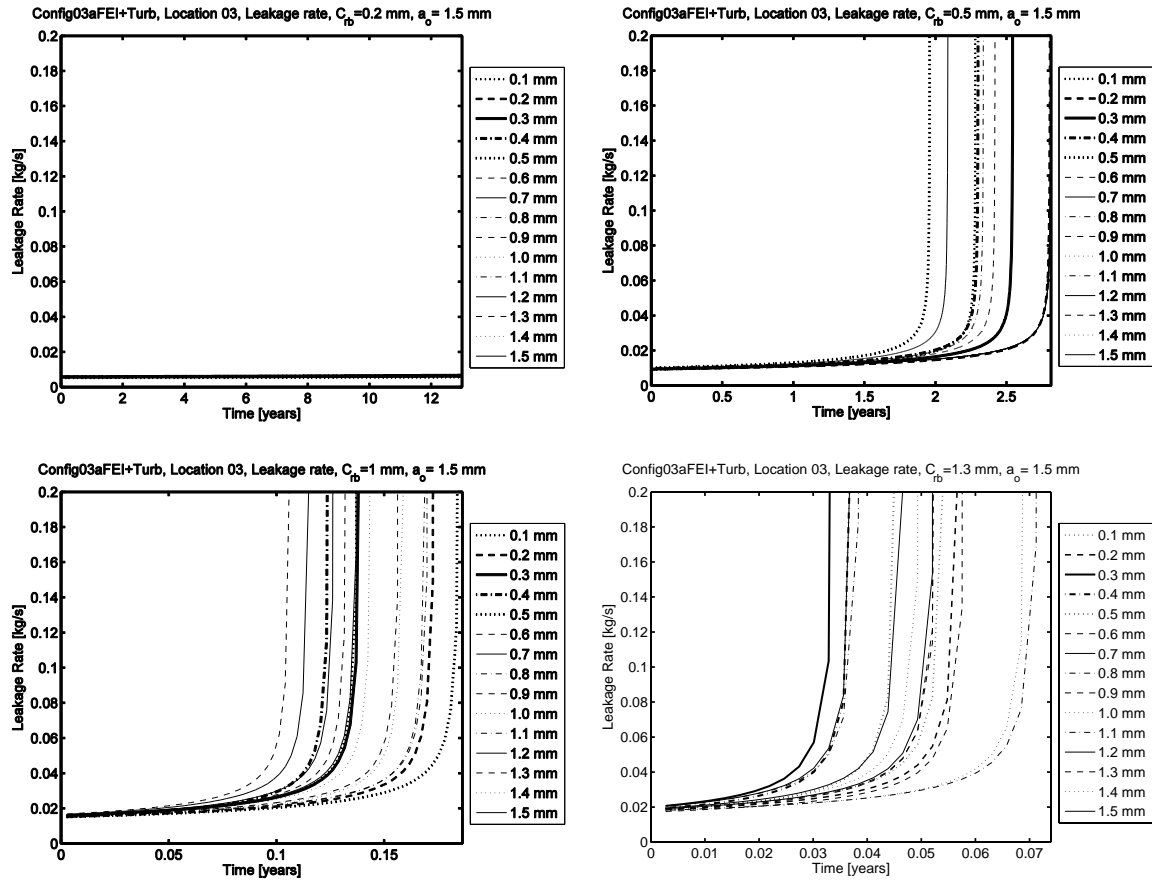
**Figure 21: Leakage rate for initial crack size a<sub>o</sub>=1.5 mm, configuration 3a.**
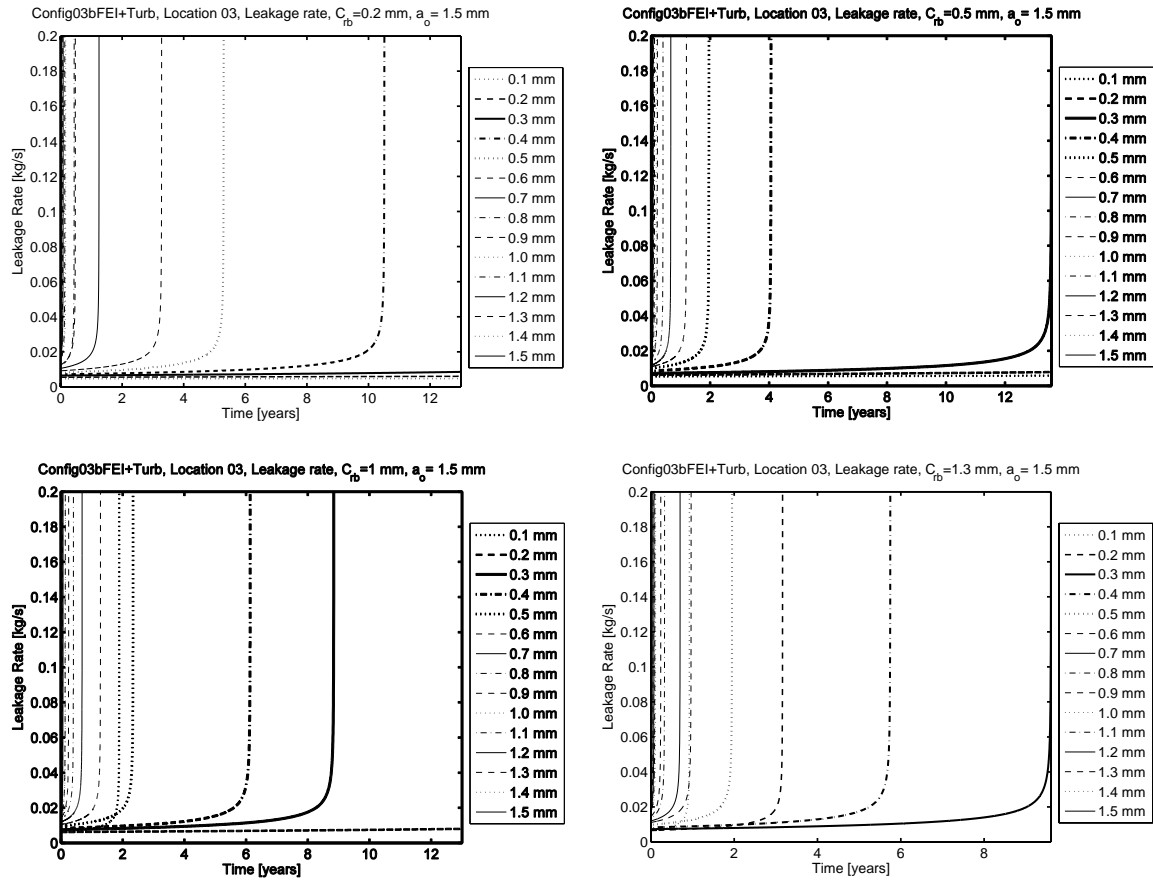
**Figure 22: Leakage rate for initial crack size $a_o$=1.5 mm, configuration 3b.**

**Table 8: Minimum clearance combinations yielding a tube life less than 10 years for configuration 3a, surface circumferential cracks, and a 45% crack ratio.**

| Base Clearance [mm] | SB1 clearance [mm] | | | | |
|---|---|---|---|---|---|
| | Location 1 | Location 2 | Location 3 | Location 4 | Location 5 |
| 0.1 | - | - | - | - | - |
| 0.2 | - | - | - | - | - |
| 0.3 | - | - | 0.2 | - | - |
| 0.4 | - | - | 0.1 | - | - |
| 0.5 | - | 0.4 | 0.1 | - | - |
| 0.6 | - | 0.5 | 0.1 | 0.1 | - |
| 0.7 | - | 0.4 | 0.1 | 0.1 | - |
| 0.8 | - | 0.2 | 0.1 | 0.1 | - |
| 0.9 | 1 | 0.1 | 0.1 | 0.1 | - |
| 1 | 0.8 | 0.1 | 0.1 | 0.1 | - |
| 1.1 | 0.7 | 0.1 | 0.1 | 0.1 | - |
| 1.2 | - | 0.1 | 0.1 | 0.1 | - |
| 1.3 | 0.9 | 0.1 | 0.1 | 0.1 | - |
| 1.4 | 0.4 | 0.1 | 0.1 | 0.1 | 0.4 |
| 1.5 | 0.9 | 0.1 | 0.1 | 0.1 | 0.1 |

**Table 9: Minimum clearance combinations yielding a tube life less than 10 years for configuration 3b, surface circumferential cracks, and a 45% crack ratio.**

| Base Clearance [mm] | SB2 clearance [mm] | | | | |
|---|---|---|---|---|---|
| | Location 1 | Location 2 | Location 3 | Location 4 | Location 5 |
| 0.1 | - | - | 0.8 | 1.3 | - |
| 0.2 | - | - | 0.8 | 1.5 | - |
| 0.3 | - | 1.5 | 0.7 | 1.3 | - |
| 0.4 | - | 1.4 | 0.7 | 1.2 | - |
| 0.5 | - | 1.4 | 0.7 | 1.4 | - |
| 0.6 | - | 1.3 | 0.7 | 1.2 | - |
| 0.7 | - | 1.3 | 0.7 | 1.1 | - |
| 0.8 | - | 1.2 | 0.7 | 1.2 | - |
| 0.9 | - | 1.3 | 0.7 | 1.1 | - |
| 1.00 | - | 1.2 | 0.7 | 1.2 | - |
| 1.1 | 1.3 | 1.2 | 0.1 | 1.1 | - |
| 1.2 | 1.3 | 1.2 | 0.1 | 1.2 | - |
| 1.3 | - | 1.4 | 0.1 | 1.2 | - |
| 1.4 | 0.3 | 1.4 | 0.1 | 1.3 | - |
| 1.5 | 1.1 | 1.3 | 0.1 | 0.3 | - |

**Table 10: Minimum clearance combinations yielding a tube life less than 10 years for configuration 3c, surface circumferential cracks, and a 45% crack ratio.**

| Base Clearance [mm] | SB3 clearance [mm] | | | | |
|---|---|---|---|---|---|
| | Location 1 | Location 2 | Location 3 | Location 4 | Location 5 |
| 0.1 | - | - | - | - | - |
| 0.2 | - | - | - | - | - |
| 0.3 | - | - | - | - | - |
| 0.4 | - | - | - | - | - |
| 0.5 | - | - | - | - | - |
| 0.6 | - | - | 0.8 | - | - |
| 0.7 | - | - | 0.2 | - | - |
| 0.8 | - | - | 0.1 | - | - |
| 0.9 | - | - | 0.1 | - | - |
| 1.0 | - | - | 0.1 | - | - |
| 1.1 | - | - | 0.1 | 0.7 | - |
| 1.2 | - | 0.6 | 0.1 | 0.4 | - |
| 1.3 | - | 0.4 | 0.1 | 0.4 | - |
| 1.4 | 0.9 | 0.1 | 0.1 | 0.2 | - |
| 1.5 | - | 0.1 | 0.1 | 0.3 | - |

**Table 11: Minimum clearance combinations yielding a tube life less than 10 years for configuration 3a, through wall cracks, given a 1.5 mm initial crack size.**

| Base Clearance [mm] | SB1 clearance [mm] | | | | |
|---|---|---|---|---|---|
| | Location 1 | Location 2 | Location 3 | Location 4 | Location 5 |
| 0.1 | - | - | - | - | - |
| 0.2 | - | - | - | - | - |
| 0.3 | - | - | - | - | - |
| 0.4 | - | - | 0.3 | - | - |
| 0.5 | - | - | 0.1 | - | - |
| 0.6 | - | - | 0.1 | - | - |
| 0.7 | - | 0.9 | 0.1 | 0.1 | - |
| 0.8 | - | 0.3 | 0.1 | 0.1 | - |
| 0.9 | 1.0 | 0.3 | 0.1 | 0.1 | - |
| 1 | - | 0.1 | 0.1 | 0.1 | - |
| 1.1 | 0.9 | 0.1 | 0.1 | 0.1 | - |
| 1.2 | - | 0.1 | 0.1 | 0.1 | - |
| 1.3 | 1.0 | 0.1 | 0.1 | 0.1 | - |
| 1.4 | 0.4 | 0.1 | 0.1 | 0.1 | - |
| 1.5 | 0.9 | 0.1 | 0.1 | 0.1 | - |

**Table 12 Minimum clearance combinations yielding a tube life less than 10 years for configuration 3b, through wall cracks, given a 1.5 mm initial crack size.**

| Base Clearance [mm] | SB2 clearance [mm] | | | | |
|---|---|---|---|---|---|
| | Location 1 | Location 2 | Location 3 | Location 4 | Location 5 |
| 0.1 | - | 1.1 | 0.5 | 0.9 | - |
| 0.2 | - | 1.0 | 0.5 | 0.8 | - |
| 0.3 | - | 0.8 | 0.4 | 0.8 | - |
| 0.4 | - | 0.8 | 0.4 | 0.7 | - |
| 0.5 | - | 0.8 | 0.4 | 0.8 | - |
| 0.6 | - | 0.8 | 0.4 | 0.7 | - |
| 0.7 | - | 0.8 | 0.4 | 0.8 | - |
| 0.8 | - | 0.7 | 0.1 | 0.7 | - |
| 0.9 | - | 0.7 | 0.1 | 0.7 | - |
| 1 | - | 0.7 | 0.1 | 0.7 | - |
| 1.1 | - | 0.7 | 0.1 | 0.7 | - |
| 1.2 | 0.9 | 0.1 | 0.1 | 0.1 | - |
| 1.3 | 0.1 | 0.1 | 0.1 | 0.1 | - |
| 1.4 | 0.1 | 0.1 | 0.1 | 0.1 | - |
| 1.5 | 0.1 | 0.1 | 0.1 | 0.1 | |

**Table 13: Minimum clearance combinations yielding a tube life less than 10 years for configuration 3c, through wall cracks, given a 1.5 mm initial crack size.**

| Base Clearance [mm] | SB3 clearance [mm] | | | | |
|---|---|---|---|---|---|
| | Location 1 | Location 2 | Location 3 | Location 4 | Location 5 |
| 0.1 | - | - | - | - | - |
| 0.2 | - | - | - | - | - |
| 0.3 | - | - | - | - | - |
| 0.4 | - | - | 0.3 | - | - |
| 0.5 | - | - | 0.1 | - | - |
| 0.6 | - | - | 0.1 | - | - |
| 0.7 | - | 0.4 | 0.1 | - | - |
| 0.8 | - | 0.2 | 0.1 | 0.3 | - |
| 0.9 | - | 0.1 | 0.1 | 0.2 | - |
| 1 | - | 0.1 | 0.1 | 0.1 | - |
| 1.1 | - | 0.1 | 0.1 | 0.1 | - |
| 1.2 | - | 0.1 | 0.1 | 0.1 | - |
| 1.3 | 1.0 | 0.1 | 0.1 | 0.1 | - |
| 1.4 | 0.9 | 0.1 | 0.1 | 0.1 | - |
| 1.5 | - | 0.1 | 0.1 | 0.1 | - |

**Table 14: Minimum clearance combinations yielding a tube life less than 10 years for configuration 3a, leakage rates, given a 1.5 mm initial crack size.**

| Base Clearance | SB1 clearance | | | | |
|---|---|---|---|---|---|
| | Location 1 | Location 2 | Location 3 | Location 4 | Location 5 |
| 0.1 | - | - | - | - | - |
| 0.2 | - | - | - | - | - |
| 0.3 | - | - | - | - | - |
| 0.4 | - | - | - | - | - |
| 0.5 | - | - | 0.5 | - | - |
| 0.6 | - | - | 0.1 | - | - |
| 0.7 | - | - | 0.1 | - | - |
| 0.8 | - | - | 0.1 | - | - |
| 0.9 | - | - | 0.1 | 0.5 | - |
| 1 | - | 0.8 | 0.1 | 0.1 | - |
| 1.1 | 0.9 | 0.7 | 0.1 | 0.1 | - |
| 1.2 | - | 0.4 | 0.1 | 0.1 | - |
| 1.3 | 1.0 | 0.3 | 0.1 | 0.1 | - |
| 1.4 | 1.1 | 0.2 | 0.1 | 0.1 | - |
| 1.5 | - | 0.1 | 0.1 | 0.1 | - |

**Table 15: Minimum clearance combinations yielding a tube life less than 10 years for configuration 3b, leakage rates, given a 1.5 mm initial crack size.**

| Base Clearance | SB1 clearance | | | | |
|---|---|---|---|---|---|
| | Location 1 | Location 2 | Location 3 | Location 4 | Location 5 |
| 0.1 | 1.1 | 0.7 | 0.4 | 0.6 | 1.1 |
| 0.2 | 1 | 0.6 | 0.3 | 0.6 | 1 |
| 0.3 | 1.1 | 0.5 | 0.2 | 0.4 | 1.1 |
| 0.4 | 0.8 | 0.3 | 0.2 | 0.3 | 1.2 |
| 0.5 | 0.8 | 0.3 | 0.2 | 0.3 | 1.1 |
| 0.6 | 0.7 | 0.3 | 0.1 | 0.3 | 1.2 |
| 0.7 | 0.1 | 0.3 | 0.1 | 0.3 | 1 |
| 0.8 | 0.1 | 0.1 | 0.1 | 0.1 | 0.1 |
| 0.9 | 0.1 | 0.1 | 0.1 | 0.1 | 0.1 |
| 1 | 0.1 | 0.1 | 0.1 | 0.1 | 0.1 |
| 1.1 | 0.1 | 0.1 | 0.1 | 0.1 | 0.1 |
| 1.2 | 0.1 | 0.1 | 0.1 | 0.1 | 0.1 |
| 1.3 | 0.1 | 0.1 | 0.1 | 0.1 | 0.1 |
| 1.4 | 0.1 | 0.1 | 0.1 | 0.1 | 0.1 |
| 1.5 | 0.1 | 0.1 | 0.1 | 0.1 | 0.1 |

### 4.2    Monte Carlo Simulations – Probabilistic Assessment

*4.2.1    Assessing the likelihood of unstable Surface Circumferential Cracks*
A sample of a 1000 cases was fully analyzed while assuming the existence of the Surface Circumferential Cracks described in section 3 of this report. Using the present assumptions regarding clearances at the support where the heat exchanger shows little sign of aging, there does not appear to be any unstable crack growth. As a matter of fact there hasn't been any observed crack growth case in the sample 1000 simulations conducted. This is shown by figures 23 and 24, where for the entire range of crack ratios considered the cracks remain at their initial length.
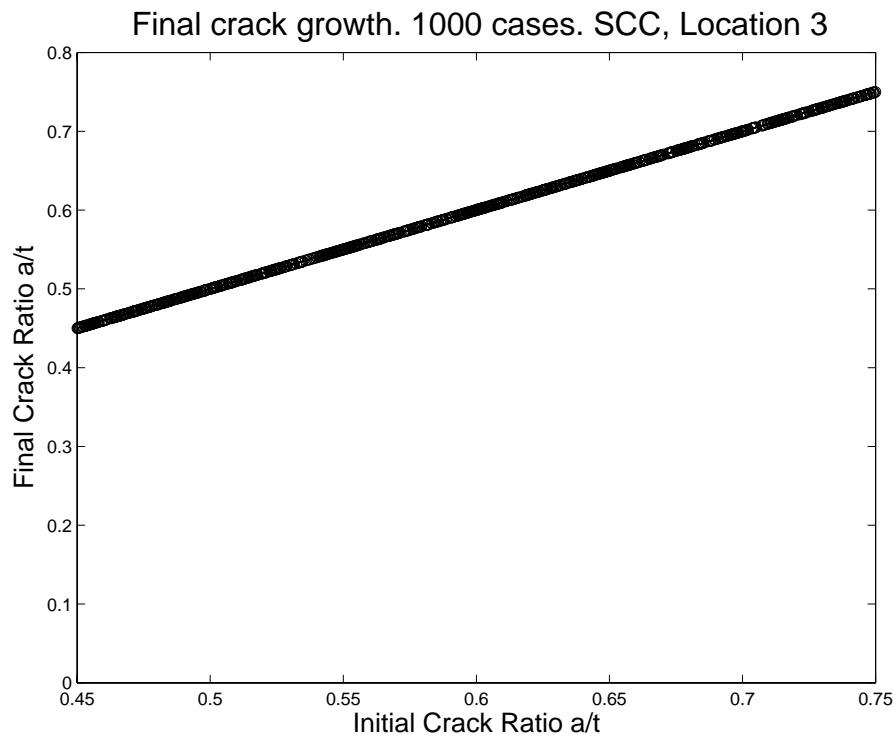


**Figure 23: Distribution of the final crack ratios *vs.* initial crack ratios for Surface Circumferential Cracks at location 3.**
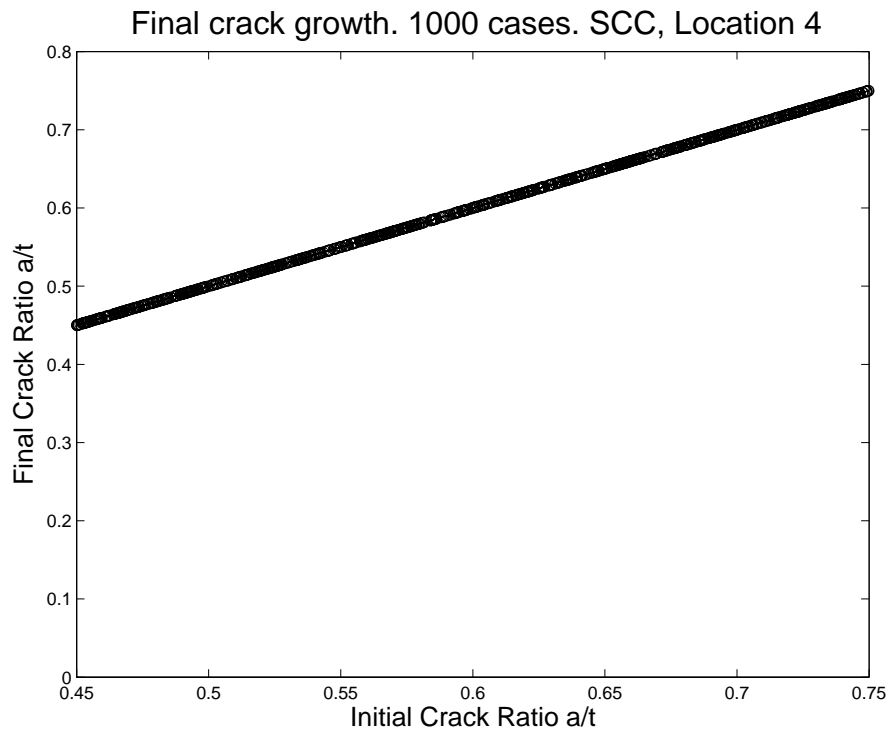
**Figure 24: Distribution of the final crack ratios *vs.* initial crack ratios for Surface Circumferential Cracks at location 4.**

### *4.2.2   Through Wall Cracks – Distribution of initial and final crack lengths*

Whereas for the large number of cases considered for SCC cracks there was little to no growth observed, the TWC cracks show a radically different behavior. As one can see in figures 25 and 26, there is a general trend such that larger initial cracks are more likely to exhibit unstable growth. This is especially apparent for location 1, where crack of an initial length between 1.5 mm and 2.5 mm are unlikely to propagate, whereas cracks that exceed 2.5 mm in initial length may grow significantly, sometimes reaching the model limit of 6 mm, for a particular subset of the simulations.
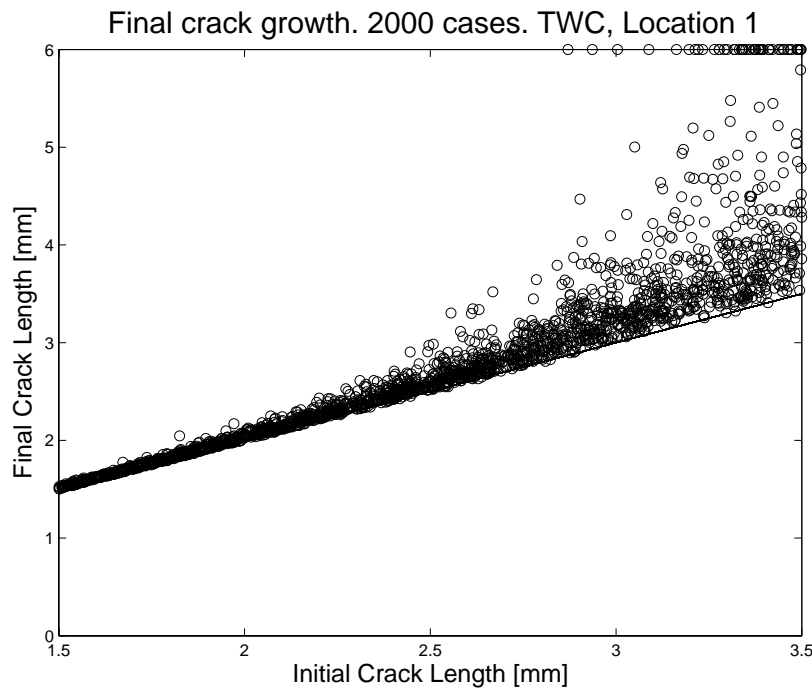


**Figure 25: Distribution of the final crack length *vs.* initial crack length for Through Wall Cracks at location 1.**

Location 3 appears to be critical as there are a number of cases over the entire range of initial crack lengths where unstable crack growth is observed. The crack behavior for the remaining locations is included in the appendix, and it can be seen that locations 1 and 5 show safe regions whereas locations 2, 3, and 4 are more prone to unstable crack growth. This is in line with the previous findings that emphasized the existence of higher stresses in the middle of the U-bend. While the conditions applied to the cold and hot leg of the heat exchanger (such as the flow parameters and the effects of corrosion) are rather different, locations on either side show similar behavior. For instance, locations 2 and 4 show similar crack growth behavior.
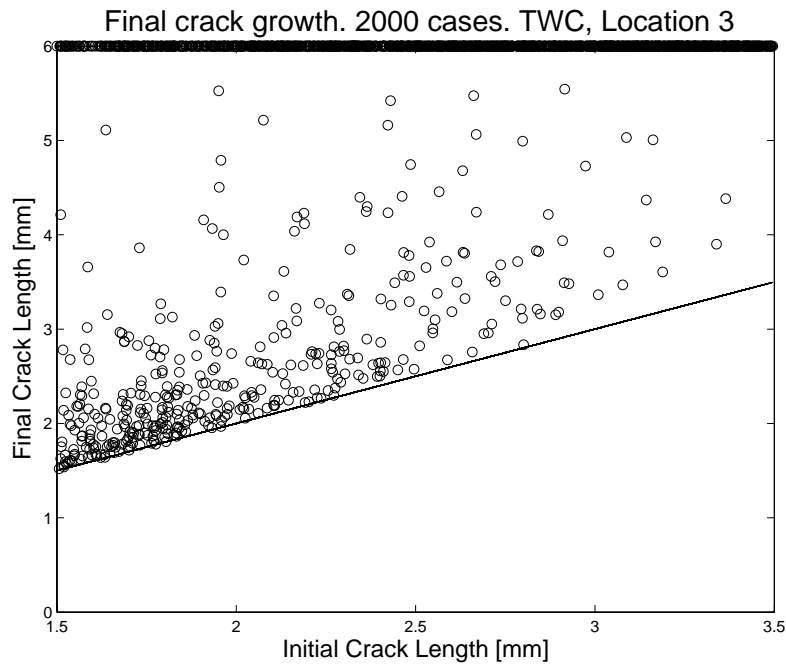
**Figure 26: Distribution of the final crack length *vs.* initial crack length for Through Wall Cracks at location 3.**
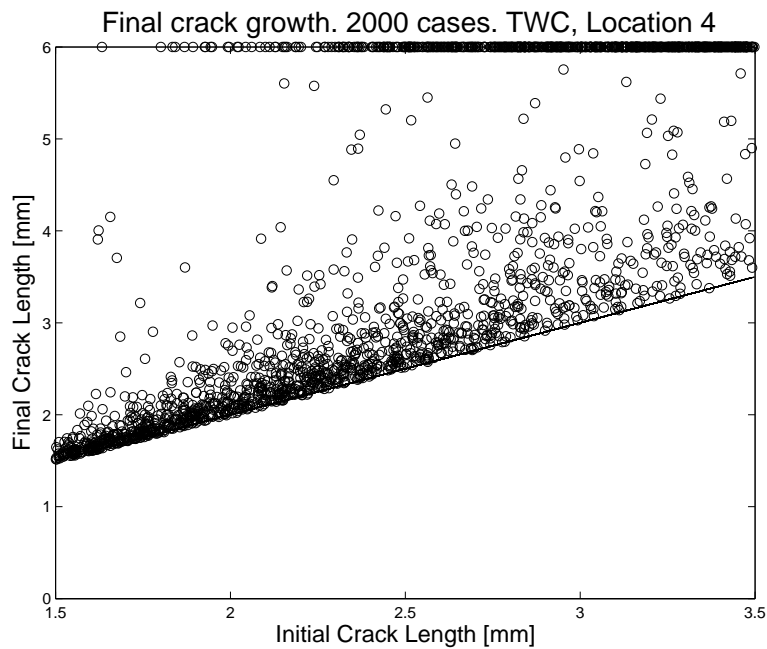


**Figure 27: Distribution of the final crack length *vs.* initial crack length for Through Wall Cracks at location 4.**

*4.2.3   Through Wall Cracks – Assessing tube life based on initial crack lengths*
The focus of the previous section was on determining which initial crack conditions would cause significant or unstable growth. One factor that was not taken into account was time. This is rather crucial as two cracks may eventually reach the same size while taking a different amount of time to develop. Figures 28 and 29 show the time required for cracks to reach 6 mm, with a ceiling of 13 years if the crack fails to develop significantly. For location 1 only cracks exceeding 2.8 mm in initial length appear to reduce the tube's life in any significant manner, with a minimum observed of 6 years for cracks of 3.1-3.5 mm.
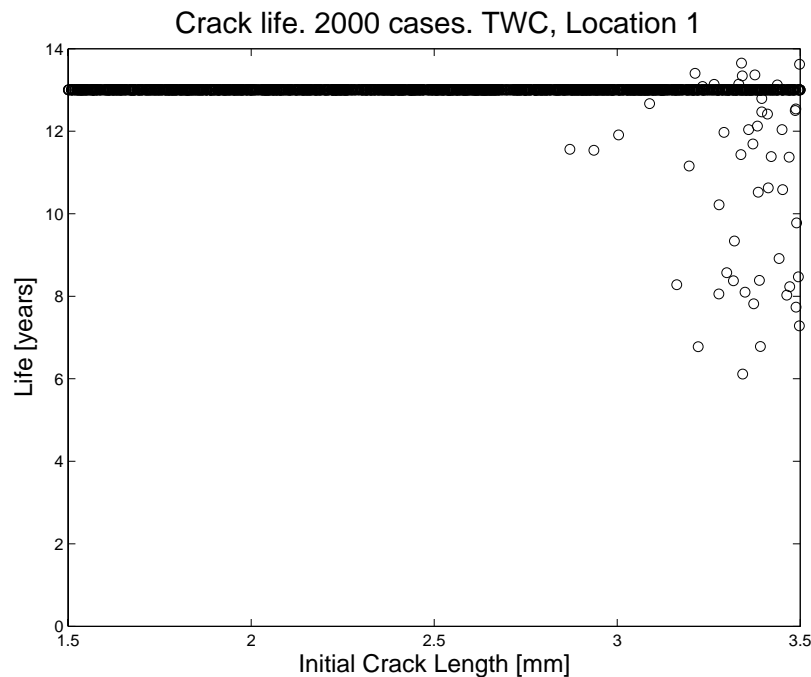


**Figure 28: Distribution of the life prediction *vs.* initial crack length for Through Wall cracks at location 1.**

Location 3 shows that there may be critical failure for cracks considered over the whole range, with an increasing proportion failing early as the initial crack length is increased, as shown by the dense cloud of results. Whereas for small initial crack lengths there is a significant portion of the cases that reaches the ceiling life of 13 years, for higher initial crack lengths there is only a small portion that is expected to reach the same tube life.
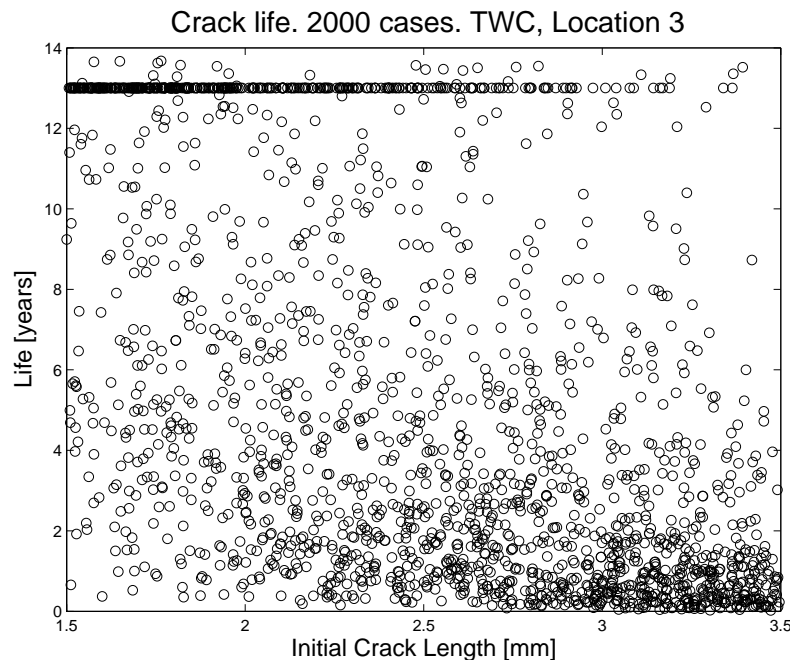
**Figure 29: Distribution of the life predictions *vs.* initial crack length for Through Wall Cracks at location 3.**

*4.2.4   Through Wall Cracks – Classification of Crack Growth Results*

When dealing with a sample of this size, a useful way to make sense of the results is to solely observe the distribution of the relative crack growth, that is, the difference between the final and initial crack length, independent of all other parameters. This provides a general idea of the expected behavior regardless of the other randomized parameters. This is shown by the histograms in figures 30 and 31. It can be seen that at location 1 over half of the cracks developing grow less than 0.1 mm over the course of 13 years. Location 3 shows different yet interesting results. There are two clusters of cases that could be classified into two regimes. The first regime is for $\Delta a$ cases comprised between 0 and 2.5 mm whereas the second regime is between 2.5 mm and 3.5 mm. The former regime describes the survival cases whereas the latter regime shows the tube failure cases.

Figures 32 and 33 show the scatter of $\Delta a$ results against the clearance of the closest support. For instance the growth at location 1 is plotted against the clearance of the CM support on the hot leg. Note that the H07FBS clearance is normally distributed with a mean of 0.22 mm as shown in figure 8. It is possible to see once again that for location 1 most cases are survival cases, whereas location 3 shows a large proportion of failure cases.

Figures 34 and 35 show similar $\Delta a$ results represented against the stresses at the current location. The two regimes are once again apparent, but there is a distinct trend showing the increased likelihood of crack growth and failure as the stresses are increased at the location. Once again location 3 appears to be critical, which is consistent with prior findings.

Thus far it is apparent that crack growth is not directly dependent of support clearance. That is, by looking at figures 33 and 34 higher clearances do not seem to result in a larger proportion of failure cases. However, high stresses at a particular location will directly result in an increased

proportion of unstable crack growth scenarios. Finally, location 3 is susceptible to high stresses that exceed 4 MPa for some cases with the current steam generator configuration, which may result in unstable crack growth.
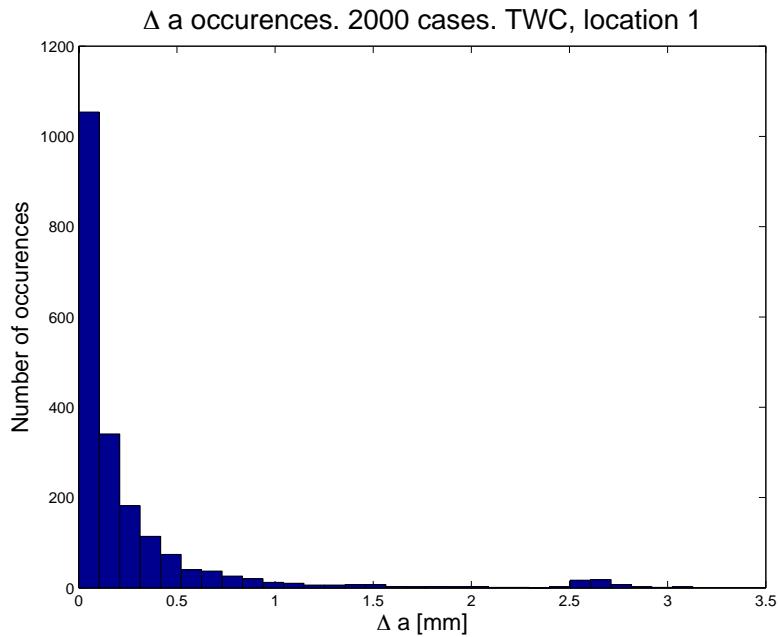


**Figure 30: Histogram showing crack growth occurrences for through wall cracks at location 1.**
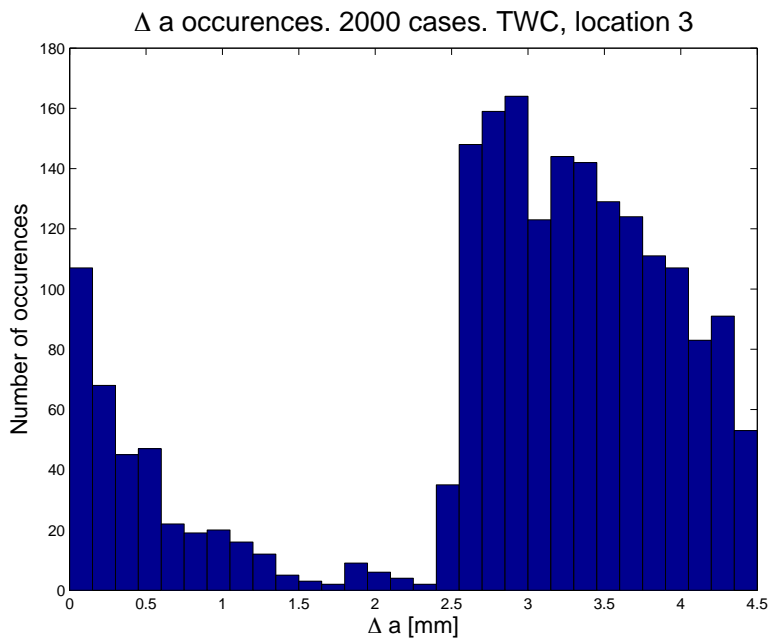


**Figure 31: Histogram showing crack growth occurrences for through wall cracks at location 3.**
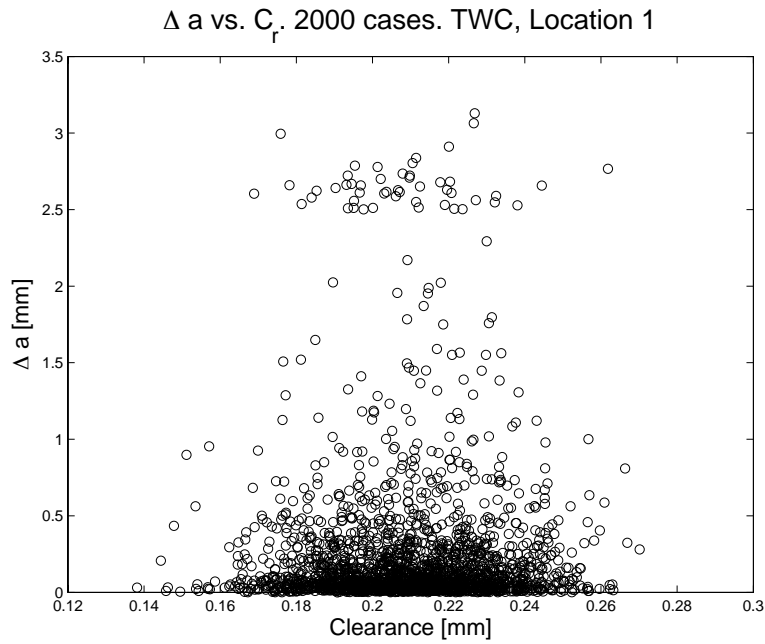
**Figure 32: Crack growth at location 1 *vs.* H07FBS support clearance.**
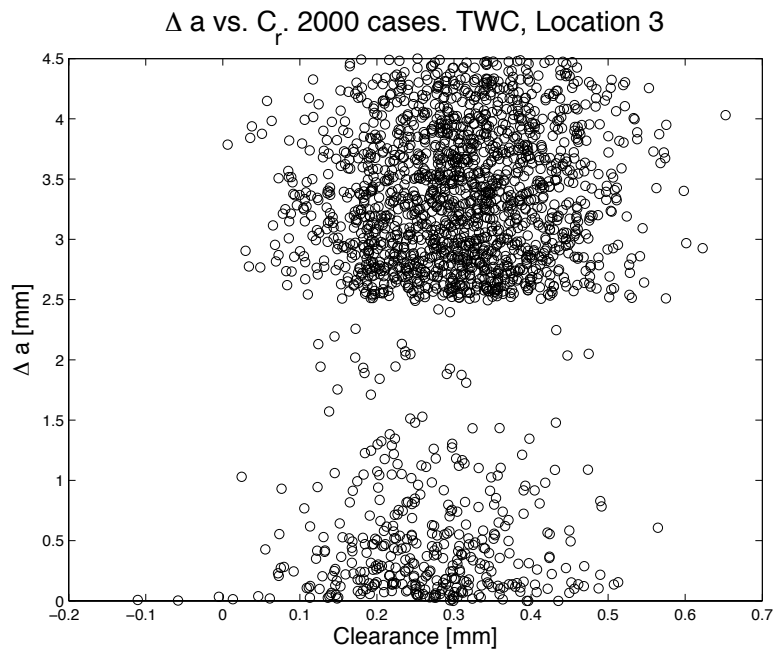


**Figure 33: Crack growth at location 3 *vs*. SB2 support clearance.**
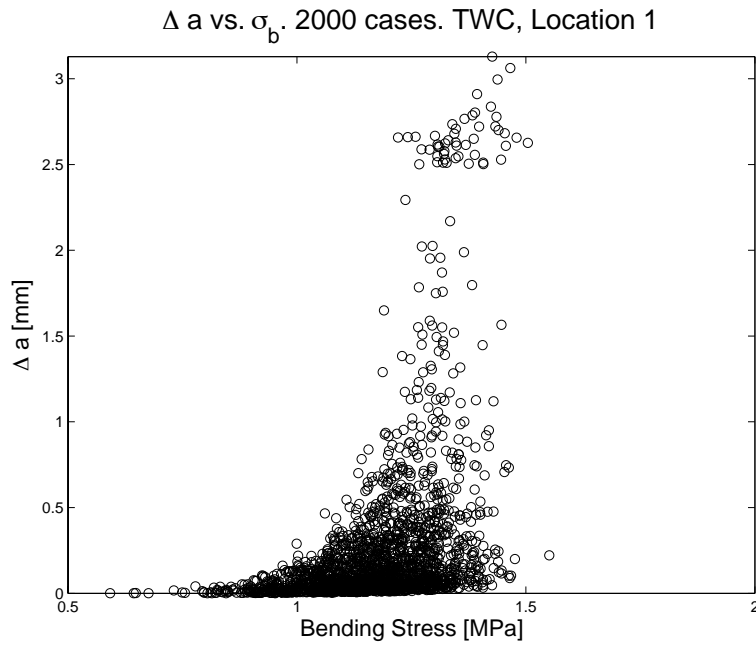
**Figure 34: Crack growth at location 1 *vs.* bending stress at location 1.**
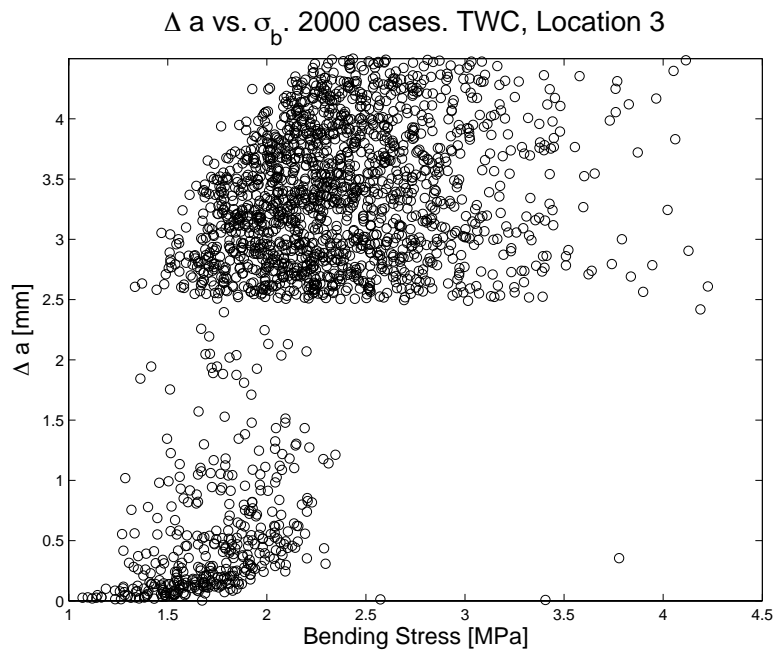


**Figure 35: Crack growth at location 3 *vs.* bending stress at location 3.**

### 4.2.5   Monte Carlo Simulations – Probabilistic Assessment of Tube Life

The results gathered thus far provide a valuable source of information regarding tube life. The latter is done by determining the proportion of initial crack length cases that may fail within various time limits. The results are summarized in figures 36 to 40. These figures exhibit some interesting features, such as the apparent symmetry between locations 1 and 5, and between locations 2 and 4. They show similar life characteristics.

In addition, it is possible to see that location 1 is rather safe, and for all initial cracks below 3.1 mm the probability of exceeding a tube life of 12 years is 100%. Location 2 shows that above 95% of all cracks below 2.2 mm will show a tube life of more than 12 years. This cannot be stated for cracks of 2.5 mm, which have an 80% chance of exceeding 12 years, 90% of exceeding 8 years, and 95% chance of exceeding 5 years. Cracks exceeding 3 mm for location 2 have a 35% chance of exceeding 12 years.

Location 3 does not appear to have a safe region, since only 90% of 1.6 mm initial size cracks may exceed a life of 3 years, and there is an 80% probability of exceeding a tube life of 5 years. These life predictions decrease to 20% and 10% respectively if the initial crack size exceeds 3 mm.

Probability of tube life exceeding thresholds. TWC, Location 1
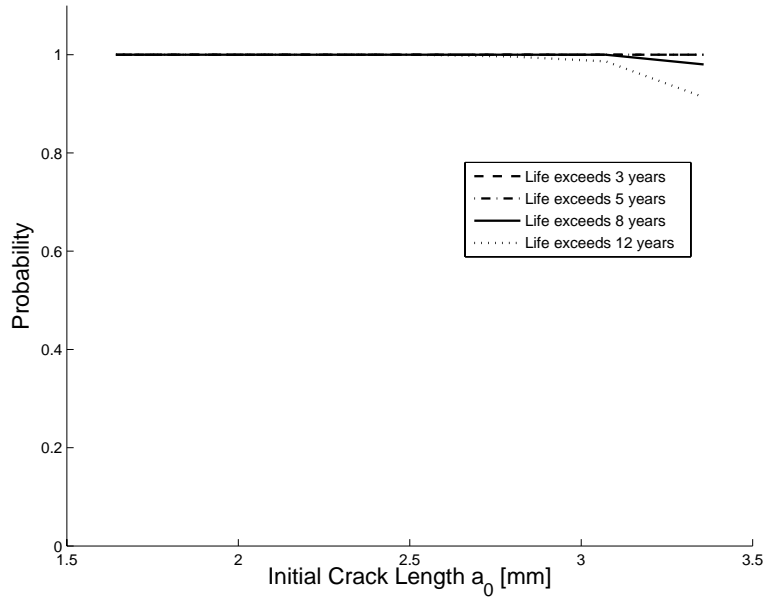


**Figure 36: Probability of unstable crack growth beyond various time limits at location 1.**

Probability of tube life exceeding thresholds. TWC, Location 2
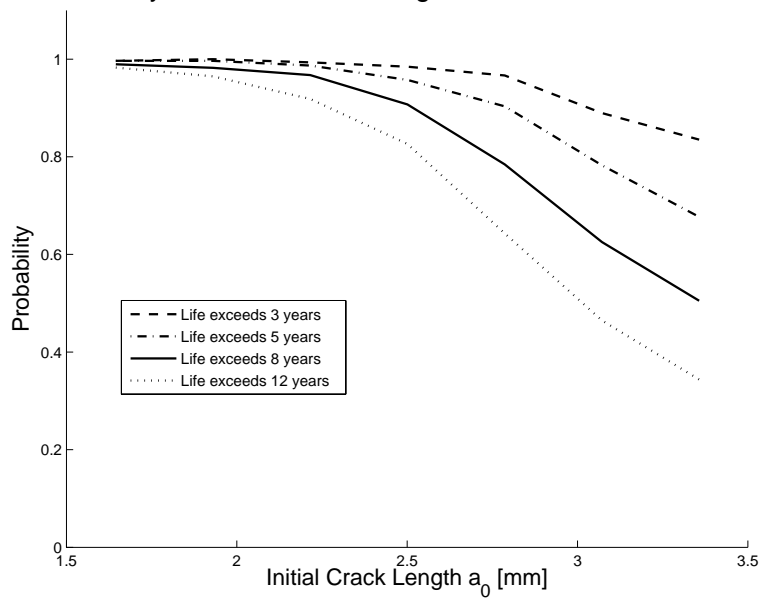


**Figure 37: Probability of unstable crack growth beyond various time limits at location 2.**

Probability of tube life exceeding thresholds. TWC, Location 3
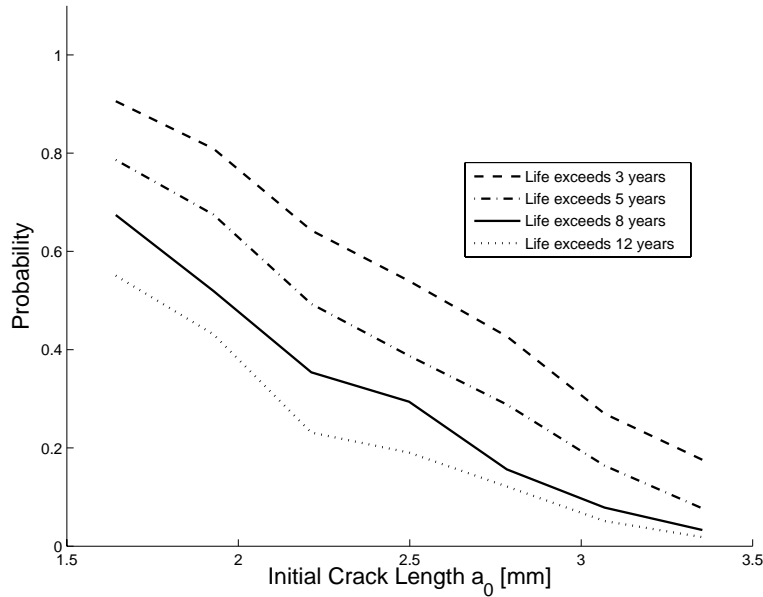


**Figure 38: Probability of unstable crack growth beyond various time limits at location 3.**

Probability of tube life exceeding thresholds. TWC, Location 4
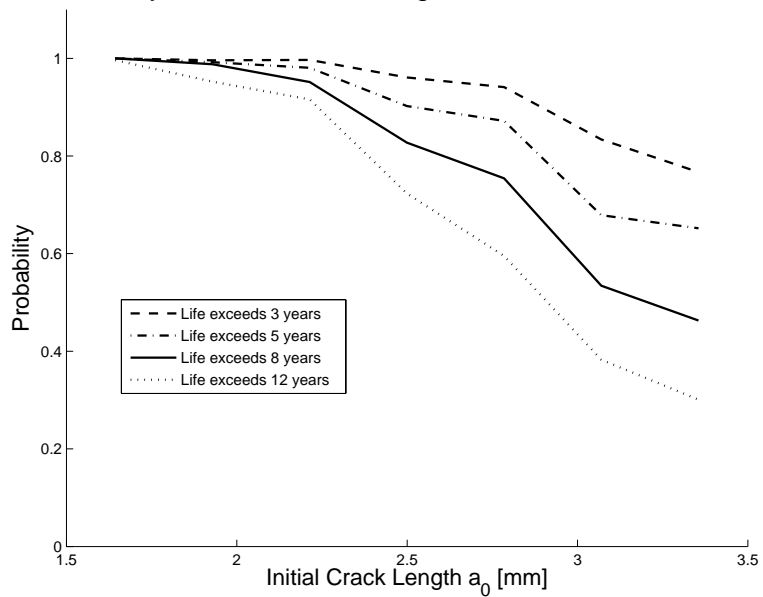


**Figure 39: Probability of unstable crack growth beyond various time limits at location 4.**

Probability of tube life exceeding thresholds. TWC, Location 5
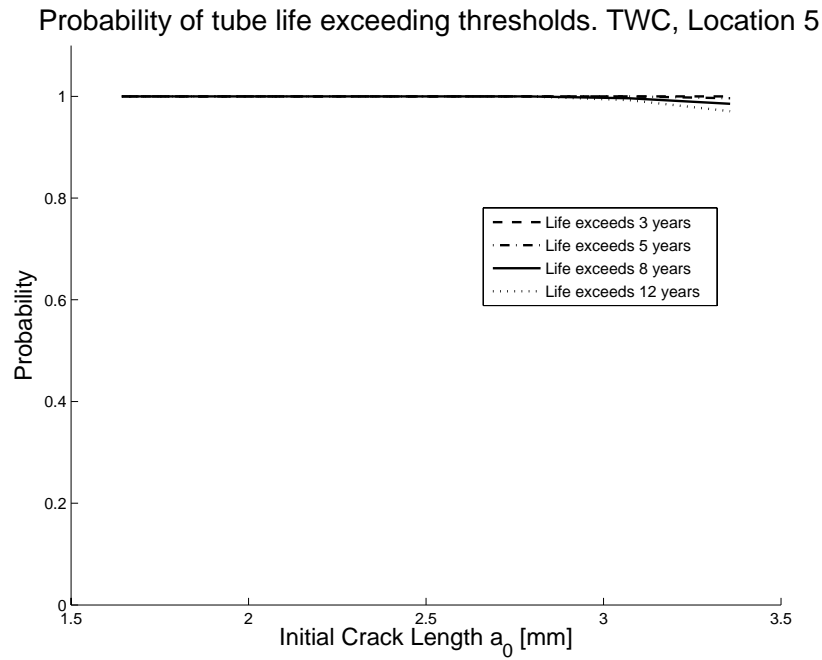


**Figure 40: Probability of unstable crack growth beyond various time limits at location 5.**

*4.2.6   Leakage Potential of Through Wall Cracks – Results:*

The leakage rates and leakage life is shown in figures 41 to 46 for 2000 cases as a function of a number of parameters, such as initial crack length and clearance at the nearest support. What is seen is that a number of leakage scenarios at location 3 show a very shortened life. Especially for cracks exceeding 2.5 mm. The clearance at the support does not seem to have as much effect as it did previously, except for the fact that we still observe two regimes.

Figure 41 shows the expected leakage life at location 1 as a function of the initial crack length. For cracks below 2.7 mm there are only a few cases where tube life is shortened.

Figure 42 shows similar results for location 3, the main difference is in the fact that at any initial crack length between 1.5 mm and 3.5 mm leakage rates may be significant.
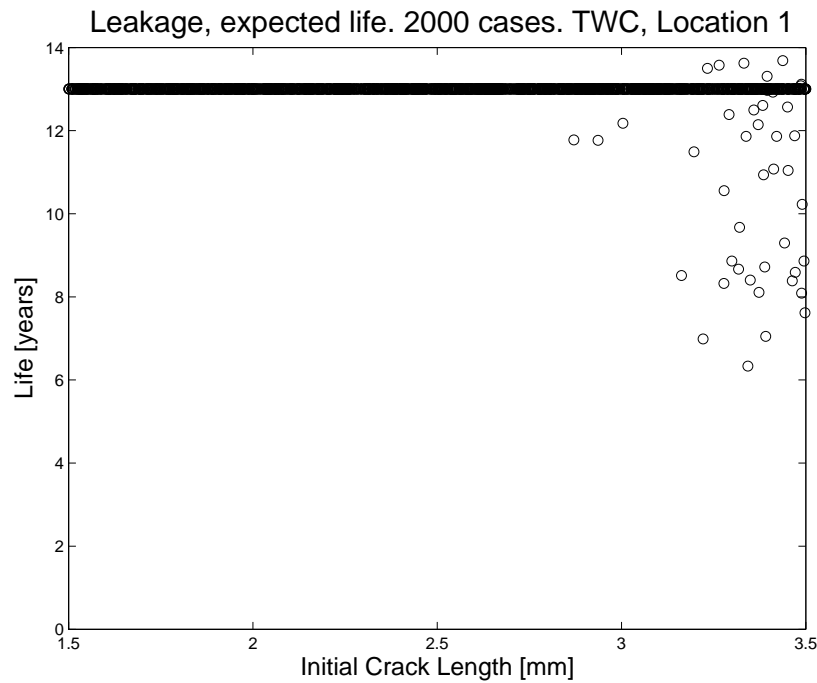
**Figure 41: Leakage life at location 1 *vs.* initial crack length.**
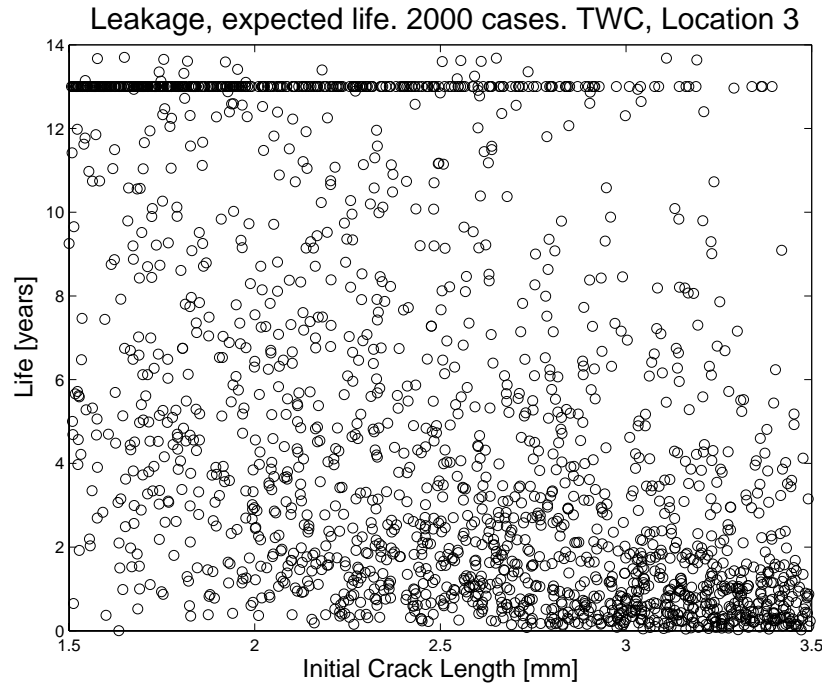


**Figure 42: Leakage life at location 3 *vs.* initial crack length.**
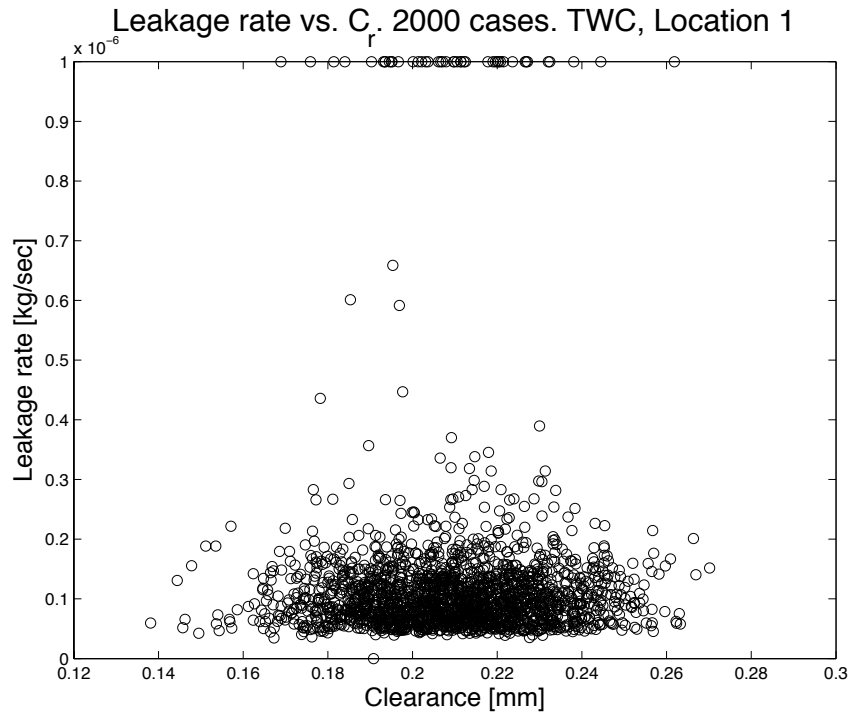
**Figure 43: Leakage rate at location 1 *vs.* clearance at H07FBS.**
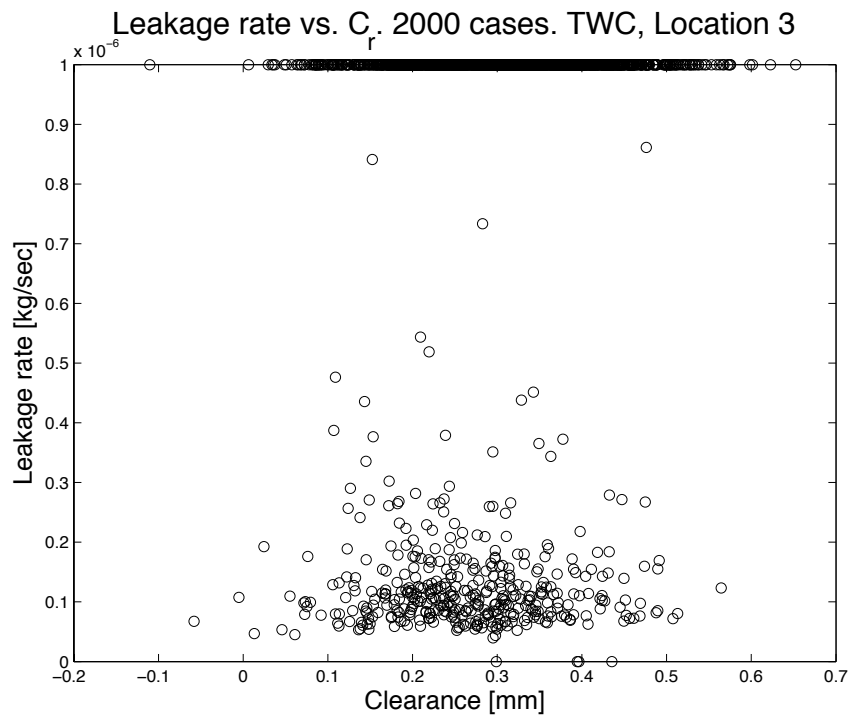


**Figure 44: Leakage rate at location 1 *vs.* clearance at SB2.**
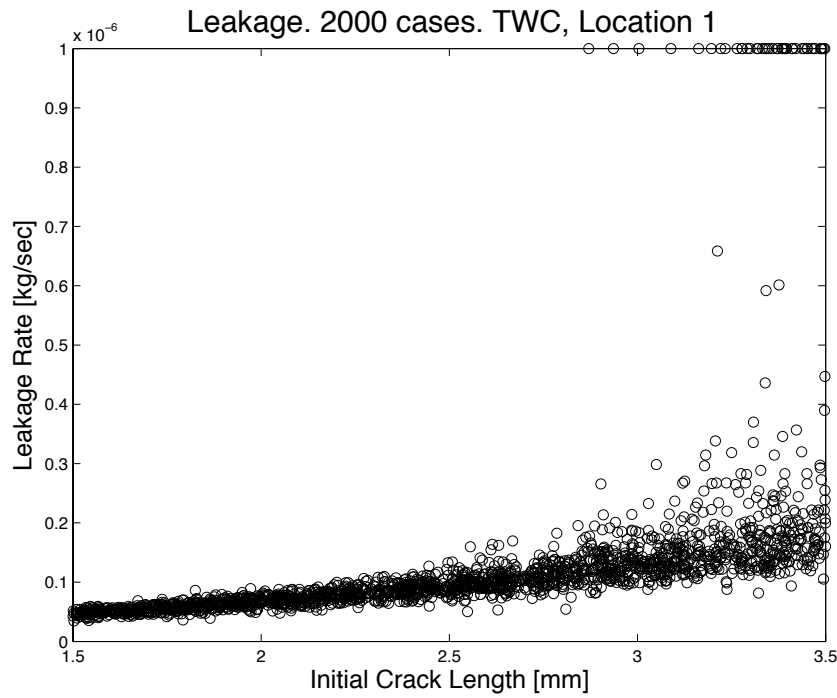
**Figure 45: Leakage rate at location 3 *vs.* initial crack length.**
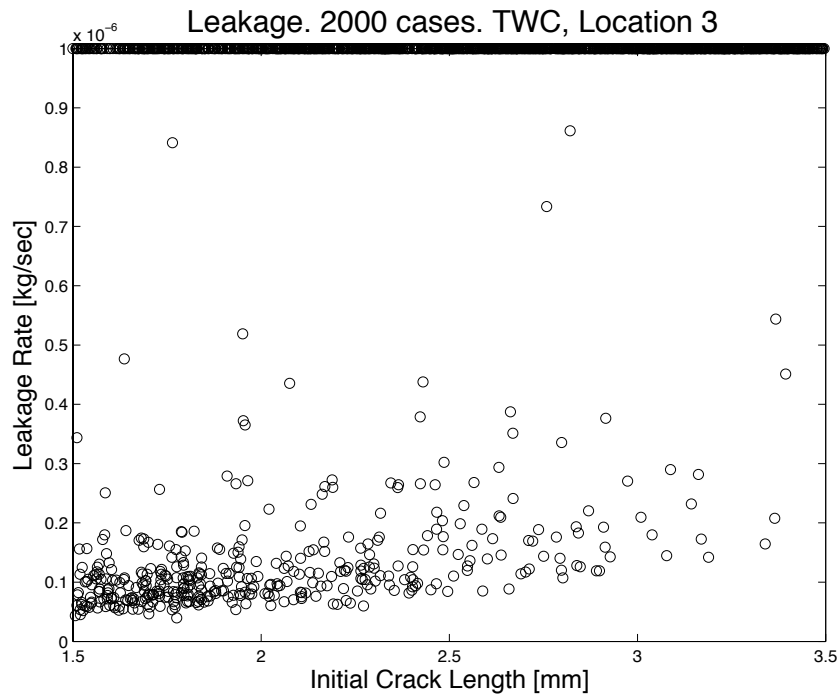


**Figure 46: Leakage rate at location 3 *vs.* initial crack length.**

*4.2.7   Monte Carlo Simulations – Evaluating the Probability of Leakage*

Figures 47 and 48 show the probability that the leakage rate would exceed thresholds of 0.1, 0.3, 0.5 and 0.8 mg/sec as a function of initial crack size. At location 1 the probability of the leakage rate reaching any appreciable value is below 5% until crack sizes reach 2.25 mm. After this point the likelihood that the crack at location rate will leak at a rate of at least 0.1 mg/sec almost linearly increases to 95 % at a crack size of 3 mm. The likelihood of leakage rate exceeding 0.3 mg/sec is negligible until crack sizes exceed 3 mm.

Probability of leakage rate exceeding thresholds. TWC, Location 1
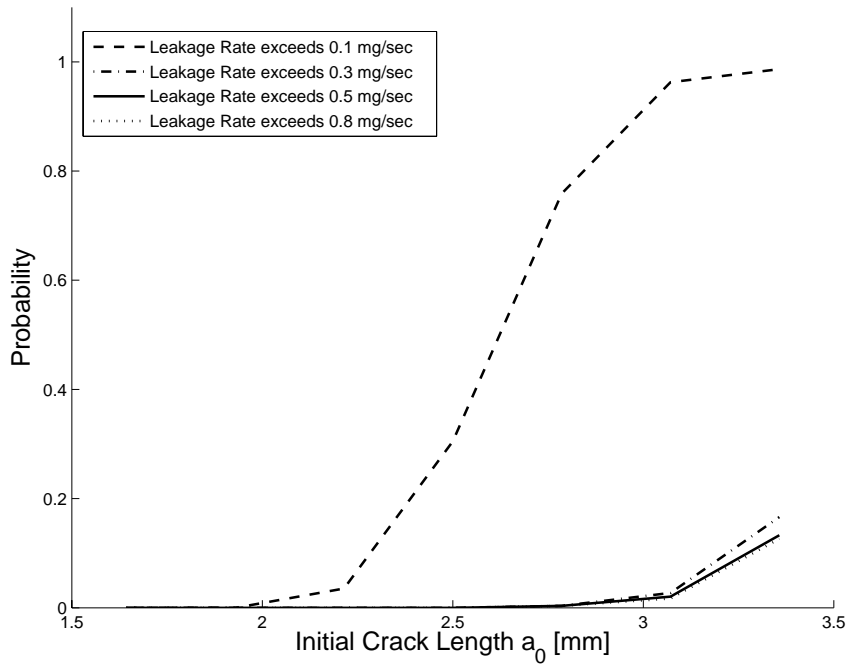


**Figure 47: Probability of leakage rates exceeding certain thresholds for a range of initial crack lengths at location 1**

Probability of leakage rate exceeding thresholds. TWC, Location 3
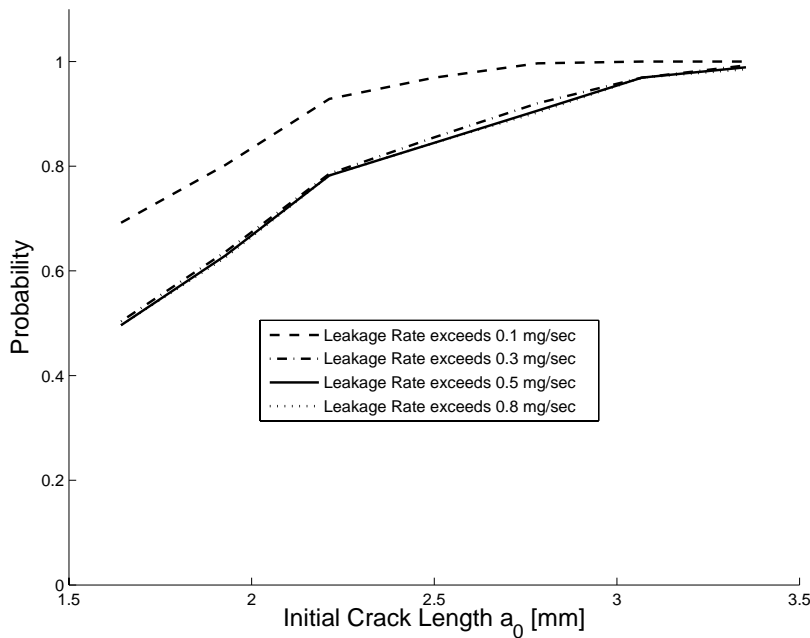


**Figure 48: Probability of leakage rates exceeding certain thresholds for a range of initial crack lengths at location 3**

# 5    Conclusion and Recommendations

This project investigated the integrity of U-bend steam generators. A deterministic and probabilistic assessment of the crack propagation and leakage rate potential was conducted for the steam generator at the Bruce Site Unit 8. Nonlinear finite element analysis is used to model the dynamics of the structure of the U-bend while accounting for the loose supports and friction and the support. The effects of turbulence and fluidelastic instability were assumed to be the principal sources of excitation in this study. The crack growth model employed is the one developed by Zahoor *et al.* The deterministic analysis provided valuable information regarding critical failure locations and critical support clearance thresholds whereas the probabilistic evaluation provided tube life due to crack propagation and leakage for actual clearance distributions.

In the deterministic analysis it was found that:
- Bending stresses are significantly high at the apex of the U-bend. It was also seen that stresses would increase at the U-bend if the support clearances increase; however, they are well below static and fatigue failure thresholds.
- SCC Cracks at location 3 are believed to be critical as they may experience an accelerated growth.
- For a base clearance below 0.3 mm the SCC crack size remained below any appreciable growth.
- For base clearances greater than 0.5 mm significant SCC crack propagation was observed. Higher base clearances may result in a very short tube lifespan, in some cases less than a year.
- Configuration 03b, where the SB support at the apex reaches high values while the other SB supports are held at base clearance values, is believed to be the most critical configuration for SCC cracks.
- TWC cracks will grow at an accelerated rate as well if located near location 3.
- To preserve tube life tube support clearances should be kept below 0.3 mm.

In the probabilistic assessment it was found that:
- SCC cracks did not prove to be critical and did not grow for nominal clearance distributions as well as distributions predicted to occur after a service life of 10 years.
- TWC cracks showed many cases that experienced unstable crack growth.
- Location 3 still proved to be critical with an appreciable number of unstable crack growth cases for cracks of any size.
- The probability of life exceeding various lifespan thresholds almost linearly decreases at location 3 with the initial crack size. For instance, the probability that the tube life will exceed 12 years for an initial crack size of 2 mm is 40%.
- Clearances below 0.2 mm will minimize the risk of unstable crack growth.
- Inspecting the extreme values of the response amplitude shows that for an average clearance of 0.3 mm the maximum tube amplitude is less that 2.0 mm in the hot leg in the span above H06.  The response in general is dominated by random components which resulting from turbulence and irregular impacts at the supports.  The region at the U-bend also represents an area of concern since the response amplitude is high.  However, the

maximum, detected response amplitude is less than 0.5 mm.  In any case, the required maximum tube amplitude to cause tube-to-tube impact is 3.9 mm with the assumption that the neighboring tube will reach the same peak at the same time at the opposite direction.  The probability of such event under the current simulation assumptions and support conditions is extremely low. Validating these assumptions would require further investigation utilizing the effect of in-flow fluidelastic instability and multiple tube simulations.

# 6 References

Axisa, F., Antunes, J. & Villard, B. "Overview of numerical methods for predicting flow-induced vibration. ASME Journal of Pressure Vessel Technology", 110, 6–14, 1988.

Downing, S.D., Socie, D.F., "Simple Rainflow Counting Algorithms", Int Jour Fatigue, 1982, 31-40

Green, S. J. and Hetsroni, G., 1995,"PWR Steam Generators", Int. J. Multiphase Flow Vol. 21, Suppl. pp. 1-97.

Hassan, M., and Hayder, M., "Modelling of fluidelastic vibrations of heat exchanger tubes with loose supports". Nuclear Engineering and Design, 238(10):2507 – 2520, 2008.

Hassan, M., and Hossen, A. "Time domain models for damping-controlled fluidelastic instability forces in tubes with loose supports", ASME Journal of Pressure Vessel Technology, 132(4):041302, 2010.

Hassan, M.A., and Rogers, R.J. "Friction modelling of preloaded tube contact dynamics. Nuclear Engineering and Design", 235:2349–2357, Dec. 2005.

Hassan M., Rogers, R.J., and Gerber, A.G. "Damping-controlled fluidelastic instability forces in multi-span tubes with loose supports", Nuclear Engineering and Design, 241(8):2666 – 2673, 2011.

Hassan, M., Weaver, D., and Dokainish, M. "A simulation of the turbulence response of heat exchanger tubes in lattice-bar supports", Journal of Fluids and Structures, 16(8):1145–1176, 2002.

Heppner, K., Laroche, S., and Pietralik, J.. "The Thirst Chemistry Module as a Tool To Determine Optimal Steam Generator Corrosion Control Strategies". In Proceedings of the 5th CNS International Steam Generator Conference, Toronto, Canada, November 2006. Canadian Nuclear Society.

Kozluk, M.J., "Near-Threshold Fatigue-Crack-Growth Rate Models for I600/I800", Ontario Hydro Nuclear, Engineering Analysis Department Technical Brief EMCD/TB-FM-03.0; Revision 1; July, 1998

Oengoren A., and Ziada, S., "An in-Depth Study of Vortex Shedding, Acoustic Resonance and Turbulent Forces in Normal Triangle Tube Arrays". Journal of Fluids and Structures, 12:717–758, 1998.

Ogundele, G.I., Lepik, O., Manolescu, A.V., Wright, M., Pagan, S., Mirzai, M., and Maruska, C. "The Cracking of Alloy 600 in Simulated BNGS "A" Crevice Environment", OHT Report 3167-010-1997-RA-0001-R00/COG Report COG-98-123 draft; September 30, 1998

Paris, P.C., and Tada, H. "Application of fracture-proof design methods using tearing-instability theory to nuclear piping postulating circumferential through-wall cracks" (No. NUREG/CR-3464). Del Research Corp., St. Louis, MO (USA), 1983.

Revankar S. T. and  Riznic J. R., "Assessment of Steam Generator Tube Flaw Size and Leak Rate Models", Nuclear Plant Operations and Control, 167:157-168, 2009.

Rogers, R. & Pick, R. "Factors associated with support plate forces due to heat exchanger tube vibratory contact". Nuclear Engineering and Design 44, 247–253, 1977.

Sauvé, R. G., Morandin, G., and Savoia, D. "Probabilistic Methods for the Prediction of Damage in Process Equipment Tubes under Nonlinear Flow Induced Vibration", ASME PVP Conference on *Flow-Induced Vibration and Noise, 53-2*, 283-289, 1997**.**

Sauvé , R. & Teper, W.  "Impact simulation of process equipment tubes and support plates-a numerical algorithm". ASME Journal of Pressure Vessel Technology 109, 70–79, 1987.

Zahoor A., "Ductile Fracture Handbook", Electric Power Research Institute, Palo Alto, California 1989.

# **Appendix A**

Configuration 03a, Surface flaw crack growth for U-bend tube subjected to turbulence in addition to fluid-elastic instability excitation.
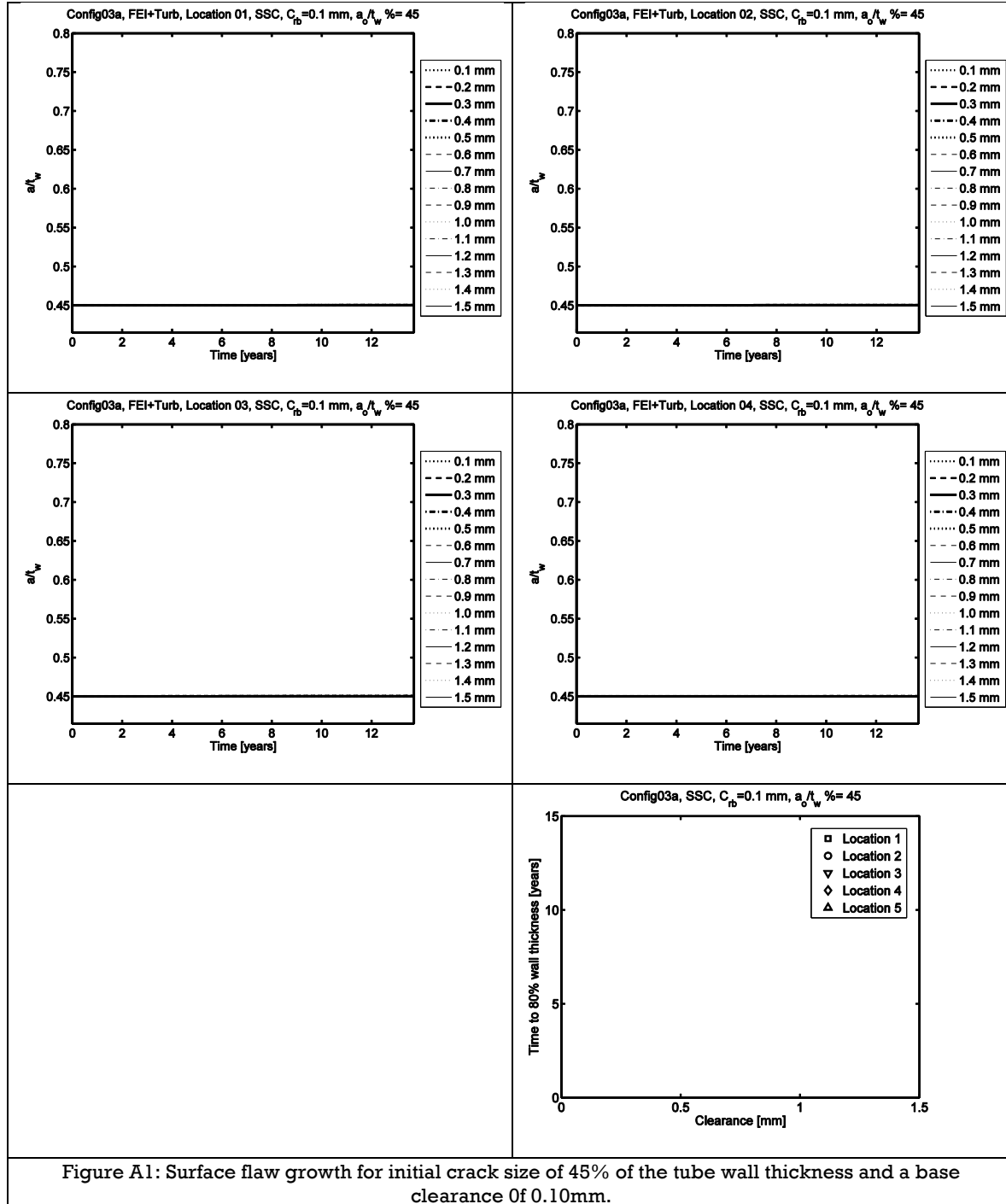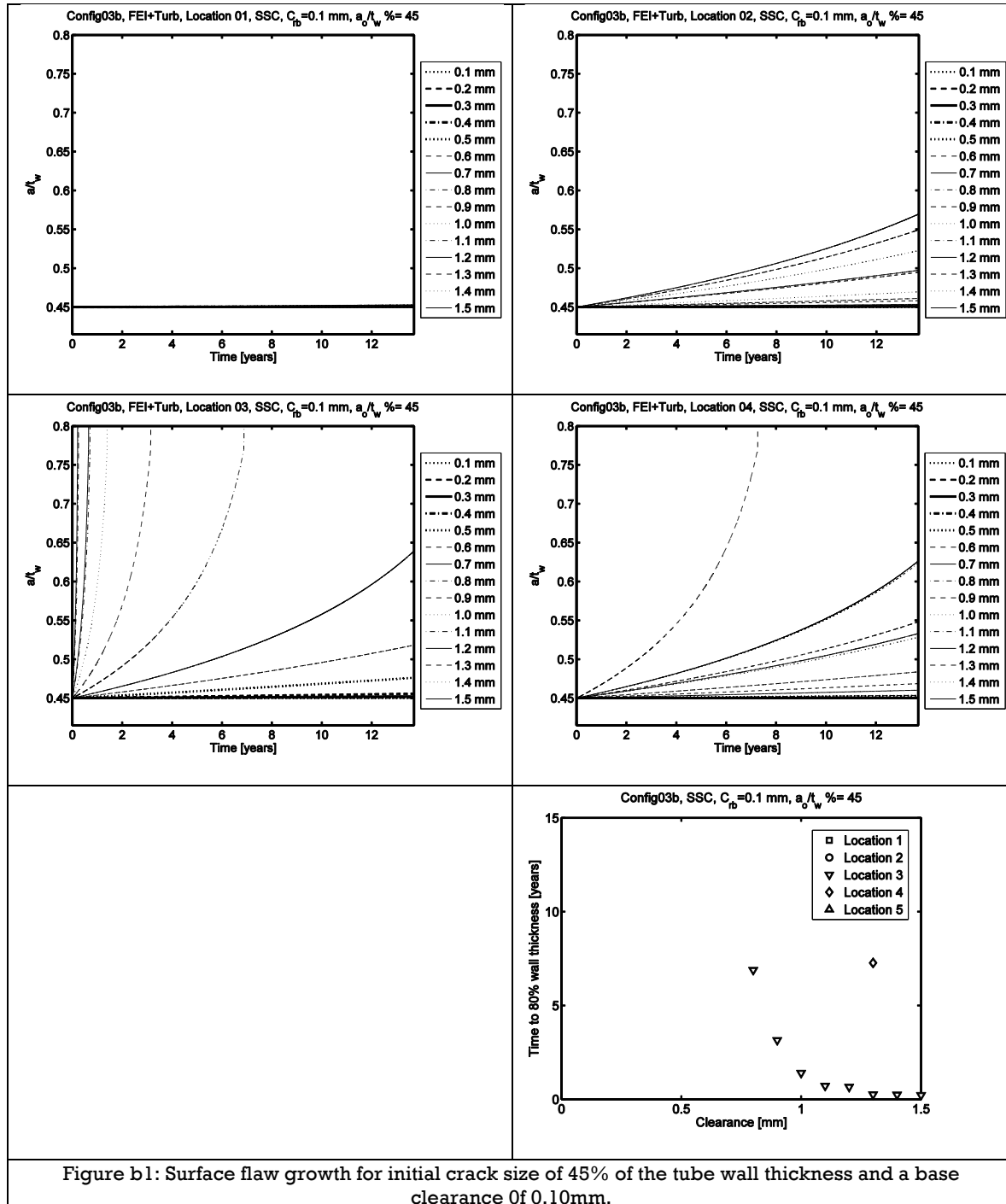


Figure A1: Surface flaw growth for initial crack size of 45% of the tube wall thickness and a base clearance 0f 0.10mm.
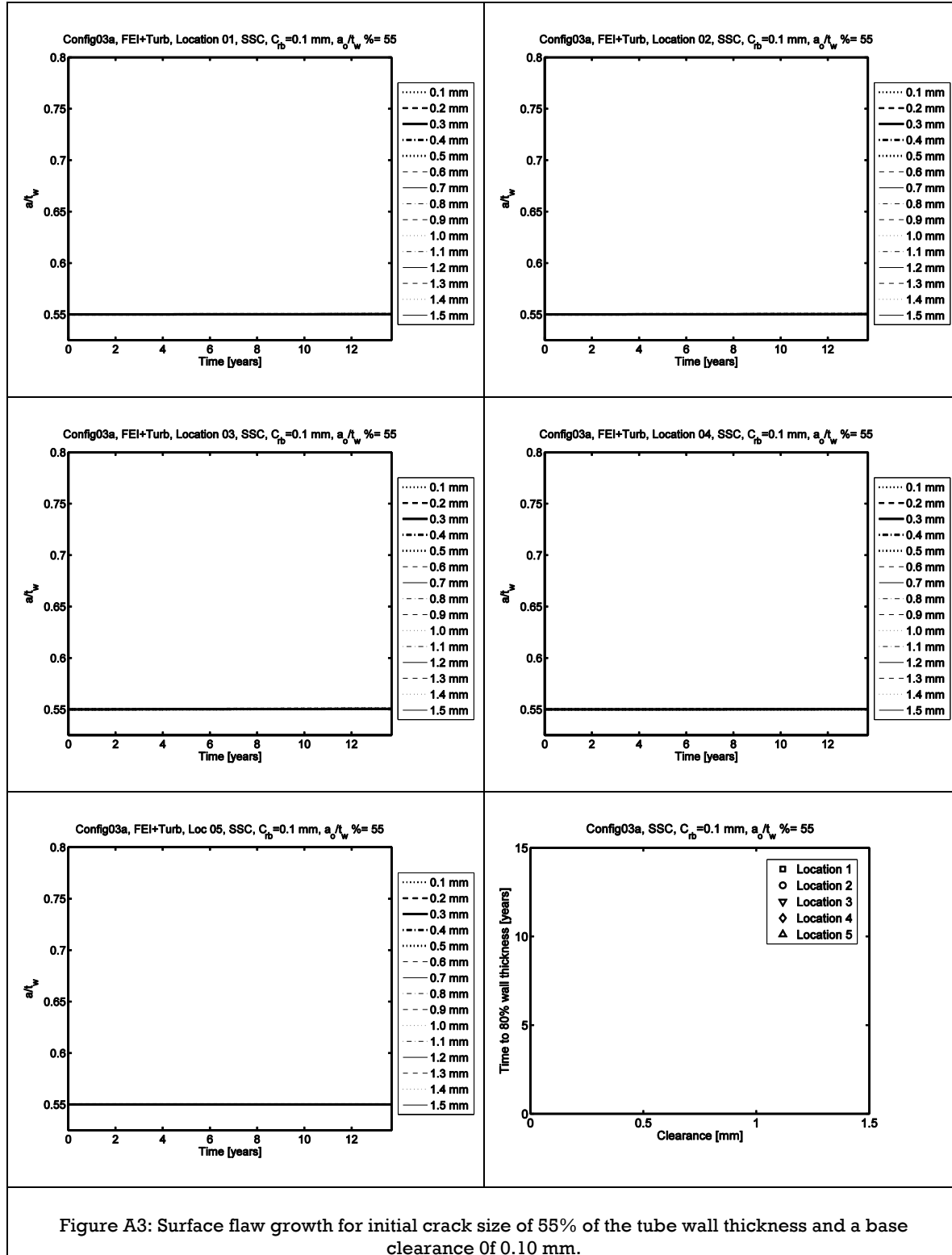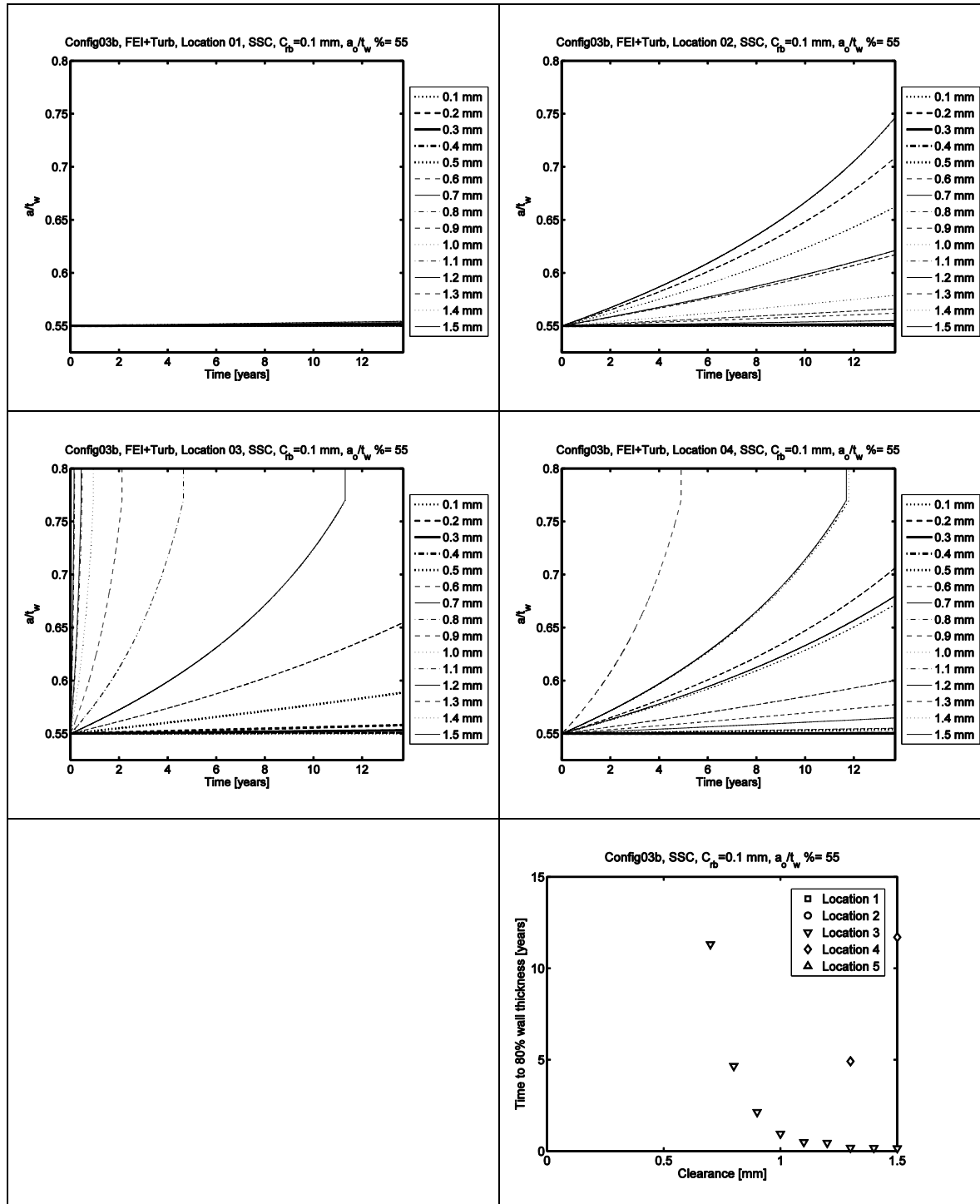
Figure A3: Surface flaw growth for initial crack size of 55% of the tube wall thickness and a base clearance 0f 0.10 mm.
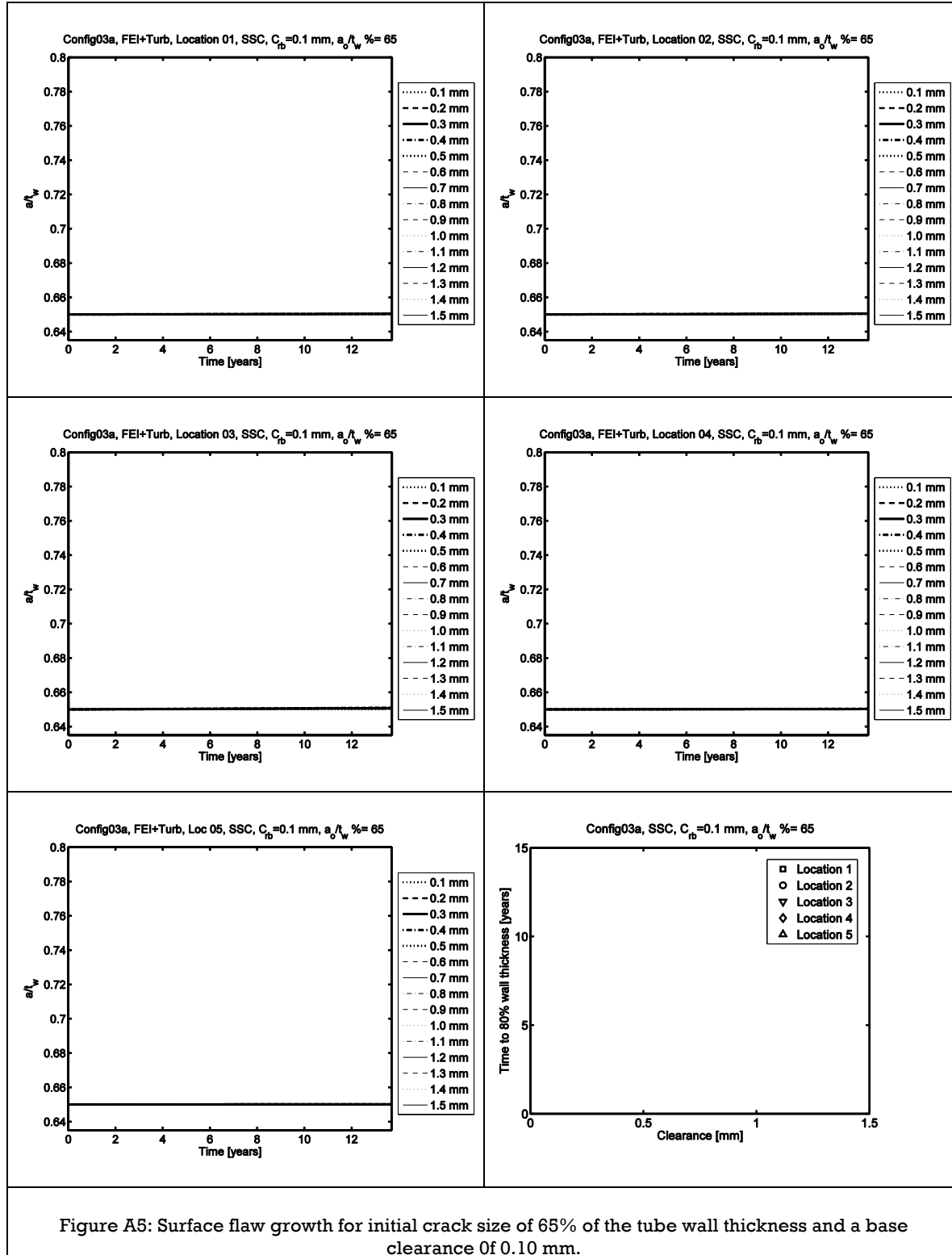
Figure A5: Surface flaw growth for initial crack size of 65% of the tube wall thickness and a base clearance 0f 0.10 mm.
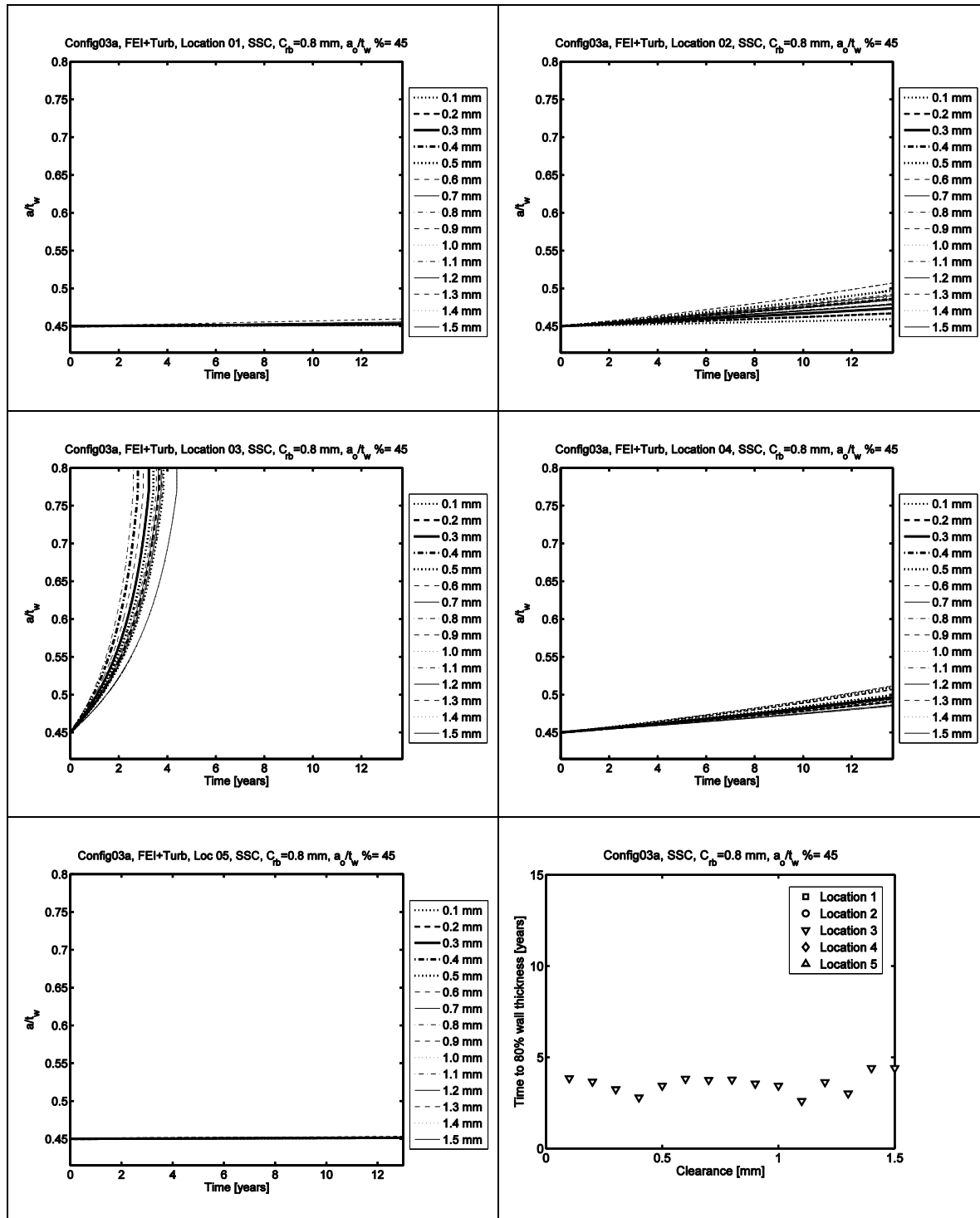
Figure A50: Surface flaw growth for initial crack size of 45% of the tube wall thickness and a base clearance 0f 0.80 mm.
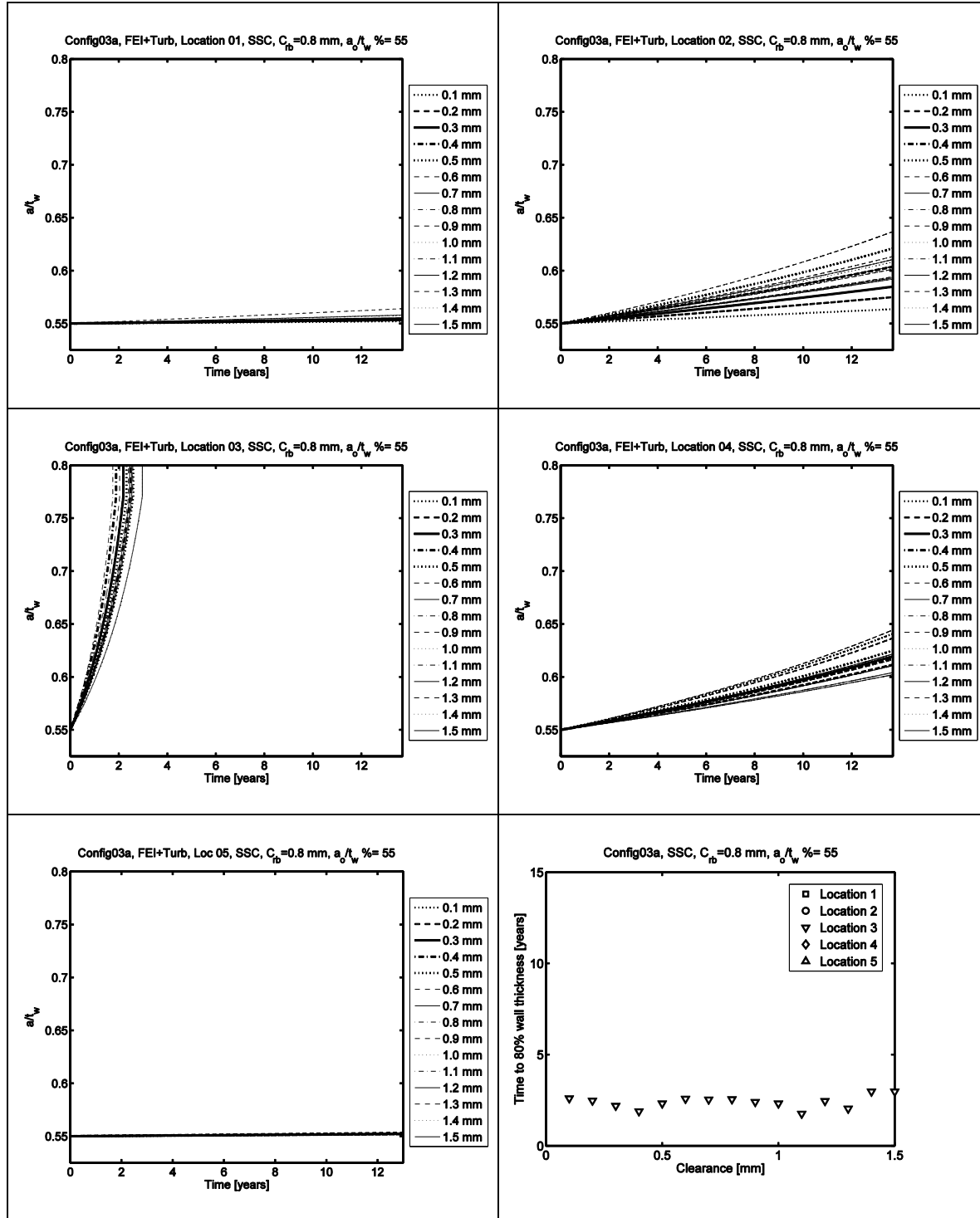
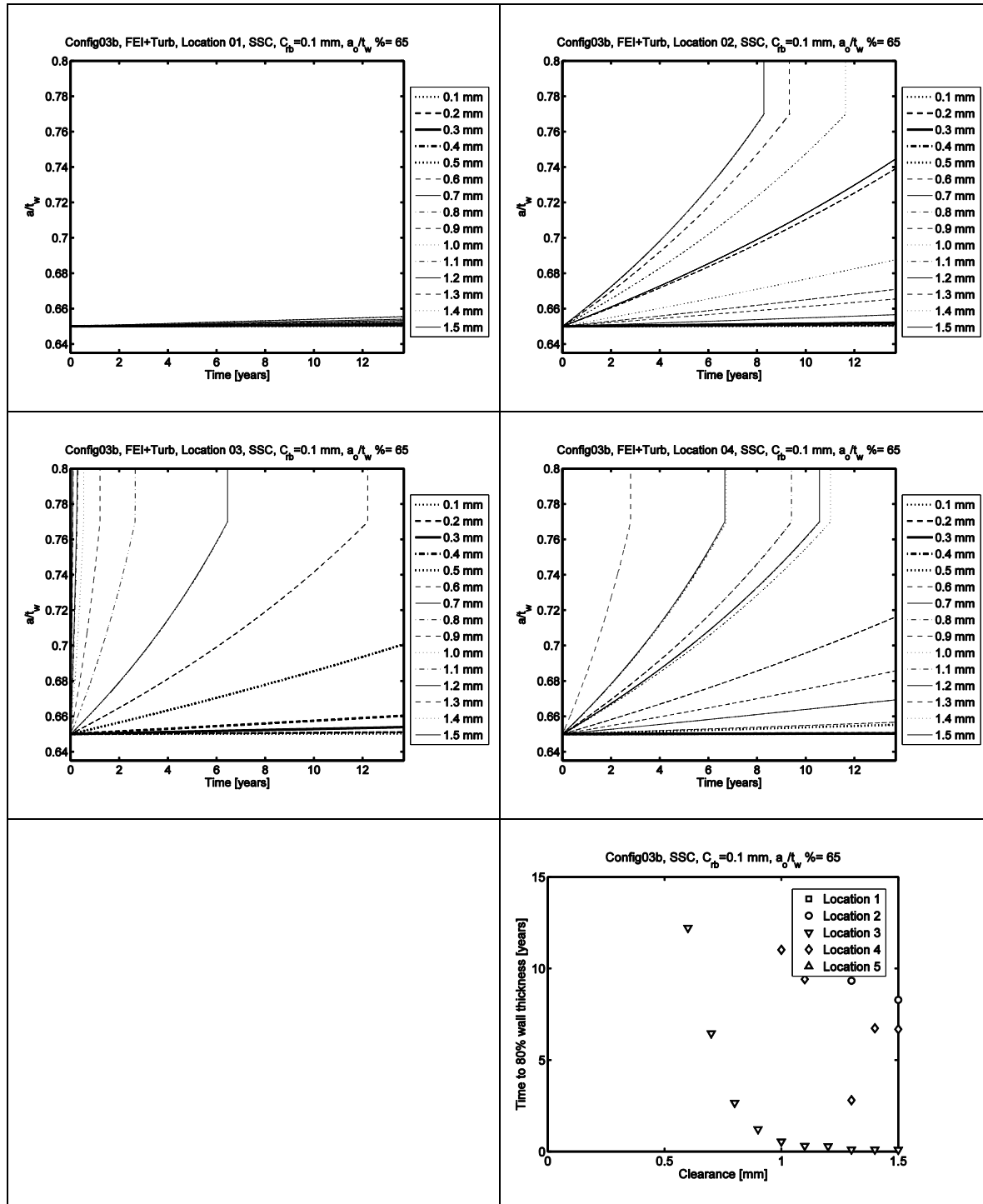Figure A52: Surface flaw growth for initial crack size of 55% of the tube wall thickness and a base clearance 0f 0.80 mm.
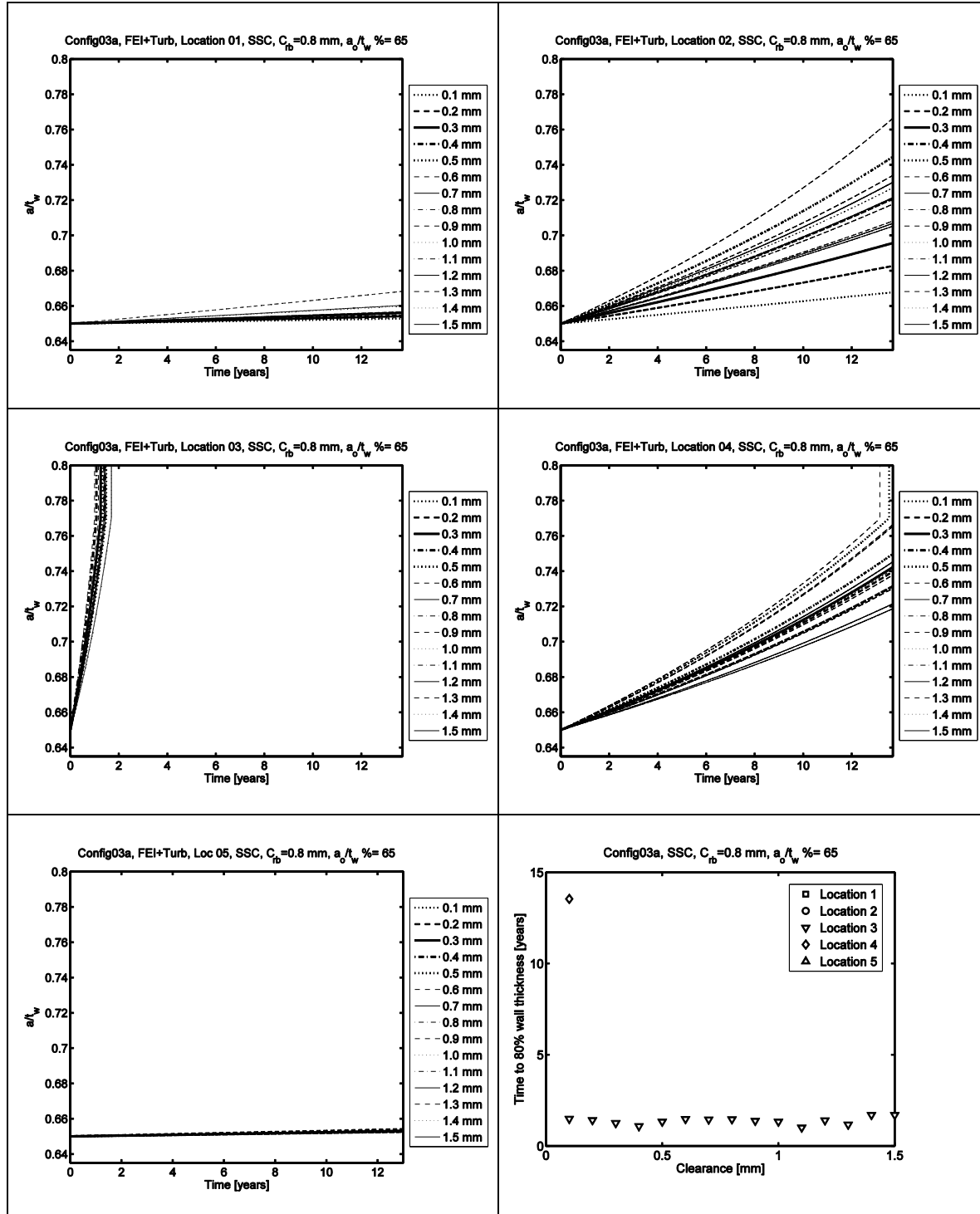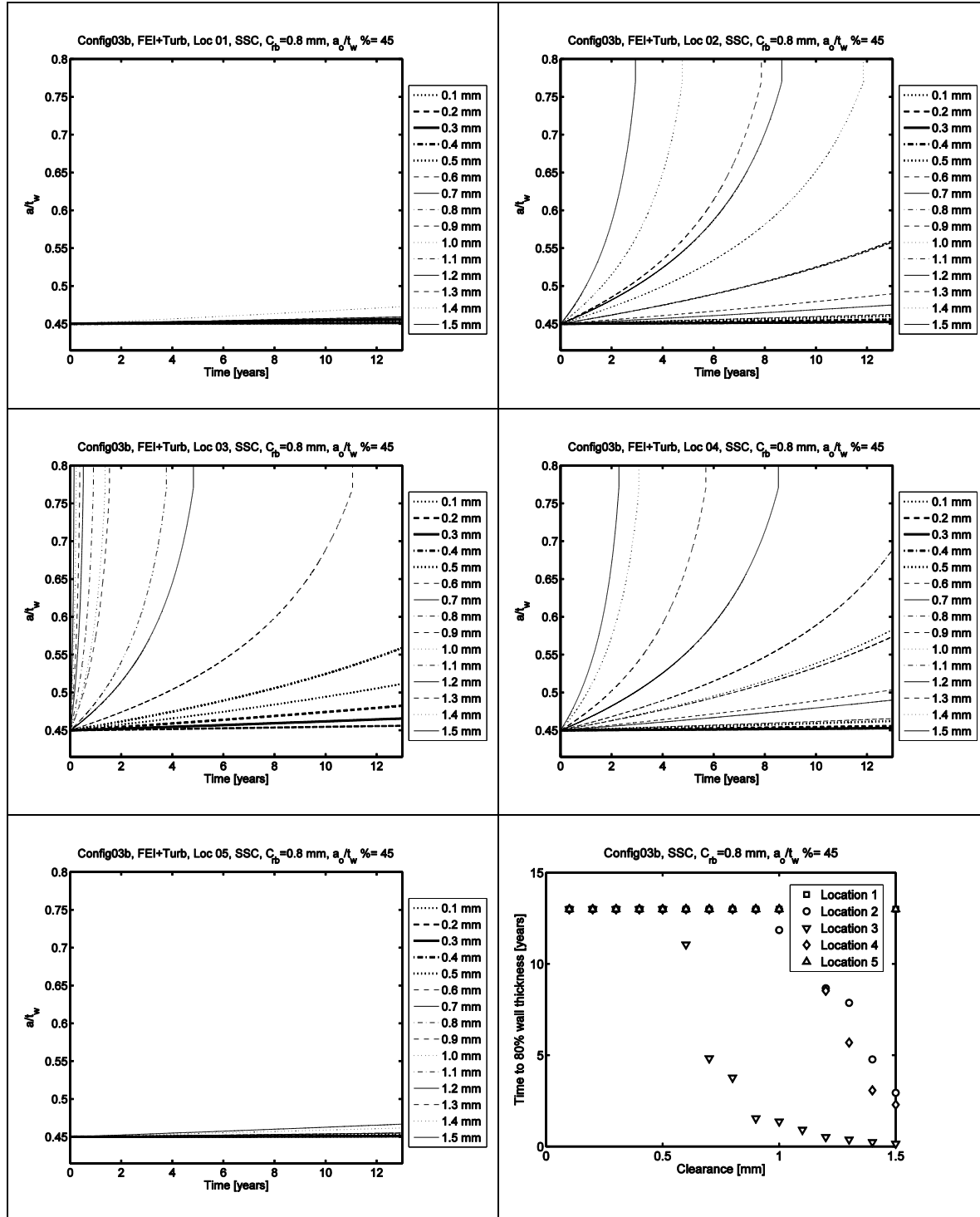
Figure A54: Surface flaw growth for initial crack size of 65% of the tube wall thickness and a base clearance 0f 0.80 mm.
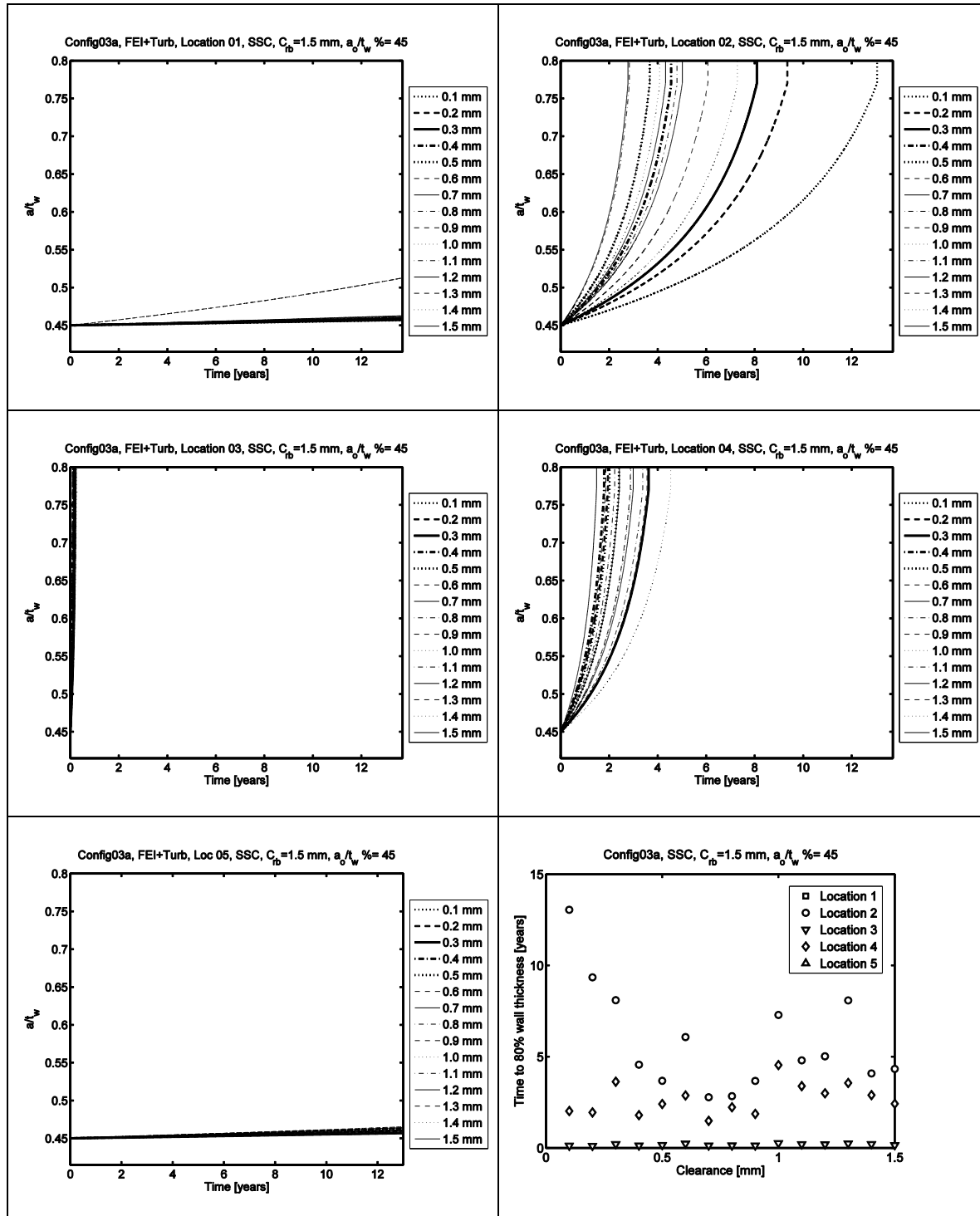
Figure A99: Surface flaw growth for initial crack size of 45% of the tube wall thickness and a base clearance 0f 1.50 mm.
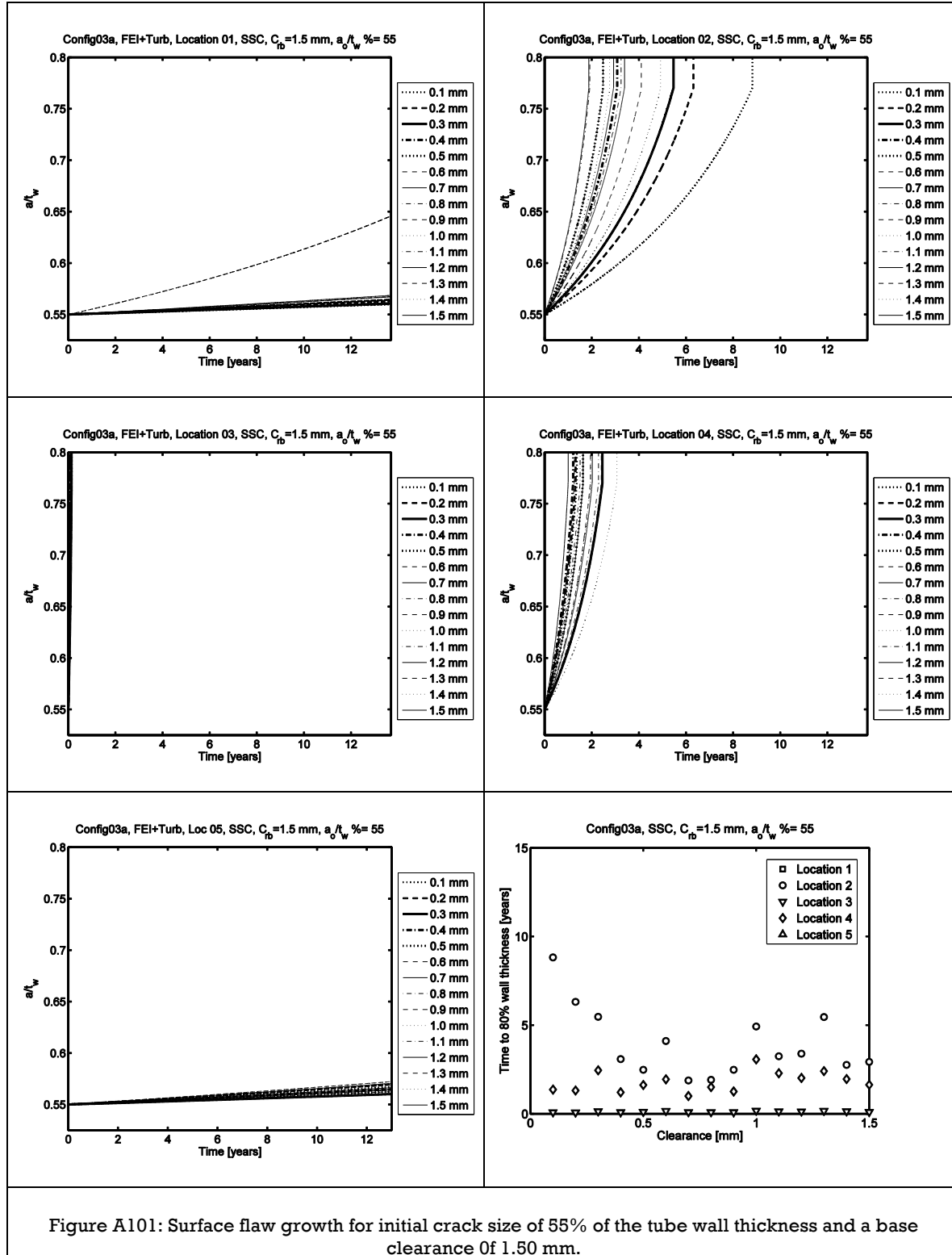
Figure A101: Surface flaw growth for initial crack size of 55% of the tube wall thickness and a base clearance 0f 1.50 mm.
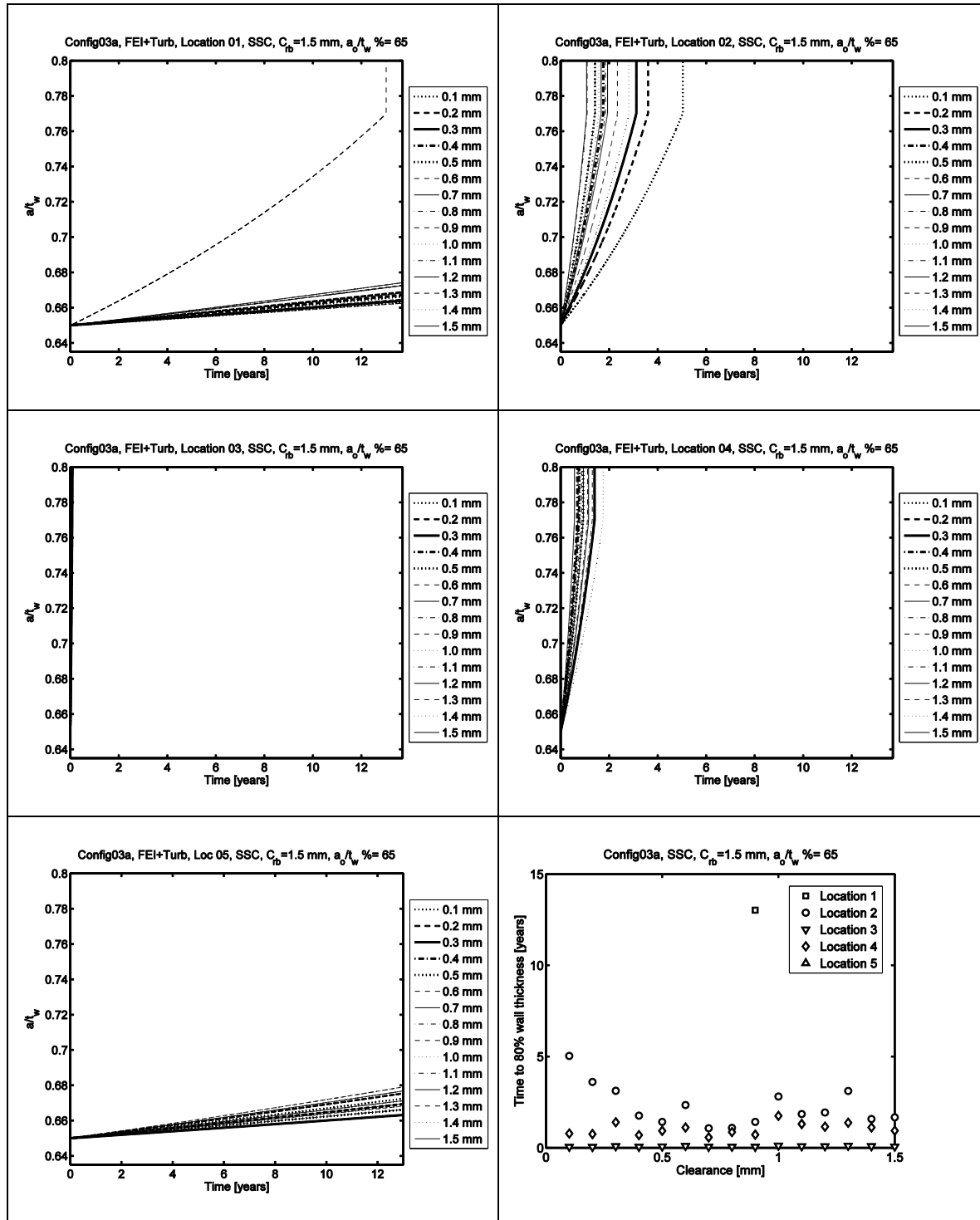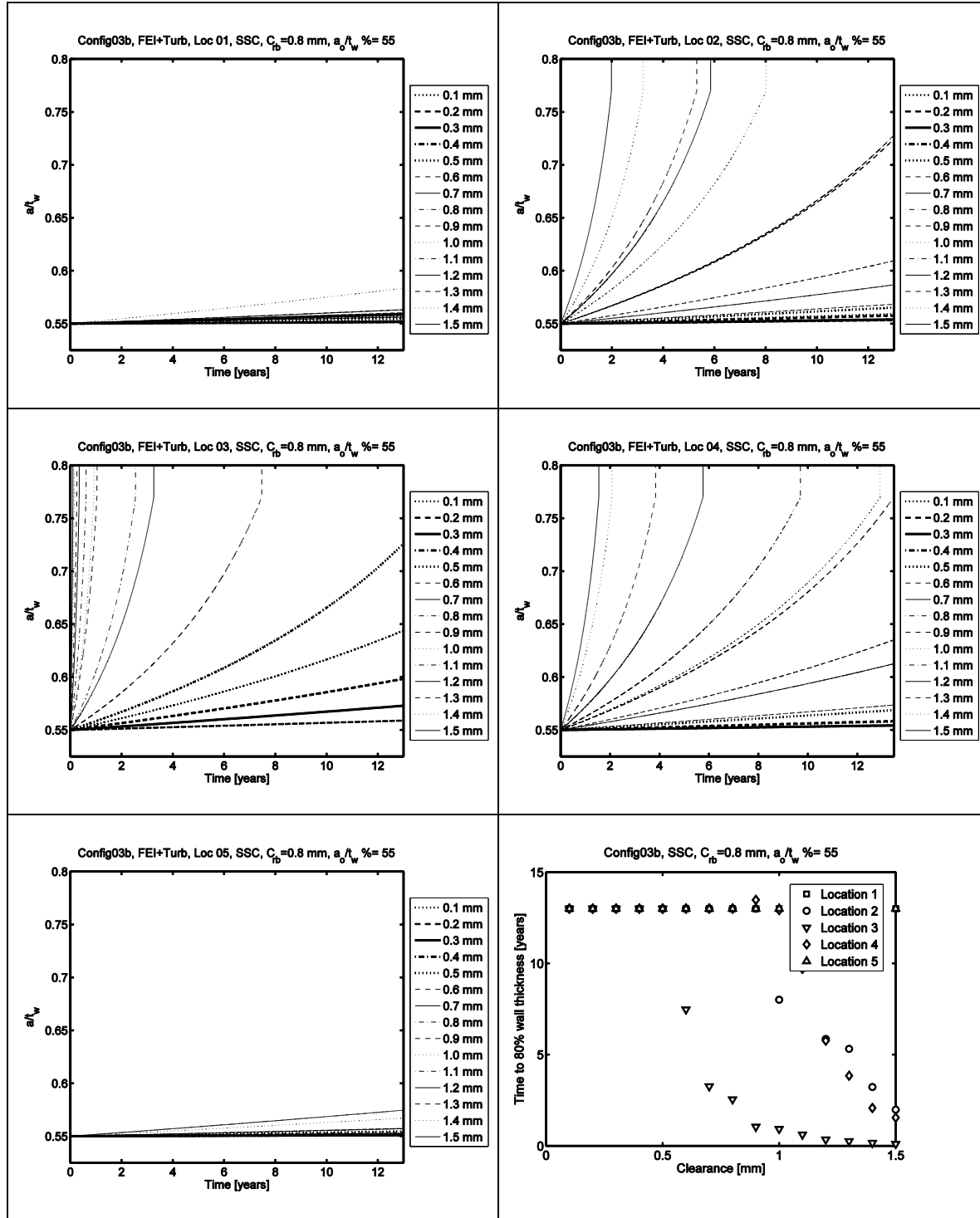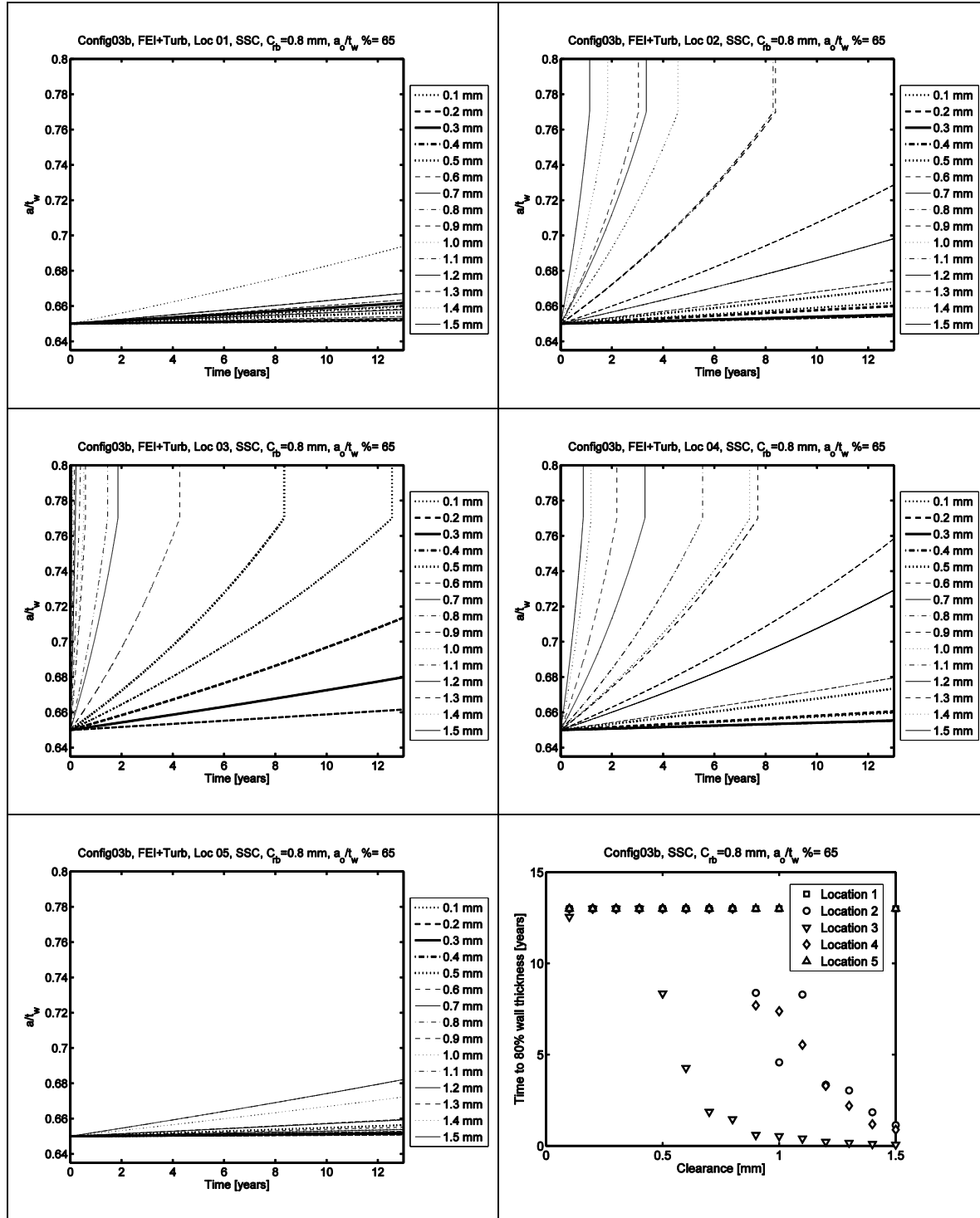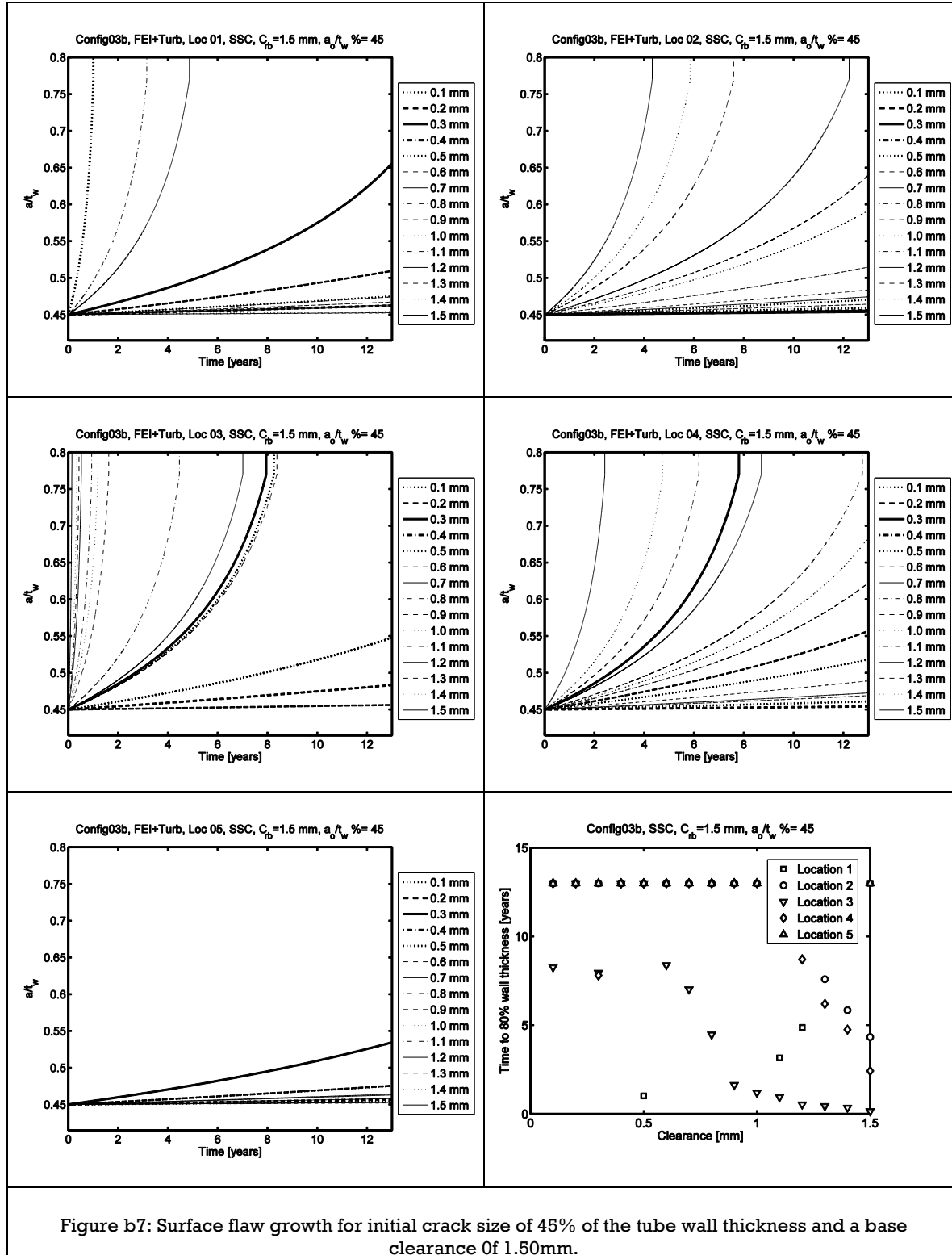
Figure A103: Surface flaw growth for initial crack size of 65% of the tube wall thickness and a base clearance 0f 1.50 mm.
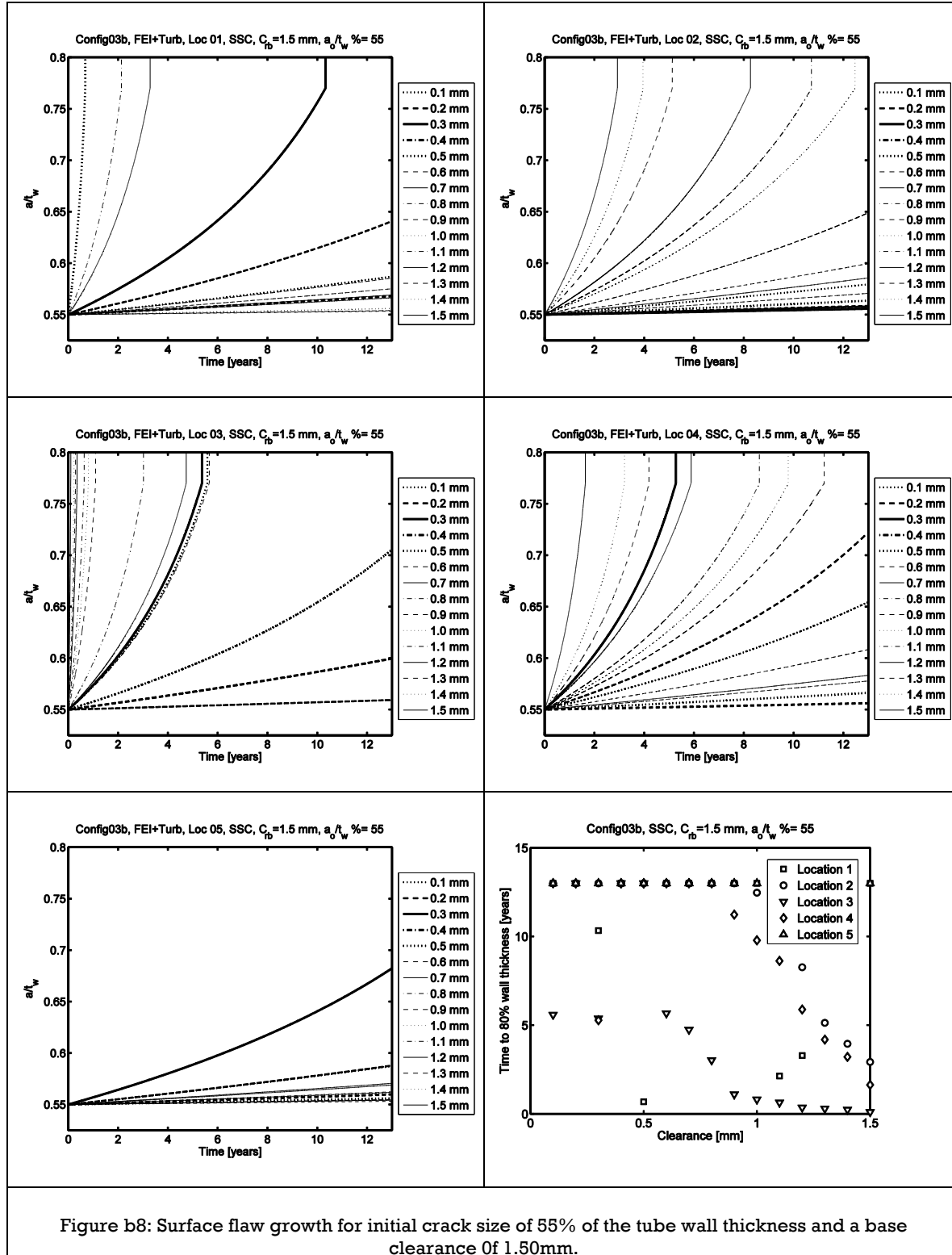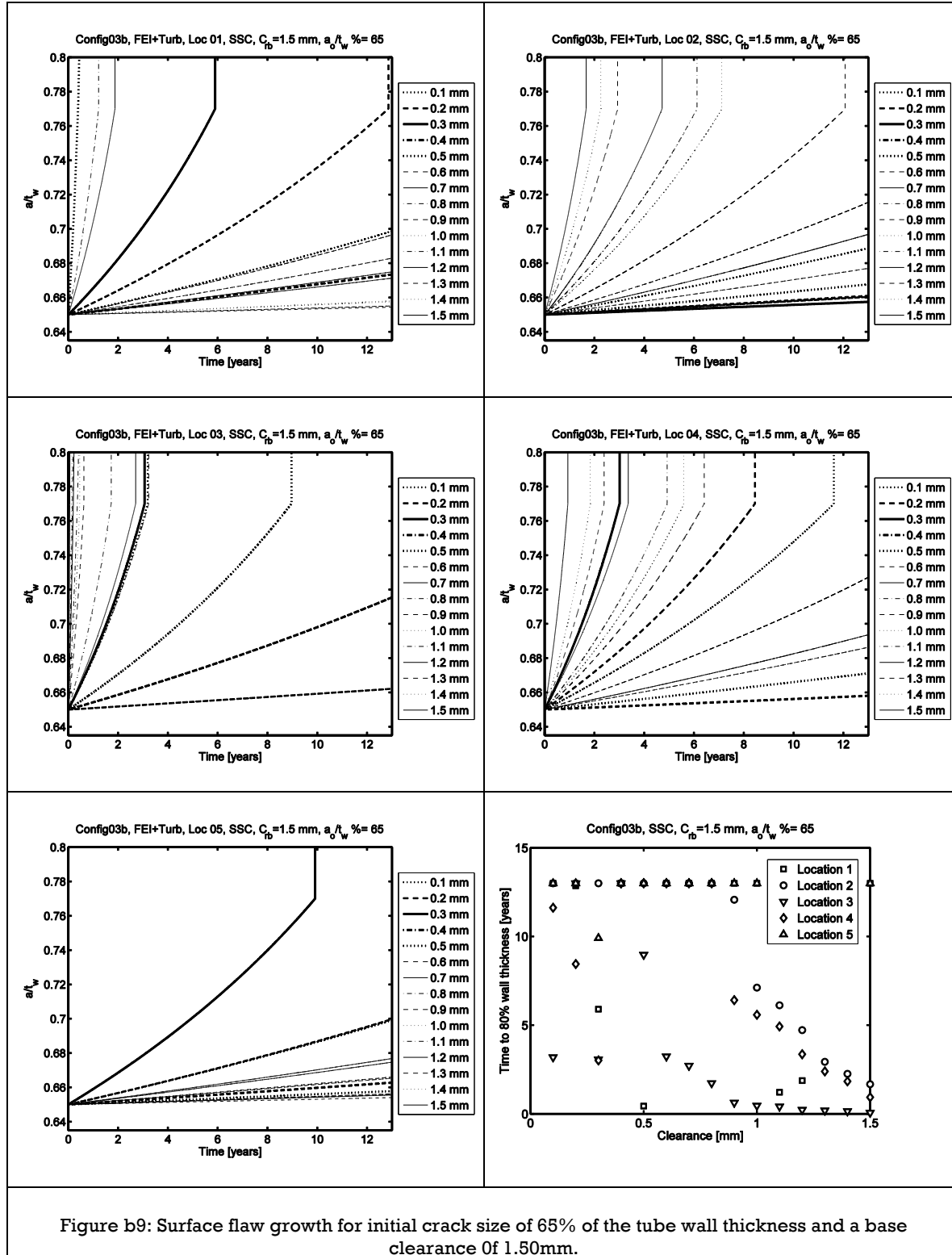
**Table a1: Config03a, SCC, 45%**

| Base Clearance | SB1 clearance | | | | |
|---|---|---|---|---|---|
| | Location 1 | Location 2 | Location 3 | Location 4 | Location 5 |
| 0.10 | - | - | - | - | - |
| 0.20 | - | - | - | - | - |
| 0.30 | - | - | - | - | - |
| 0.40 | - | - | - | - | - |
| 0.50 | - | - | - | - | - |
| 0.60 | - | - | 0.4 | - | - |
| 0.70 | - | - | 0.1 | - | - |
| 0.80 | - | - | 0.1 | - | - |
| 0.90 | - | - | 0.1 | - | - |
| 1.00 | - | - | 0.1 | 0.9 | - |
| 1.10 | - | 0.7 | 0.1 | 0.1 | - |
| 1.20 | - | 0.6 | 0.1 | 0.1 | - |
| 1.30 | - | 0.7 | 0.1 | 0.1 | - |
| 1.40 | - | 0.3 | 0.1 | 0.1 | - |
| 1.50 | - | 0.2 | 0.1 | 0.1 | - |

**Table a2: Config03a, SCC, 50%**

| Base Clearance | SB1 clearance | | | | |
|---|---|---|---|---|---|
| | Location 1 | Location 2 | Location 3 | Location 4 | Location 5 |
| 0.10 | - | - | - | - | - |
| 0.20 | - | - | - | - | - |
| 0.30 | - | - | - | - | - |
| 0.40 | - | - | - | - | - |
| 0.50 | - | - | - | - | - |
| 0.60 | - | - | 0.4 | - | - |
| 0.70 | - | - | 0.1 | - | - |
| 0.80 | - | - | 0.1 | - | - |
| 0.90 | - | - | 0.1 | - | - |
| 1.00 | - | 0.9 | 0.1 | 0.9 | - |
| 1.10 | - | 0.7 | 0.1 | 0.1 | - |
| 1.20 | - | 0.4 | 0.1 | 0.1 | - |
| 1.30 | - | 0.3 | 0.1 | 0.1 | - |
| 1.40 | - | 0.3 | 0.1 | 0.1 | - |
| 1.50 | - | 0.2 | 0.1 | 0.1 | - |

**Table a3: Config03a, SCC, 55%**

| Base Clearance | SB1 clearance | | | | |
|---|---|---|---|---|---|
| | Location 1 | Location 2 | Location 3 | Location 4 | Location 5 |
| 0.1 | - | - | - | - | - |
| 0.2 | - | - | - | - | - |
| 0.3 | - | - | - | - | - |
| 0.4 | - | - | - | - | - |
| 0.5 | - | - | - | - | - |
| 0.6 | - | - | 0.3 | - | - |
| 0.7 | - | - | 0.1 | - | - |
| 0.8 | - | - | 0.1 | - | - |
| 0.9 | - | - | 0.1 | - | - |
| 1 | - | 0.9 | 0.1 | 0.9 | - |
| 1.1 | - | 0.7 | 0.1 | 0.1 | - |
| 1.2 | - | 0.4 | 0.1 | 0.1 | - |
| 1.3 | 1.1 | 0.3 | 0.1 | 0.1 | - |
| 1.4 | 1.1 | 0.3 | 0.1 | 0.1 | - |
| 1.5 | - | 0.1 | 0.1 | 0.1 | - |

**Table a4: Config03a, SCC, 60%**

| Base Clearance | SB1 clearance | | | | |
|---|---|---|---|---|---|
| | Location 1 | Location 2 | Location 3 | Location 4 | Location 5 |
| 0.1 | - | - | - | - | - |
| 0.2 | - | | - | - | - |
| 0.3 | - | | - | - | - |
| 0.4 | - | - | - | - | - |
| 0.5 | - | | 0.5 | - | - |
| 0.6 | - | | 0.1 | - | - |
| 0.7 | - | - | 0.1 | - | - |
| 0.8 | - | - | 0.1 | - | - |
| 0.9 | - | 0.9 | 0.1 | 0.9 | - |
| 1 | - | 0.8 | 0.1 | 0.1 | - |
| 1.1 | 0.9 | 0.7 | 0.1 | 0.1 | - |
| 1.2 | - | 0.4 | 0.1 | 0.1 | - |
| 1.3 | 1.1 | 0.3 | 0.1 | 0.1 | - |
| 1.4 | 1.1 | 0.2 | 0.1 | 0.1 | - |
| 1.5 | - | 0.1 | 0.1 | 0.1 | - |

**Table a5: Config03a, SCC, 65%**

| Base Clearance | SB1 clearance | | | | |
|---|---|---|---|---|---|
| | Location 1 | Location 2 | Location 3 | Location 4 | Location 5 |
| 0.1 | - | - | - | - | - |
| 0.2 | - | - | - | - | - |
| 0.3 | - | - | - | - | - |
| 0.4 | - | - | - | - | - |
| 0.5 | - | - | 0.1 | - | - |
| 0.6 | - | - | 0.1 | - | - |
| 0.7 | - | - | 0.1 | - | - |
| 0.8 | - | - | 0.1 | - | - |
| 0.9 | - | 0.5 | 0.1 | 0.9 | - |
| 1 | - | 0.4 | 0.1 | 0.1 | - |
| 1.1 | 0.9 | 0.4 | 0.1 | 0.1 | - |
| 1.2 | - | 0.4 | 0.1 | 0.1 | - |
| 1.3 | 1.1 | 0.2 | 0.1 | 0.1 | - |
| 1.4 | 1.1 | 0.2 | 0.1 | 0.1 | - |
| 1.5 | - | 0.1 | 0.1 | 0.1 | - |

**Table a6: Config03a, SCC, 70%**

| Base Clearance | SB1 clearance | | | | |
|---|---|---|---|---|---|
| | Location 1 | Location 2 | Location 3 | Location 4 | Location 5 |
| 0.1 | - | - | - | - | - |
| 0.2 | - | - | - | - | - |
| 0.3 | - | - | - | - | - |
| 0.4 | - | - | - | - | - |
| 0.5 | - | - | 0.1 | - | - |
| 0.6 | - | - | 0.1 | - | - |
| 0.7 | - | - | 0.1 | 1.1 | - |
| 0.8 | - | 0.5 | 0.1 | 0.1 | - |
| 0.9 | 1.0 | 0.5 | 0.1 | 0.1 | - |
| 1 | - | 0.3 | 0.1 | 0.1 | - |
| 1.1 | 0.9 | 0.1 | 0.1 | 0.1 | - |
| 1.2 | - | 0.1 | 0.1 | 0.1 | - |
| 1.3 | 1.0 | 0.1 | 0.1 | 0.1 | - |
| 1.4 | 1.1 | 0.1 | 0.1 | 0.1 | - |
| 1.5 | 0.9 | 0.1 | 0.1 | 0.1 | - |

**Table a7: Config03a, SCC, 75%**

| Base Clearance | SB1 clearance | | | | |
|---|---|---|---|---|---|
| | Location 1 | Location 2 | Location 3 | Location 4 | Location 5 |
| 0.1 | - | - | - | - | - |
| 0.2 | - | - | - | - | - |
| 0.3 | - | - | 0.2 | - | - |
| 0.4 | - | - | 0.1 | - | - |
| 0.5 | - | 0.4 | 0.1 | - | - |
| 0.6 | - | 0.5 | 0.1 | 0.1 | - |
| 0.7 | - | 0.4 | 0.1 | 0.1 | - |
| 0.8 | - | 0.2 | 0.1 | 0.1 | - |
| 0.9 | 1 | 0.1 | 0.1 | 0.1 | - |
| 1 | 0.8 | 0.1 | 0.1 | 0.1 | - |
| 1.1 | 0.7 | 0.1 | 0.1 | 0.1 | - |
| 1.2 | - | 0.1 | 0.1 | 0.1 | - |
| 1.3 | 0.9 | 0.1 | 0.1 | 0.1 | - |
| 1.4 | 0.4 | 0.1 | 0.1 | 0.1 | 0.4 |
| 1.5 | 0.9 | 0.1 | 0.1 | 0.1 | 0.1 |

# Appendix B

Configuration 03b, Surface flaw crack growth for U-bend tube subjected to turbulence in addition to fluid-elastic instability excitation.



Figure b1: Surface flaw growth for initial crack size of 45% of the tube wall thickness and a base clearance 0f 0.10mm.

Figure b2: Surface flaw growth for initial crack size of 55% of the tube wall thickness and a base clearance 0f 0.10mm.
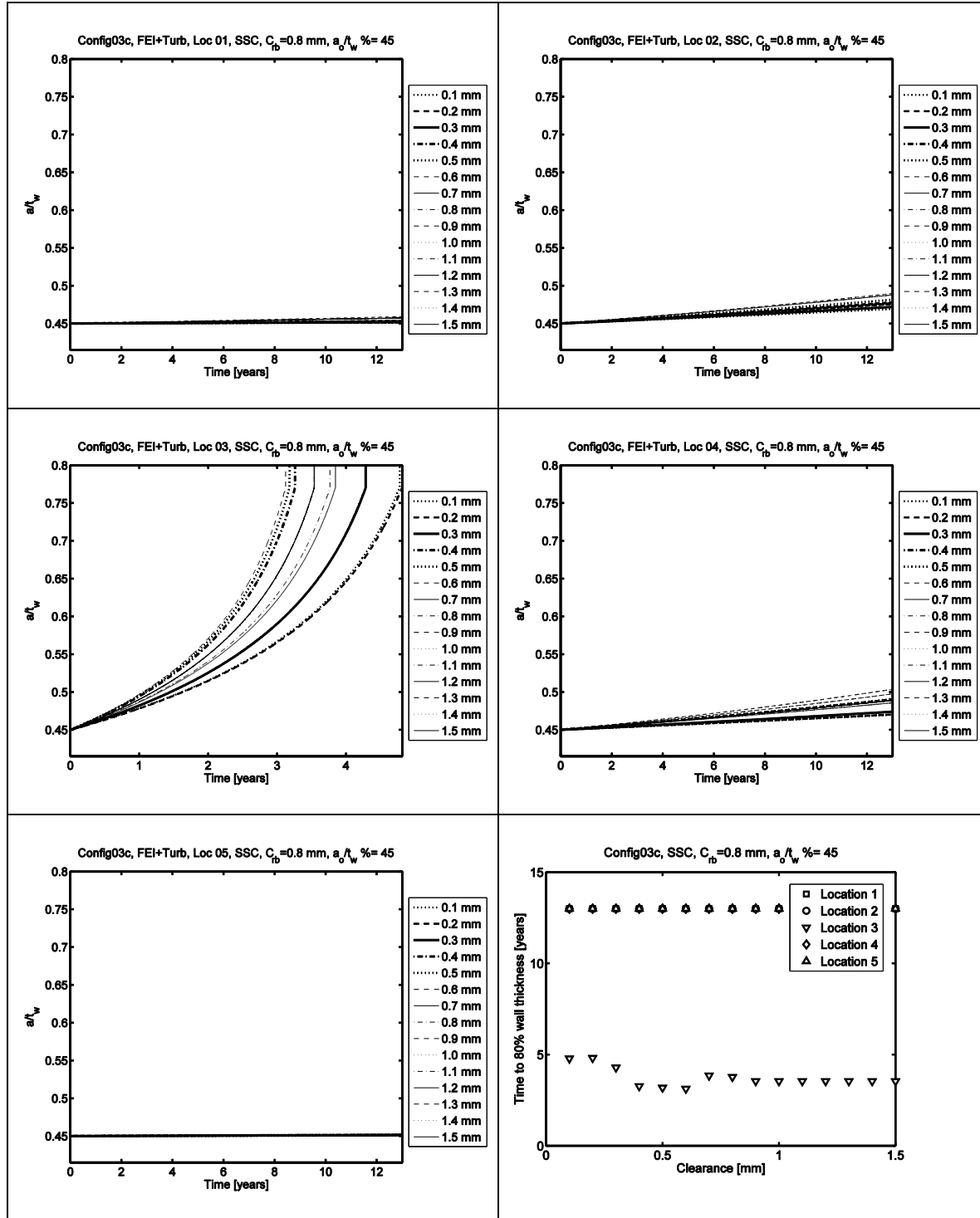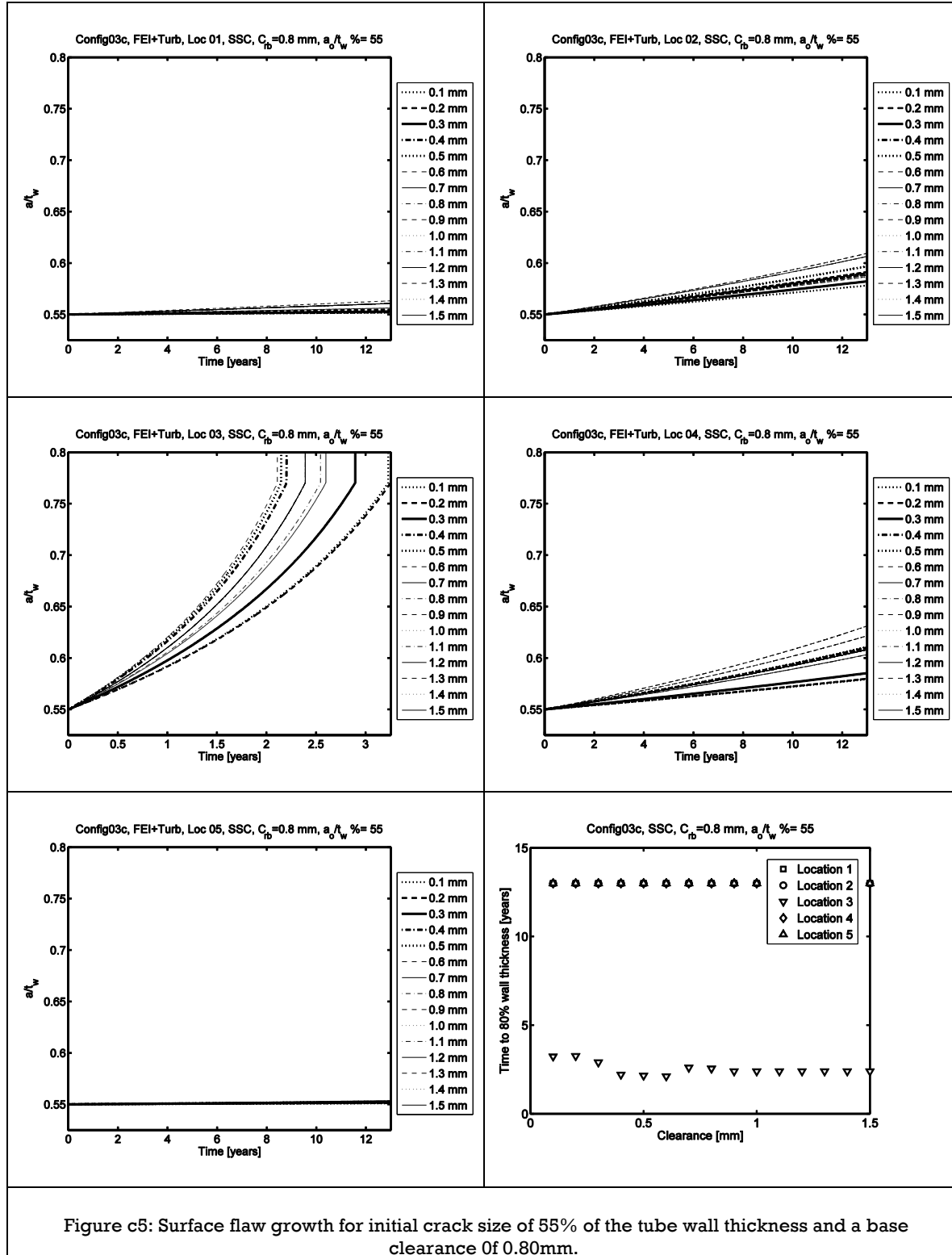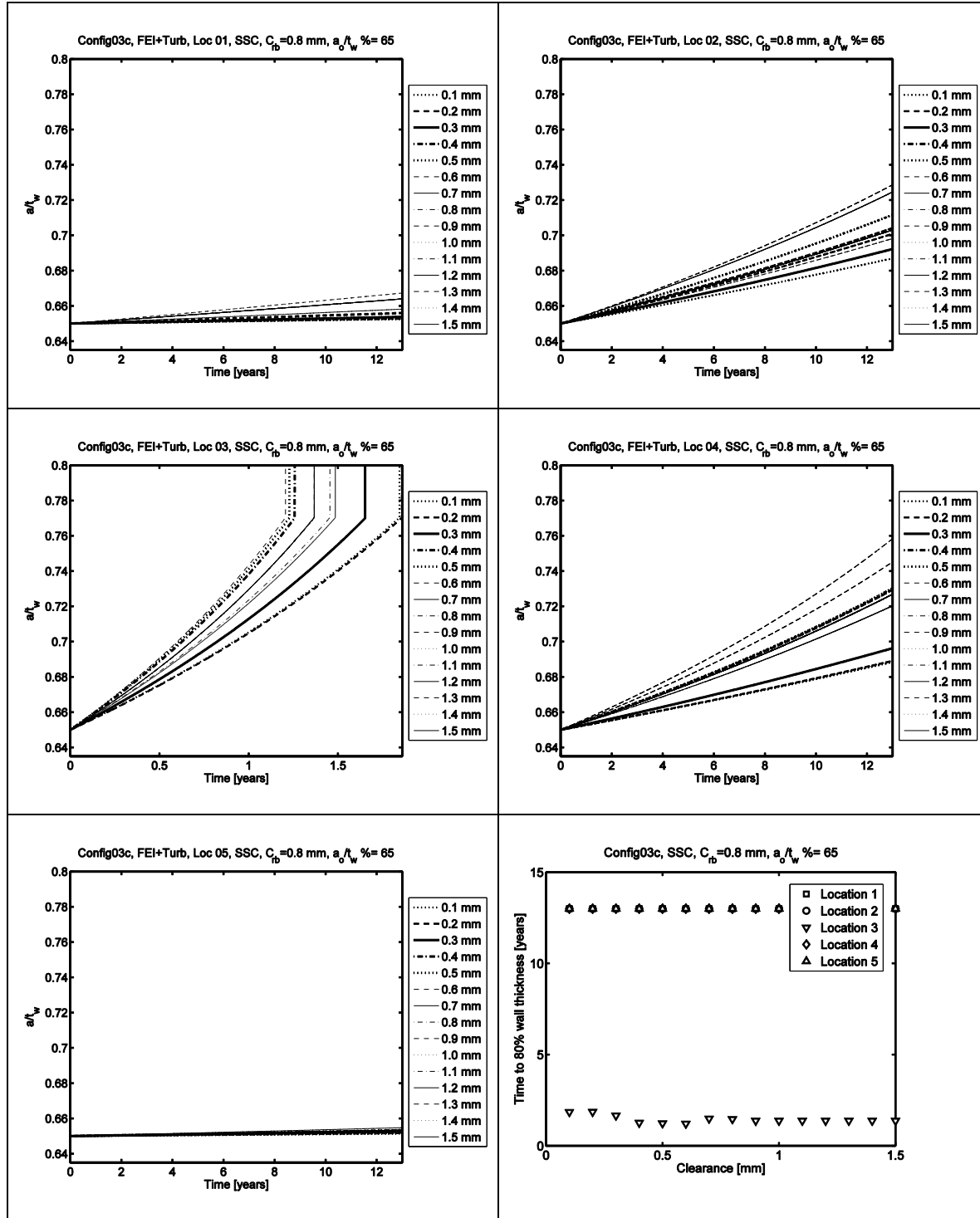
Figure b3: Surface flaw growth for initial crack size of 65% of the tube wall thickness and a base clearance 0f 0.10mm.
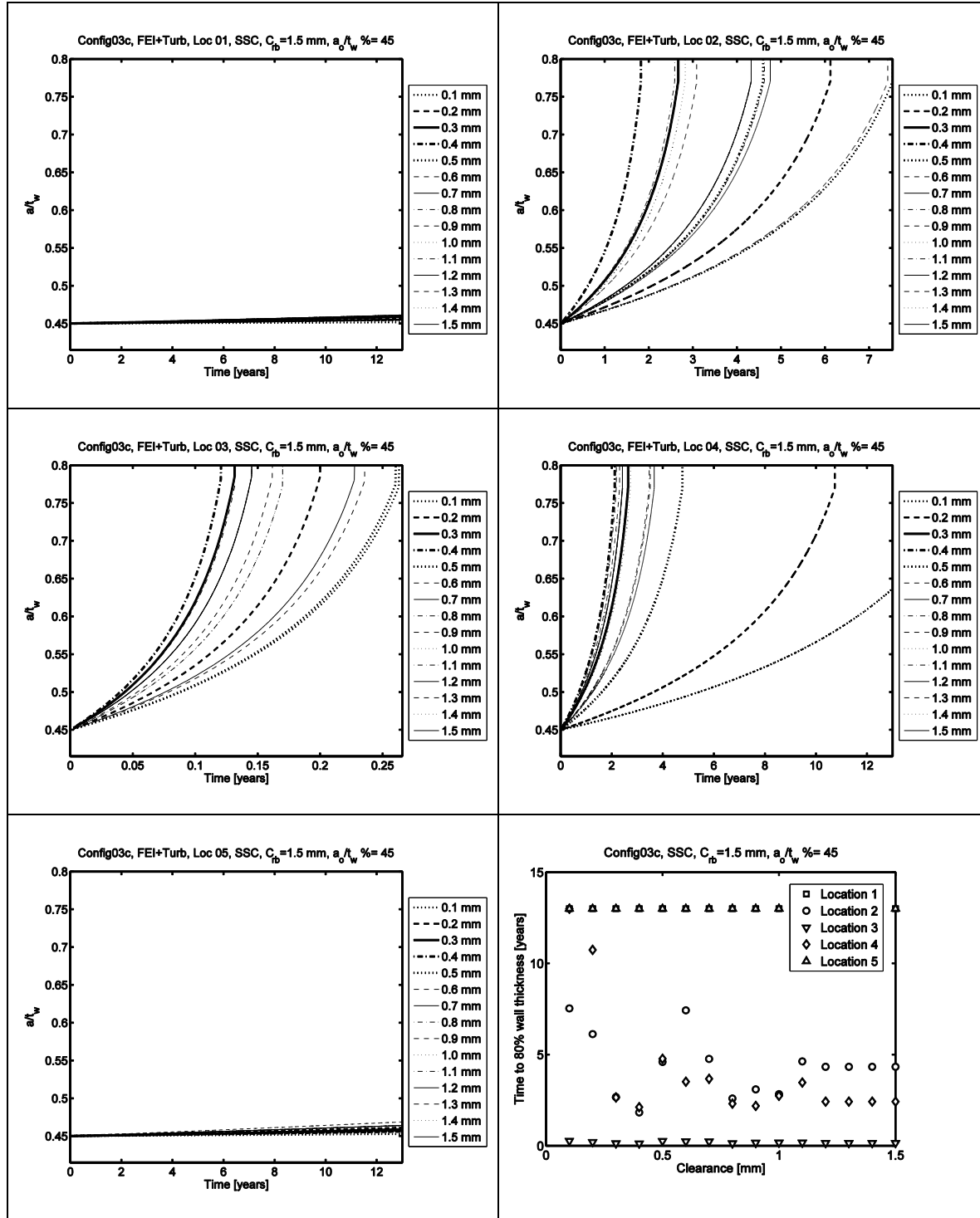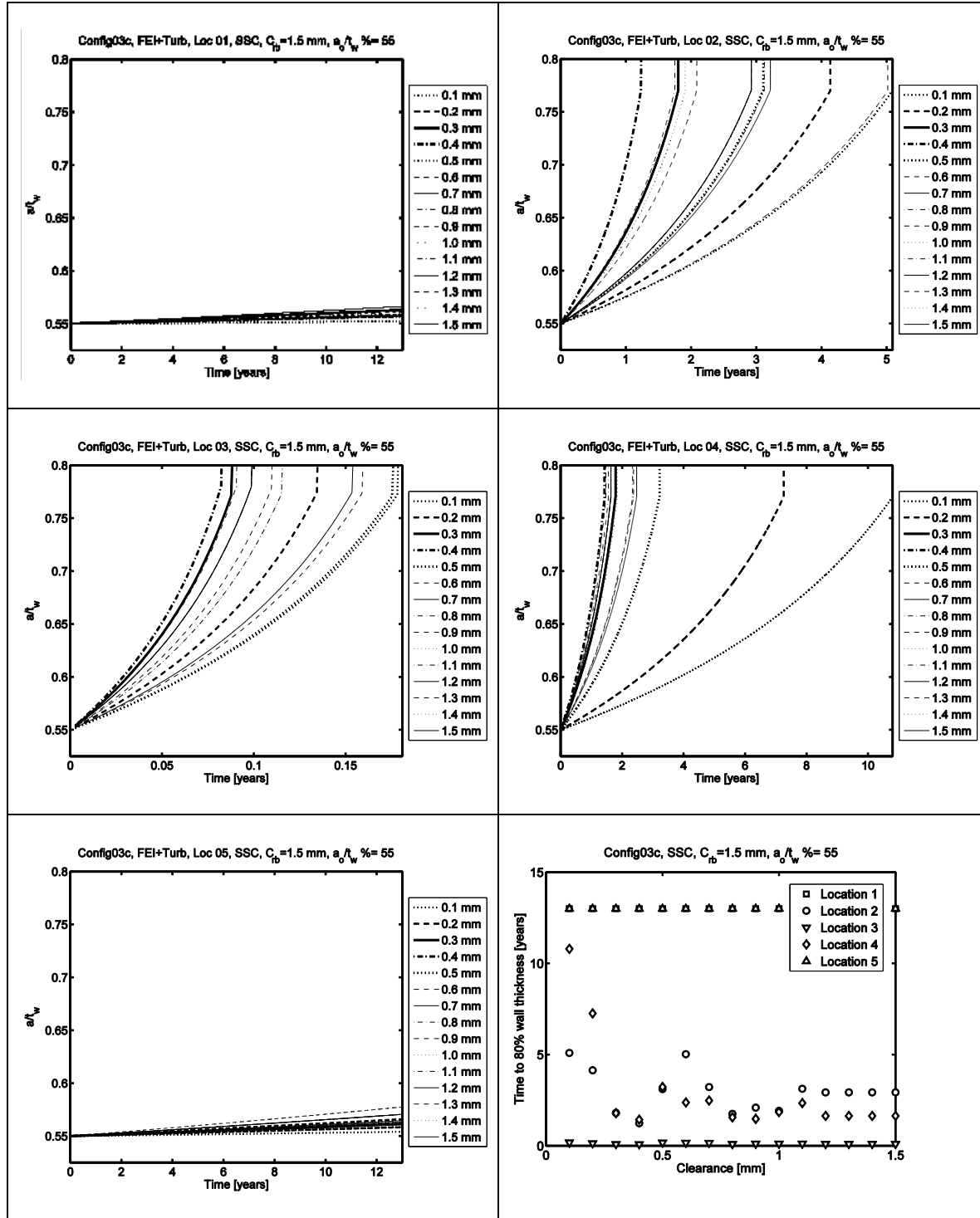
Figure b4: Surface flaw growth for initial crack size of 45% of the tube wall thickness and a base clearance 0f 0.80mm.
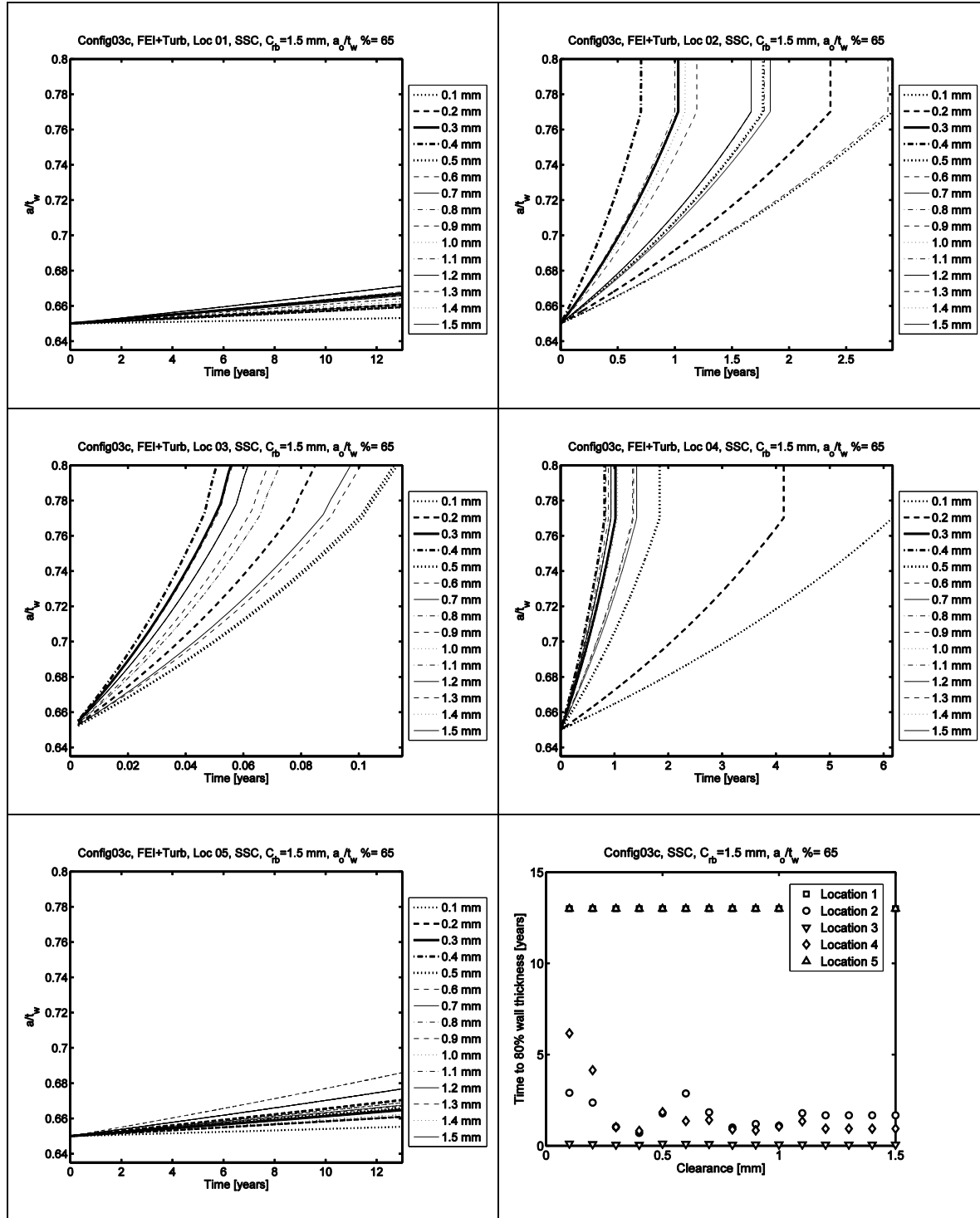
Figure b5: Surface flaw growth for initial crack size of 55% of the tube wall thickness and a base clearance 0f 0.8mm.

Figure b6: Surface flaw growth for initial crack size of 65% of the tube wall thickness and a base clearance 0f 0.80mm.

Figure b7: Surface flaw growth for initial crack size of 45% of the tube wall thickness and a base clearance 0f 1.50mm.

Figure b8: Surface flaw growth for initial crack size of 55% of the tube wall thickness and a base clearance 0f 1.50mm.

Figure b9: Surface flaw growth for initial crack size of 65% of the tube wall thickness and a base clearance 0f 1.50mm.

**Table b1: Config03a, SCC, 45%**

| Base Clearance | SB2 clearance | | | | |
|---|---|---|---|---|---|
| | Location 1 | Location 2 | Location 3 | Location 4 | Location 5 |
| 0.10 | - | - | 0.8 | 1.3 | - |
| 0.20 | - | - | 0.8 | 1.5 | - |
| 0.30 | - | 1.5 | 0.7 | 1.3 | - |
| 0.40 | - | 1.4 | 0.7 | 1.2 | - |
| 0.50 | - | 1.4 | 0.7 | 1.4 | - |
| 0.60 | - | 1.3 | 0.7 | 1.2 | - |
| 0.70 | - | 1.3 | 0.7 | 1.1 | - |
| 0.80 | - | 1.2 | 0.7 | 1.2 | - |
| 0.90 | - | 1.3 | 0.7 | 1.1 | - |
| 1.00 | - | 1.2 | 0.7 | 1.2 | - |
| 1.10 | 1.3 | 1.2 | 0.1 | 1.1 | - |
| 1.20 | 1.3 | 1.2 | 0.1 | 1.2 | |
| 1.30 | - | 1.4 | 0.1 | 1.2 | |
| 1.40 | 0.3 | 1.4 | 0.1 | 1.3 | |
| 1.50 | 1.1 | 1.3 | 0.1 | 0.3 | |

**Table b2: Config03a, SCC, 50%**

| Base Clearance | SB2 clearance | | | | |
|---|---|---|---|---|---|
| | Location 1 | Location 2 | Location 3 | Location 4 | Location 5 |
| 0.10 | - | - | 0.8 | 1.3 | - |
| 0.20 | - | - | 0.7 | 1.3 | - |
| 0.30 | - | 1.5 | 0.7 | 1.3 | - |
| 0.40 | - | 1.3 | 0.7 | 1.2 | - |
| 0.50 | - | 1.2 | 0.6 | 1.4 | - |
| 0.60 | - | 1.3 | 0.6 | 1.1 | - |
| 0.70 | - | 1.3 | 0.6 | 1.1 | - |
| 0.80 | - | 1 | 0.6 | 1.2 | - |
| 0.90 | - | 1.2 | 0.7 | 1.1 | - |
| 1.00 | - | 1.2 | 0.6 | 1.2 | - |
| 1.10 | 1.3 | 1.2 | 0.1 | 1.1 | - |
| 1.20 | 1 | 1 | 0.1 | 1 | - |
| 1.30 | - | 1.4 | 0.1 | 1 | - |
| 1.40 | 0.3 | 1.2 | 0.1 | 0.3 | - |
| 1.50 | 0.5 | 1.3 | 0.1 | 0.3 | - |

**Table b3: Config03a, SCC, 55%**

| Base Clearance | SB2 clearance | | | | |
|---|---|---|---|---|---|
| | Location 1 | Location 2 | Location 3 | Location 4 | Location 5 |
| 0.1 | - | - | 0.8 | 1.3 | - |
| 0.2 | - | 1.5 | 0.7 | 1.2 | - |
| 0.3 | - | 1.1 | 0.7 | 1.2 | - |
| 0.4 | - | 1.2 | 0.6 | 1.2 | - |
| 0.5 | - | 1.4 | 0.6 | 1.2 | - |
| 0.6 | - | 1 | 0.6 | 1 | - |
| 0.7 | - | 1.2 | 0.6 | 1 | - |
| 0.8 | - | 1 | 0.6 | 1.1 | - |
| 0.9 | - | 1 | 0.6 | 1 | - |
| 1 | - | 1 | 0.6 | 1 | - |
| 1.1 | 1.3 | 1 | 0.1 | 1.1 | - |
| 1.2 | 1 | 1 | 0.1 | 1 | - |
| 1.3 | - | 1 | 0.1 | 1 | - |
| 1.4 | 0.3 | 1 | 0.1 | 0.3 | - |
| 1.5 | 1.1 | 1.2 | 0.1 | 0.3 | - |

**Table b4: Config03a, SCC, 60%**

| Base Clearance | SB2 clearance | | | | |
|---|---|---|---|---|---|
| | Location 1 | Location 2 | Location 3 | Location 4 | Location 5 |
| 0.1 | - | - | 0.7 | 1.3 | - |
| 0.2 | - | 1.3 | 0.7 | 1.2 | - |
| 0.3 | - | 1.1 | 0.6 | 1.1 | - |
| 0.4 | - | 1.2 | 0.6 | 1.1 | - |
| 0.5 | - | 1.2 | 0.5 | 1.1 | - |
| 0.6 | - | 1 | 0.6 | 1 | - |
| 0.7 | - | 1.2 | 0.6 | 1 | - |
| 0.8 | - | 1 | 0.6 | 1 | - |
| 0.9 | - | 1 | 0.6 | 0.9 | - |
| 1 | - | 1 | 0.1 | 0.9 | - |
| 1.1 | 1.3 | 1 | 0.1 | 1 | - |
| 1.2 | 1 | 1 | 0.1 | 1 | - |
| 1.3 | - | 1 | 0.1 | 0.3 | - |
| 1.4 | 0.3 | 1 | 0.1 | 0.3 | - |
| 1.5 | 0.3 | 1 | 0.1 | 0.3 | - |

**Table b5: Config03a, SCC, 65%**

| Base Clearance | SB2 clearance | | | | |
| --- | --- | --- | --- | --- | --- |
| | Location 1 | Location 2 | Location 3 | Location 4 | Location 5 |
| 0.1 | - | 1.3 | 0.7 | 1.1 | - |
| 0.2 | - | 1.3 | 0.7 | 1 | - |
| 0.3 | - | 1.1 | 0.6 | 1 | - |
| 0.4 | - | 1.2 | 0.6 | 0.9 | - |
| 0.5 | - | 1.1 | 0.5 | 1 | - |
| 0.6 | - | 1 | 0.5 | 0.9 | - |
| 0.7 | - | 1 | 0.6 | 1 | - |
| 0.8 | - | 0.9 | 0.5 | 0.9 | - |
| 0.9 | - | 0.9 | 0.1 | 0.9 | - |
| 1 | - | 1 | 0.1 | 0.9 | - |
| 1.1 | 1.3 | 0.9 | 0.1 | 0.1 | - |
| 1.2 | 1 | 1 | 0.1 | 0.9 | - |
| 1.3 | - | 1 | 0.1 | 0.2 | - |
| 1.4 | 0.3 | 1 | 0.1 | 0.2 | 0.5 |
| 1.5 | 0.3 | 1 | 0.1 | 0.2 | 0.3 |

**Table b6: Config03a, SCC, 70%**

| Base Clearance | SB2 clearance | | | | |
| --- | --- | --- | --- | --- | --- |
| | Location 1 | Location 2 | Location 3 | Location 4 | Location 5 |
| 0.1 | - | 1.3 | 0.6 | 1 | - |
| 0.2 | - | 1.2 | 0.6 | 1 | - |
| 0.3 | - | 1 | 0.5 | 0.9 | - |
| 0.4 | - | 0.9 | 0.5 | 0.8 | - |
| 0.5 | - | 0.9 | 0.4 | 0.9 | - |
| 0.6 | - | 0.8 | 0.4 | 0.8 | - |
| 0.7 | - | 0.9 | 0.5 | 0.9 | - |
| 0.8 | - | 0.9 | 0.1 | 0.8 | - |
| 0.9 | - | 0.9 | 0.1 | 0.8 | - |
| 1 | - | 0.9 | 0.1 | 0.8 | - |
| 1.1 | 0.2 | 0.9 | 0.1 | 0.1 | - |
| 1.2 | 0.1 | 0.9 | 0.1 | 0.1 | - |
| 1.3 | 0.2 | 0.8 | 0.1 | 0.1 | 0.3 |
| 1.4 | 0.2 | 0.9 | 0.1 | 0.1 | 0.5 |
| 1.5 | 0.2 | 0.9 | 0.1 | 0.1 | 0.3 |

**Table b7: Config03a, SCC, 75%**

| Base Clearance | SB2 clearance | | | | |
|---|---|---|---|---|---|
| | Location 1 | Location 2 | Location 3 | Location 4 | Location 5 |
| 0.1 | - | 1 | 0.5 | 0.8 | - |
| 0.2 | - | 0.9 | 0.4 | 0.8 | - |
| 0.3 | - | 0.7 | 0.4 | 0.7 | - |
| 0.4 | - | 0.7 | 0.3 | 0.6 | - |
| 0.5 | - | 0.6 | 0.3 | 0.6 | - |
| 0.6 | - | 0.6 | 0.3 | 0.6 | - |
| 0.7 | - | 0.6 | 0.1 | 0.6 | - |
| 0.8 | - | 0.6 | 0.1 | 0.5 | - |
| 0.9 | - | 0.6 | 0.1 | 0.2 | - |
| 1 | 0.3 | 0.7 | 0.1 | 0.1 | - |
| 1.1 | 0.1 | 0.1 | 0.1 | 0.1 | 0.1 |
| 1.2 | 0.1 | 0.1 | 0.1 | 0.1 | 0.1 |
| 1.3 | 0.1 | 0.1 | 0.1 | 0.1 | 0.1 |
| 1.4 | 0.1 | 0.1 | 0.1 | 0.1 | 0.1 |
| 1.5 | 0.1 | 0.1 | 0.1 | 0.1 | 0.1 |

# Appendix C

Configuration 03C, Surface flaw crack growth for U-bend tube subjected to turbulence in addition to fluid-elastic instability excitation.
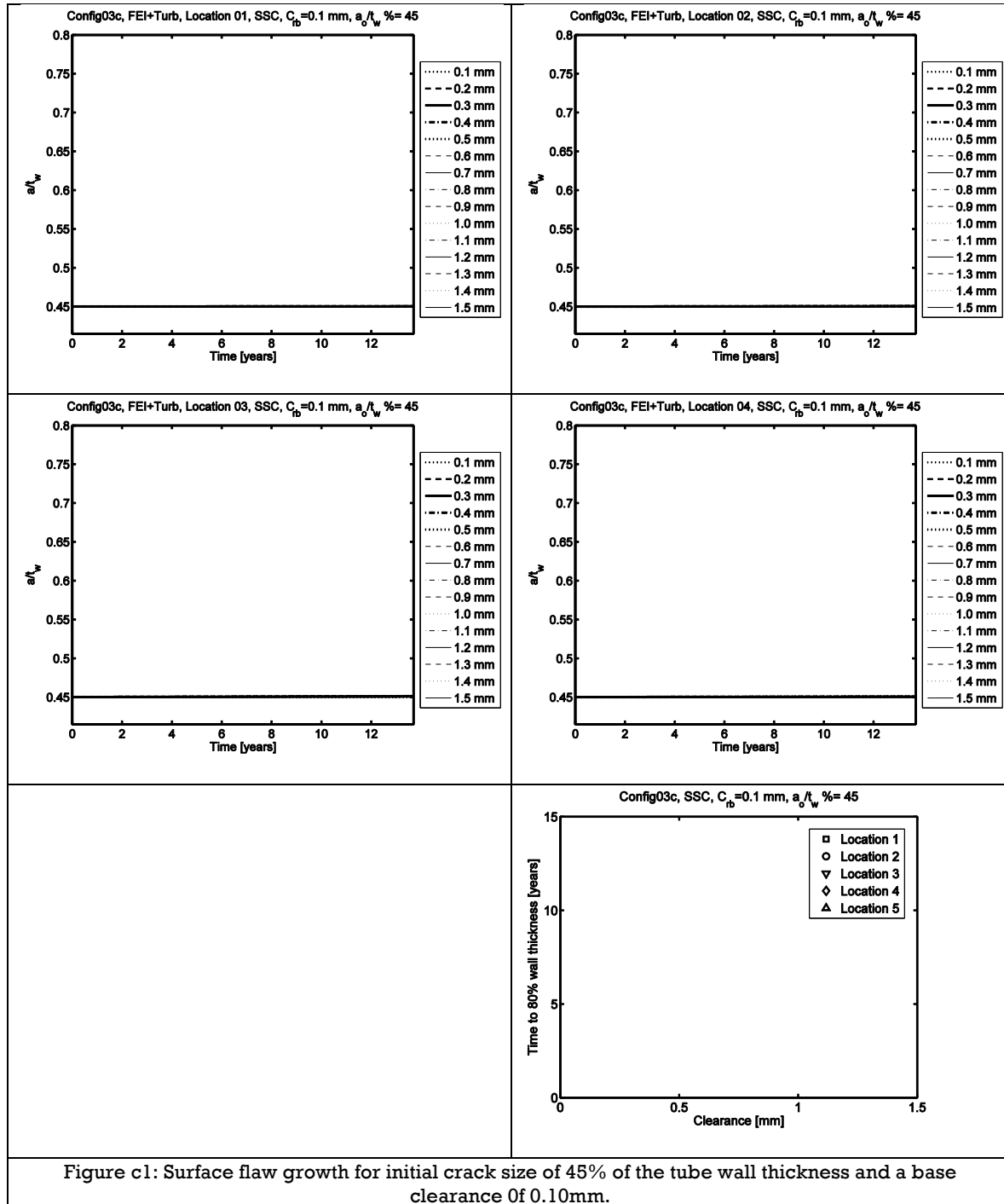


Figure c1: Surface flaw growth for initial crack size of 45% of the tube wall thickness and a base clearance 0f 0.10mm.

Config03c, FEI+Turb, Location 01, SSC, $C_{rb}$=0.1 mm, $a_o/t_w$ %= 55

Config03c, FEI+Turb, Location 02, SSC, $C_{rb}$=0.1 mm, $a_o/t_w$ %= 55

Config03c, FEI+Turb, Location 03, SSC, $C_{rb}$=0.1 mm, $a_o/t_w$ %= 55

Config03c, FEI+Turb, Location 04, SSC, $C_{rb}$=0.1 mm, $a_o/t_w$ %= 55

Config03c, SSC, $C_{rb}$=0.1 mm, $a_o/t_w$ %= 55
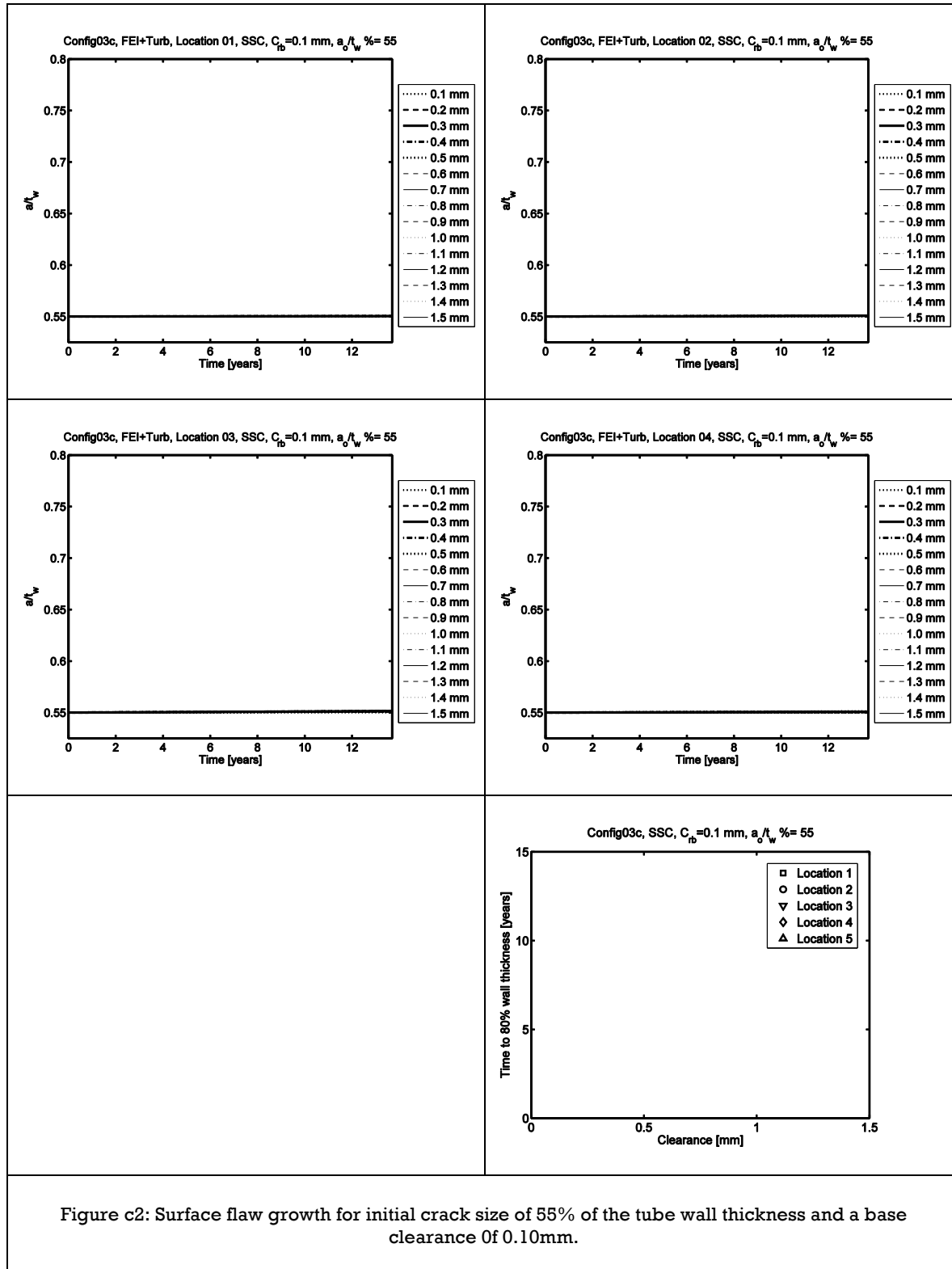
Figure c2: Surface flaw growth for initial crack size of 55% of the tube wall thickness and a base clearance 0f 0.10mm.
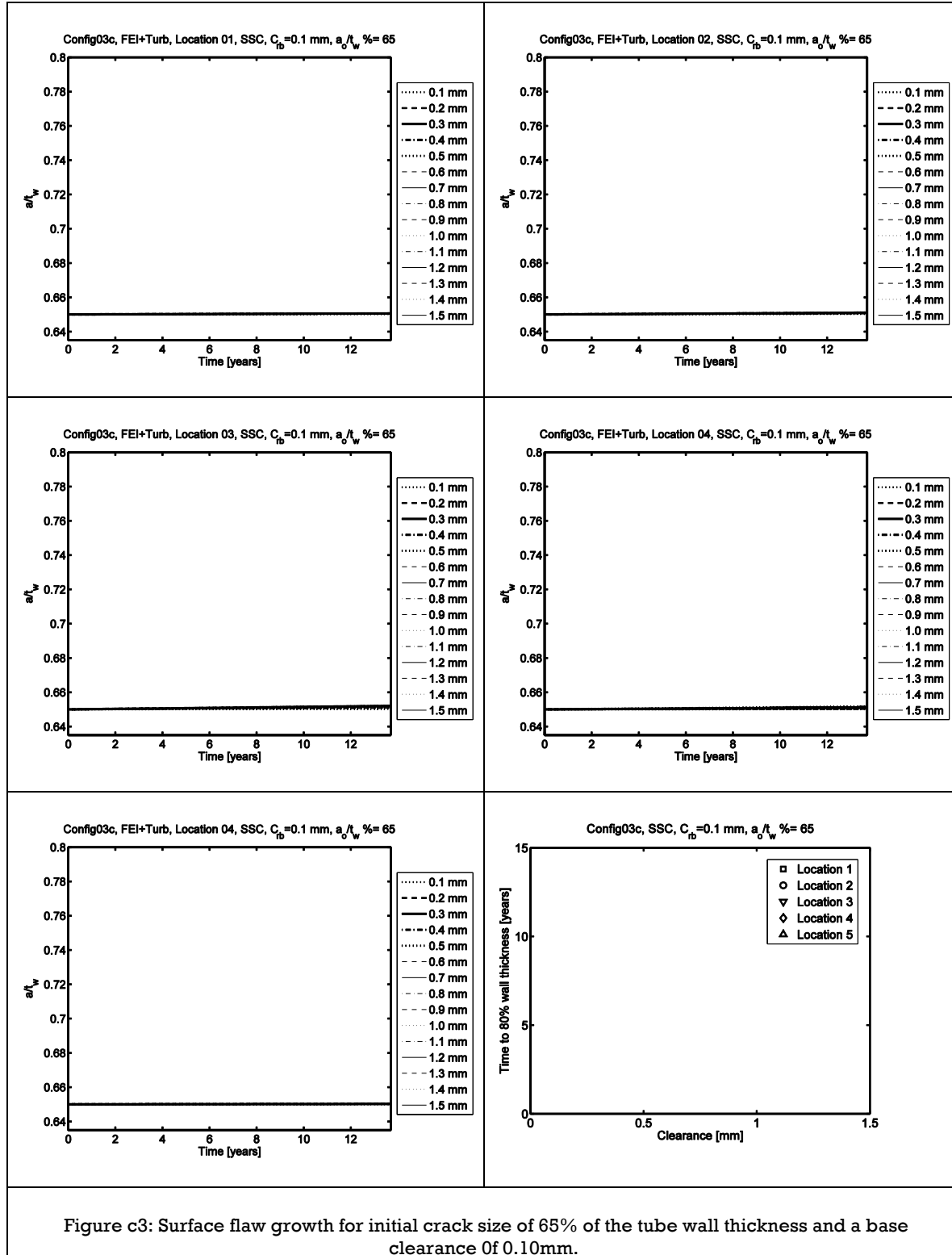
Figure c3: Surface flaw growth for initial crack size of 65% of the tube wall thickness and a base clearance 0f 0.10mm.

Figure c4: Surface flaw growth for initial crack size of 45% of the tube wall thickness and a base clearance 0f 0.80mm.

Figure c5: Surface flaw growth for initial crack size of 55% of the tube wall thickness and a base clearance 0f 0.80mm.

Figure c6: Surface flaw growth for initial crack size of 65% of the tube wall thickness and a base clearance 0f 0.80mm.

Figure c7: Surface flaw growth for initial crack size of 45% of the tube wall thickness and a base clearance 0f 1.50mm.

Figure c8: Surface flaw growth for initial crack size of 55% of the tube wall thickness and a base clearance 0f 1.50mm.

Figure c9: Surface flaw growth for initial crack size of 65% of the tube wall thickness and a base clearance 0f 1.50mm.

**Table b1: Config03a, SCC, 45%**

| Base Clearance | SB3 clearance | | | | |
|---|---|---|---|---|---|
| | Location 1 | Location 2 | Location 3 | Location 4 | Location 5 |
| 0.10 | - | - | - | - | - |
| 0.20 | - | - | - | - | - |
| 0.30 | - | - | - | - | - |
| 0.40 | - | - | - | - | - |
| 0.50 | - | - | - | - | - |
| 0.60 | - | - | 0.8 | - | - |
| 0.70 | - | - | 0.2 | - | - |
| 0.80 | - | - | 0.1 | - | - |
| 0.90 | - | - | 0.1 | - | - |
| 1.00 | - | - | 0.1 | - | - |
| 1.10 | - | - | 0.1 | 0.7 | - |
| 1.20 | - | 0.6 | 0.1 | 0.4 | - |
| 1.30 | - | 0.4 | 0.1 | 0.4 | - |
| 1.40 | 0.9 | 0.1 | 0.1 | 0.2 | - |
| 1.50 | - | 0.1 | 0.1 | 0.3 | - |

# Appendix D

Configuration 03a, Circumferential Through-Wall crack growth for U-bend tube subjected to turbulence in addition to fluid-elastic instability excitation.
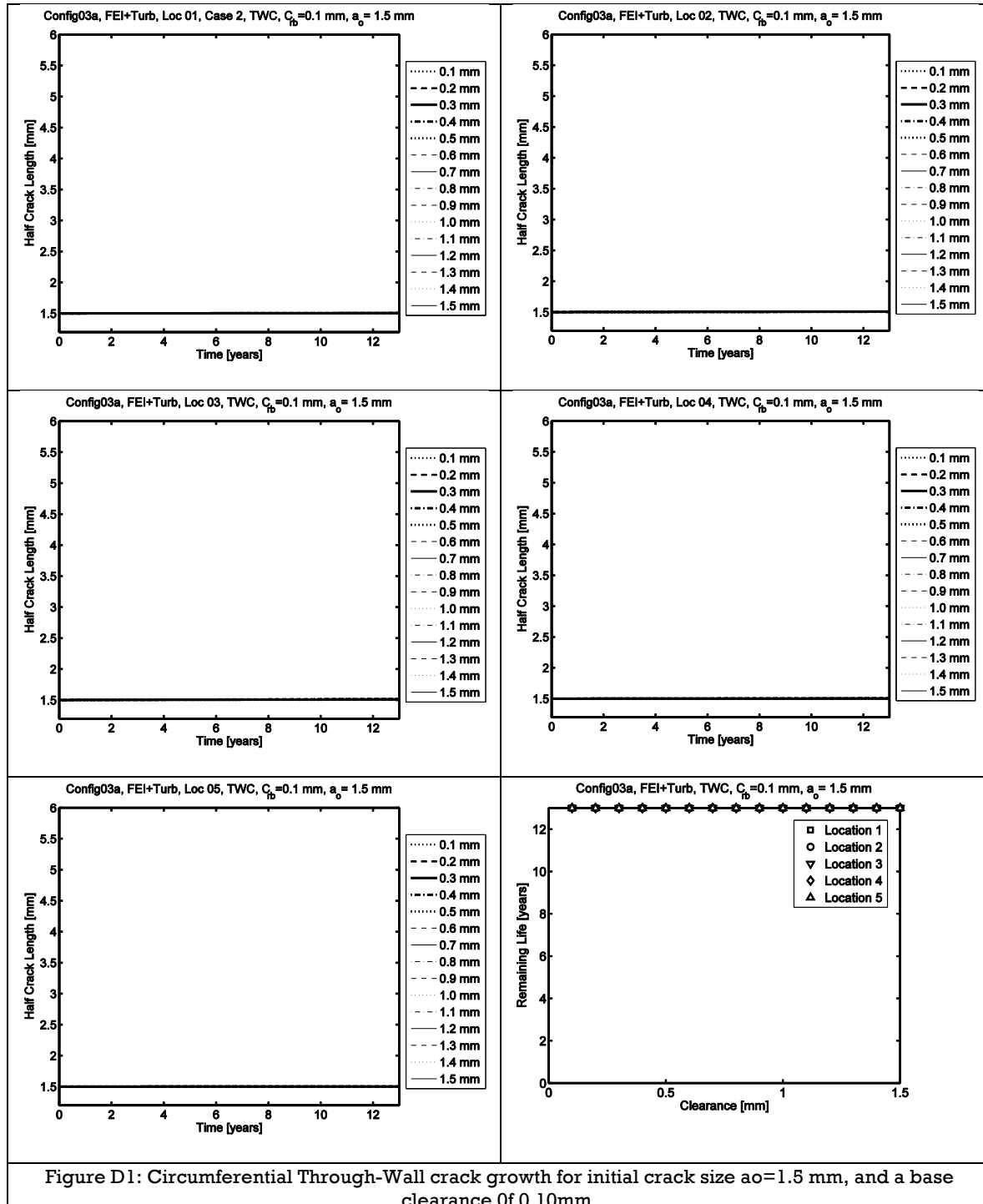


Figure D1: Circumferential Through-Wall crack growth for initial crack size ao=1.5 mm, and a base clearance 0f 0.10mm.
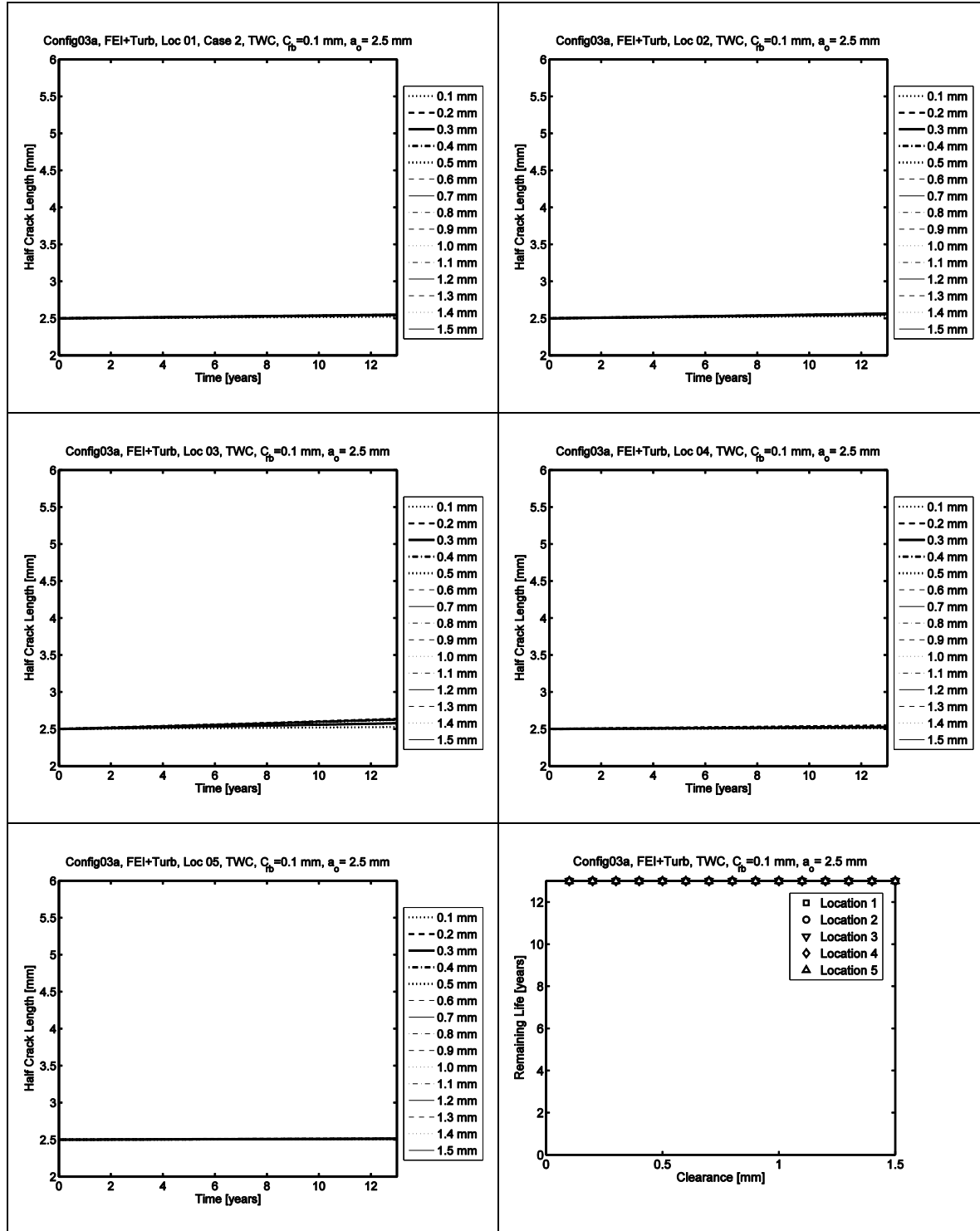
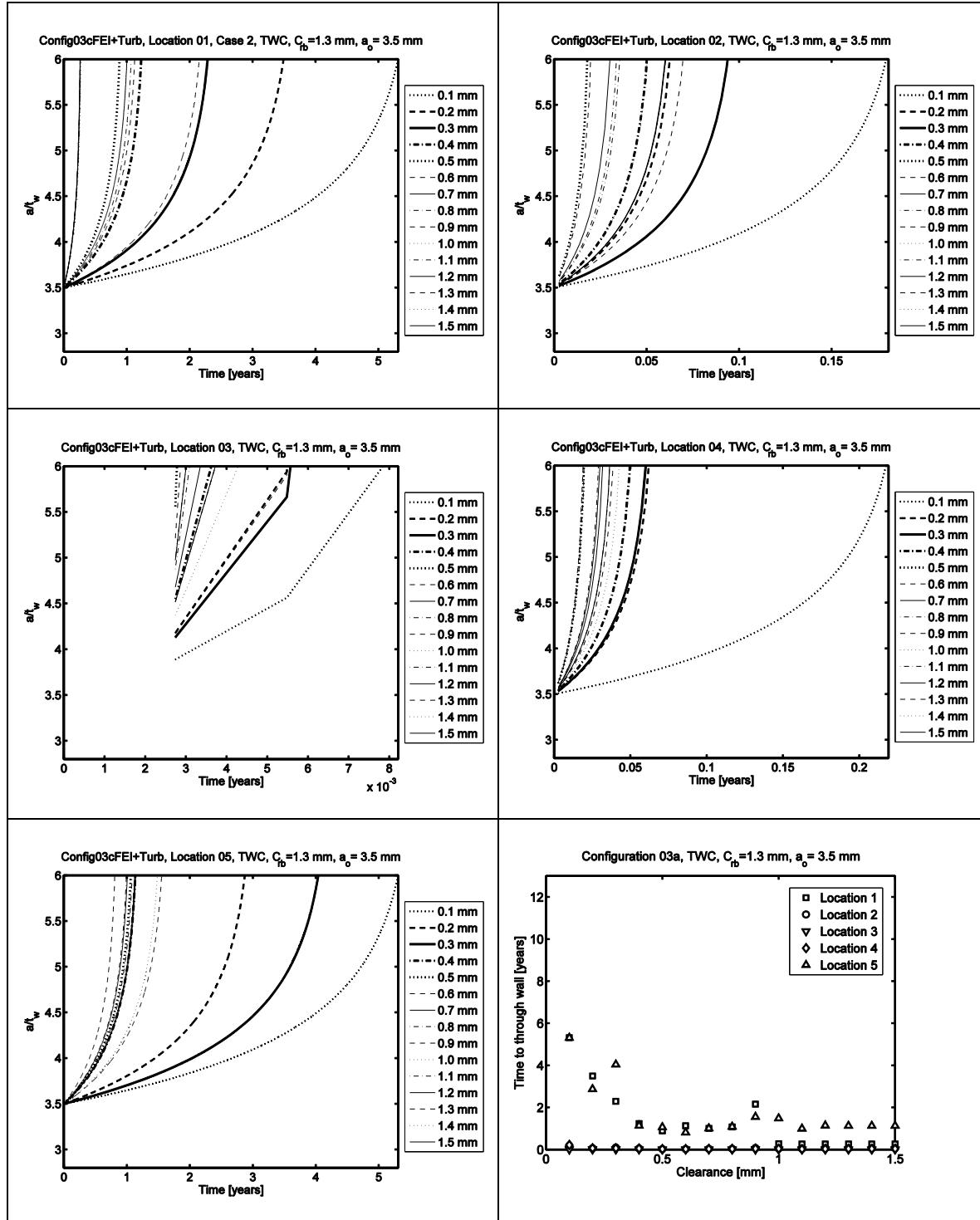Figure D2: Circumferential Through-Wall crack growth for initial crack size ao=2.5 mm, and a base clearance 0f 0.10mm.
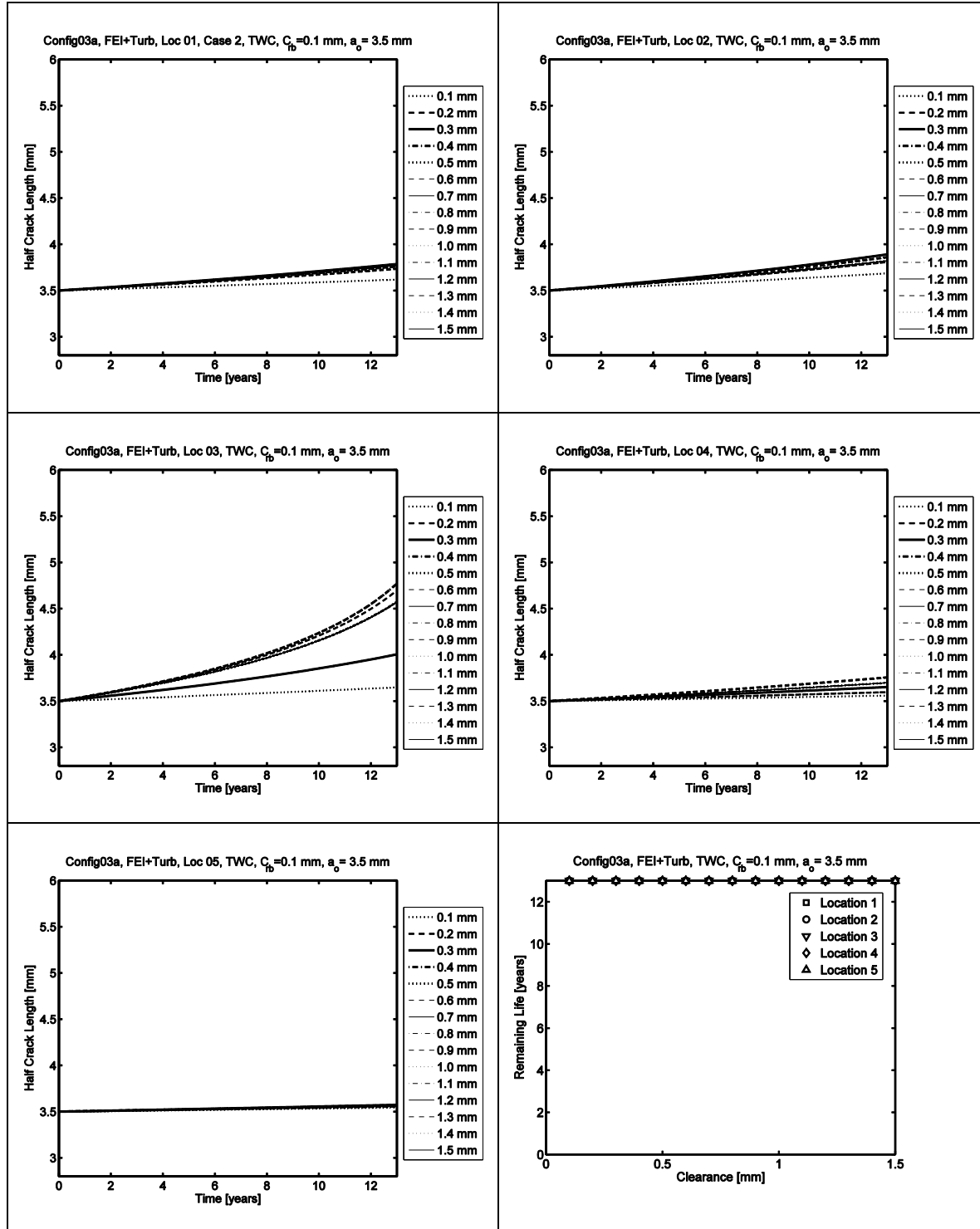
Figure D3: Circumferential Through-Wall crack growth for initial crack size ao=3.5 mm, and a base clearance 0f 0.10mm.
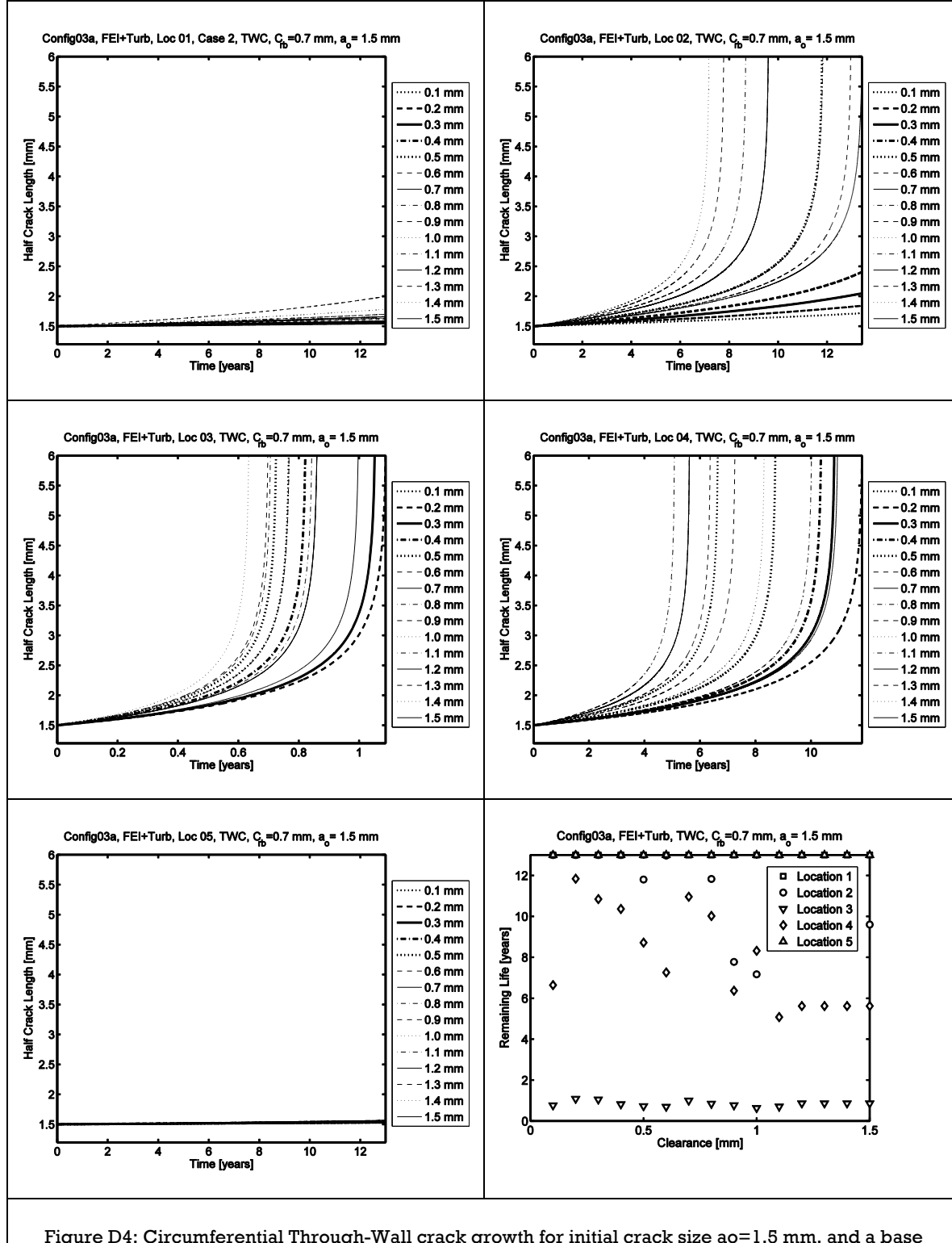
Figure D4: Circumferential Through-Wall crack growth for initial crack size ao=1.5 mm, and a base
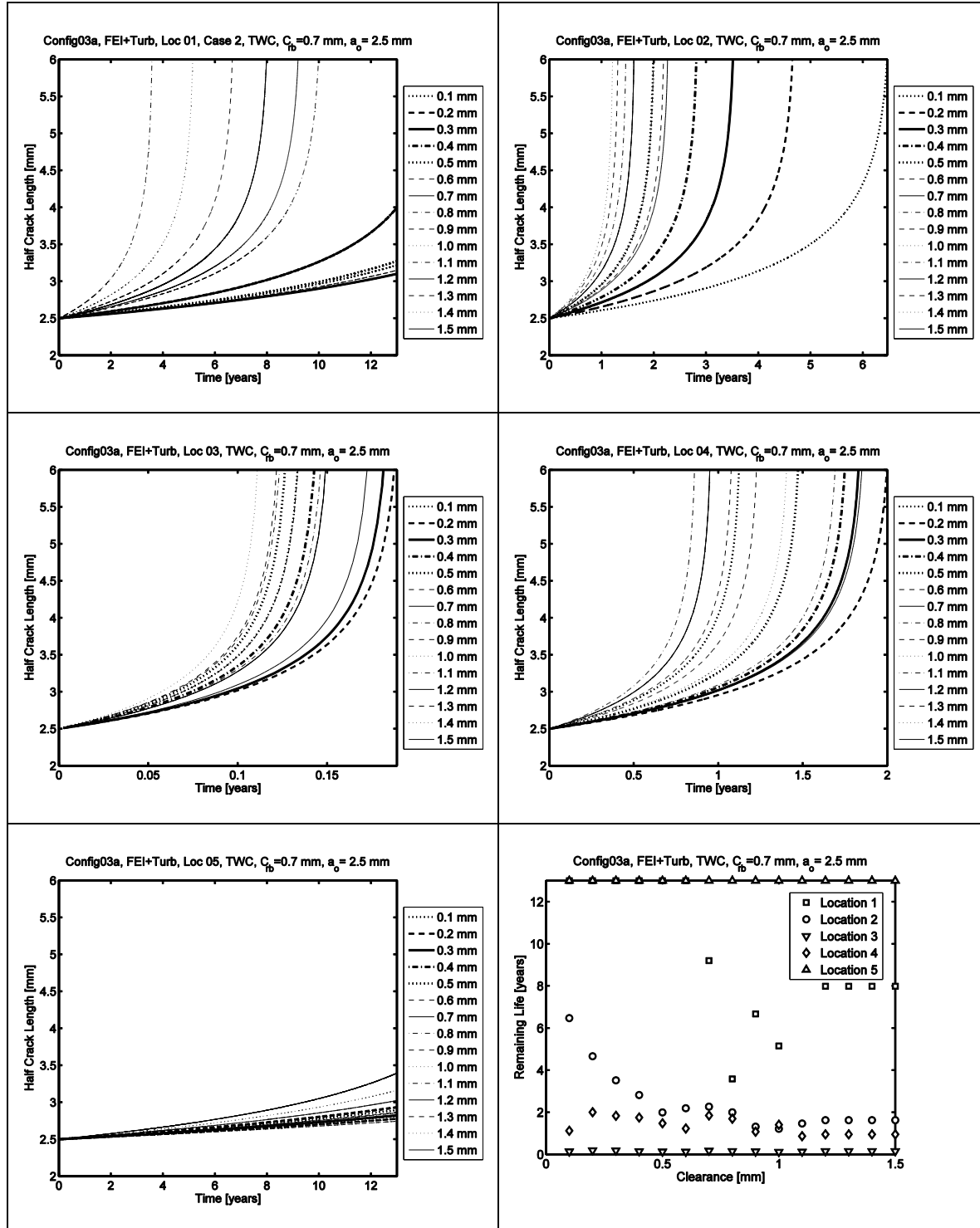
clearance 0f 0.70mm.



Figure D5: Circumferential Through-Wall crack growth for initial crack size ao=2.5 mm, and a base clearance 0f 0.70mm.
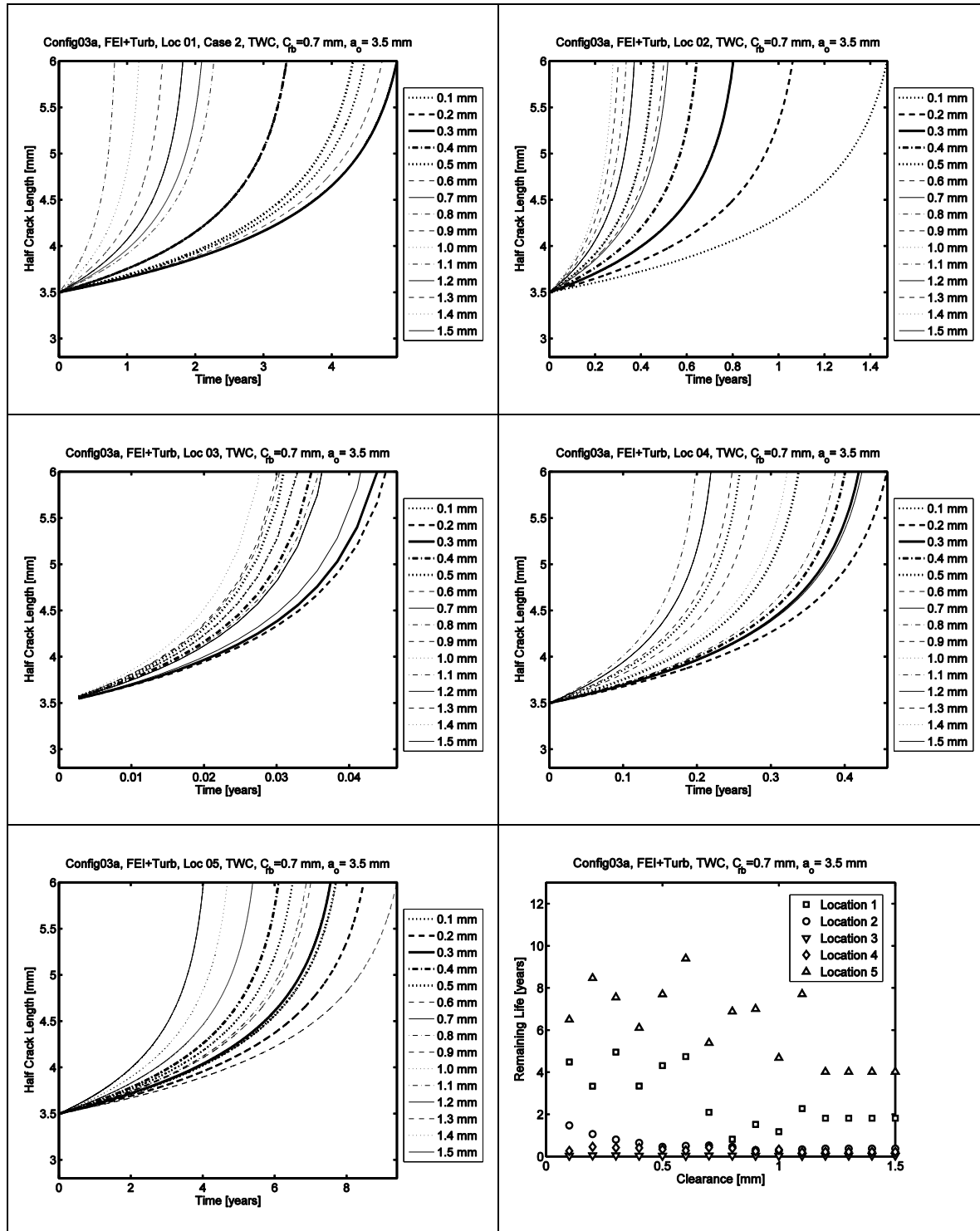
Figure D6: Circumferential Through-Wall crack growth for initial crack size ao=3.5 mm, and a base clearance 0f 0.70mm.
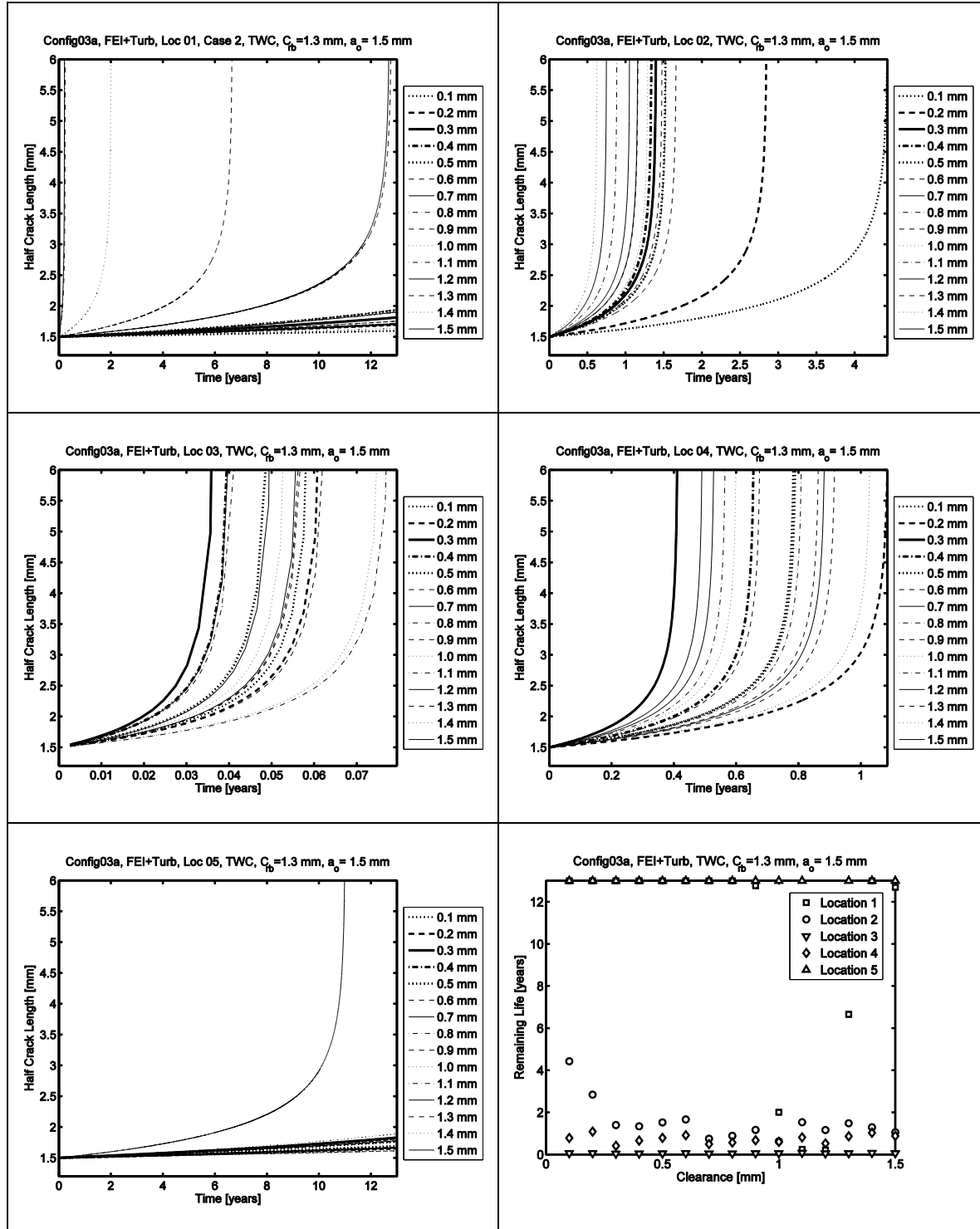
Figure D7: Circumferential Through-Wall crack growth for initial crack size ao=1.5 mm, and a base clearance 0f 1.30mm.
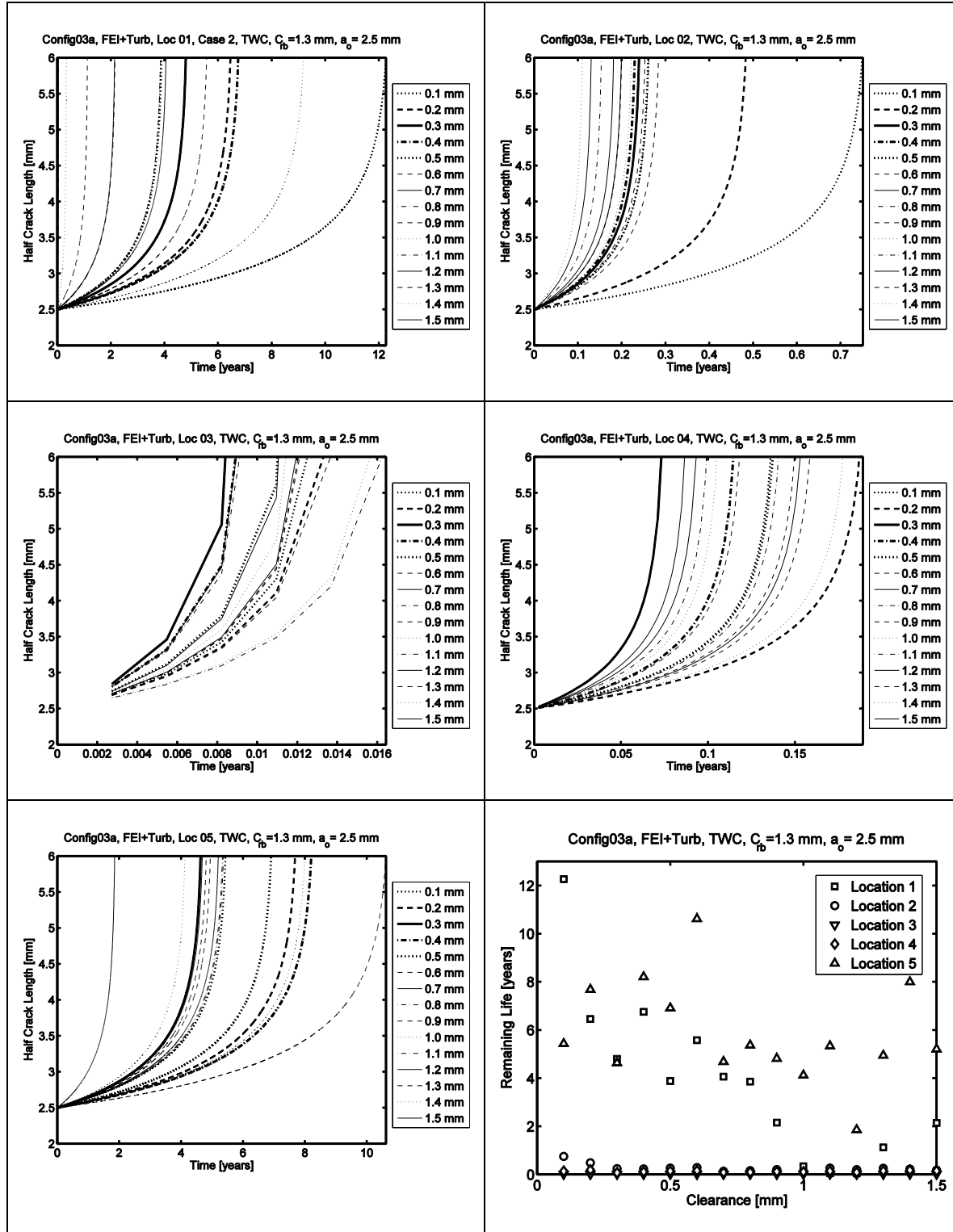
Figure D8: Circumferential Through-Wall crack growth for initial crack size ao=2.5 mm, and a base clearance 0f 1.30mm.
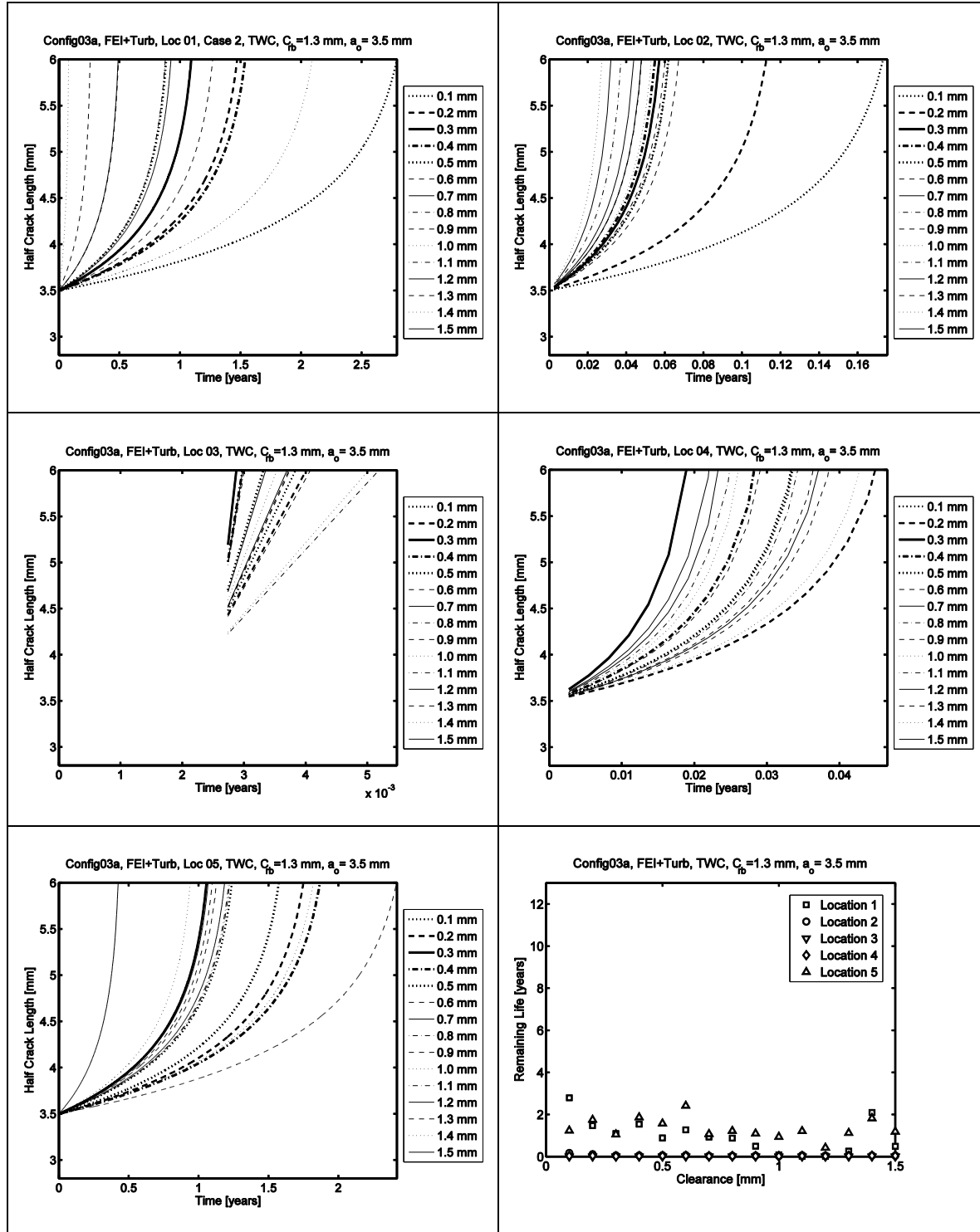
Figure D9: Circumferential Through-Wall crack growth for initial crack size ao=3.5 mm, and a base clearance 0f 1.30mm.

**Table D1: Config03a, TWC, 45%**

**Table D2: Config03a, TWC, 50%**

**Table D3: Config03a, TWC, 55%**

**Table D4: Config03a, TWC, 60%**

**Table D5: Config03a, TWC, 65%**

**Table D6: Config03a, TWC, 70%**

**Table D7: Config03a, TWC, 75%**

# Appendix E

Configuration 03b, Circumferential Through-Wall crack growth for U-bend tube subjected to turbulence in addition to fluid-elastic instability excitation.
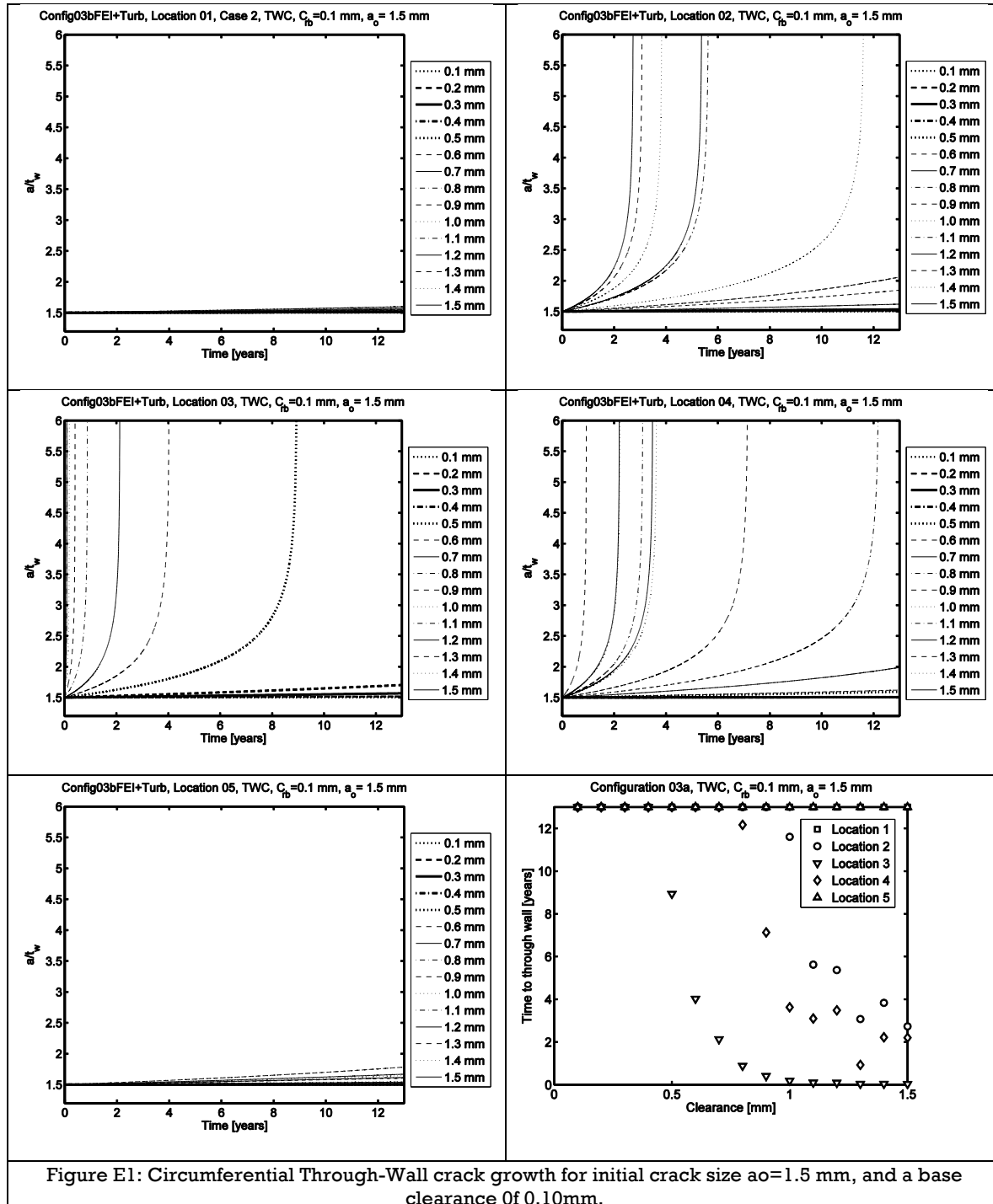


Figure E1: Circumferential Through-Wall crack growth for initial crack size ao=1.5 mm, and a base clearance 0f 0.10mm.
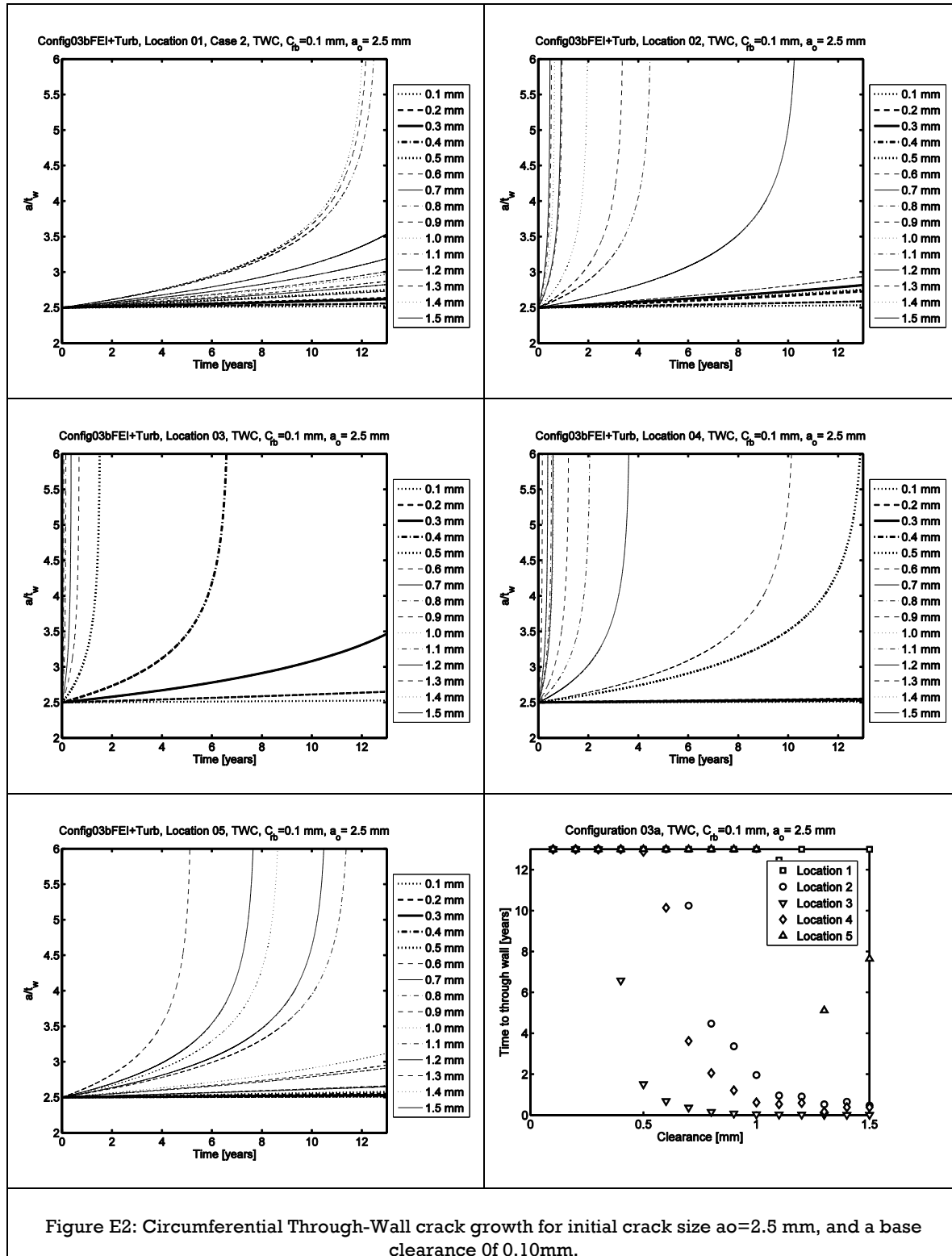
Figure E2: Circumferential Through-Wall crack growth for initial crack size ao=2.5 mm, and a base clearance 0f 0.10mm.
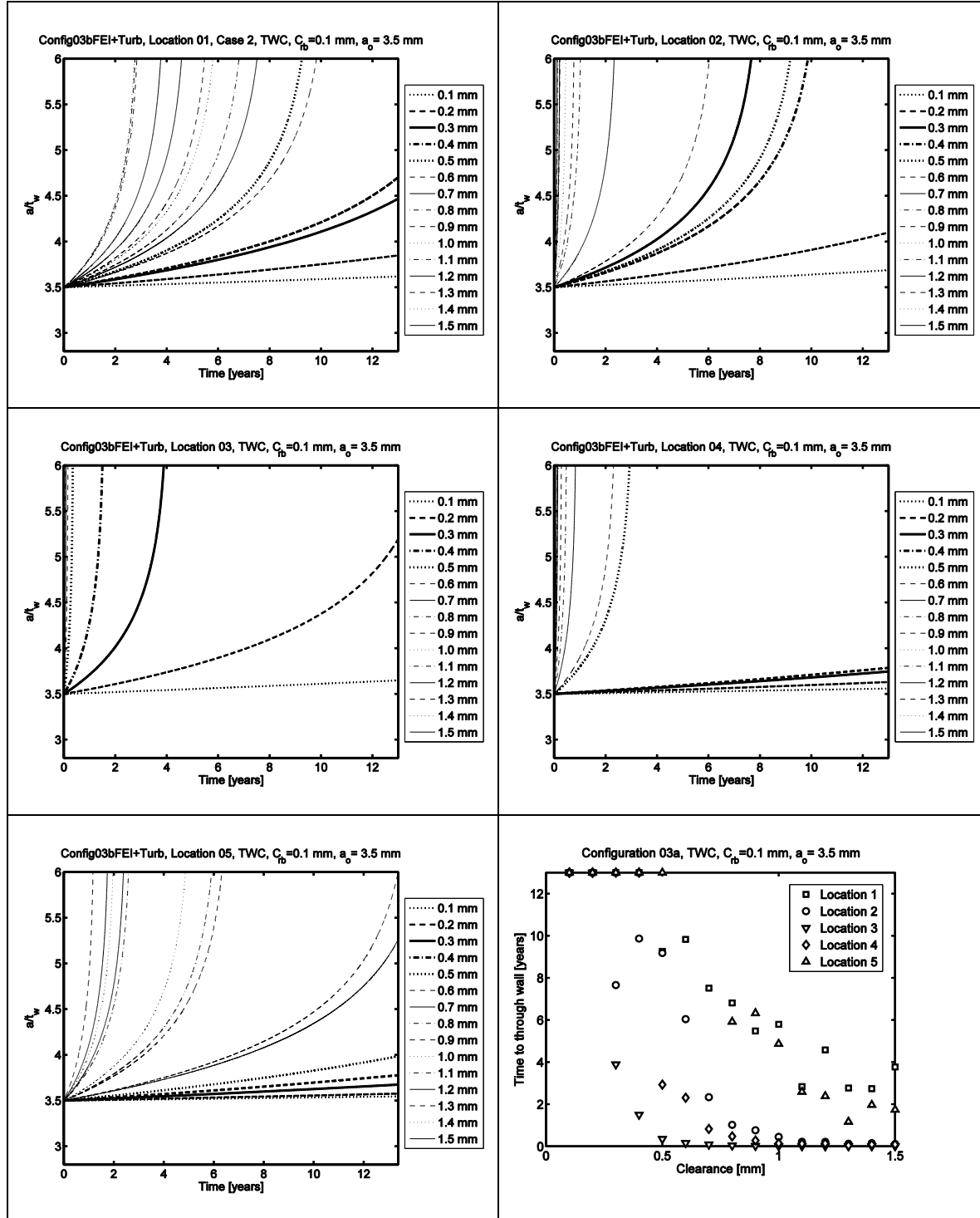
Figure E3: Circumferential Through-Wall crack growth for initial crack size ao=3.5 mm, and a base clearance 0f 0.10mm.
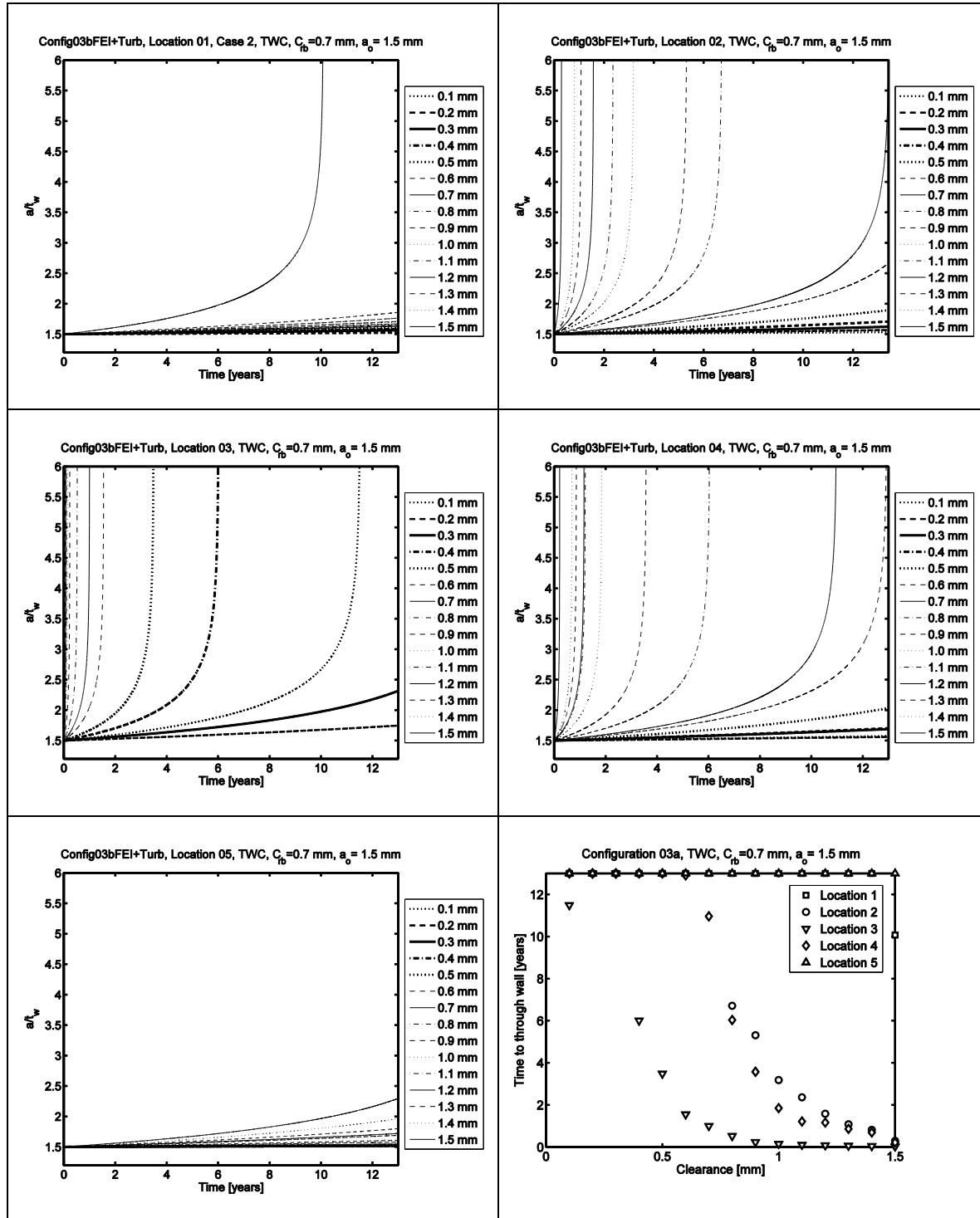
Figure E4: Circumferential Through-Wall crack growth for initial crack size ao=1.5 mm, and a base clearance 0f 0.70mm.
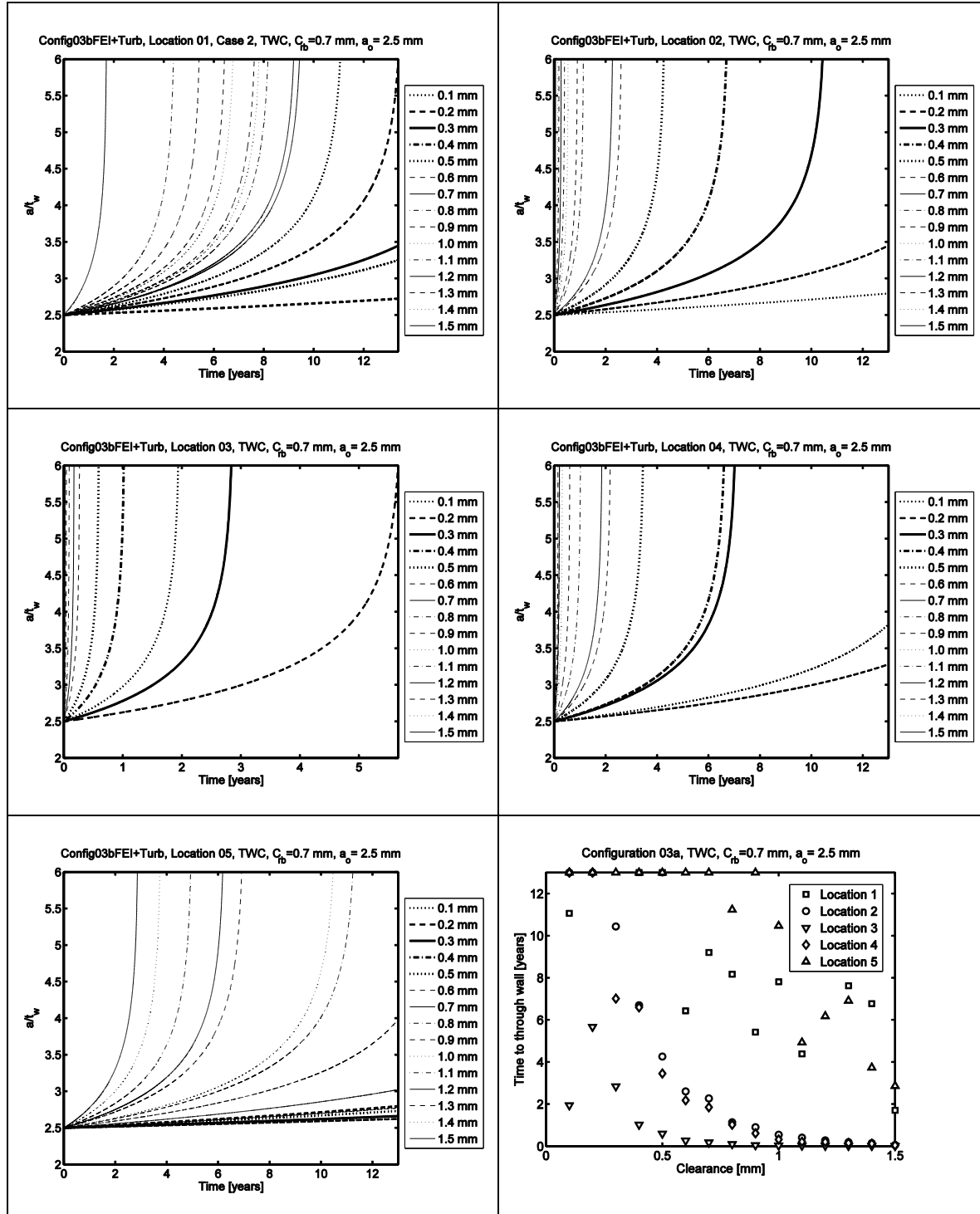
Figure E5: Circumferential Through-Wall crack growth for initial crack size ao=2.5 mm, and a base clearance 0f 0.70mm.
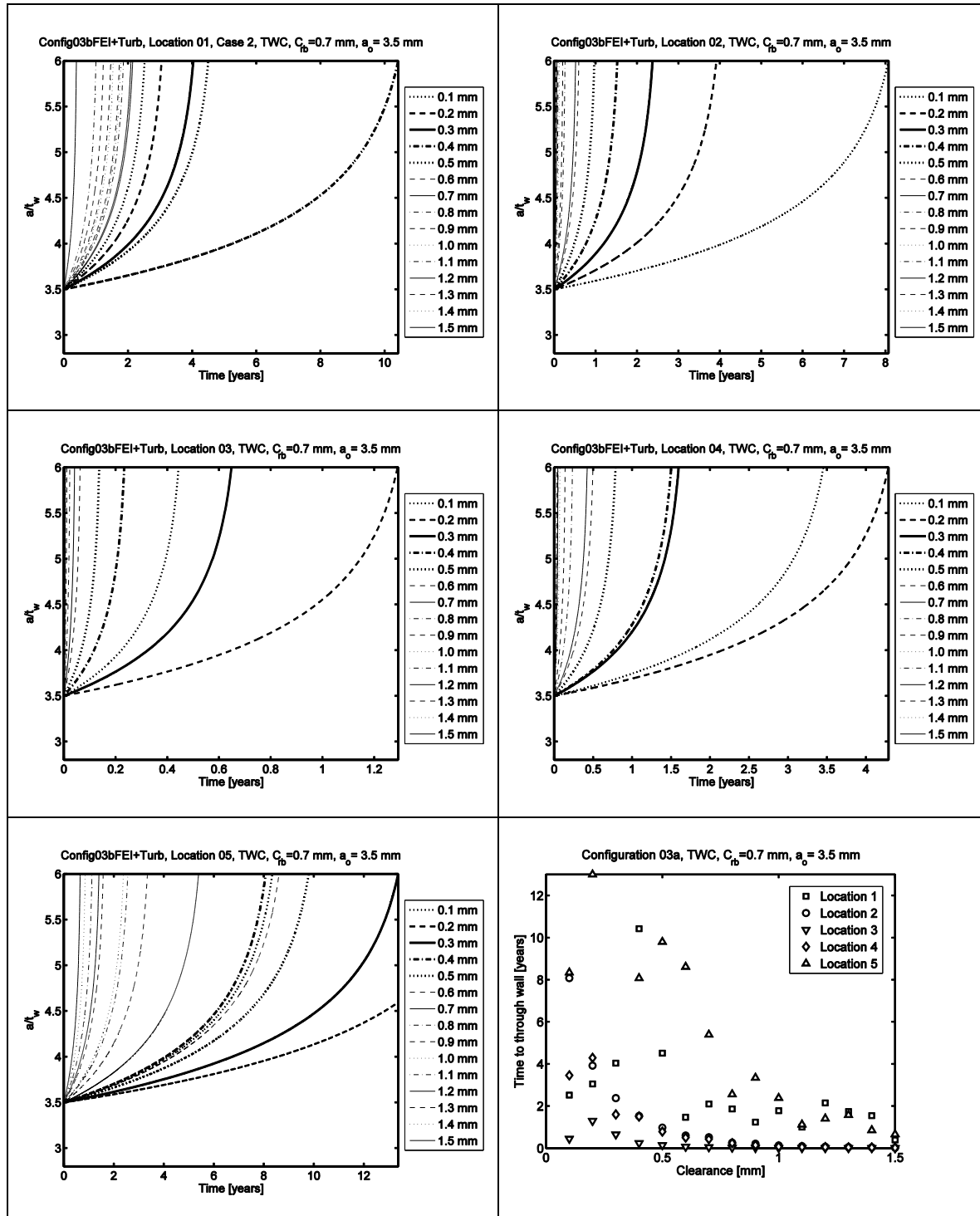
Figure E6: Circumferential Through-Wall crack growth for initial crack size ao=3.5 mm, and a base clearance 0f 0.70mm.
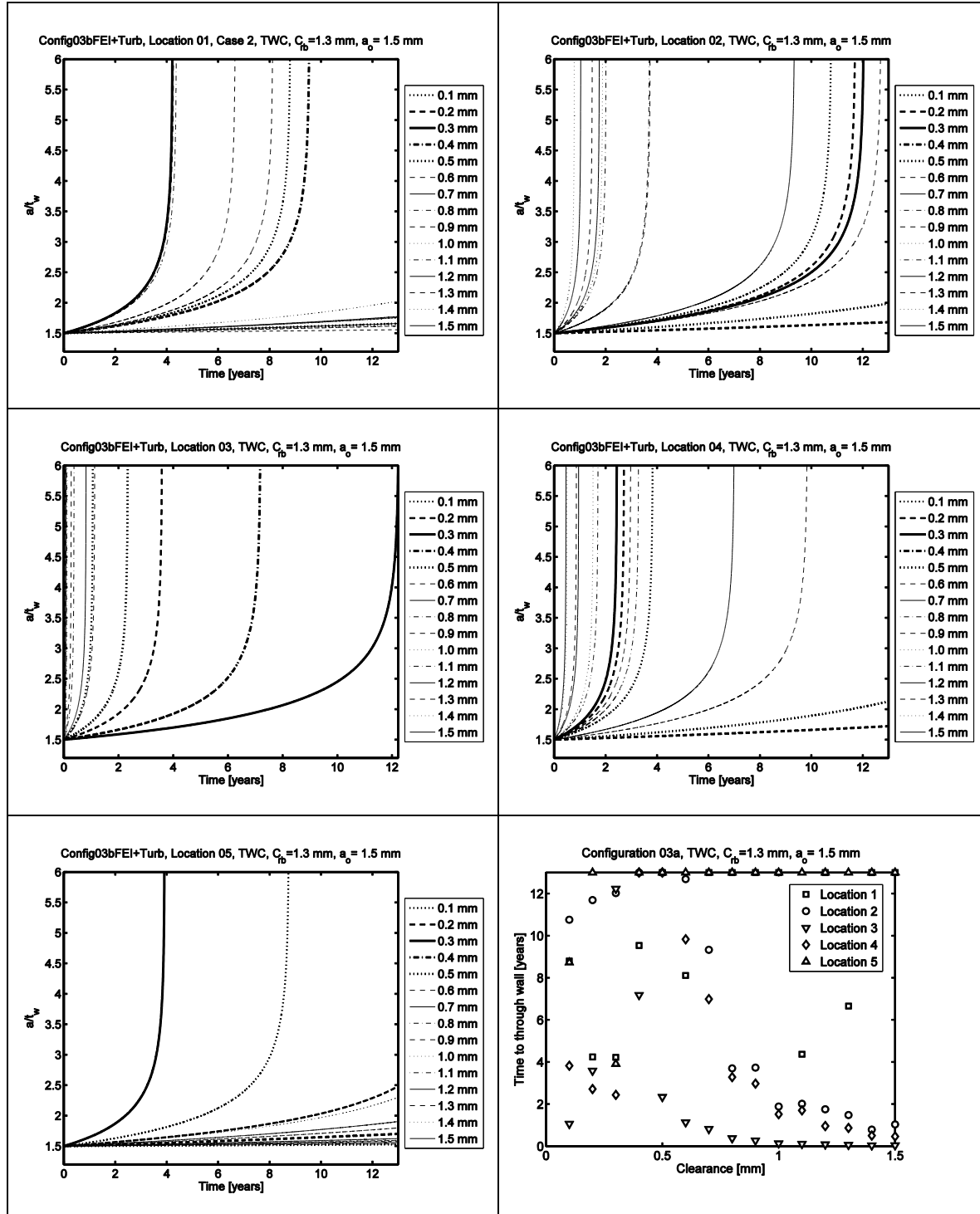
Figure E7: Circumferential Through-Wall crack growth for initial crack size ao=1.5 mm, and a base clearance 0f 1.30mm.
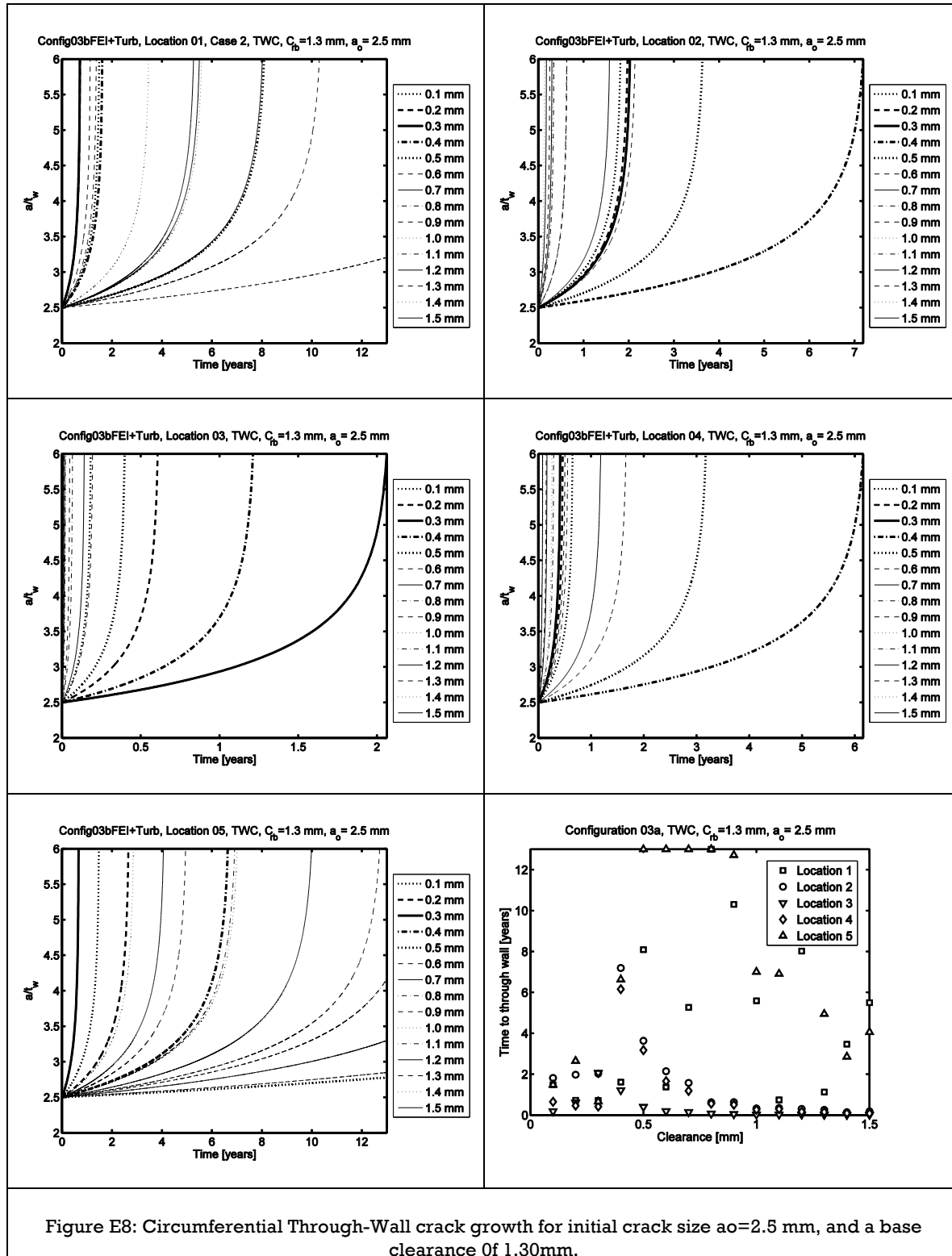
Figure E8: Circumferential Through-Wall crack growth for initial crack size ao=2.5 mm, and a base clearance 0f 1.30mm.
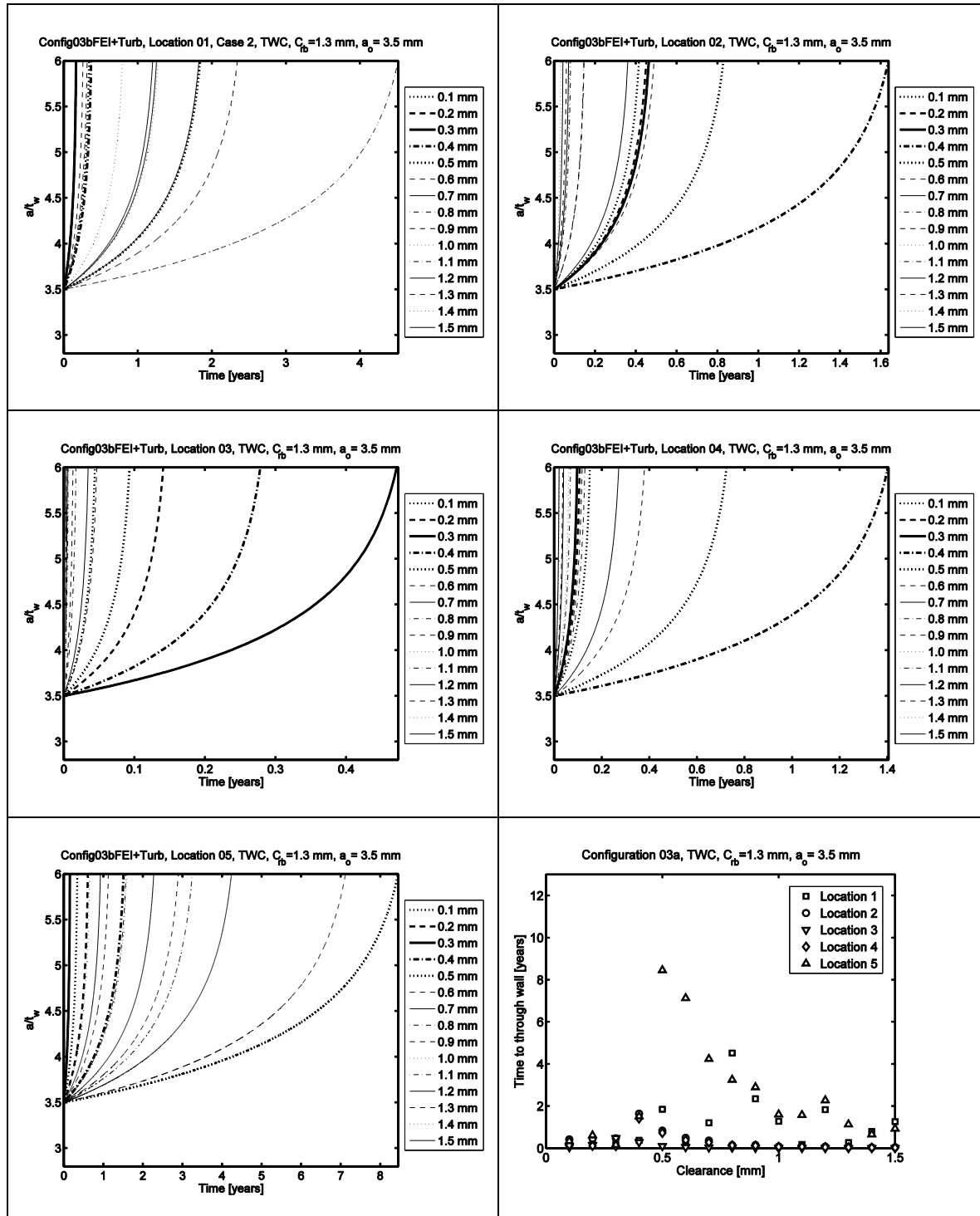
Figure E9: Circumferential Through-Wall crack growth for initial crack size ao=3.5 mm, and a base clearance 0f 1.30mm.

**Table E1: Config03b, TWC, 45%**

**Table E2: Config03b, TWC, 50%**

**Table E3: Config03b, TWC, 55%**

**Table E4: Config03b, TWC, 60%**

**Table E5: Config03b, TWC, 65%**

**Table E6: Config03b, TWC, 70%**

**Table E7: Config03b, TWC, 75%**

# Appendix F

Configuration 03c, Circumferential Through-Wall crack growth for U-bend tube subjected to turbulence in addition to fluid-elastic instability excitation.
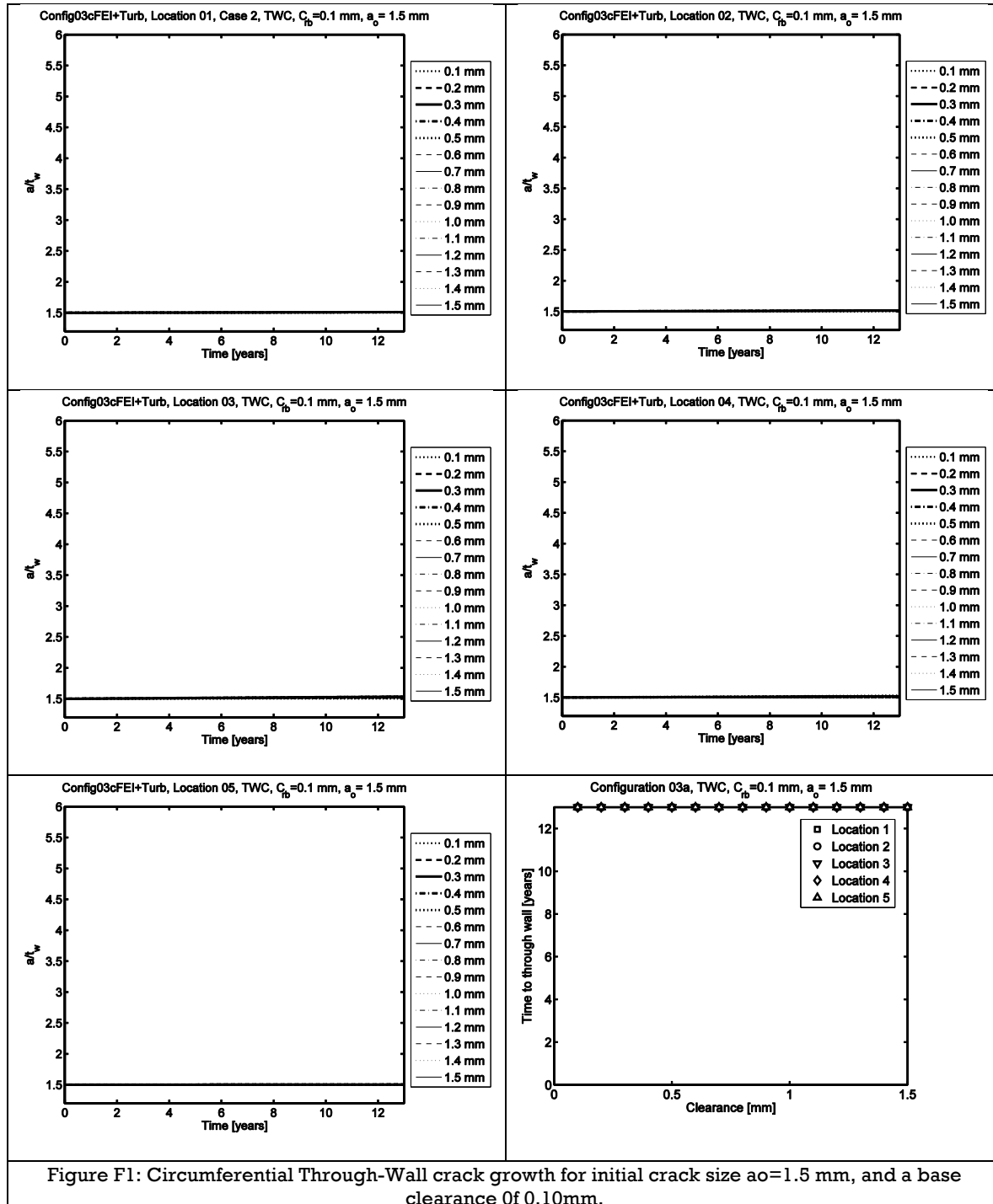


Figure F1: Circumferential Through-Wall crack growth for initial crack size ao=1.5 mm, and a base clearance 0f 0.10mm.
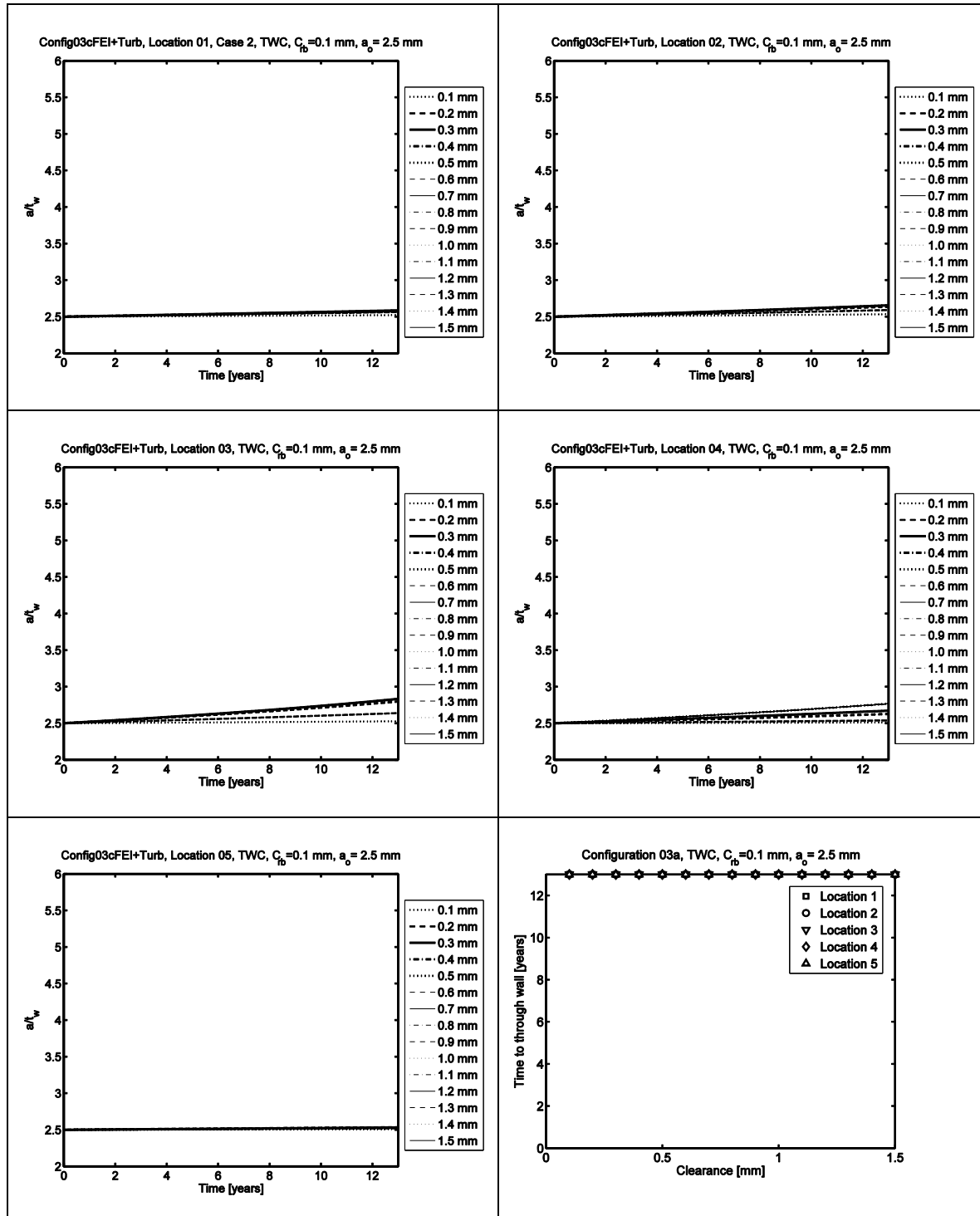
Figure F2: Circumferential Through-Wall crack growth for initial crack size ao=2.5 mm, and a base clearance 0f 0.10mm.
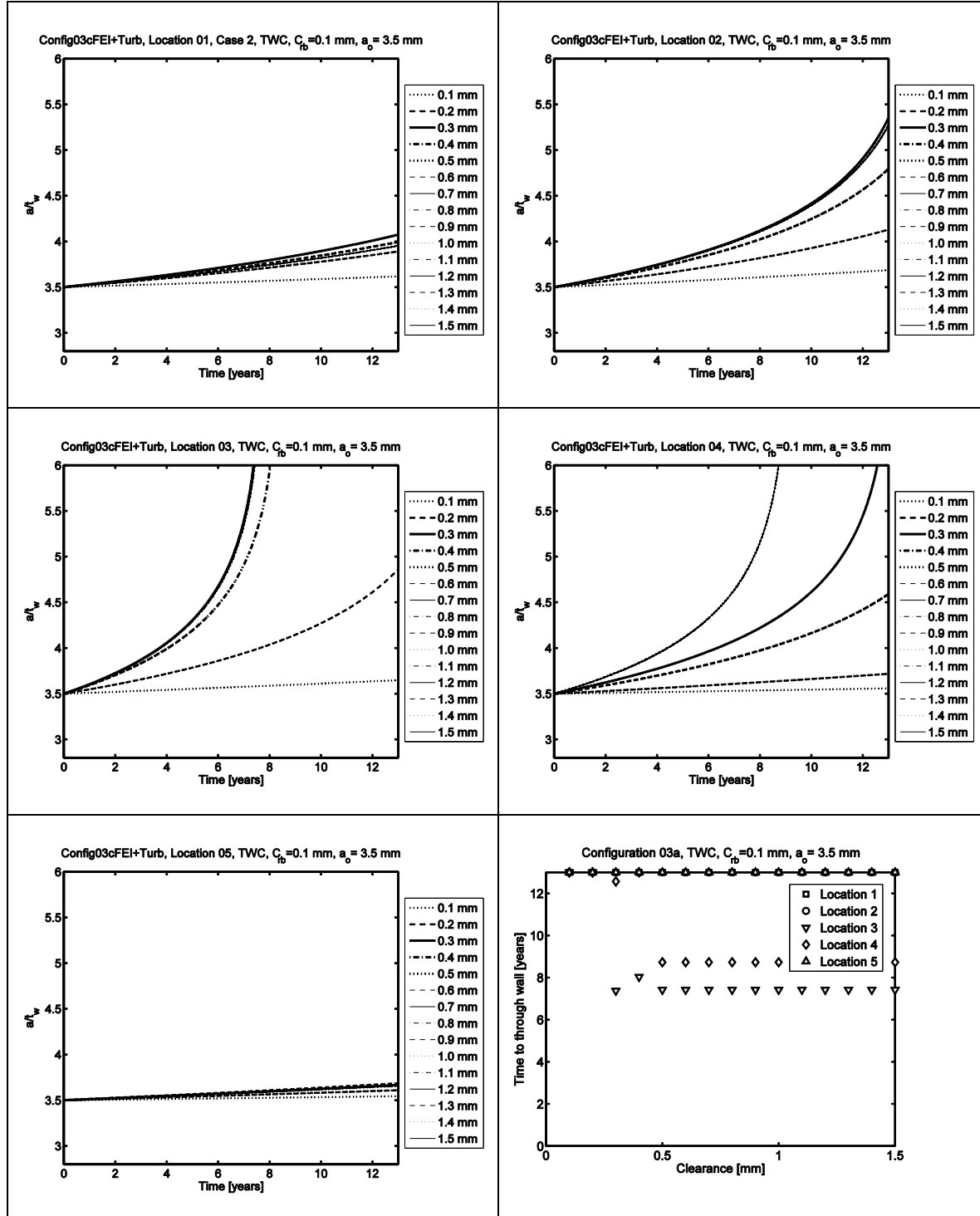
Figure F3: Circumferential Through-Wall crack growth for initial crack size ao=3.5 mm, and a base clearance 0f 0.10mm.
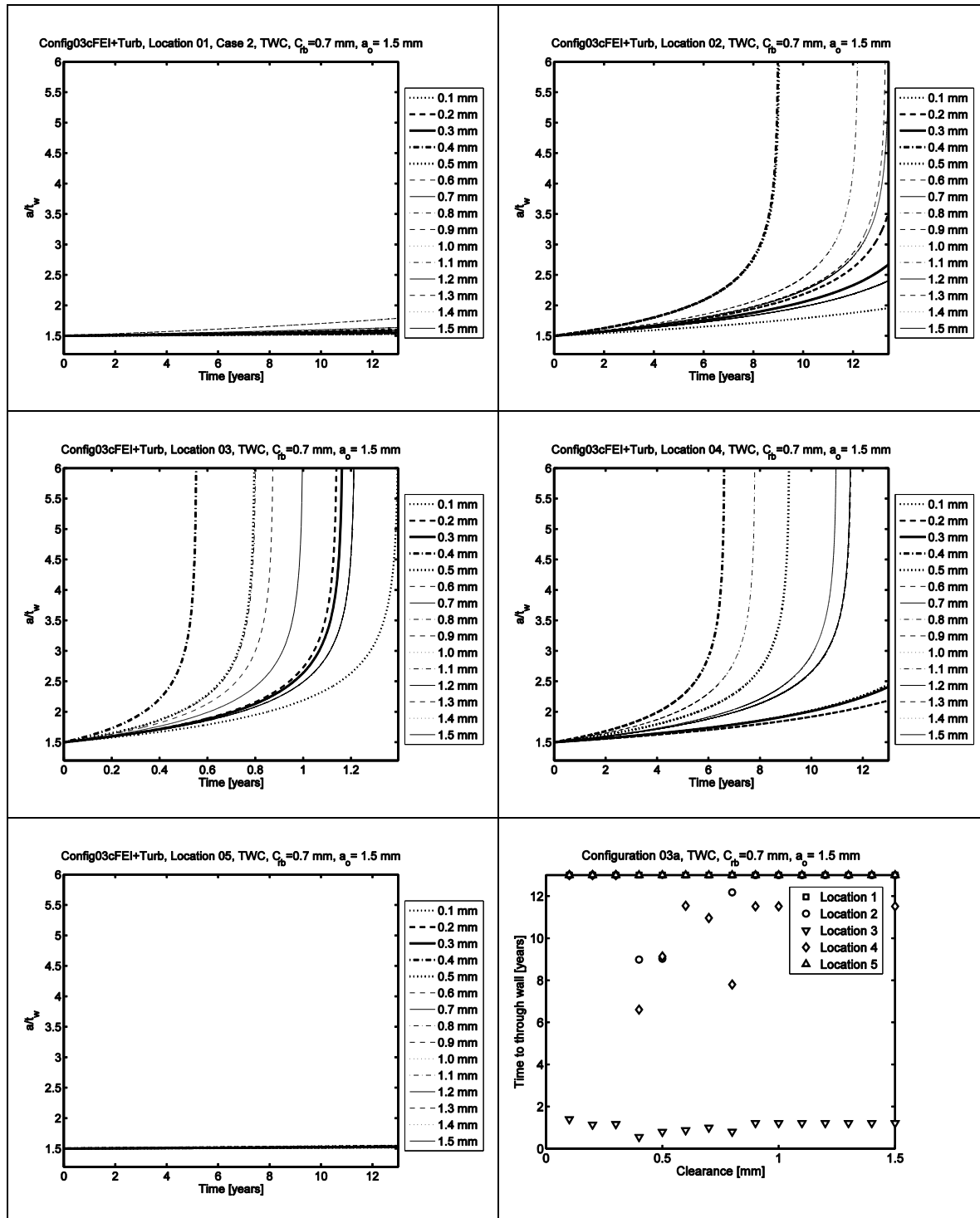
Figure F4: Circumferential Through-Wall crack growth for initial crack size ao=1.5 mm, and a base clearance 0f 0.70mm.
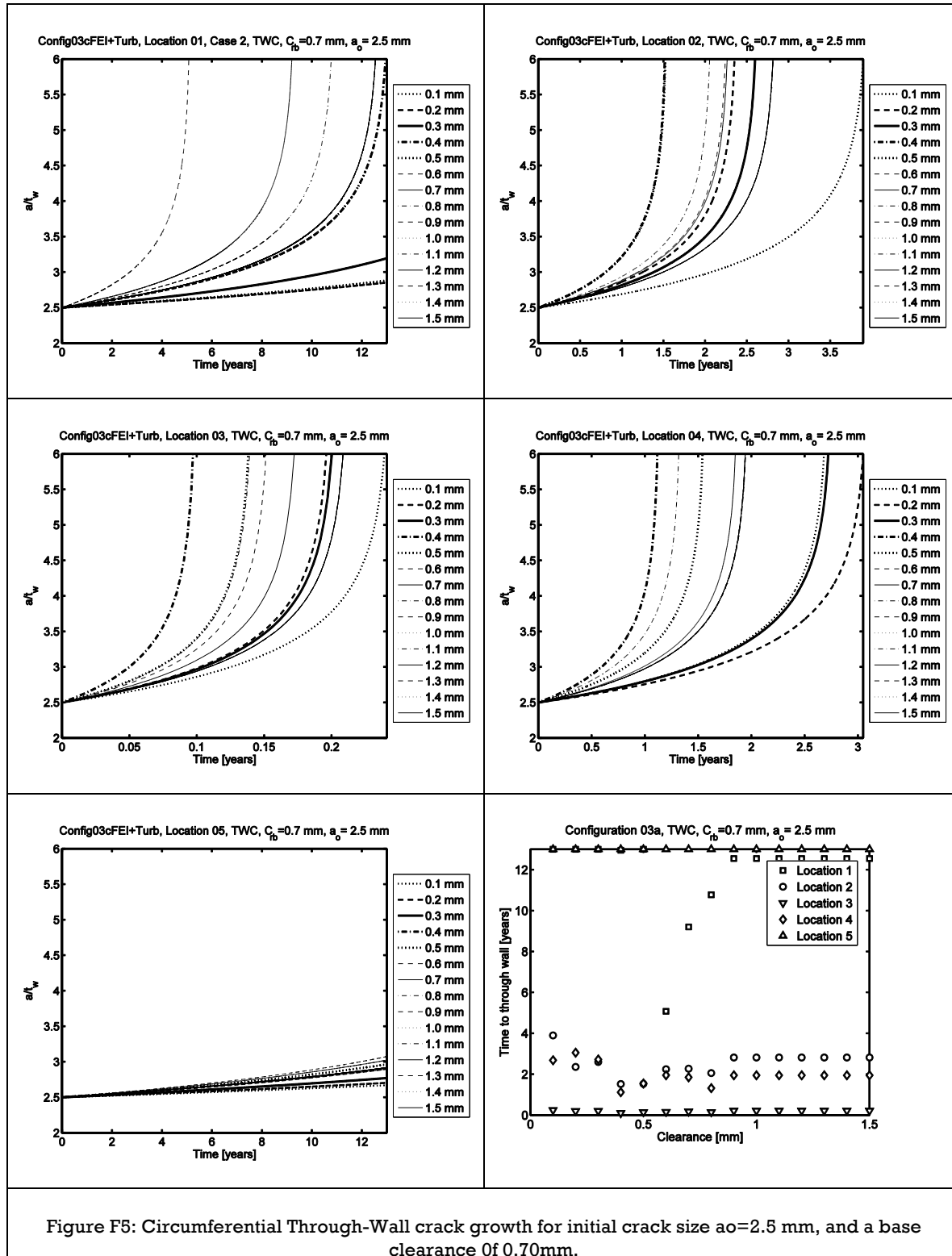
Figure F5: Circumferential Through-Wall crack growth for initial crack size ao=2.5 mm, and a base clearance 0f 0.70mm.
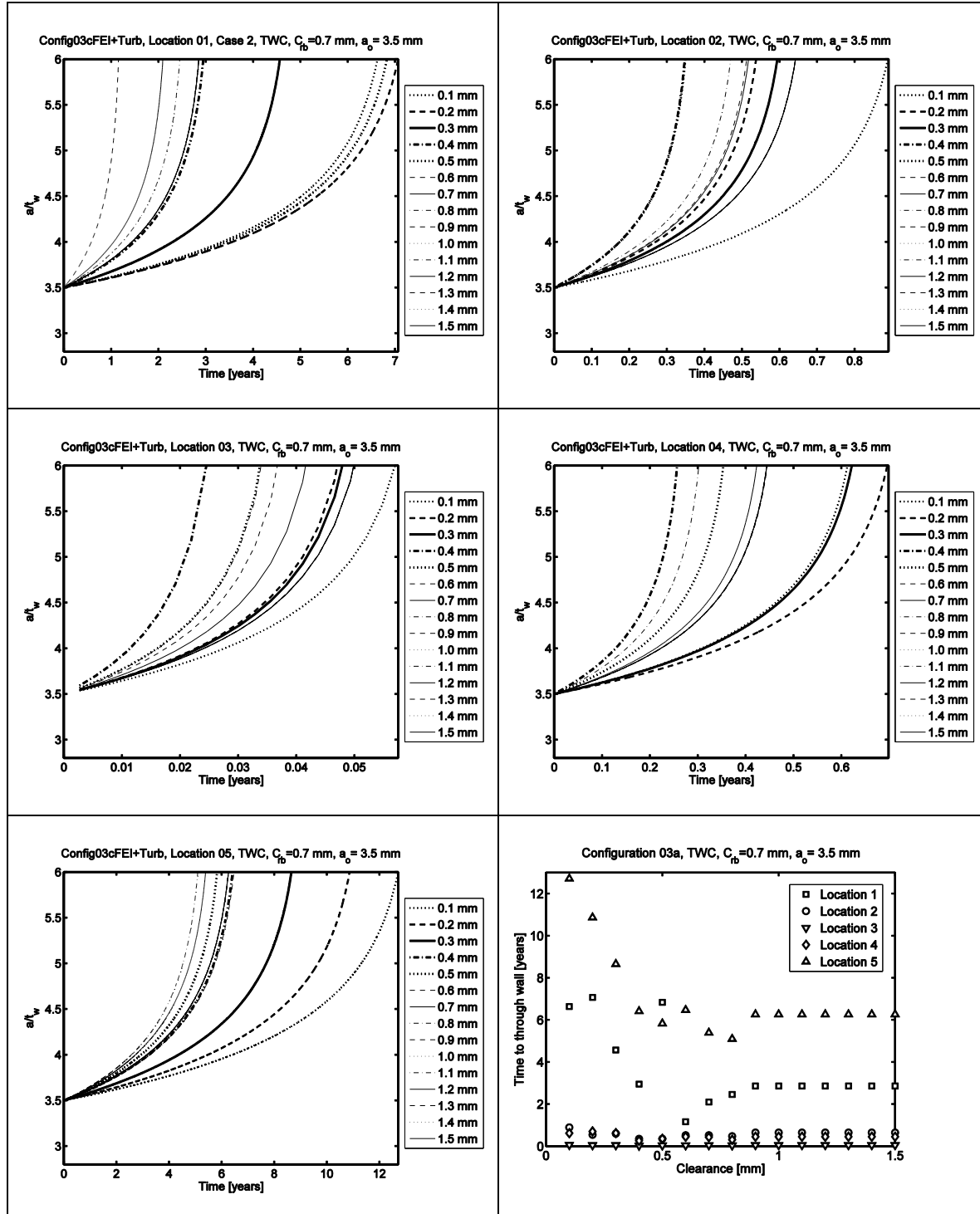
Figure F6: Circumferential Through-Wall crack growth for initial crack size ao=3.5 mm, and a base clearance 0f 0.70mm.
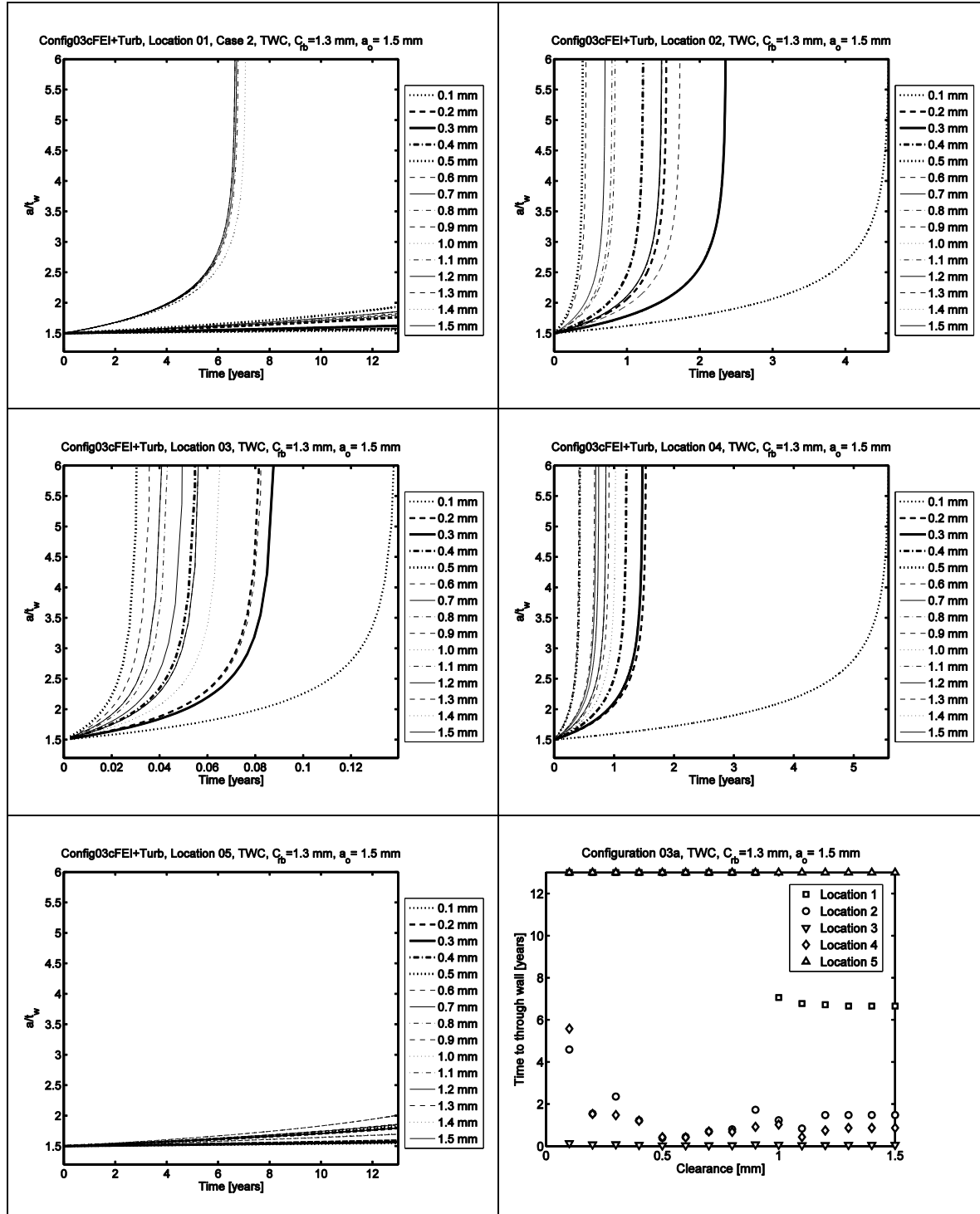
Figure F7: Circumferential Through-Wall crack growth for initial crack size ao=1.5 mm, and a base clearance 0f 1.30mm.
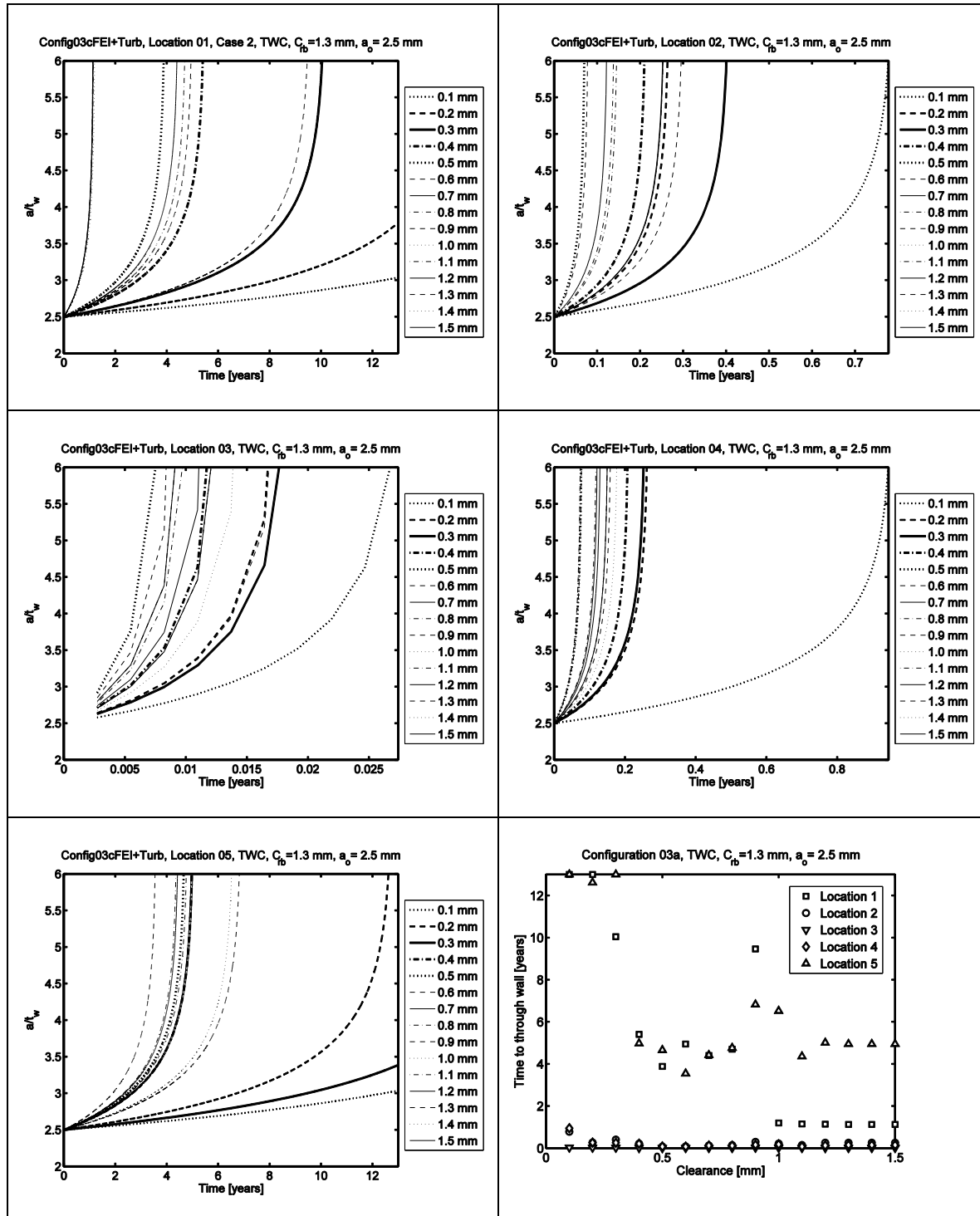
Figure F8: Circumferential Through-Wall crack growth for initial crack size ao=2.5 mm, and a base clearance 0f 1.30mm.

Figure F9: Circumferential Through-Wall crack growth for initial crack size ao=3.5 mm, and a base clearance 0f 1.30mm.

**Table b1: Config03a, SCC, 50%**

| Base Clearance | SB3 clearance | | | | |
|:---:|:---:|:---:|:---:|:---:|:---:|
| | Location 1 | Location 2 | Location 3 | Location 4 | Location 5 |
| 0.10 | - | - | - | - | - |
| 0.20 | - | - | - | - | - |
| 0.30 | - | - | - | - | - |
| 0.40 | - | - | - | - | - |
| 0.50 | - | - | - | - | - |
| 0.60 | | | 0.6 | | |
| 0.70 | - | - | 0.1 | - | - |
| 0.80 | - | - | 0.1 | - | - |
| 0.90 | - | - | 0.1 | - | - |
| 1.00 | - | 0.9 | 0.1 | 0.8 | - |
| 1.10 | - | 0.4 | 0.1 | 0.4 | - |
| 1.20 | - | 0.2 | 0.1 | 0.4 | - |
| 1.30 | - | 0.2 | 0.1 | 0.2 | - |
| 1.40 | 0.9 | 0.1 | 0.1 | 0.1 | - |
| 1.50 | - | 0.1 | 0.1 | 0.2 | - |

**Table b3: Config03a, SCC, 55%**

| Base Clearance | SB3 clearance | | | | |
|:---:|:---:|:---:|:---:|:---:|:---:|
| | Location 1 | Location 2 | Location 3 | Location 4 | Location 5 |
| 0.1 | - | - | - | - | - |
| 0.2 | - | - | - | - | - |
| 0.3 | - | - | - | - | - |
| 0.4 | - | - | - | - | - |
| 0.5 | - | - | - | - | - |
| 0.6 | - | - | 0.3 | - | - |
| 0.7 | - | - | 0.1 | - | - |
| 0.8 | - | - | 0.1 | - | - |
| 0.9 | - | - | 0.1 | - | - |
| 1 | - | 0.9 | 0.1 | 0.8 | - |
| 1.1 | - | 0.4 | 0.1 | 0.4 | - |
| 1.2 | - | 0.1 | 0.1 | 0.1 | - |
| 1.3 | - | 0.2 | 0.1 | 0.2 | - |
| 1.4 | 0.9 | 0.1 | 0.1 | 0.1 | - |
| 1.5 | - | 0.1 | 0.1 | 0.2 | - |

**Table b4: Config03a, SCC, 60%**

| Base Clearance | SB3 clearance | | | | |
|:---:|:---:|:---:|:---:|:---:|:---:|
| | Location 1 | Location 2 | Location 3 | Location 4 | Location 5 |
| 0.1 | - | - | - | - | - |
| 0.2 | - | - | - | - | - |
| 0.3 | - | - | - | - | - |
| 0.4 | - | - | - | - | - |
| 0.5 | - | - | 0.5 | - | - |
| 0.6 | - | - | 0.3 | - | - |
| 0.7 | - | - | 0.1 | - | - |
| 0.8 | - | - | 0.1 | - | - |
| 0.9 | - | - | 0.1 | 0.6 | - |
| 1 | - | 0.5 | 0.1 | 0.7 | - |
| 1.1 | - | 0.3 | 0.1 | 0.2 | - |
| 1.2 | - | 0.1 | 0.1 | 0.1 | - |
| 1.3 | - | 0.2 | 0.1 | 0.2 | - |
| 1.4 | 0.9 | 0.1 | 0.1 | 0.1 | - |
| 1.5 | - | 0.1 | 0.1 | 0.1 | - |

**Table b5: Config03a, SCC, 65%**

| Base Clearance | SB3 clearance | | | | |
|:---:|:---:|:---:|:---:|:---:|:---:|
| | Location 1 | Location 2 | Location 3 | Location 4 | Location 5 |
| 0.1 | - | - | - | - | - |
| 0.2 | - | - | - | - | - |
| 0.3 | - | - | - | - | - |
| 0.4 | - | - | - | - | - |
| 0.5 | | | 0.5 | | |
| 0.6 | - | - | 0.1 | - | - |
| 0.7 | - | - | 0.1 | - | - |
| 0.8 | - | - | 0.1 | - | - |
| 0.9 | - | 0.6 | 0.1 | 0.6 | - |
| 1 | - | 0.5 | 0.1 | 0.3 | - |
| 1.1 | - | 0.1 | 0.1 | 0.2 | - |
| 1.2 | - | 0.1 | 0.1 | 0.1 | - |
| 1.3 | - | 0.2 | 0.1 | 0.2 | - |
| 1.4 | 0.9 | 0.1 | 0.1 | 0.1 | - |
| 1.5 | - | 0.1 | 0.1 | 0.1 | - |

**Table b6: Config03a, SCC, 70%**

| Base Clearance | SB3 clearance | | | | |
|---|---|---|---|---|---|
| | Location 1 | Location 2 | Location 3 | Location 4 | Location 5 |
| 0.1 | - | - | - | - | - |
| 0.2 | - | - | - | - | - |
| 0.3 | - | - | - | - | - |
| 0.4 | - | - | - | - | - |
| 0.5 | - | - | 0.3 | - | - |
| 0.6 | - | - | 0.1 | - | - |
| 0.7 | - | - | 0.1 | - | - |
| 0.8 | - | - | 0.1 | 0.6 | - |
| 0.9 | - | 0.4 | 0.1 | 0.3 | - |
| 1 | - | 0.1 | 0.1 | 0.2 | - |
| 1.1 | - | 0.1 | 0.1 | 0.2 | - |
| 1.2 | 1.1 | 0.1 | 0.1 | 0.1 | - |
| 1.3 | - | 0.1 | 0.1 | 0.2 | - |
| 1.4 | 0.9 | 0.1 | 0.1 | - | - |
| 1.5 | - | 0.1 | 0.1 | 0.1 | - |

**Table b7: Config03a, SCC, 75%**

| Base Clearance | SB3 clearance | | | | |
|---|---|---|---|---|---|
| | Location 1 | Location 2 | Location 3 | Location 4 | Location 5 |
| 0.1 | - | - | - | - | - |
| 0.2 | - | - | - | - | - |
| 0.3 | - | - | 0.4 | - | - |
| 0.4 | - | - | 0.1 | - | - |
| 0.5 | - | - | 0.1 | 0.6 | - |
| 0.6 | - | 0.5 | 0.1 | 0.5 | - |
| 0.7 | - | 0.2 | 0.1 | 0.1 | - |
| 0.8 | - | 0.1 | 0.1 | 0.1 | - |
| 0.9 | 0.7 | 0.1 | 0.1 | 0.1 | - |
| 1 | - | 0.1 | 0.1 | 0.1 | - |
| 1.1 | 0.9 | 0.1 | 0.1 | 0.1 | - |
| 1.2 | 1.1 | 0.1 | 0.1 | 0.1 | 1.1 |
| 1.3 | 1 | 0.1 | 0.1 | 0.1 | - |
| 1.4 | 0.9 | 0.1 | 0.1 | 0.1 | 0.4 |
| 1.5 | - | 0.1 | 0.1 | 0.1 | 0.8 |

# Appendix G

Configuration 03a, Circumferential Through-Wall crack growth for U-bend tube subjected to turbulence in addition to fluid-elastic instability excitation.
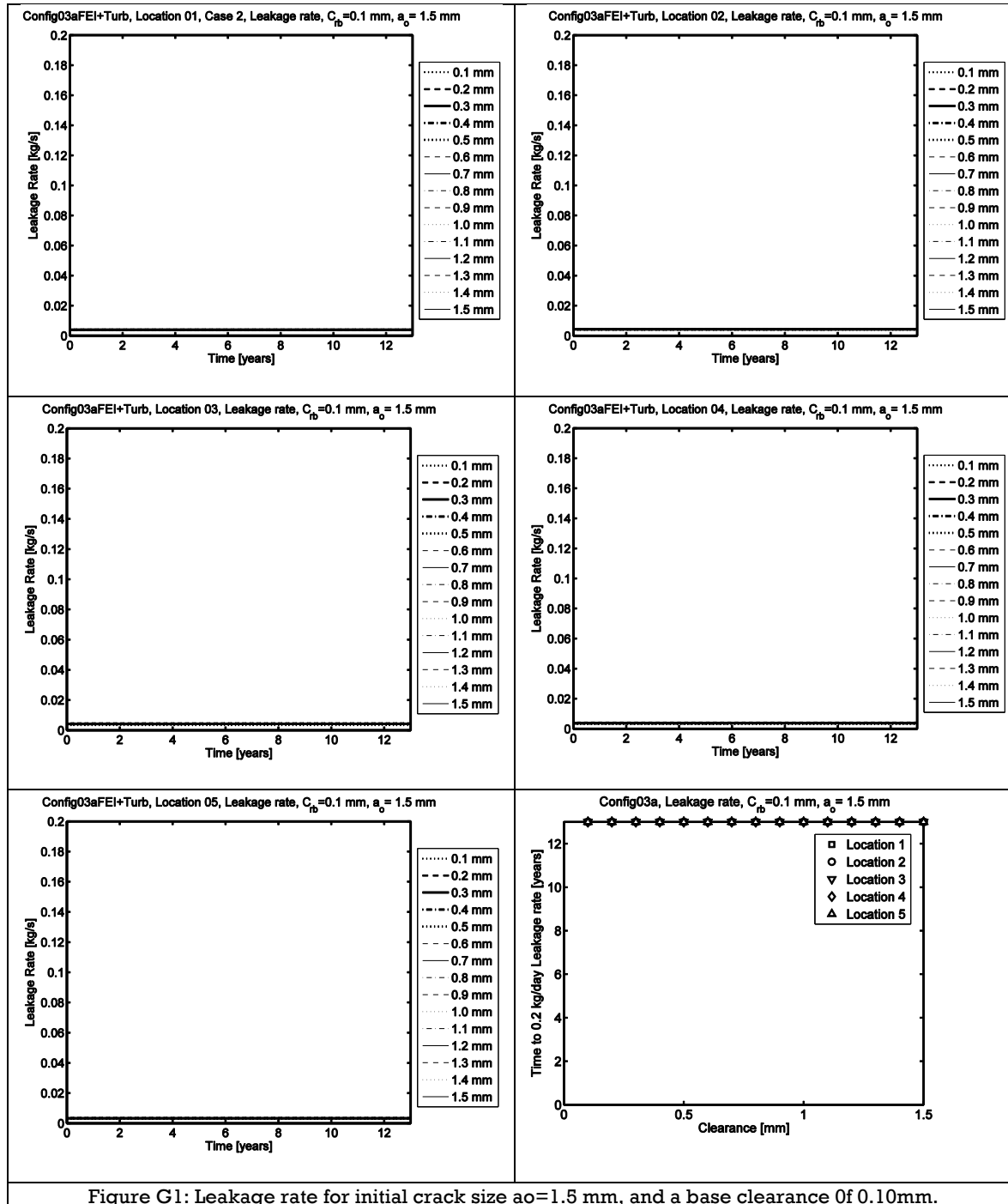


Figure G1: Leakage rate for initial crack size ao=1.5 mm, and a base clearance 0f 0.10mm.
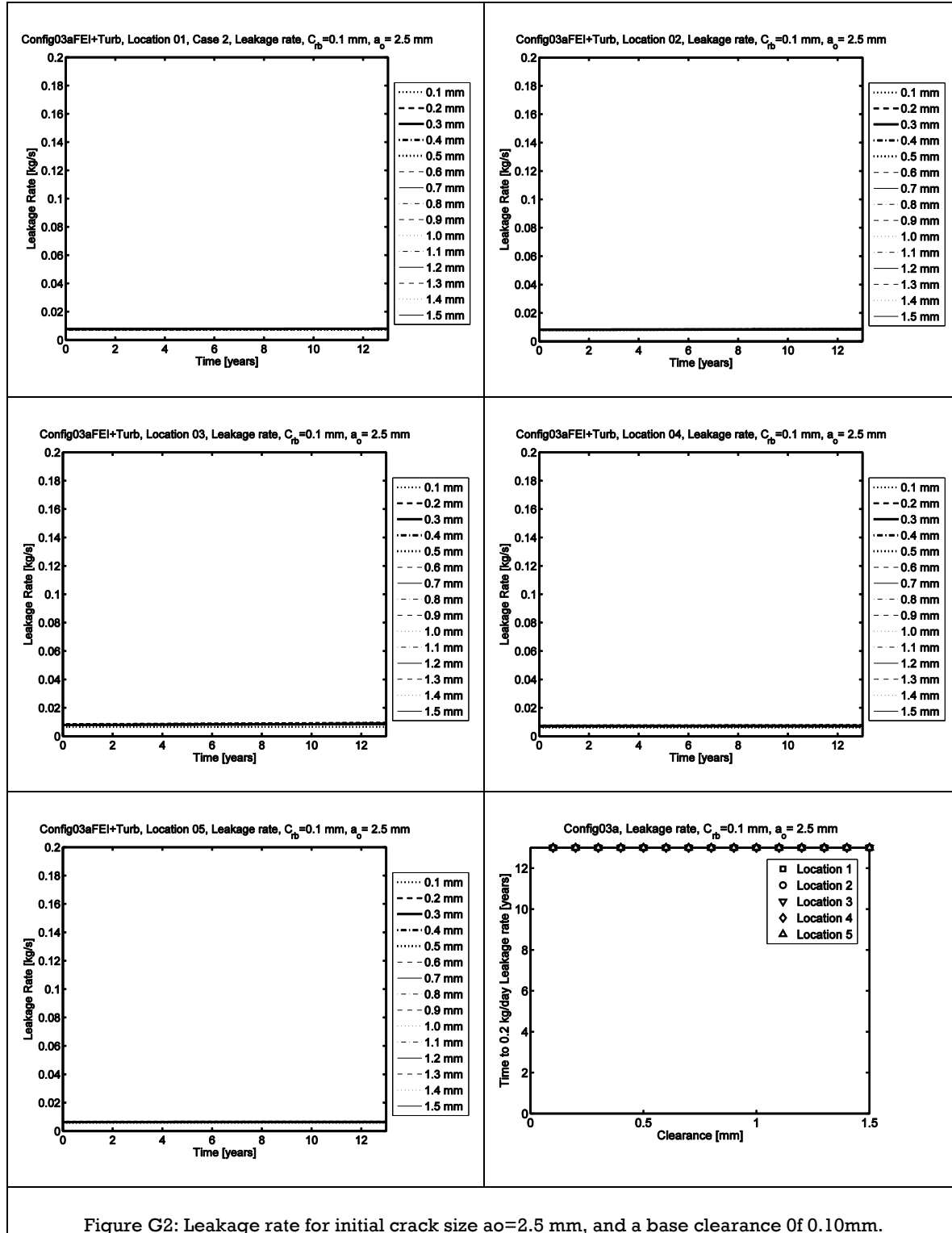
Figure G2: Leakage rate for initial crack size ao=2.5 mm, and a base clearance 0f 0.10mm.
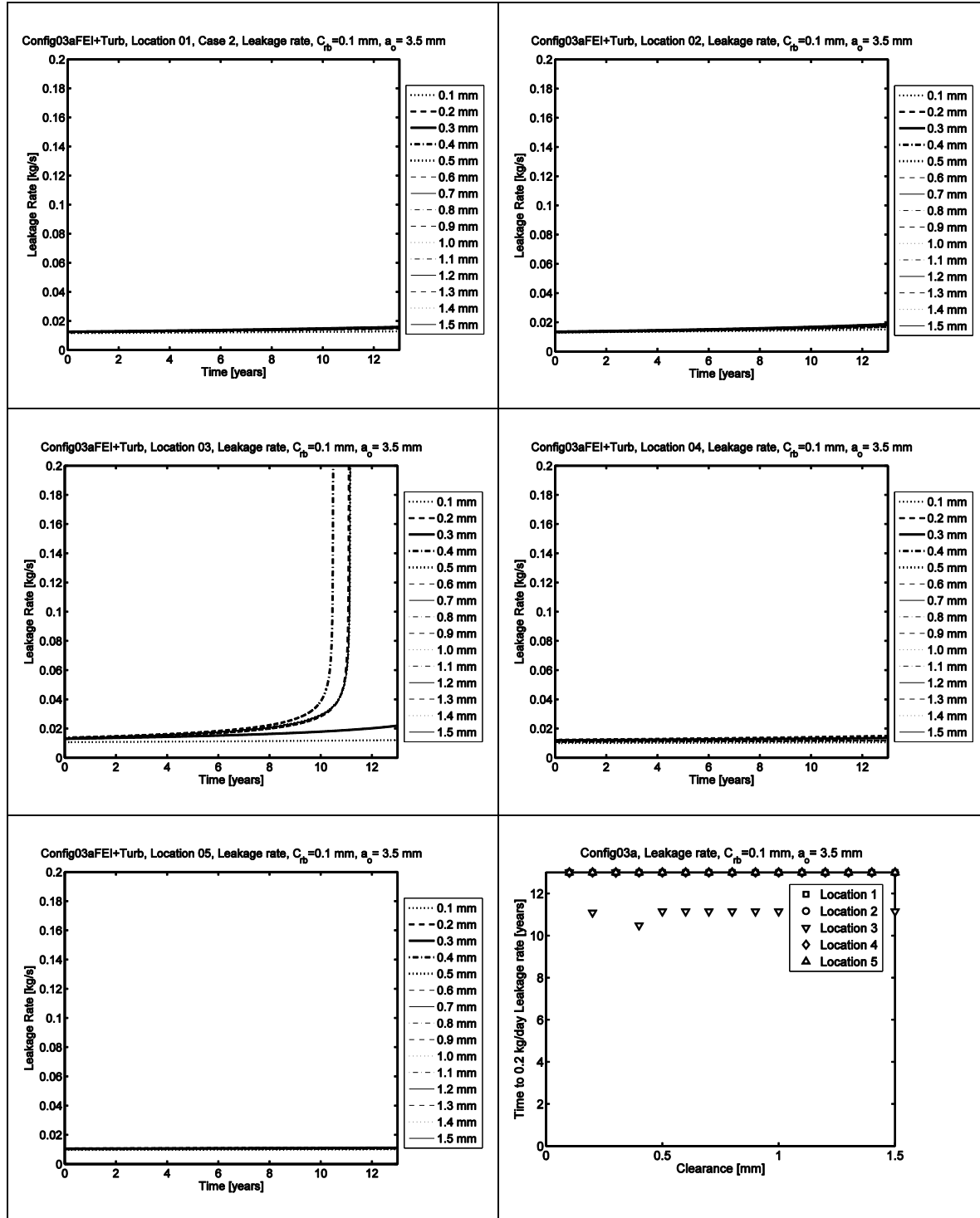
Figure G3: Leakage rate for initial crack size ao=3.5 mm, and a base clearance 0f 0.10mm.
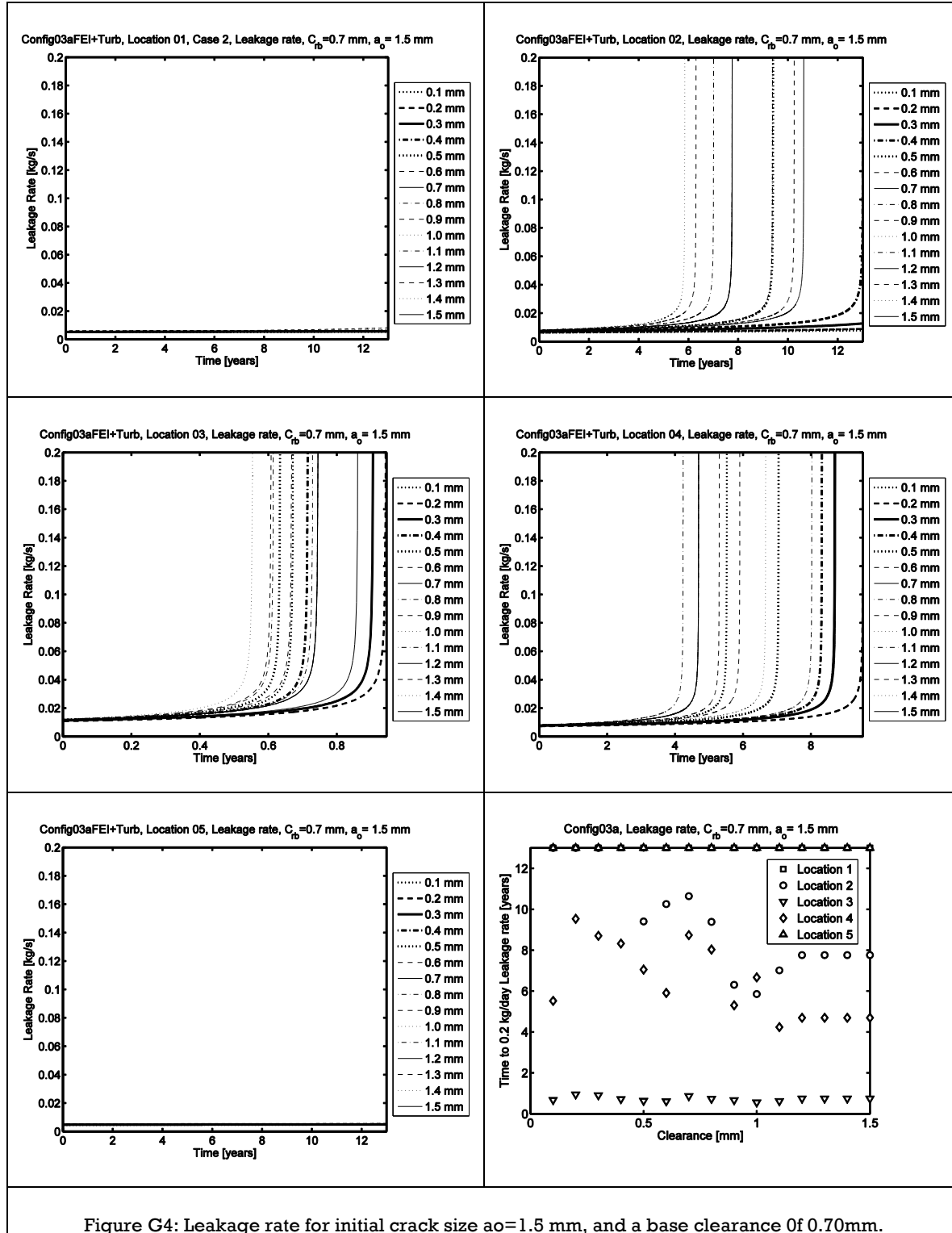
Figure G4: Leakage rate for initial crack size ao=1.5 mm, and a base clearance 0f 0.70mm.
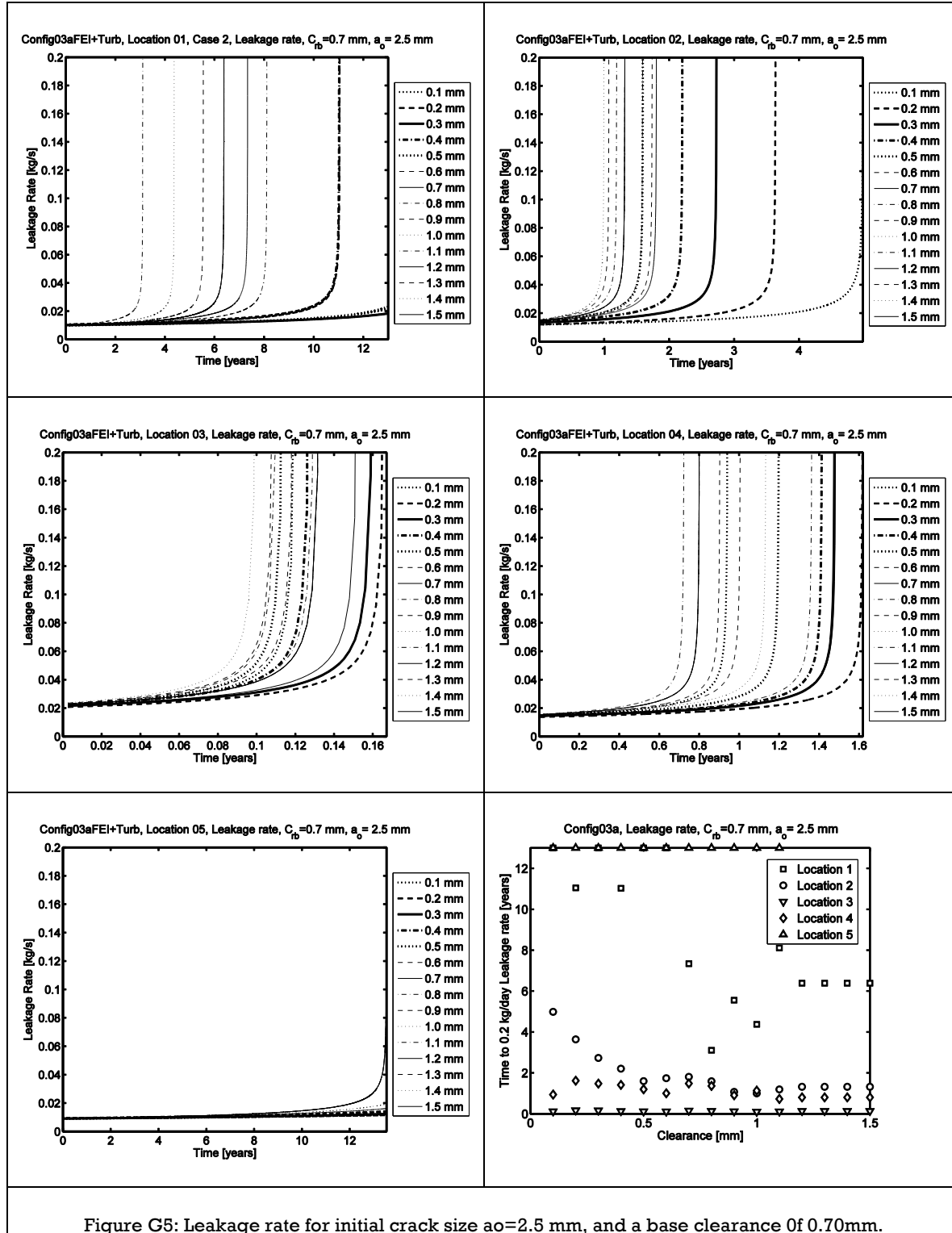
Figure G5: Leakage rate for initial crack size ao=2.5 mm, and a base clearance 0f 0.70mm.
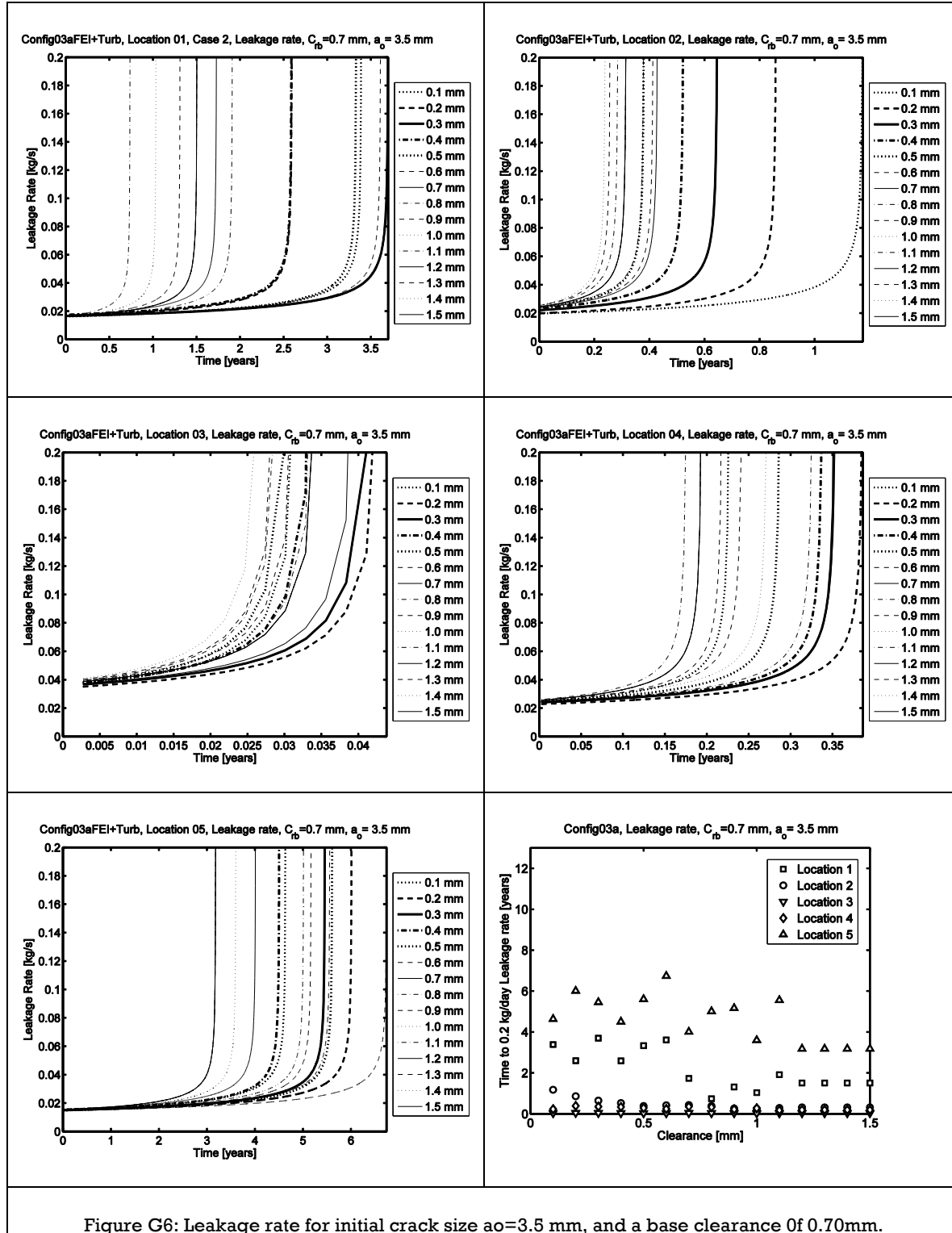
Figure G6: Leakage rate for initial crack size ao=3.5 mm, and a base clearance 0f 0.70mm.
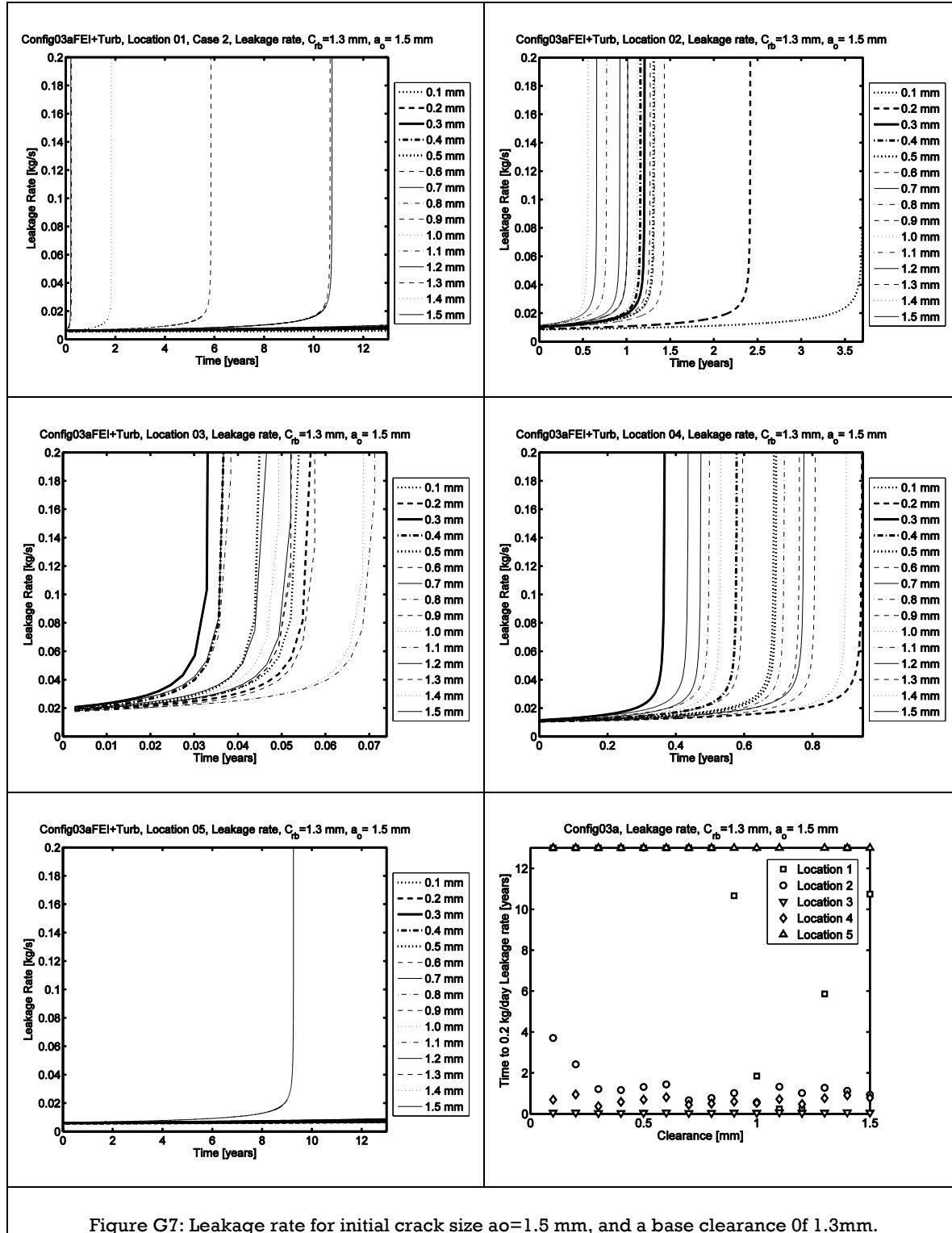
Figure G7: Leakage rate for initial crack size ao=1.5 mm, and a base clearance 0f 1.3mm.
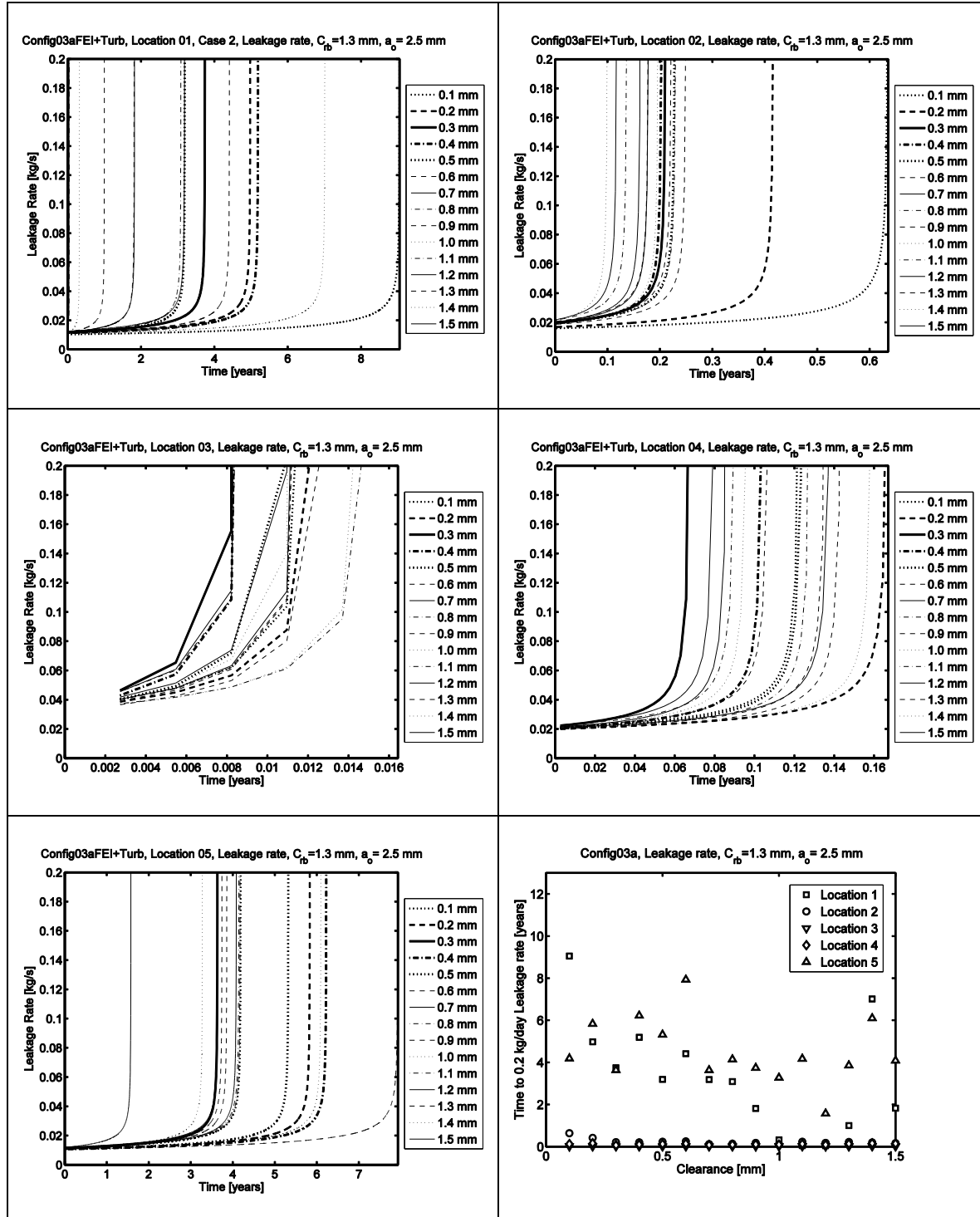
Figure G8: Leakage rate for initial crack size ao=2.5 mm, and a base clearance 0f 1.3mm.
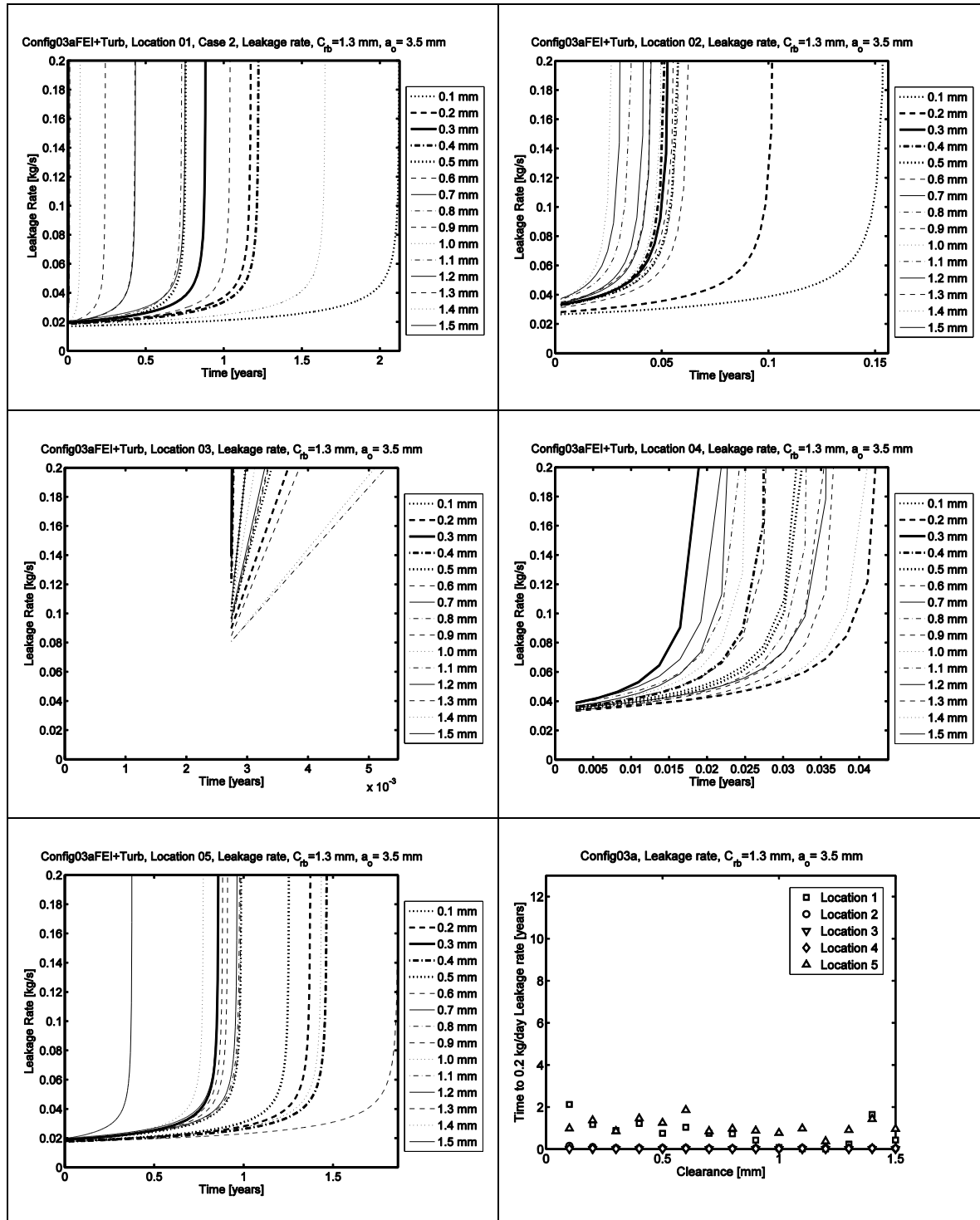
Figure G9: Leakage rate for initial crack size ao=3.5 mm, and a base clearance 0f 1.3mm.

**Table G1: Config03a, leakage rate, 45%**

**Table G2: Config03a, leakage rate, 50%**

**Table G3: Config03a, leakage rate, 55%**

**Table G4: Config03a, leakage rate, 60%**

**Table G5: Config03a, leakage rate, 65%**

**Table G6: Config03a, leakage rate, 70%**

**Table G6: Config03a, leakage rate, 75%**

# Appendix H

Configuration 03a, Circumferential Through-Wall crack growth for U-bend tube subjected to turbulence in addition to fluid-elastic instability excitation.
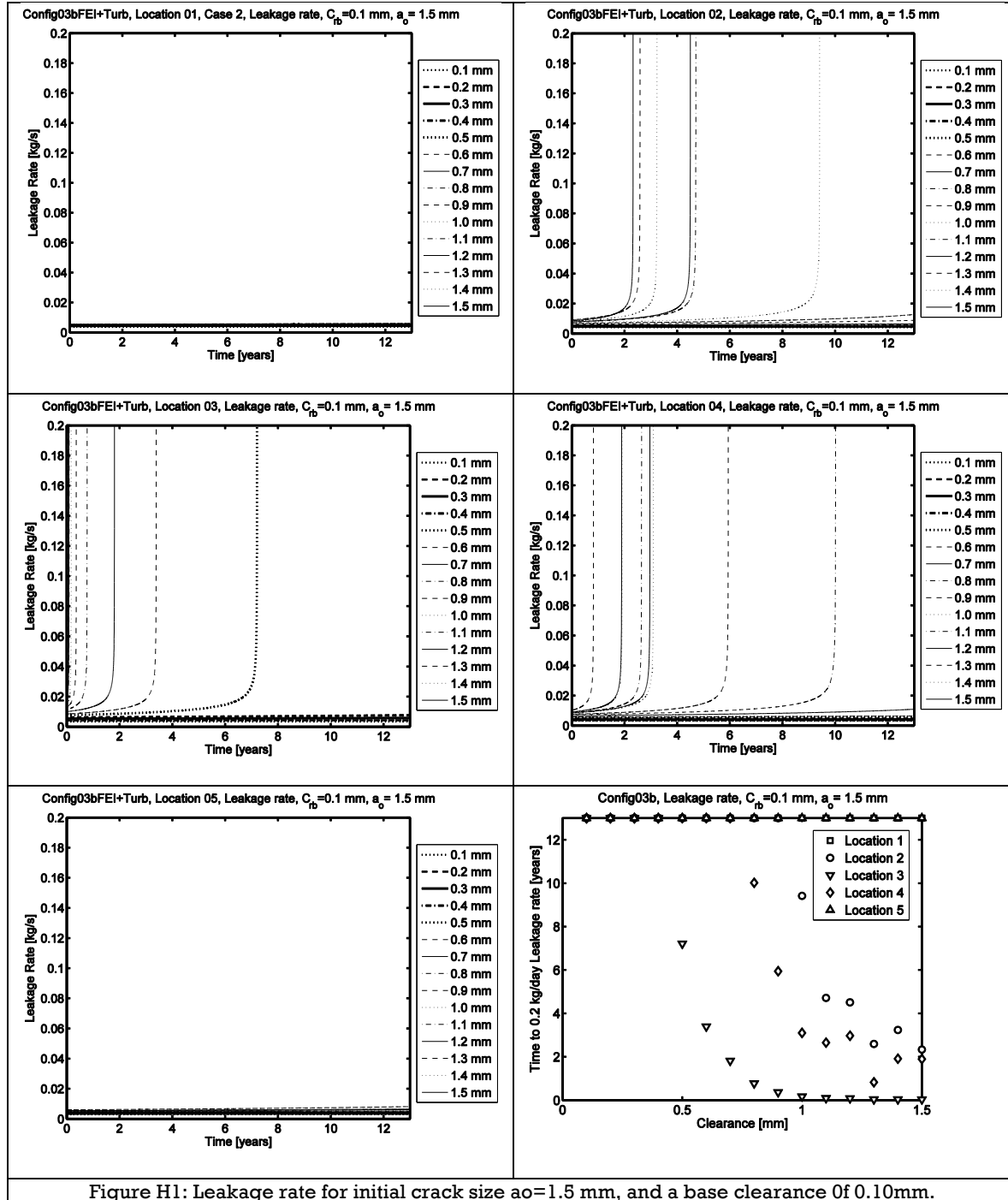


Figure H1: Leakage rate for initial crack size ao=1.5 mm, and a base clearance 0f 0.10mm.
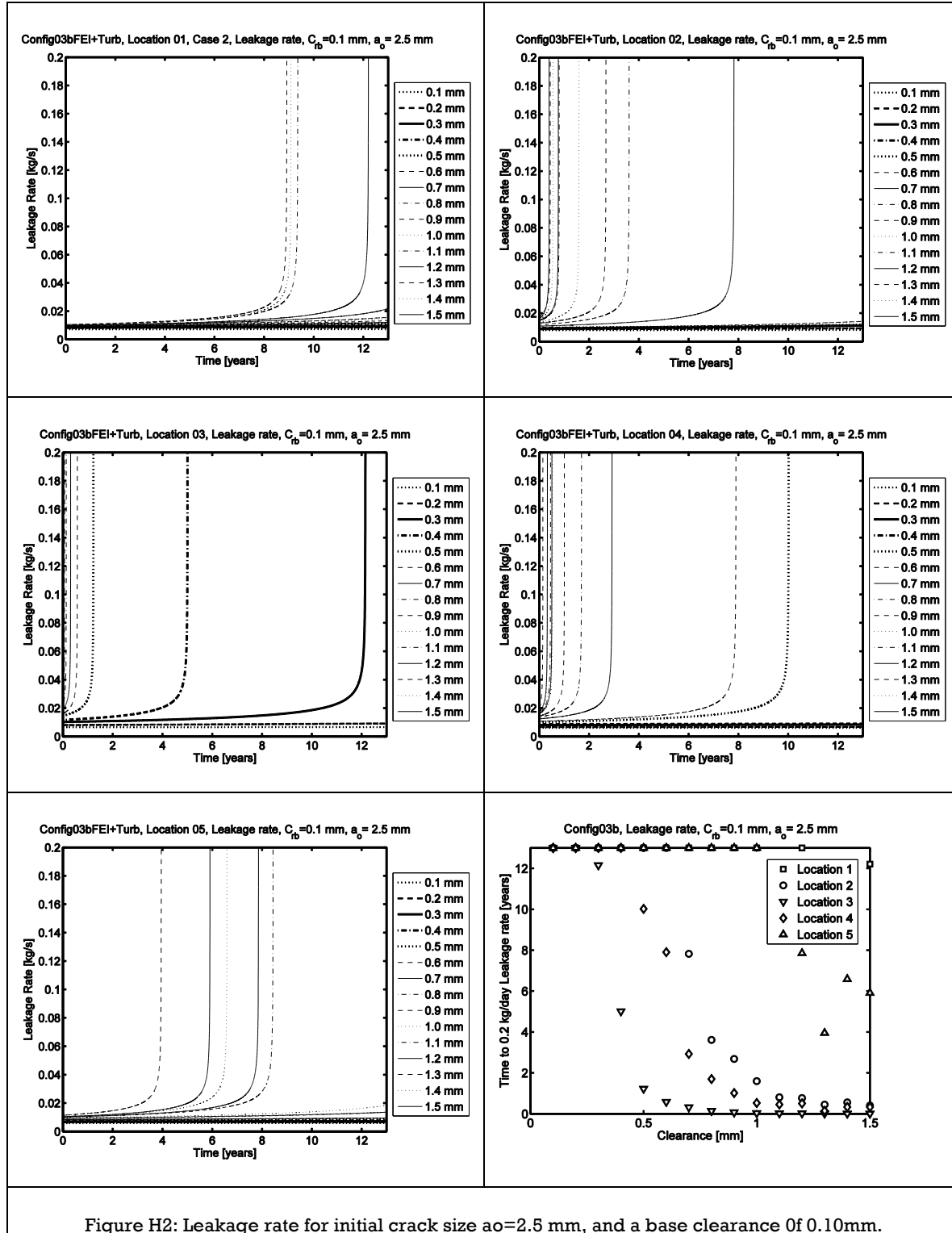
Figure H2: Leakage rate for initial crack size ao=2.5 mm, and a base clearance 0f 0.10mm.
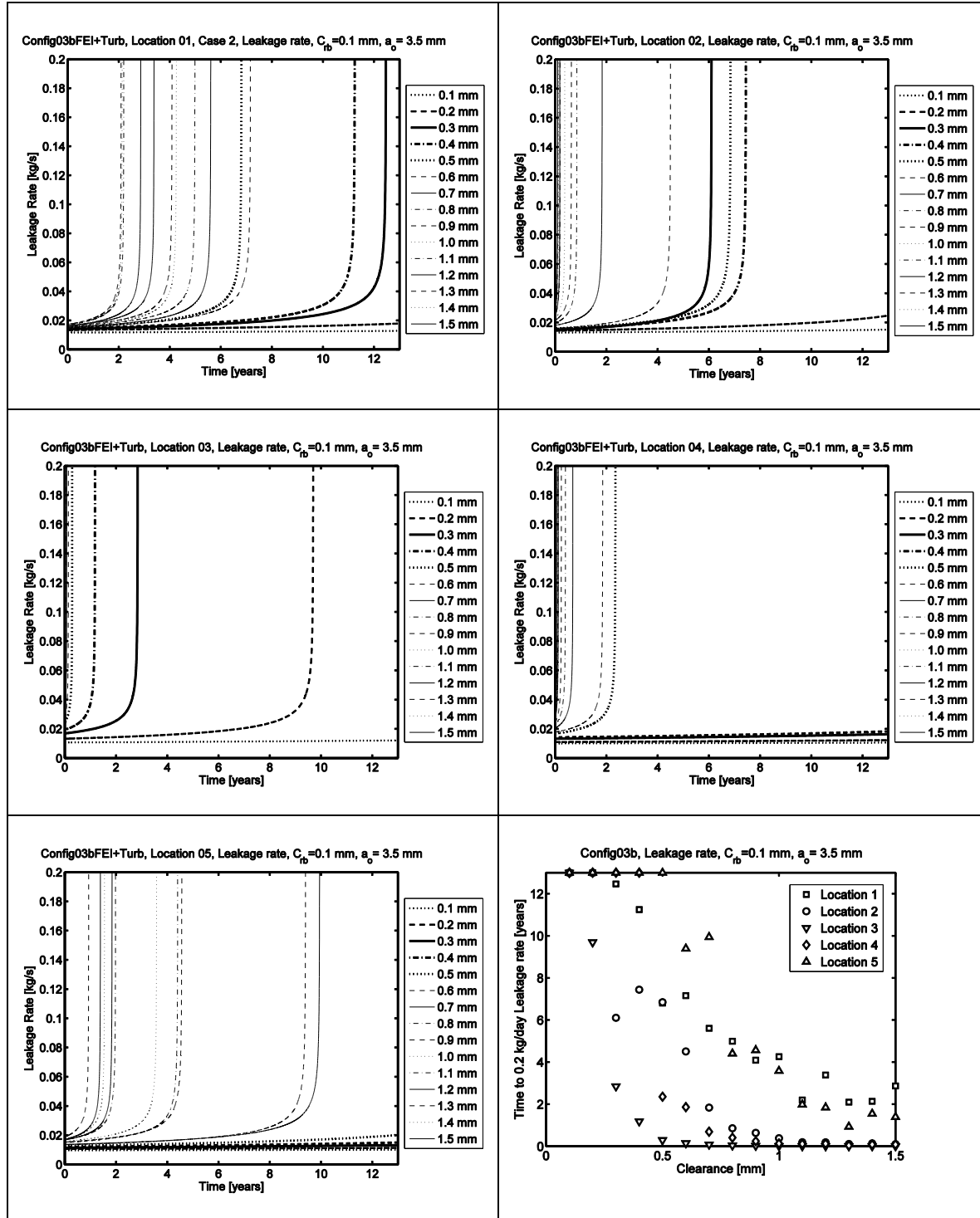
Figure H3: Leakage rate for initial crack size ao=3.5 mm, and a base clearance 0f 0.10mm.
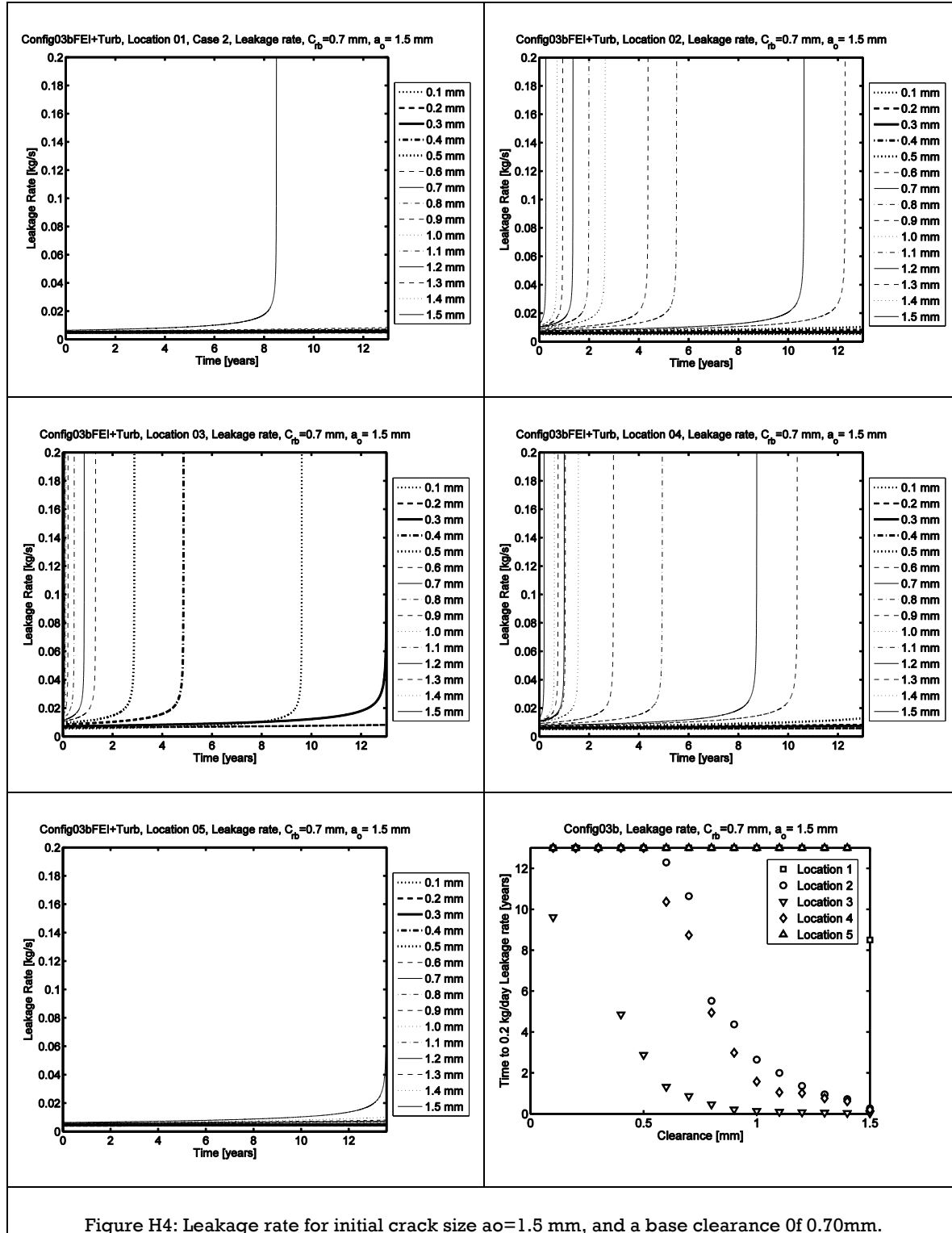
Figure H4: Leakage rate for initial crack size ao=1.5 mm, and a base clearance 0f 0.70mm.
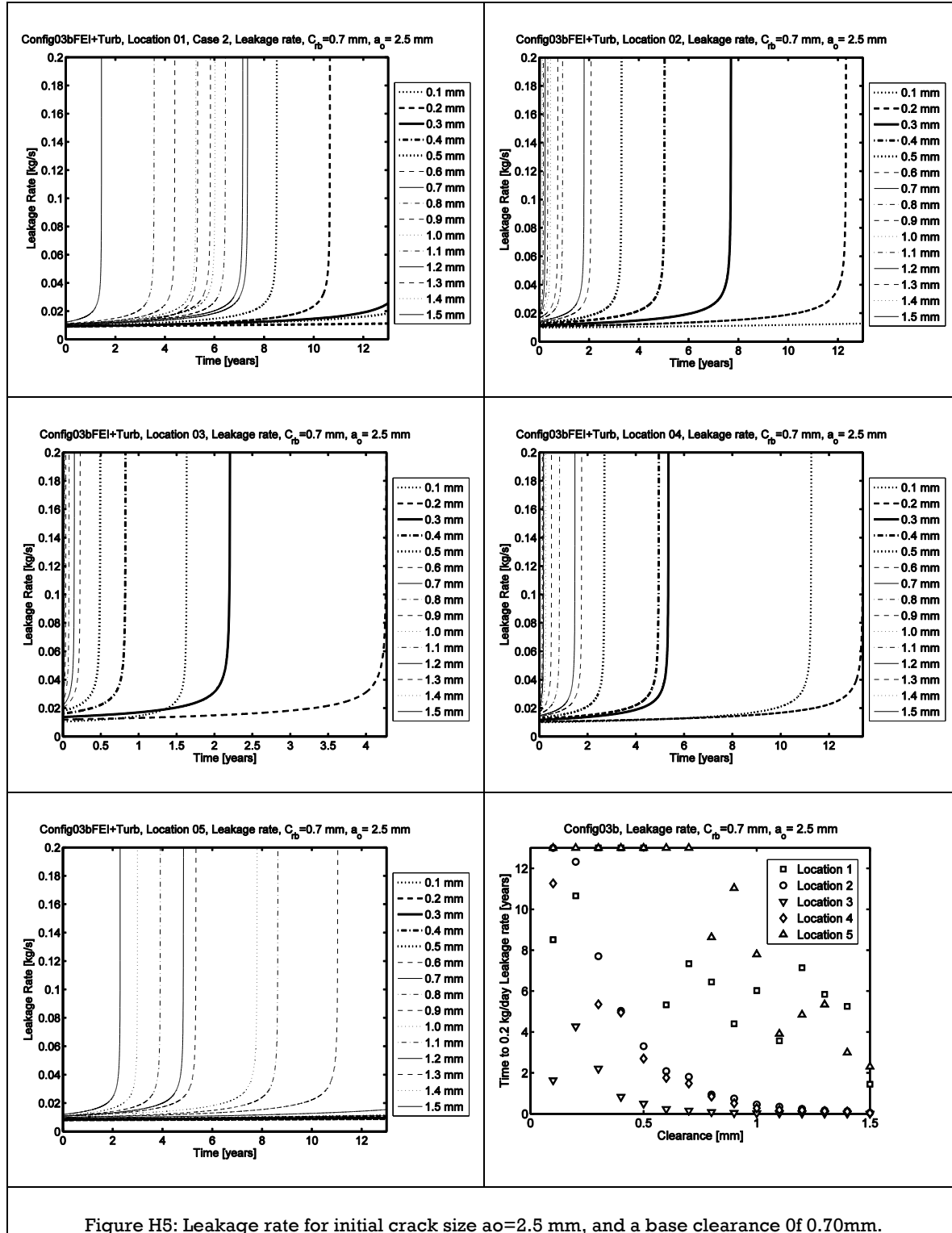
Figure H5: Leakage rate for initial crack size ao=2.5 mm, and a base clearance 0f 0.70mm.
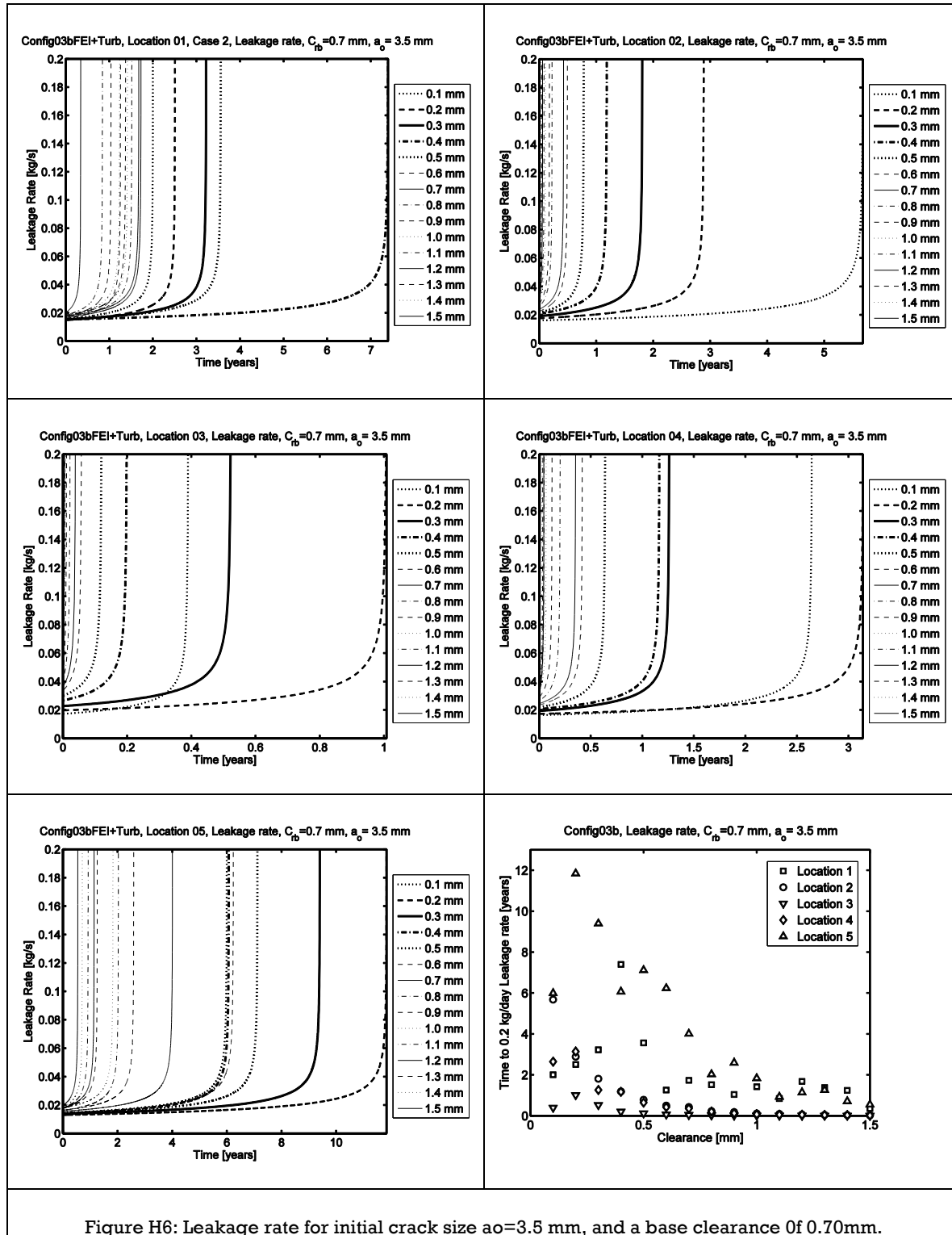
Figure H6: Leakage rate for initial crack size ao=3.5 mm, and a base clearance 0f 0.70mm.

Figure H7: Leakage rate for initial crack size ao=1.5 mm, and a base clearance 0f 1.3mm.
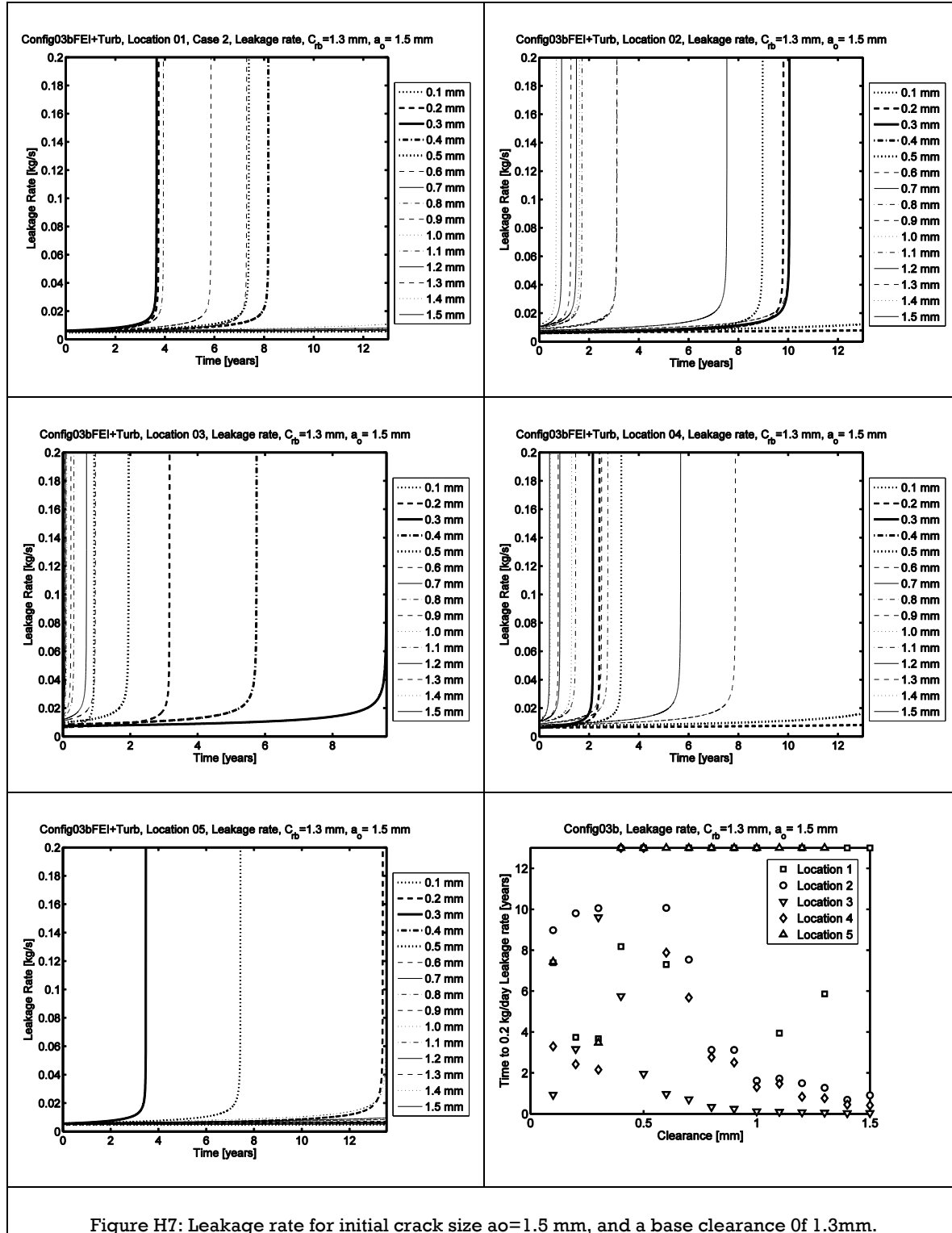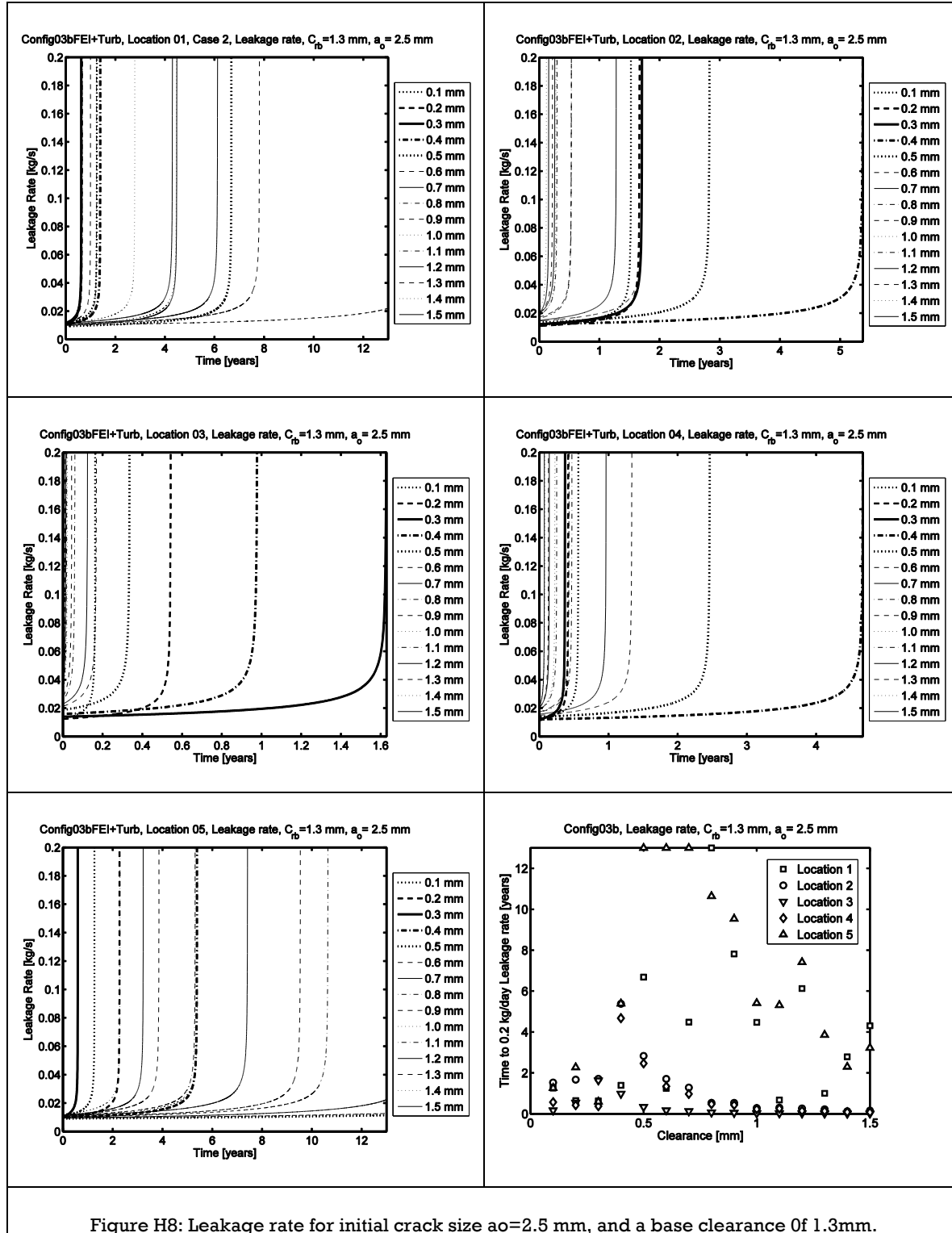
Figure H8: Leakage rate for initial crack size ao=2.5 mm, and a base clearance 0f 1.3mm.
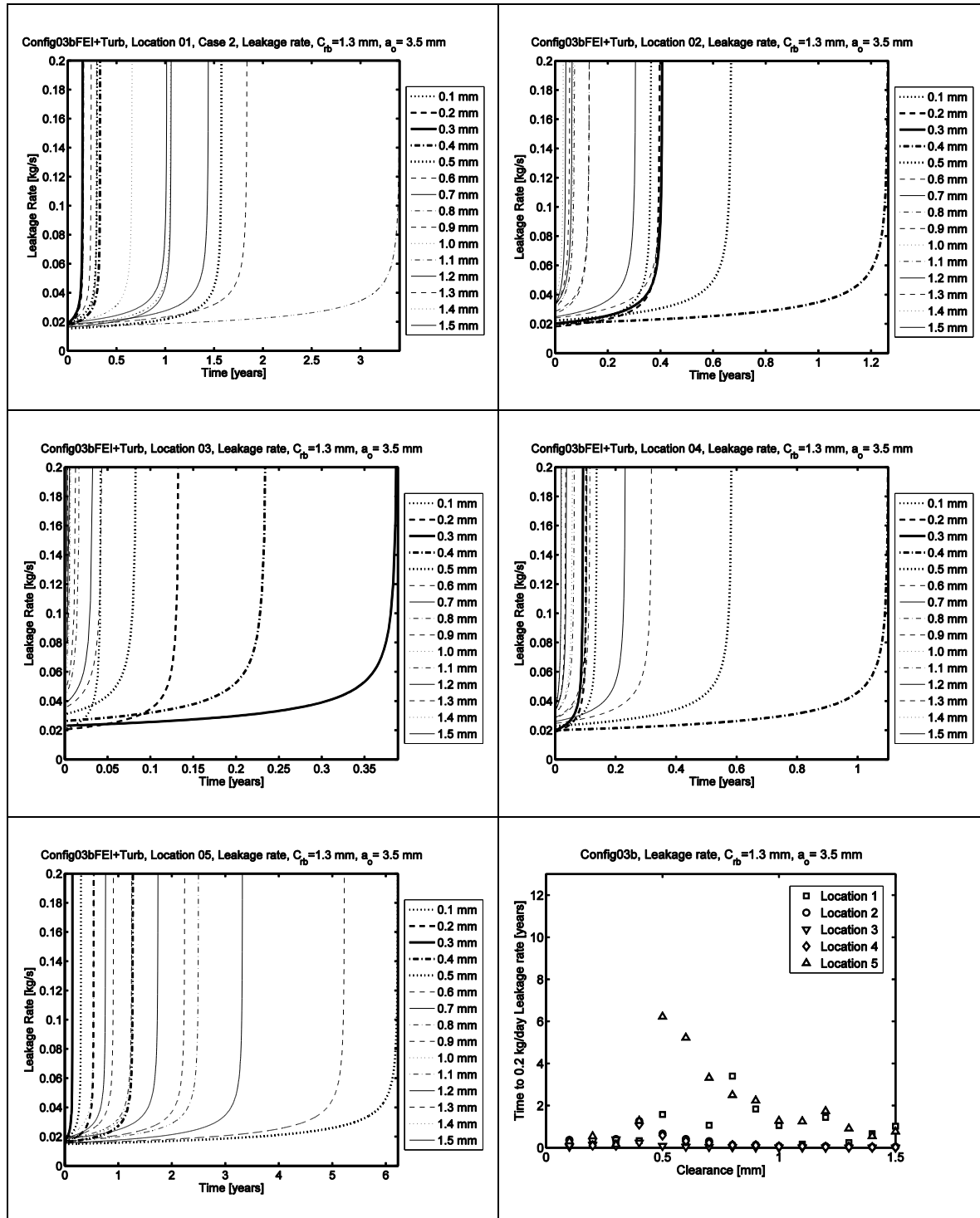
Figure H9: Leakage rate for initial crack size ao=3.5 mm, and a base clearance 0f 1.3mm.

# Appendix I: SCC Crack results



Final crack growth. 1000 cases. SCC, Location 1



Final crack growth. 1000 cases. SCC, Location 2

Final crack growth. 1000 cases. SCC, Location 3



Final crack growth. 1000 cases. SCC, Location 4
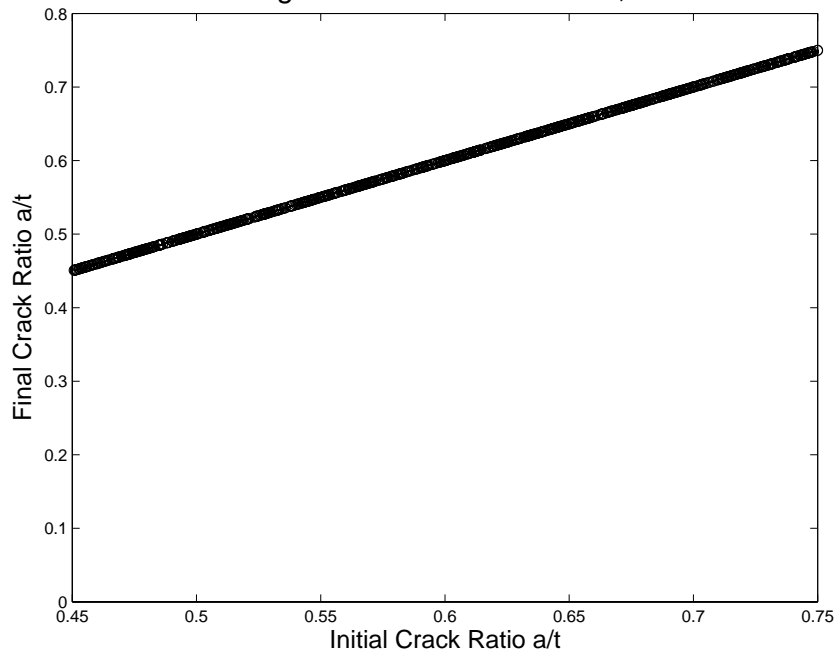
Final crack growth. 1000 cases. SCC, Location 5
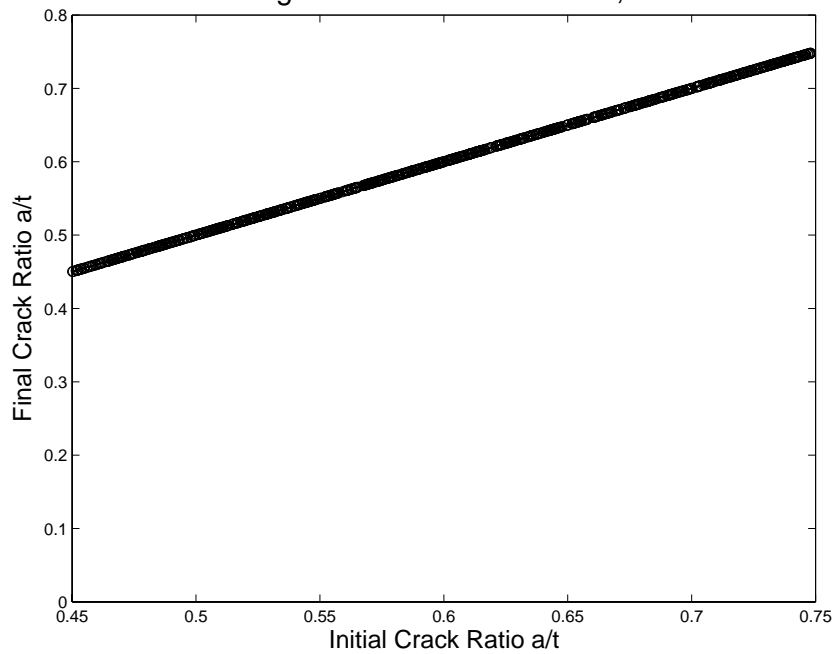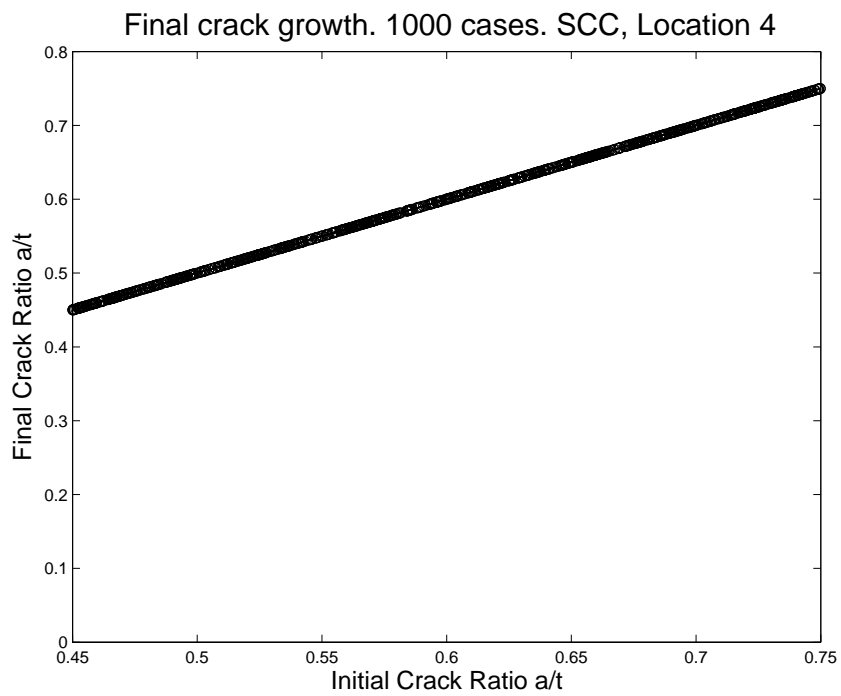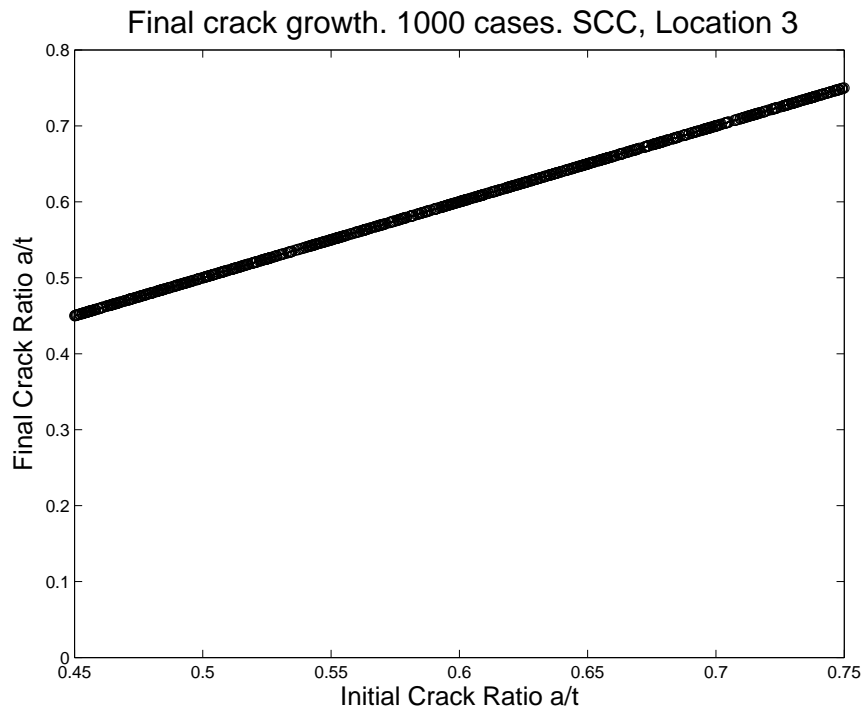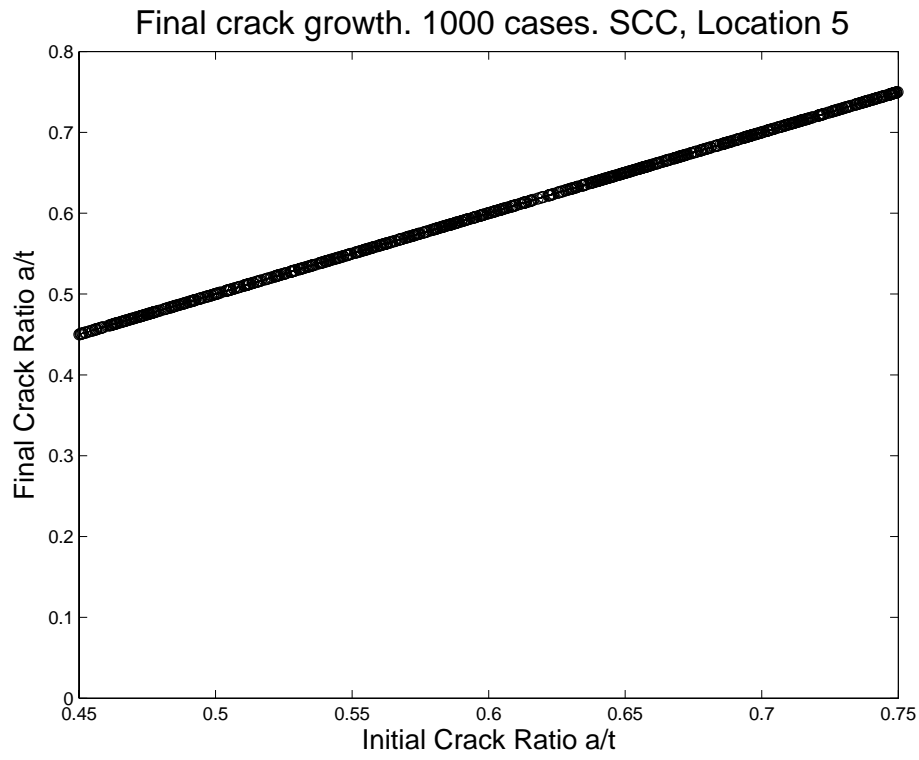
# Appendix I: TWC Final Crack Length results
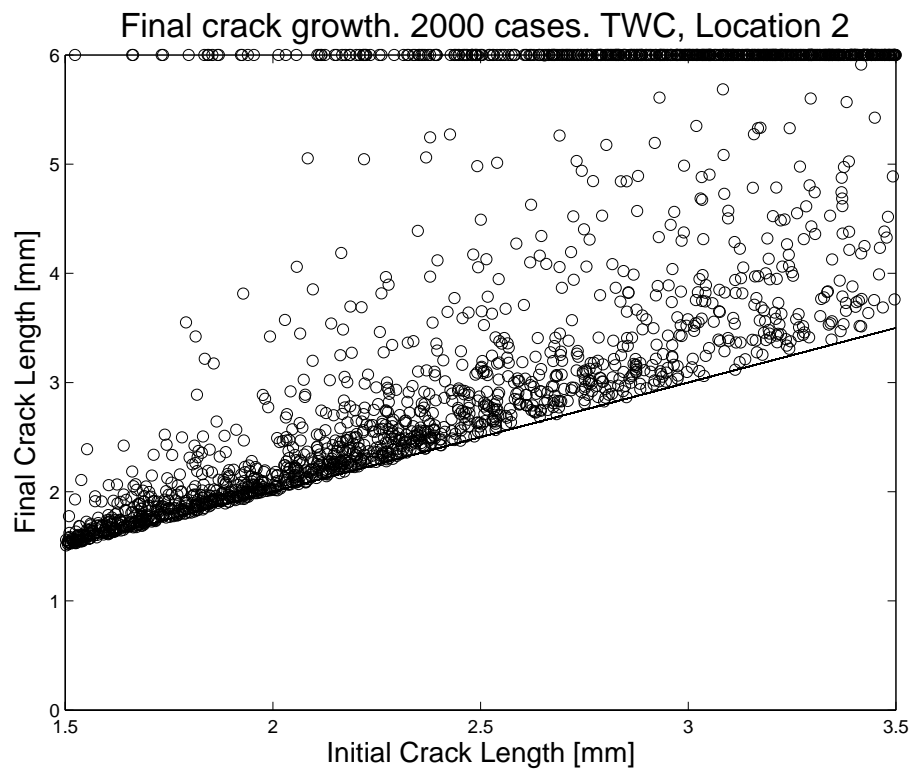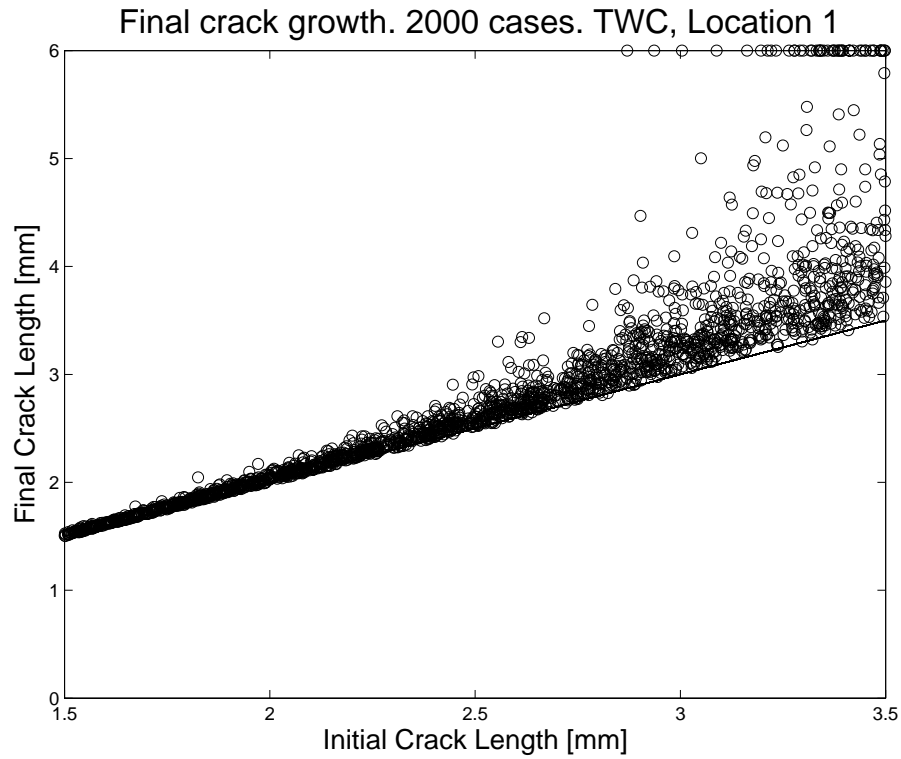
Final crack growth. 2000 cases. TWC, Location 1



Final crack growth. 2000 cases. TWC, Location 2

## Final crack growth. 2000 cases. TWC, Location 3



## Final crack growth. 2000 cases. TWC, Location 4
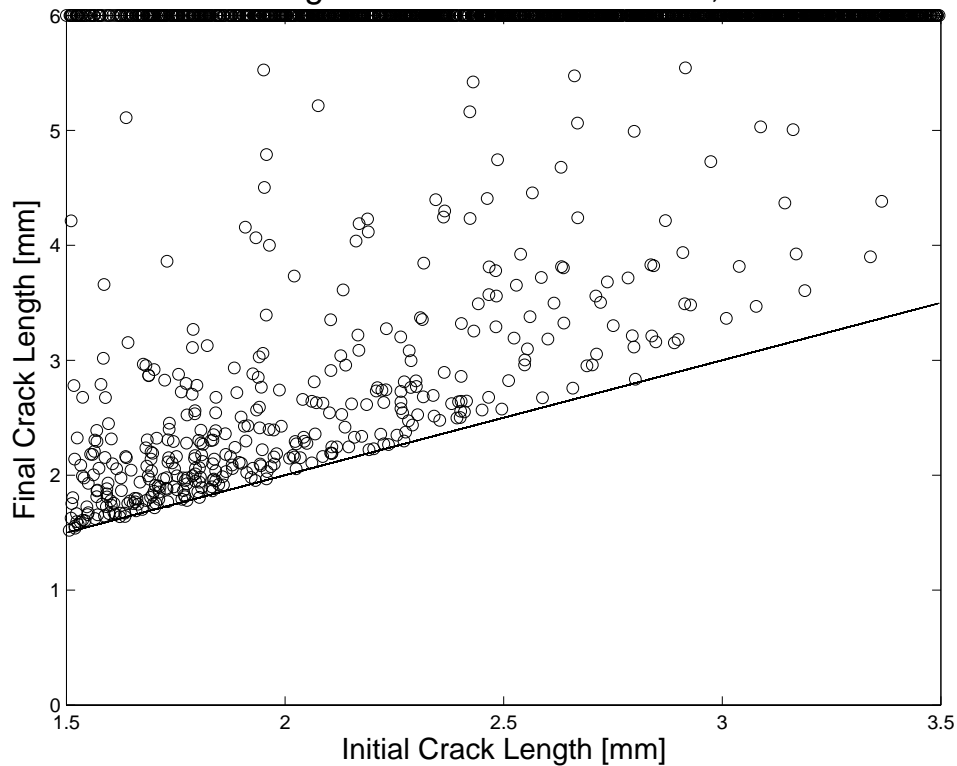
Final crack growth. 2000 cases. TWC, Location 5
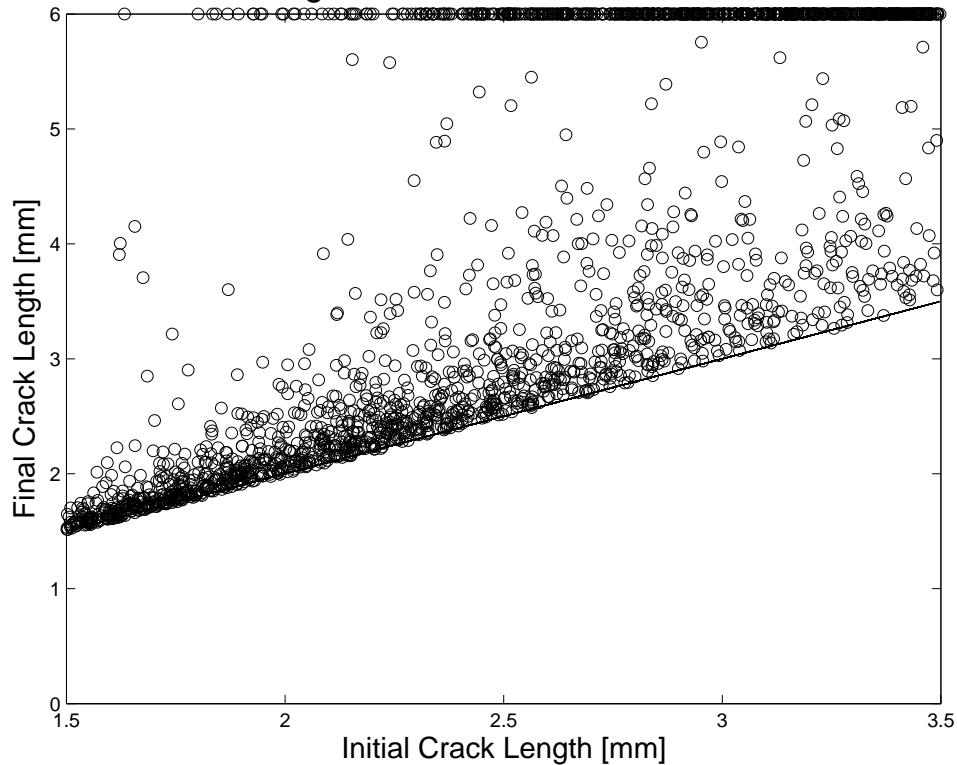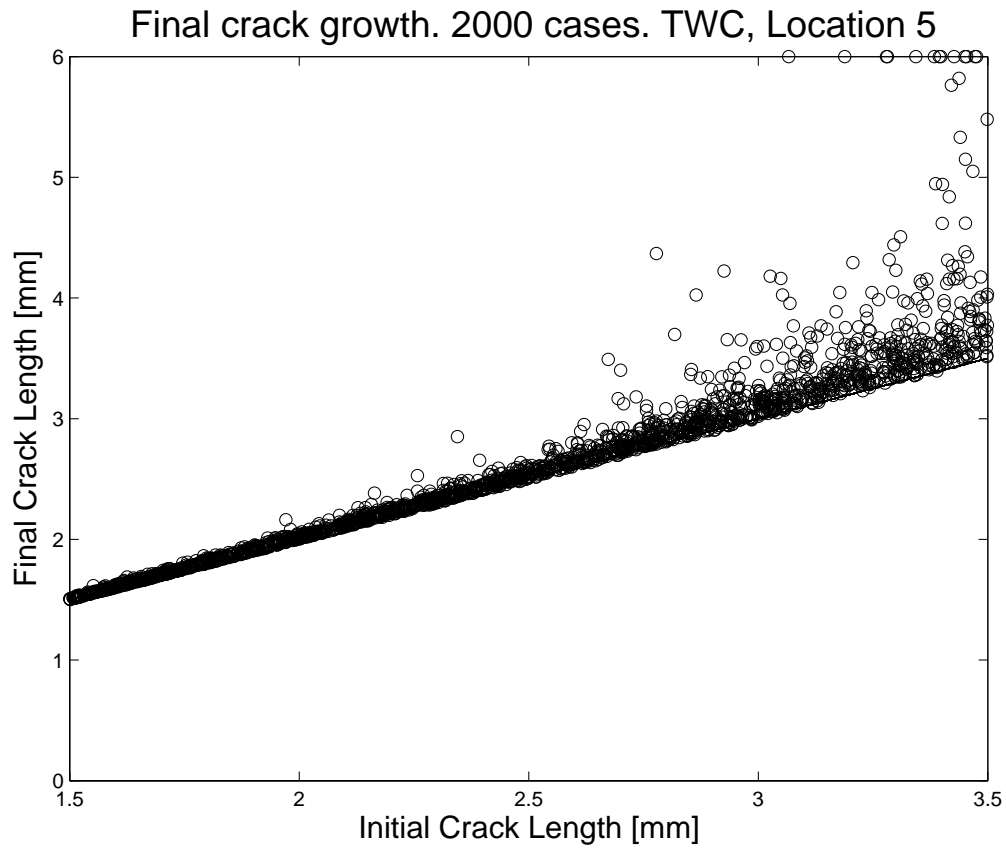
# Appendix J: TWC Crack Life Results



Crack life. 2000 cases. TWC, Location 1



Crack life. 2000 cases. TWC, Location 2

## Crack life. 2000 cases. TWC, Location 3



Life [years] vs Initial Crack Length [mm]

## Crack life. 2000 cases. TWC, Location 4



Life [years] vs Initial Crack Length [mm]
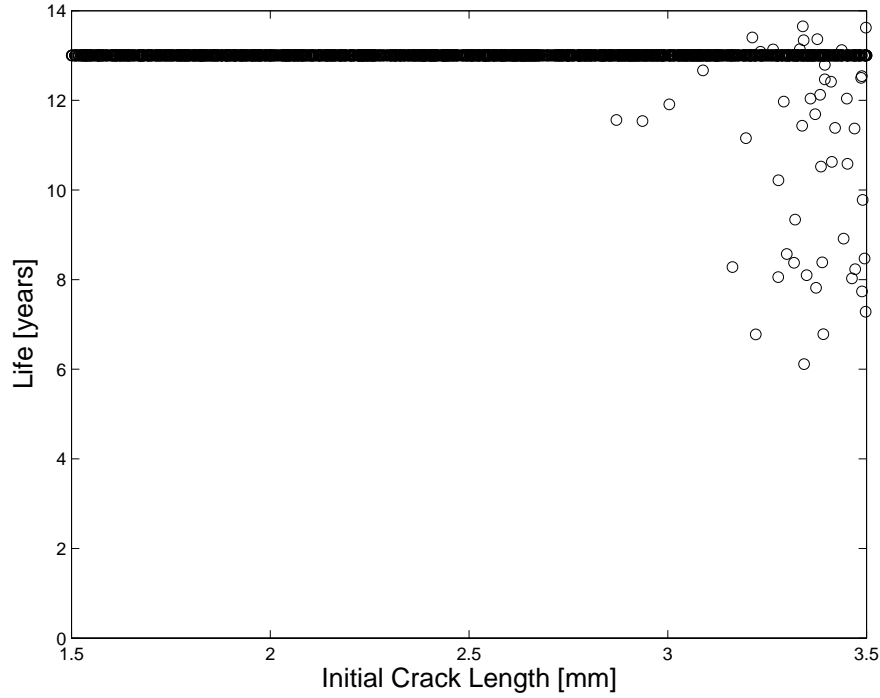
Crack life. 2000 cases. TWC, Location 5
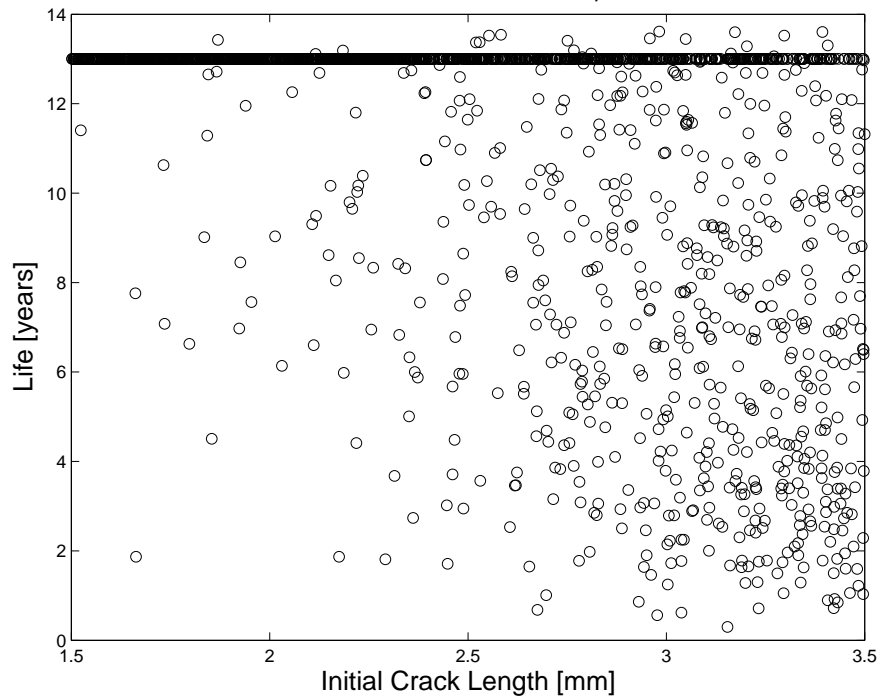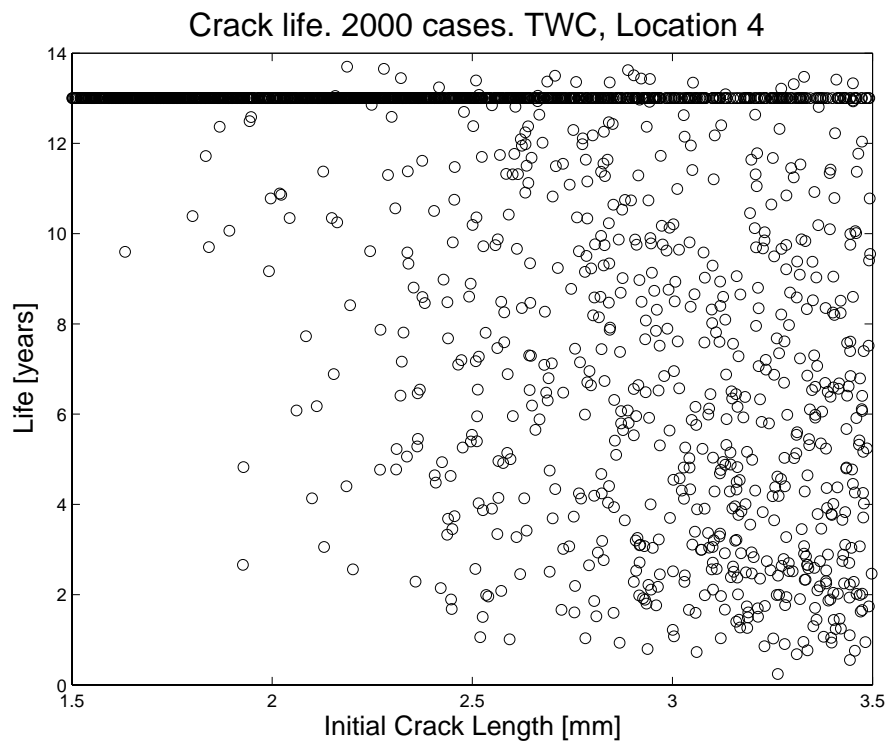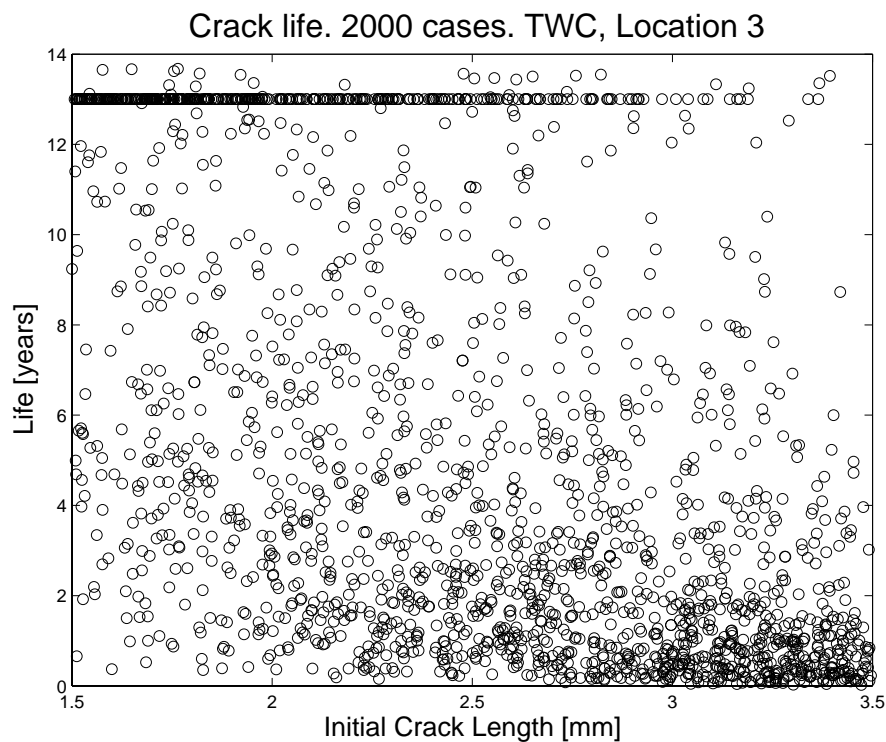
## Appendix K: TWC Crack Growth Histogram results
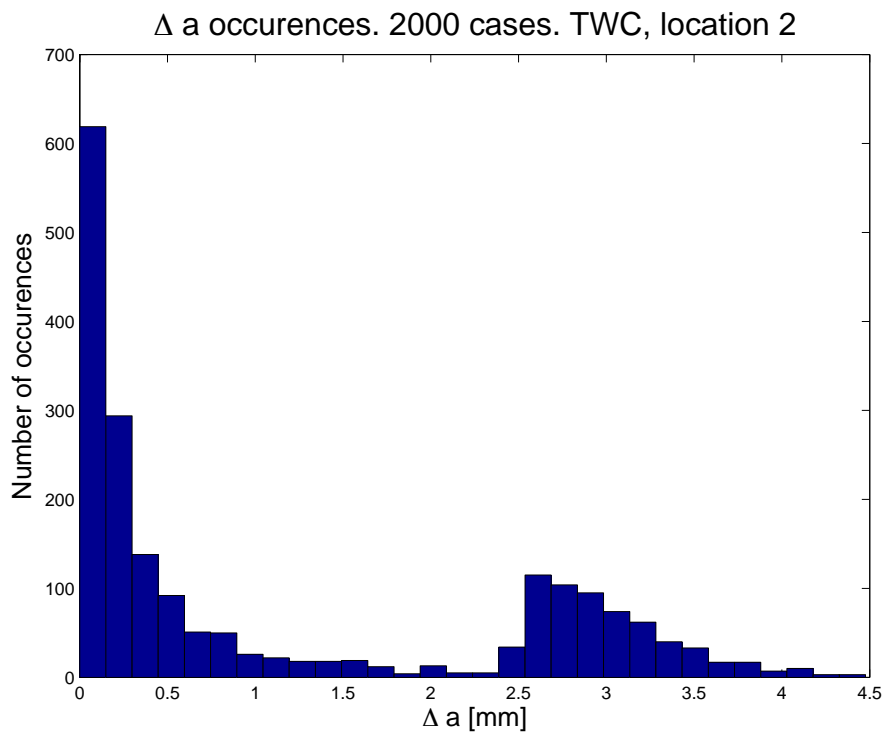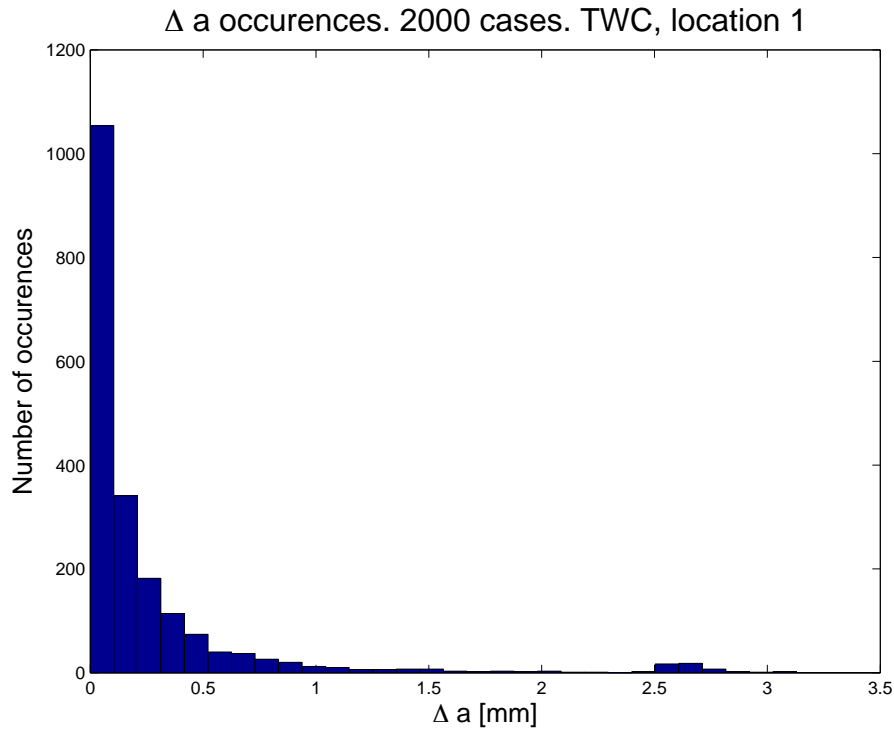
Δ a occurences. 2000 cases. TWC, location 1



Δ a occurences. 2000 cases. TWC, location 2

Δ a occurences. 2000 cases. TWC, location 3



Δ a occurences. 2000 cases. TWC, location 4
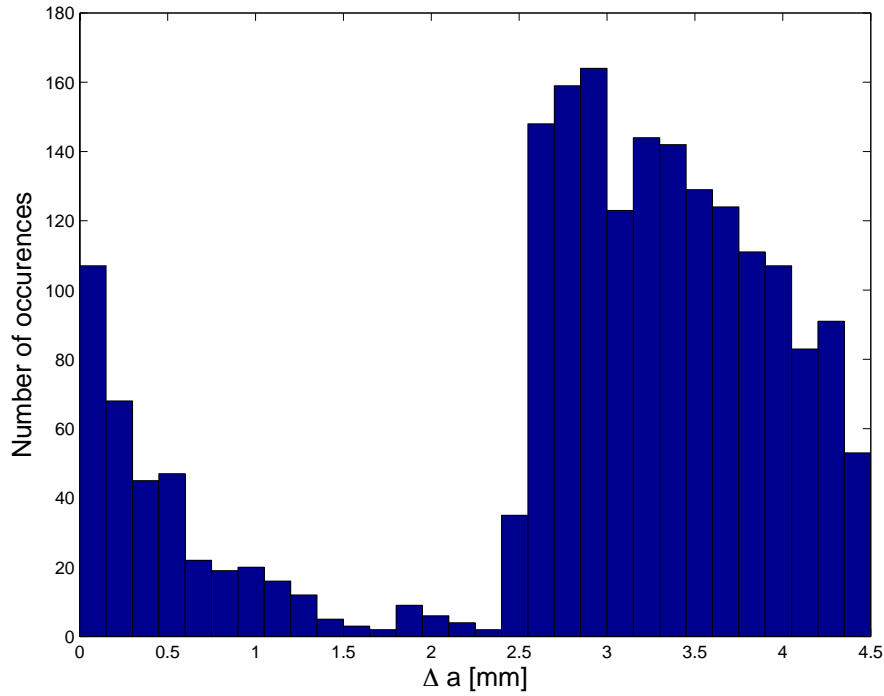
Δ a occurences. 2000 cases. TWC, location 5
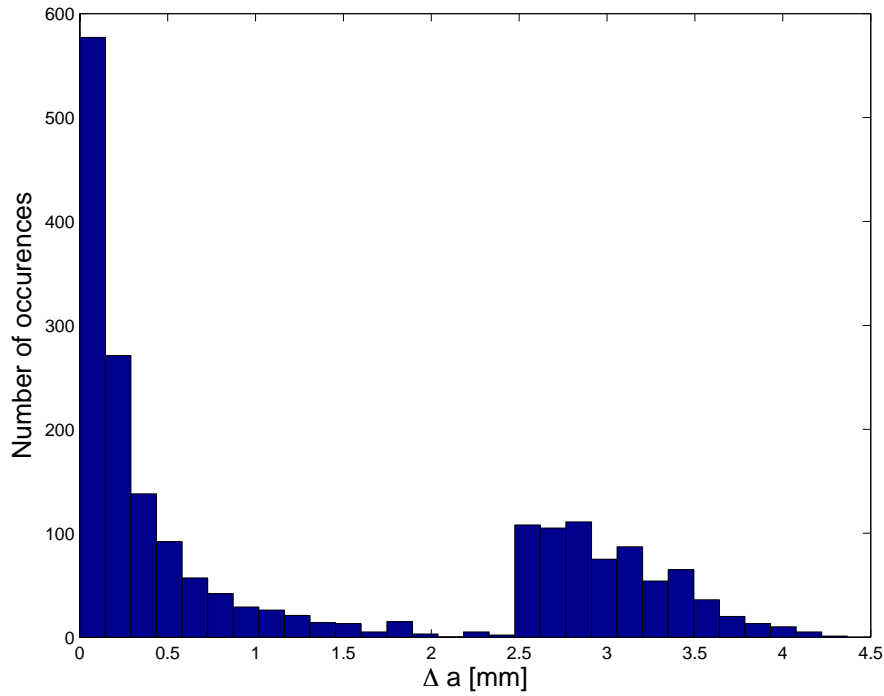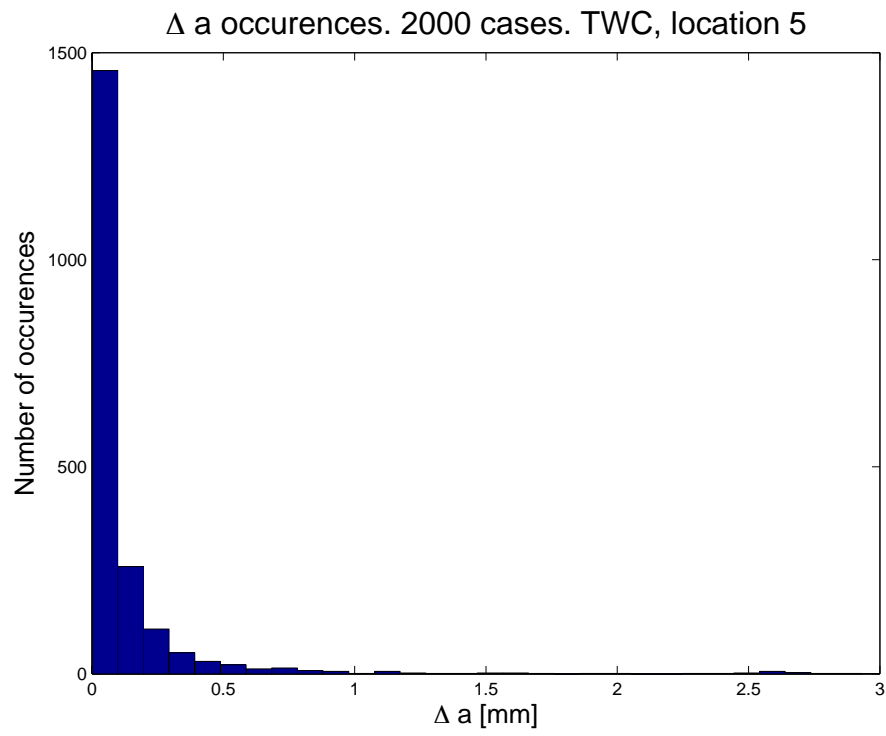
# Appendix L: TWC Crack Growth vs. Support Clearance results

## $\Delta$ a vs. $C_r$. 2000 cases. TWC, Location 1
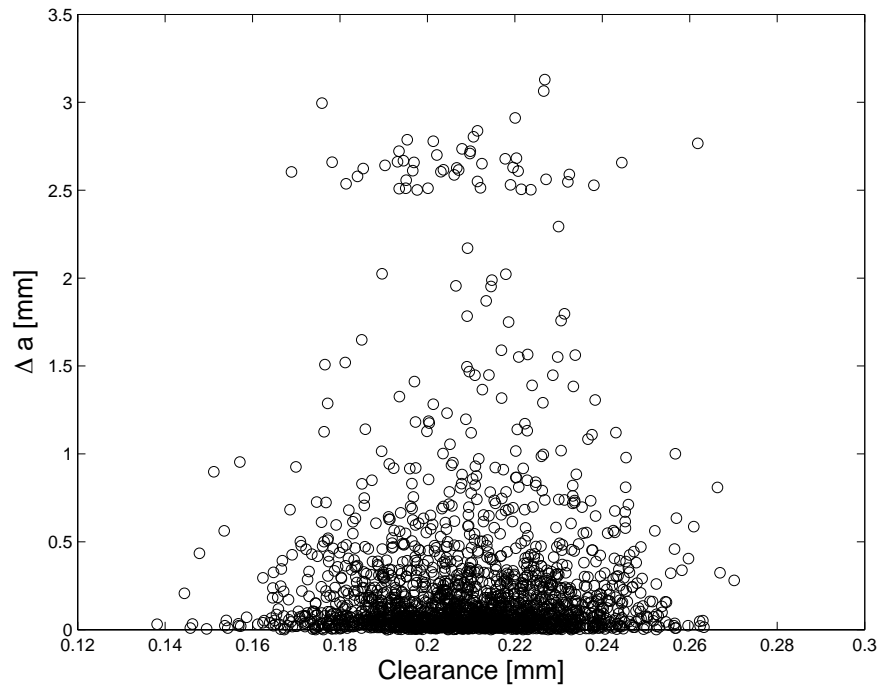


## $\Delta$ a vs. $C_r$. 2000 cases. TWC, Location 2
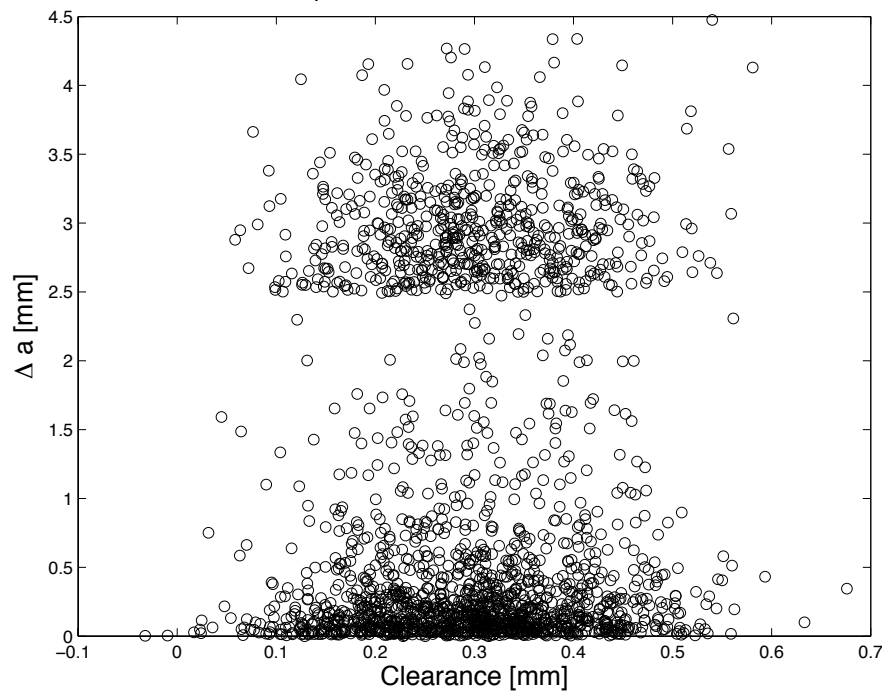
$\Delta$ a vs. C$_r$. 2000 cases. TWC, Location 3

$\Delta$ a vs. C$_r$. 2000 cases. TWC, Location 4
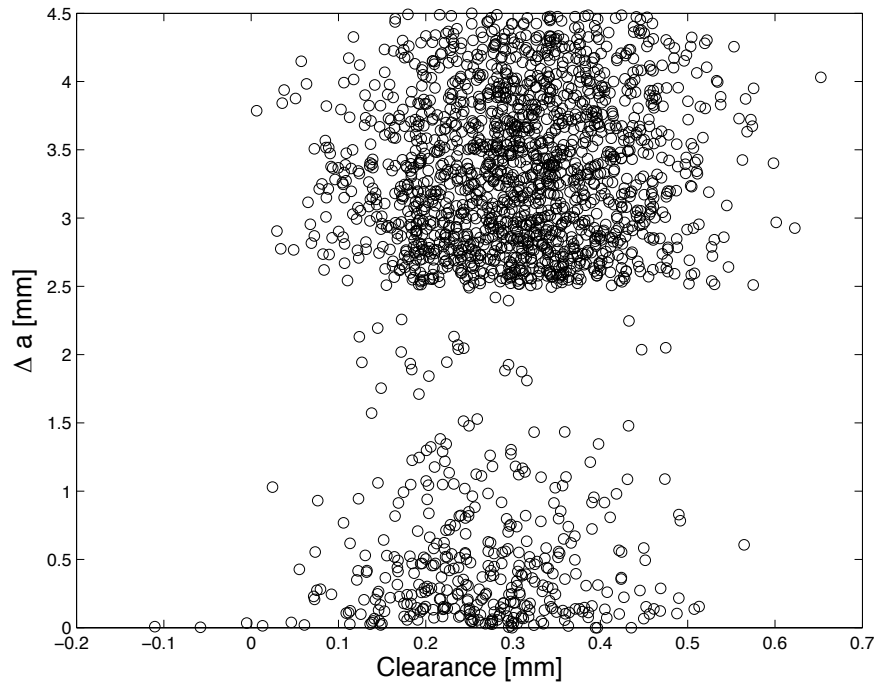
$\Delta$ a vs. $C_r$. 2000 cases. TWC, Location 5
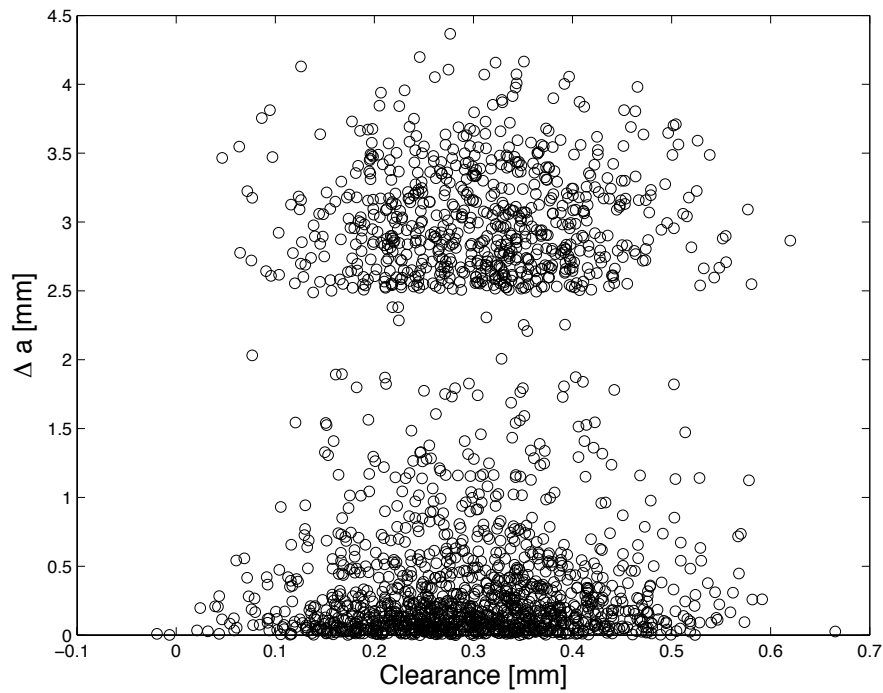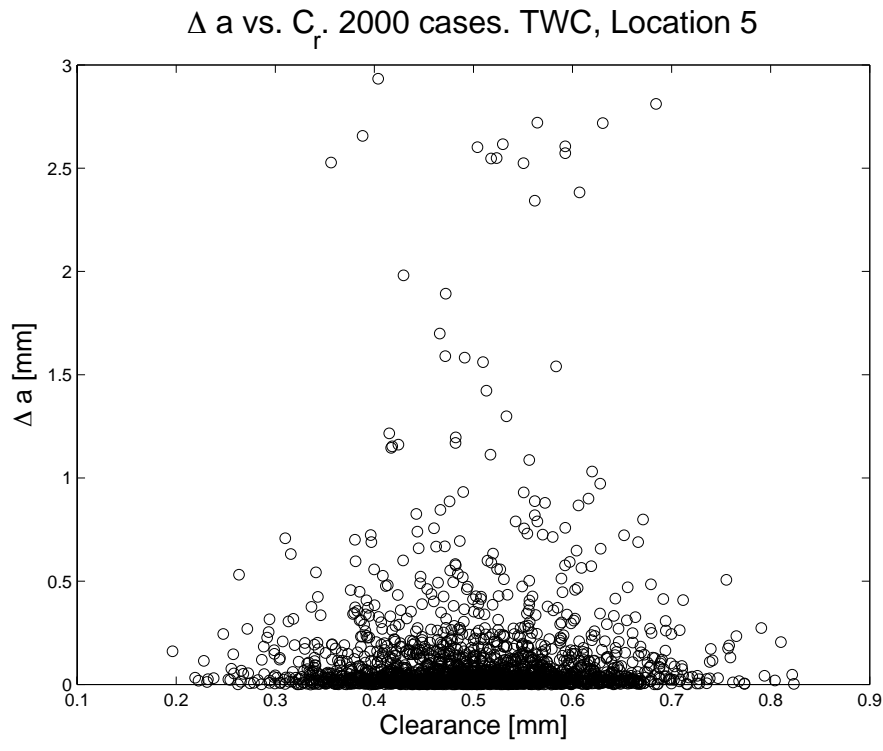
# Appendix M: TWC Crack Growth vs. Bending Stress Results

## Δ a vs. σ$_b$. 2000 cases. TWC, Location 1
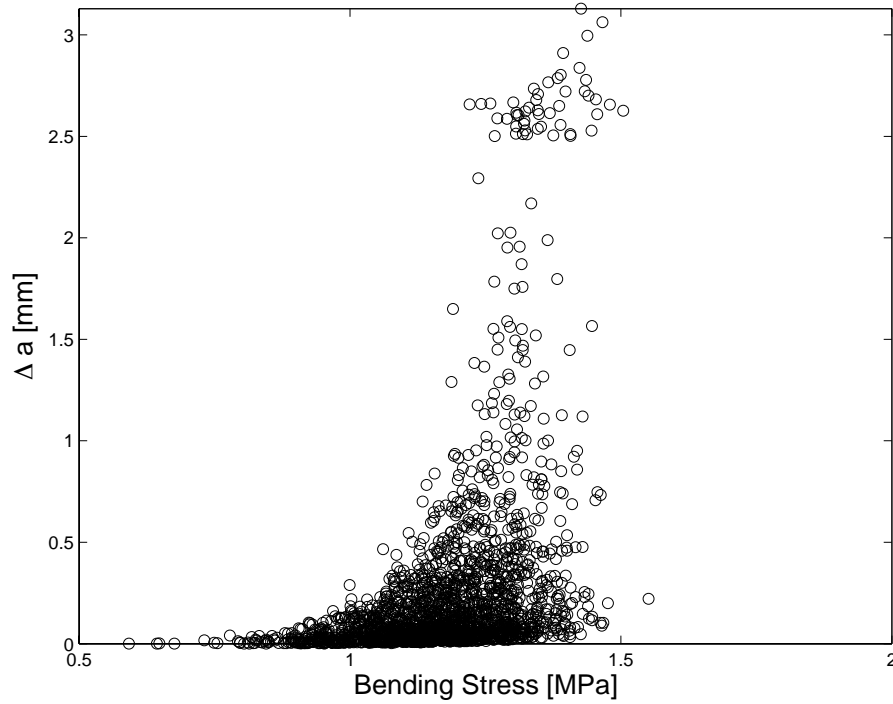


## Δ a vs. σ$_b$. 2000 cases. TWC, Location 2
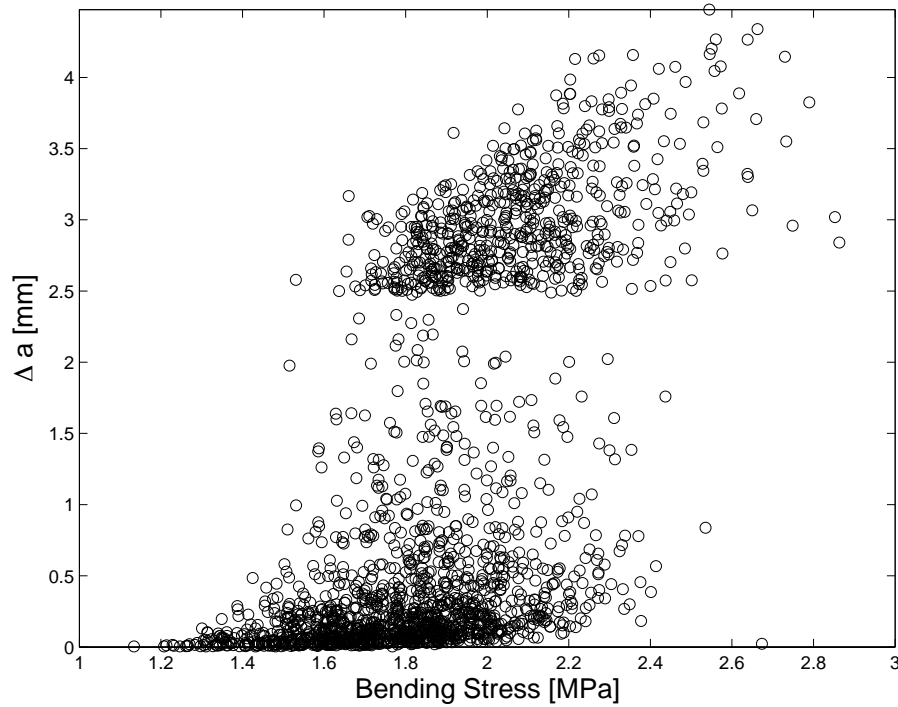
$\Delta$ a vs. $\sigma_b$. 2000 cases. TWC, Location 3
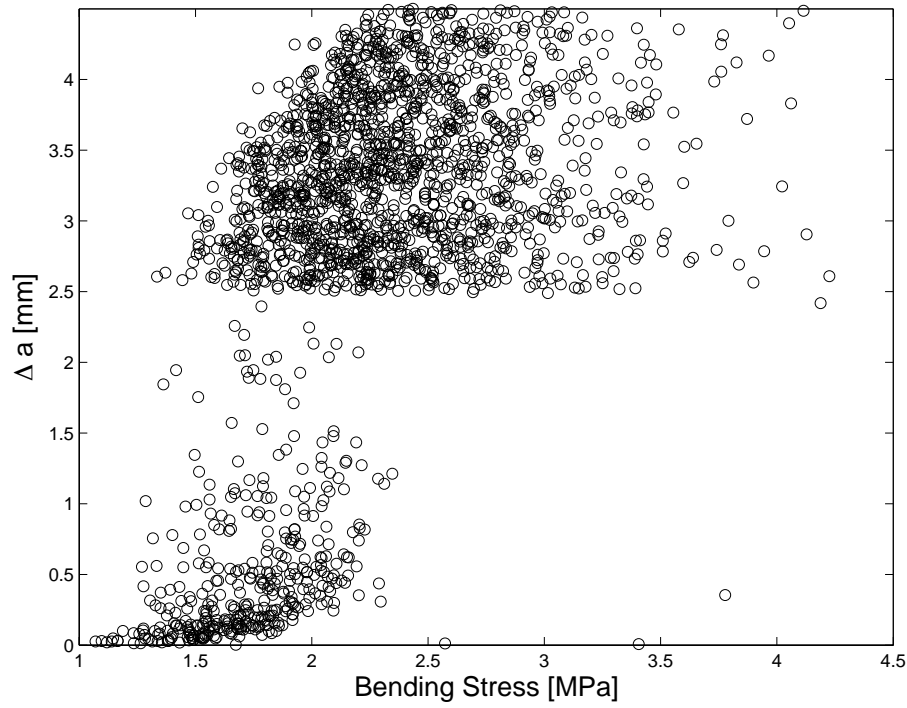
$\Delta$ a vs. $\sigma_b$. 2000 cases. TWC, Location 4
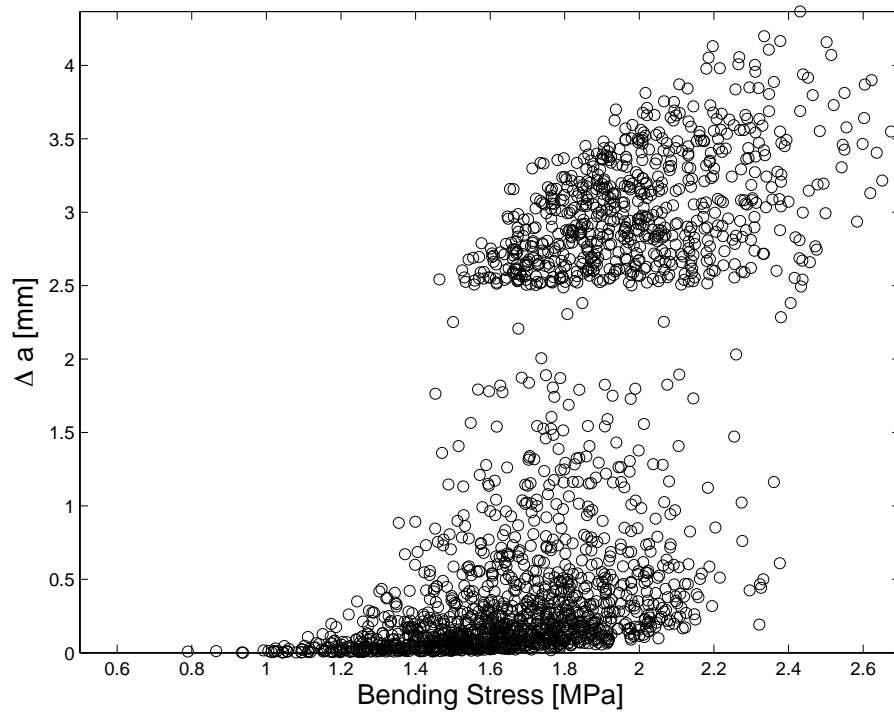
## Δ a vs. σ_b. 2000 cases. TWC, Location 5
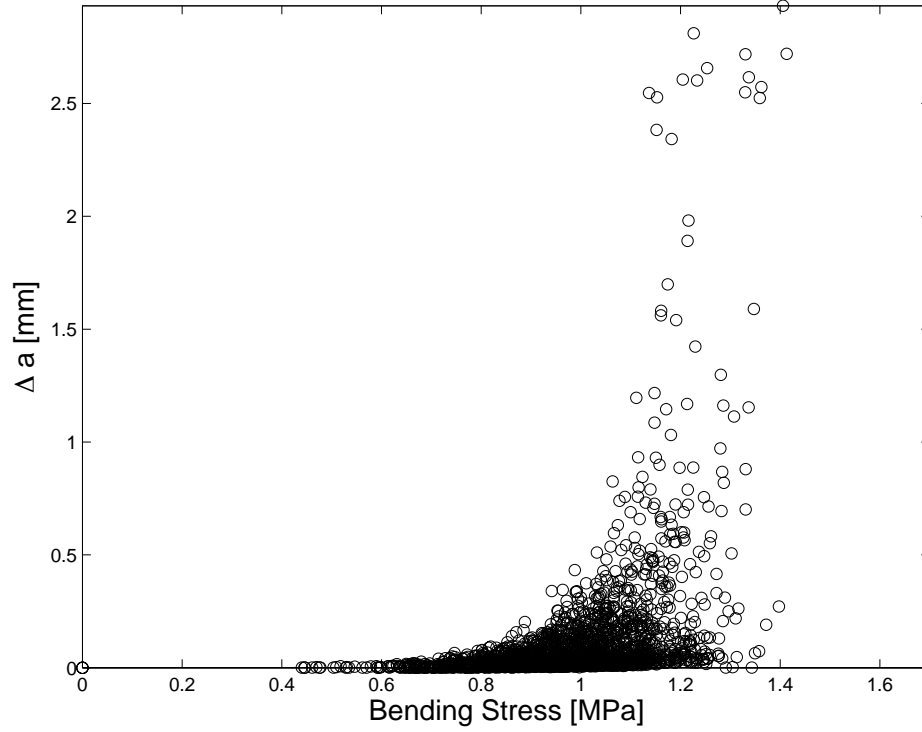
# Appendix N: TWC Tube Life Probability vs. Initial Crack Length

Probability of tube life exceeding thresholds. TWC, Location 1
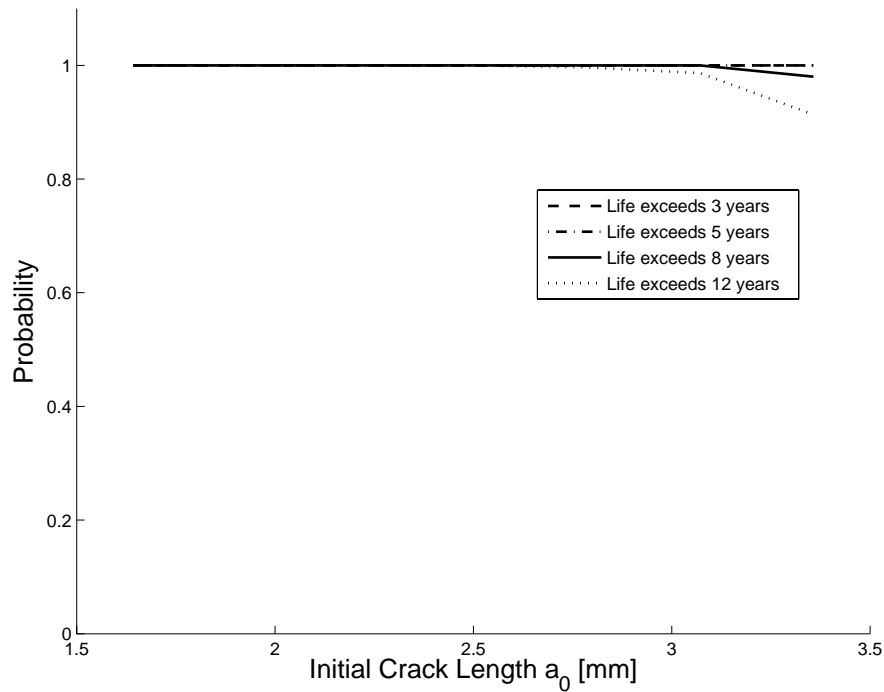


Probability of tube life exceeding thresholds. TWC, Location 2
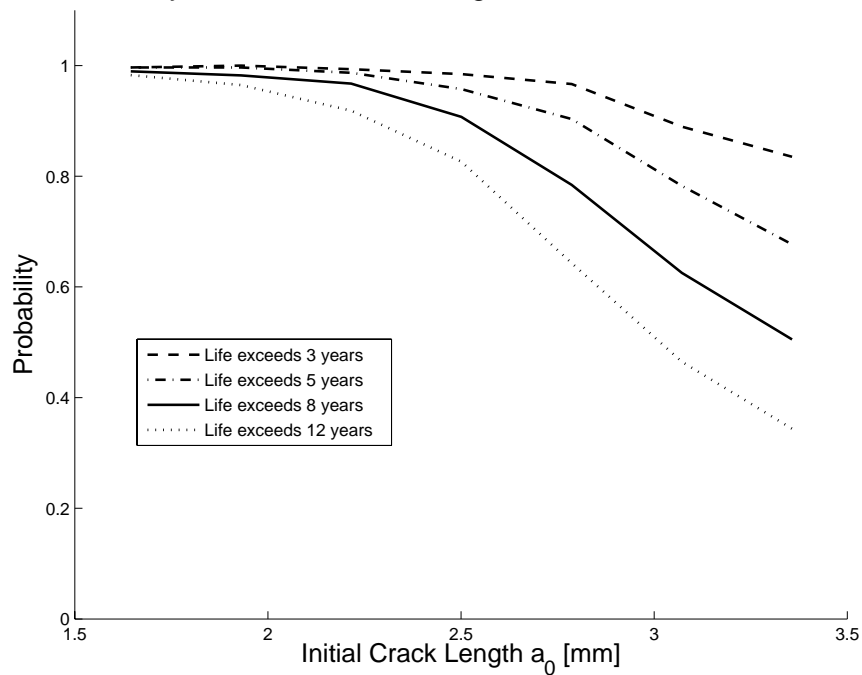
Probability of tube life exceeding thresholds. TWC, Location 3
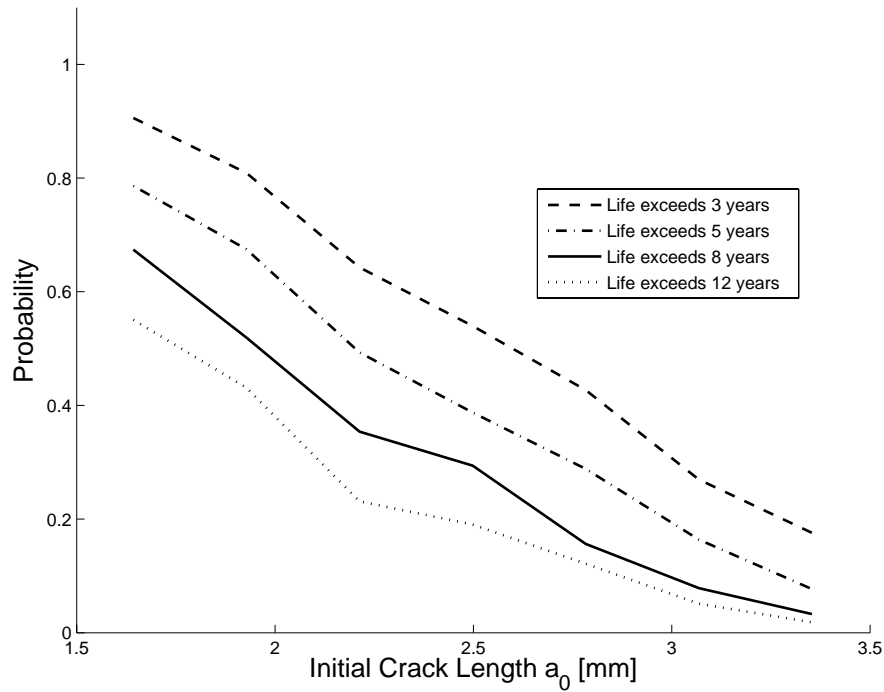


Probability of tube life exceeding thresholds. TWC, Location 4
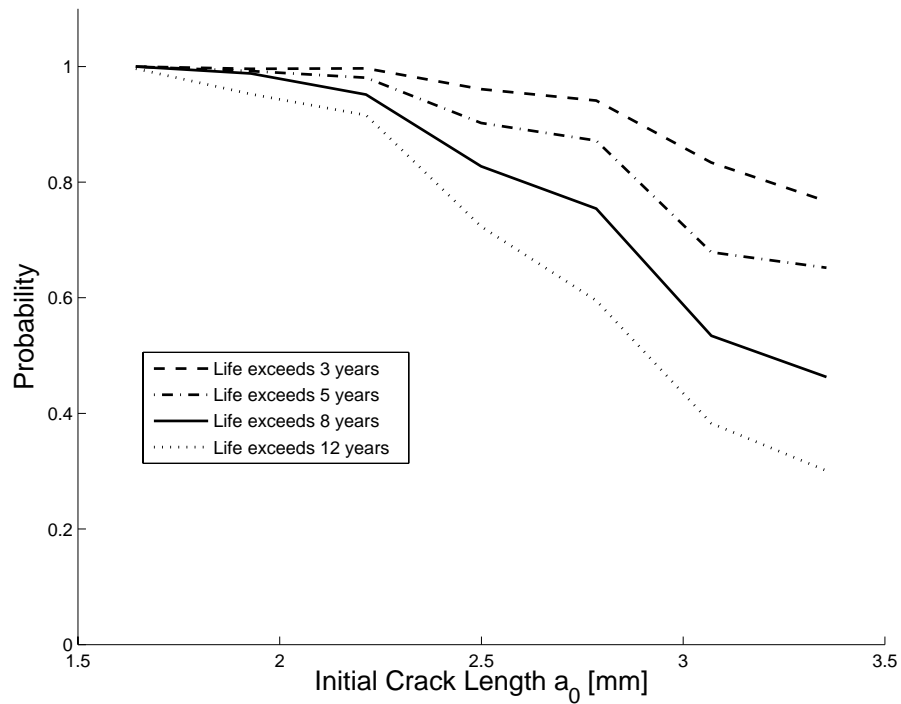
Probability of tube life exceeding thresholds. TWC, Location 5
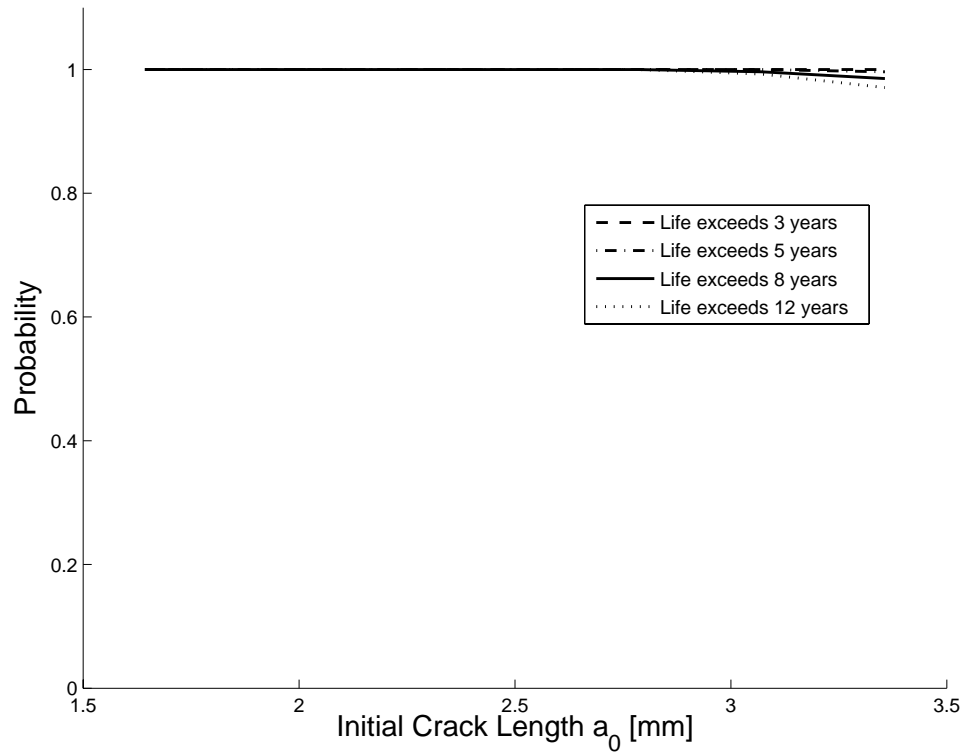
## Appendix O: Leakage Tube Life vs. Initial Crack Length

Leakage, expected life. 2000 cases. TWC, Location 1



Leakage, expected life. 2000 cases. TWC, Location 2

### Leakage, expected life. 2000 cases. TWC, Location 3



### Leakage, expected life. 2000 cases. TWC, Location 4

Leakage, expected life. 2000 cases. TWC, Location 5
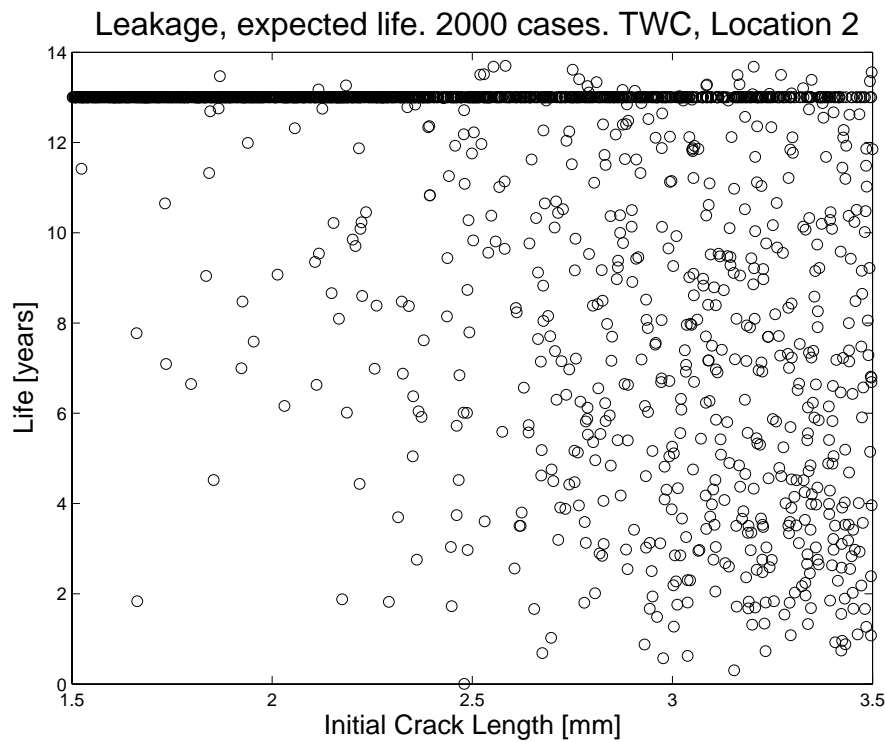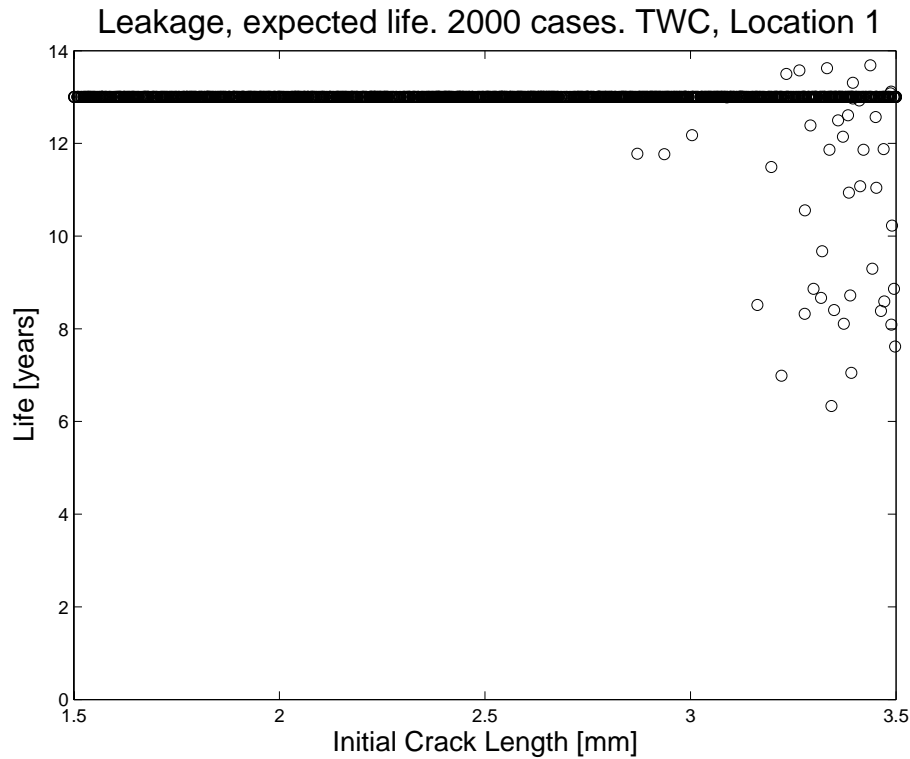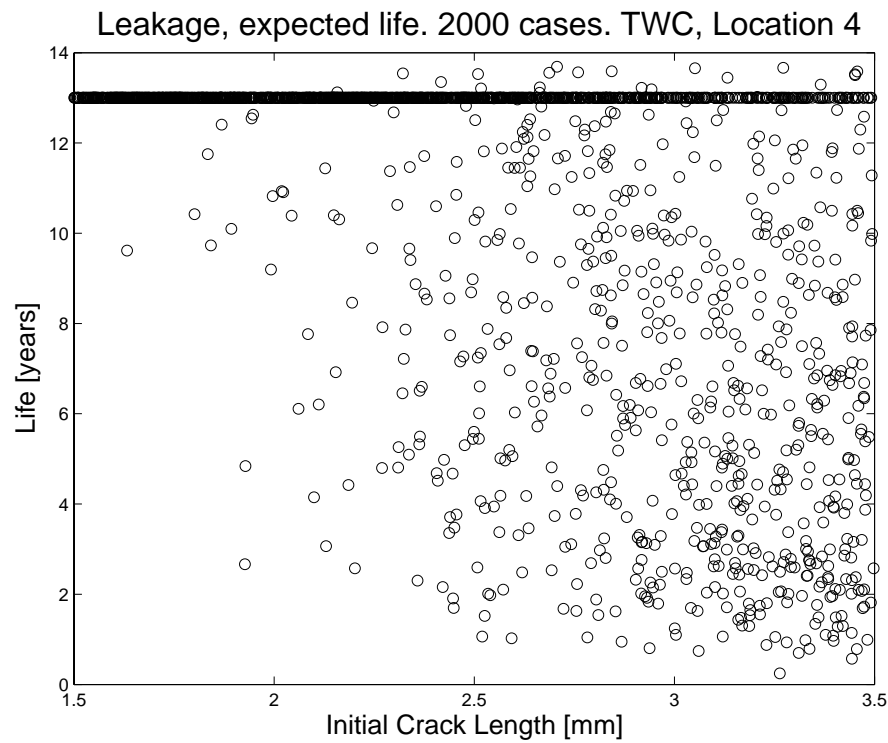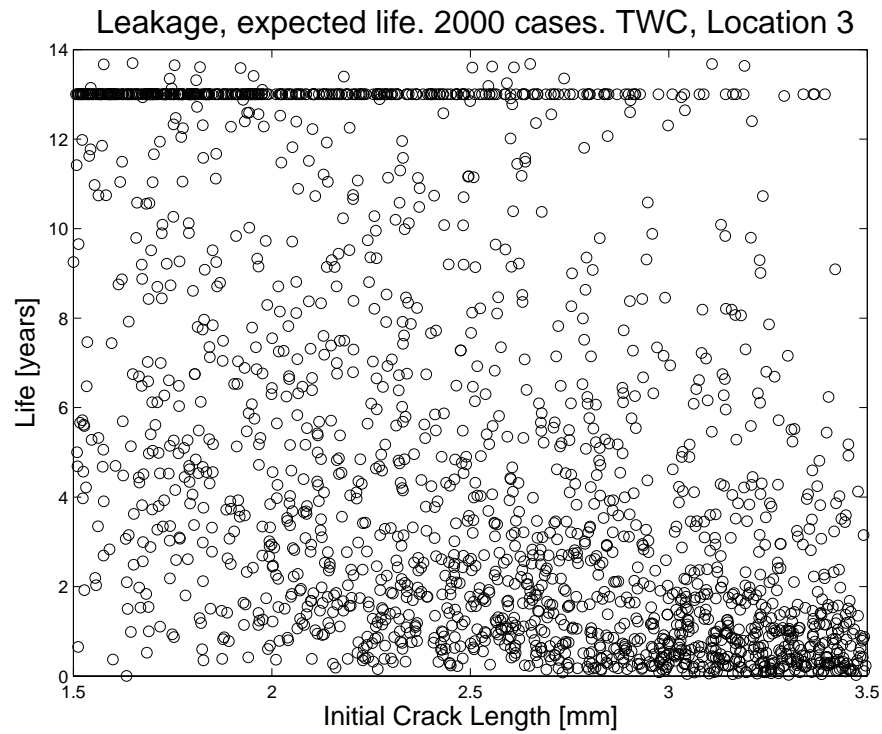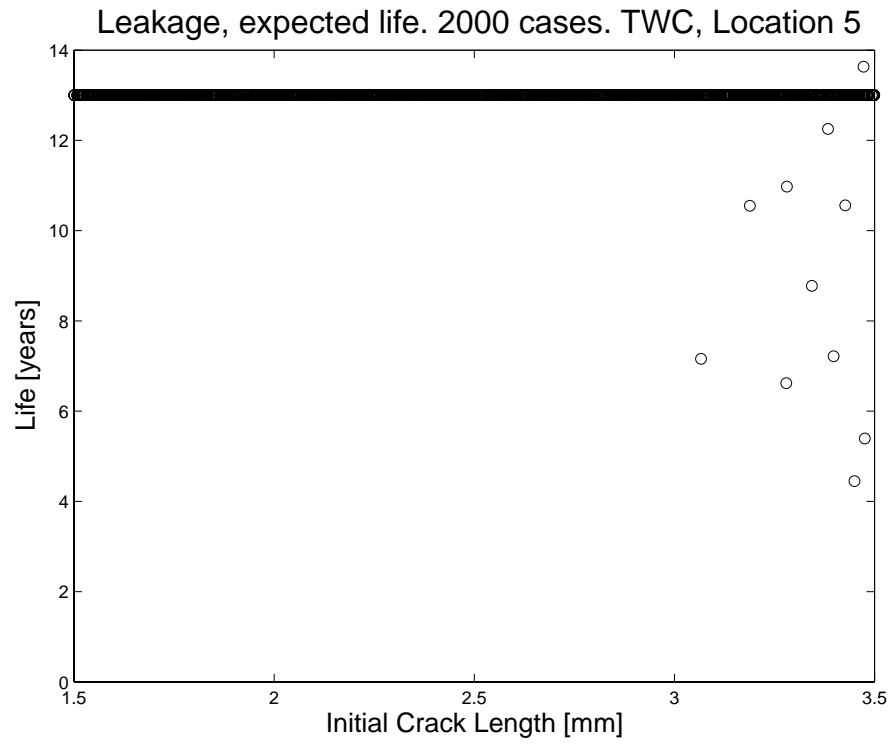
## Appendix P: Leakage Rate vs. Initial Crack Length



Leakage. 2000 cases. TWC, Location 1



Leakage. 2000 cases. TWC, Location 2

Leakage. 2000 cases. TWC, Location 3



Leakage. 2000 cases. TWC, Location 4

Leakage. 2000 cases. TWC, Location 5
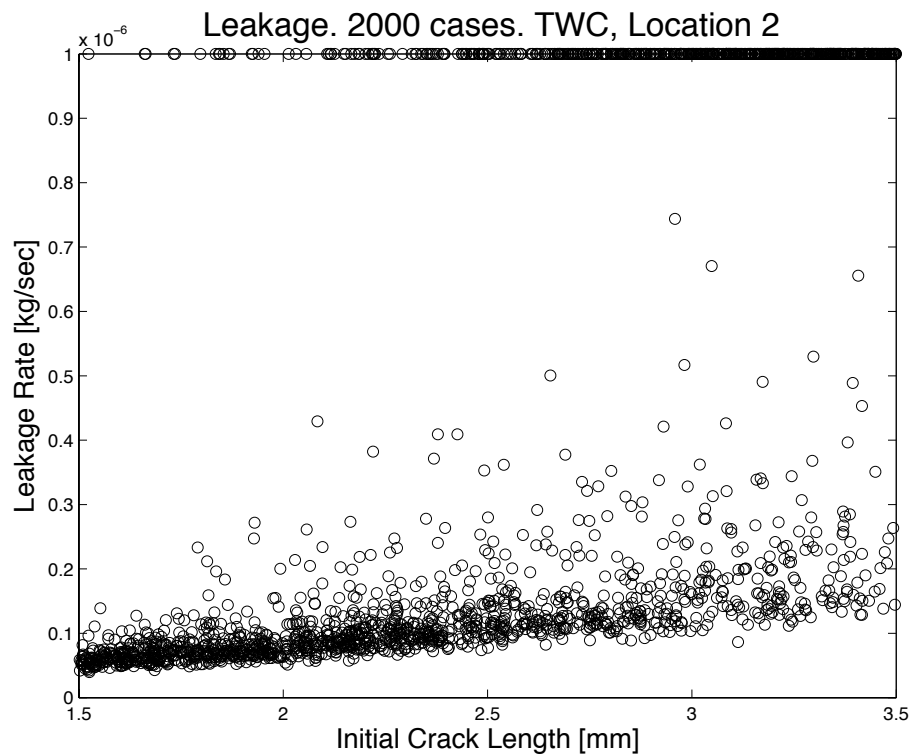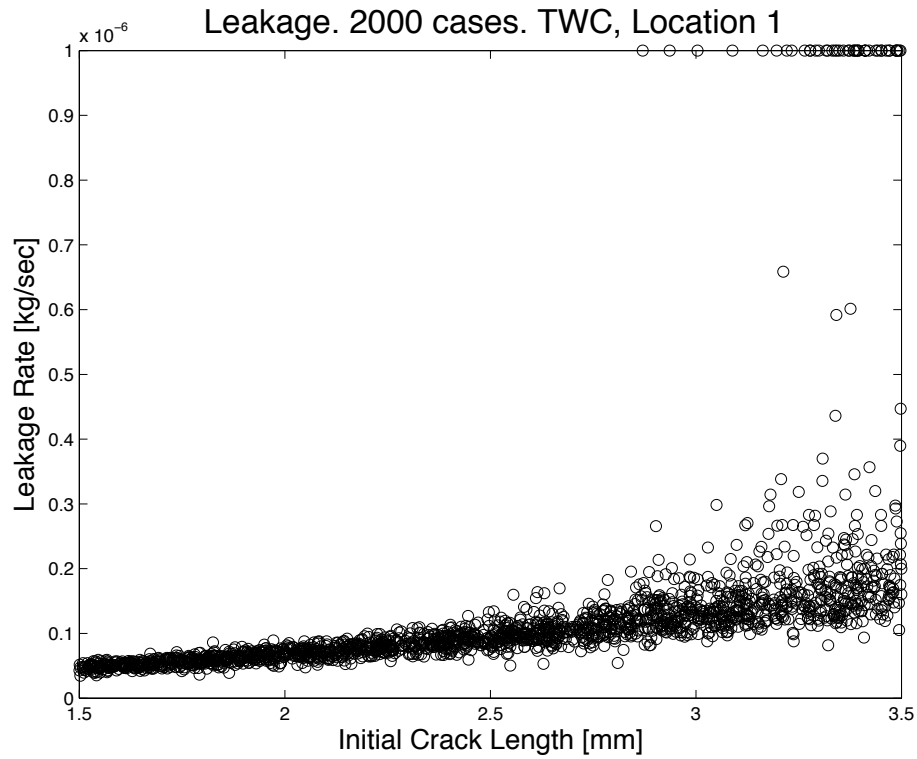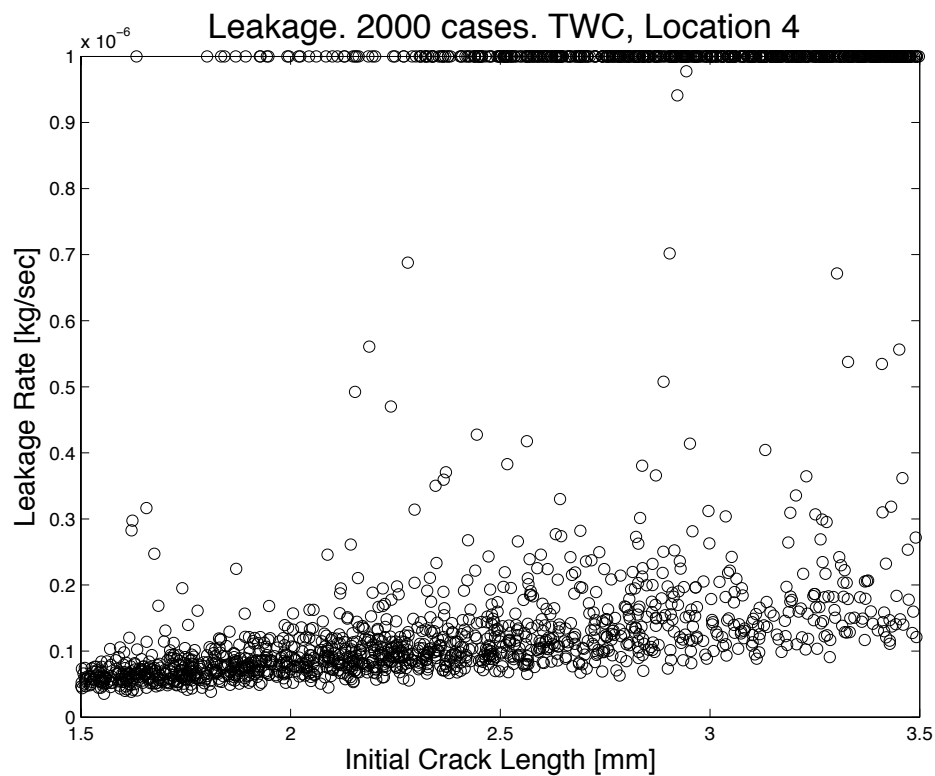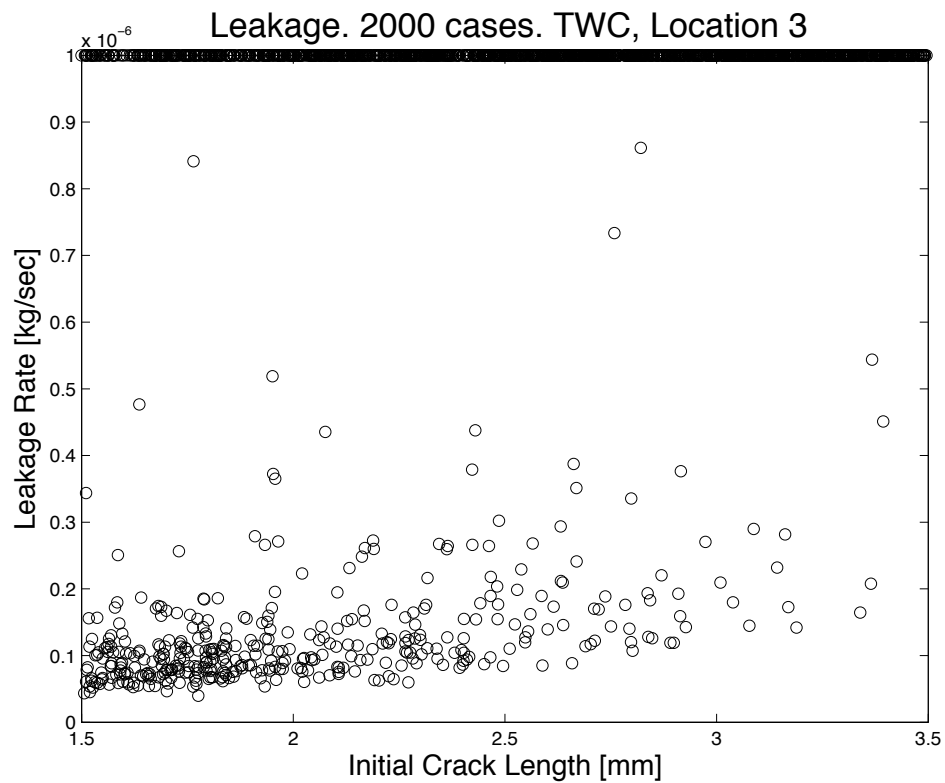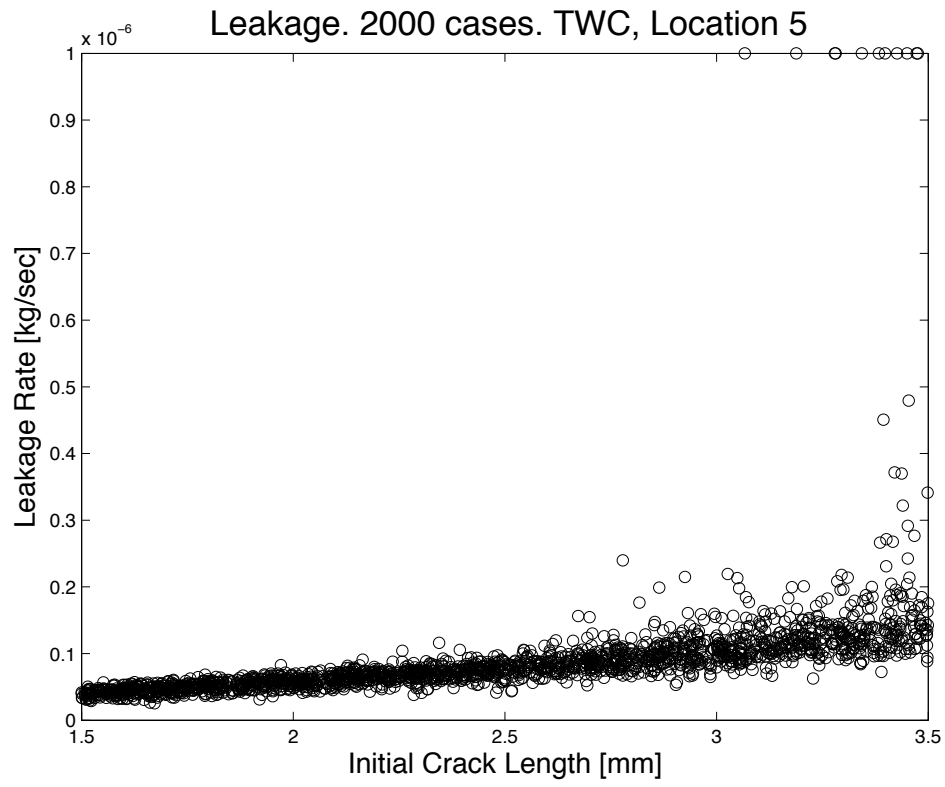
# Appendix Q: Leakage Tube Life vs. Support Clearances



Leakage rate vs. $C_r$. 2000 cases. TWC, Location 1



Leakage rate vs. $C_r$. 2000 cases. TWC, Location 2

Leakage rate vs. C$_r$. 2000 cases. TWC, Location 3



Leakage rate vs. C$_r$. 2000 cases. TWC, Location 4
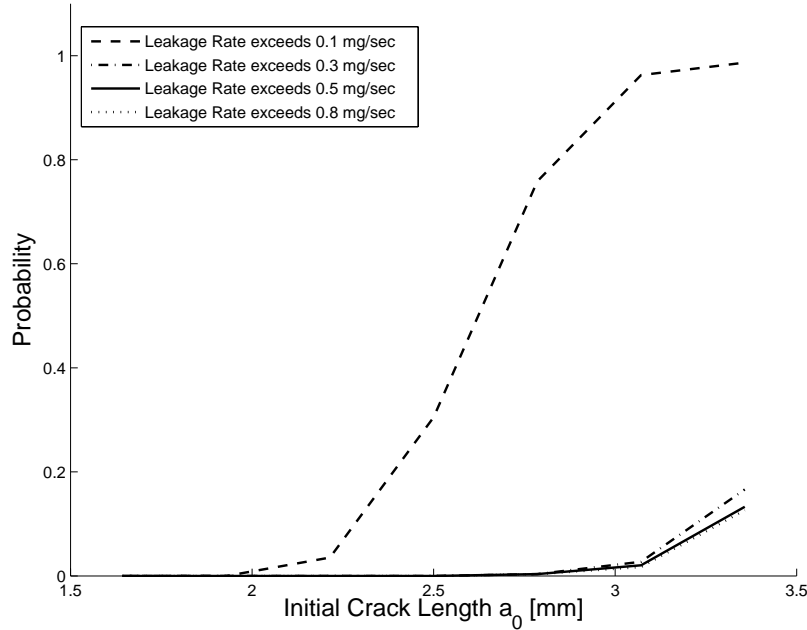
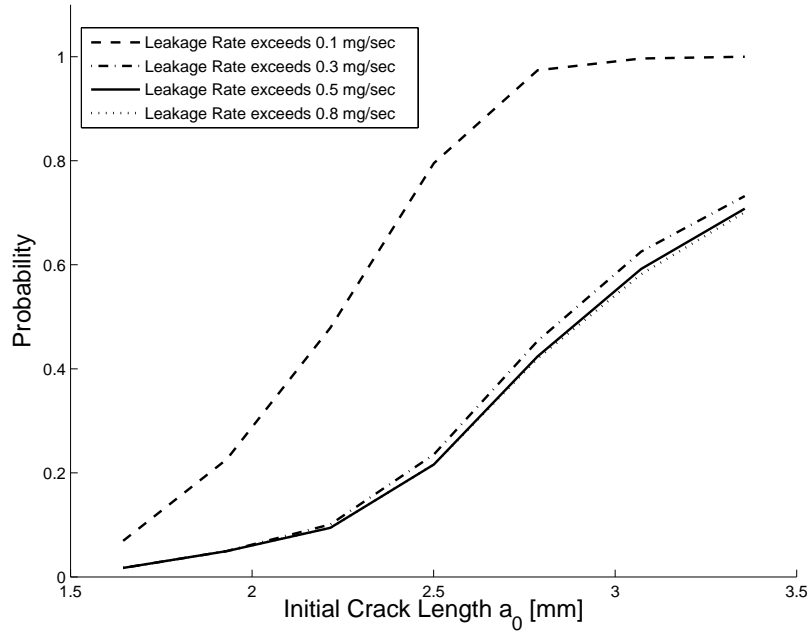Leakage rate vs. $C_r$. 2000 cases. TWC, Location 5
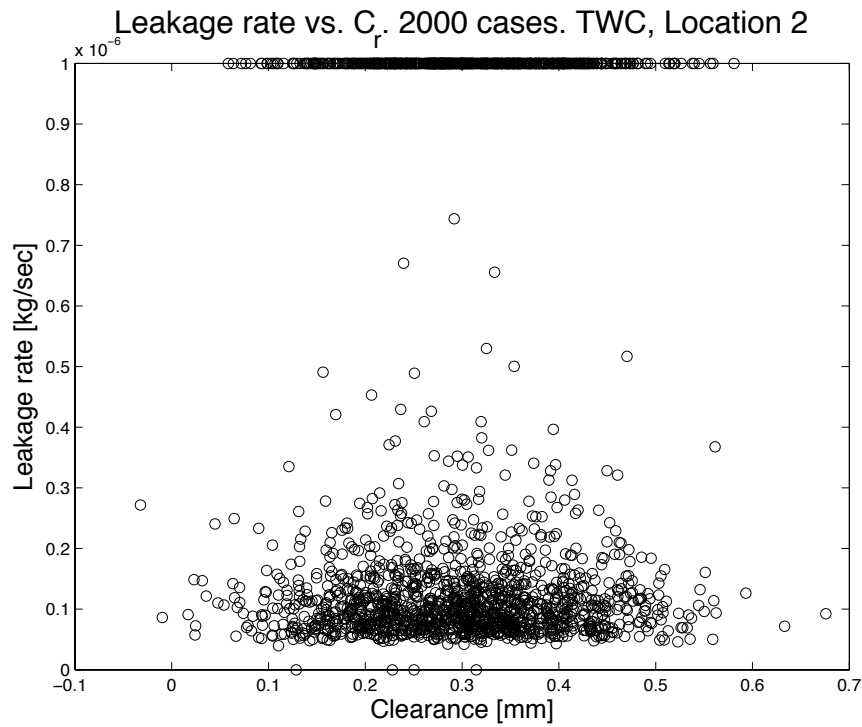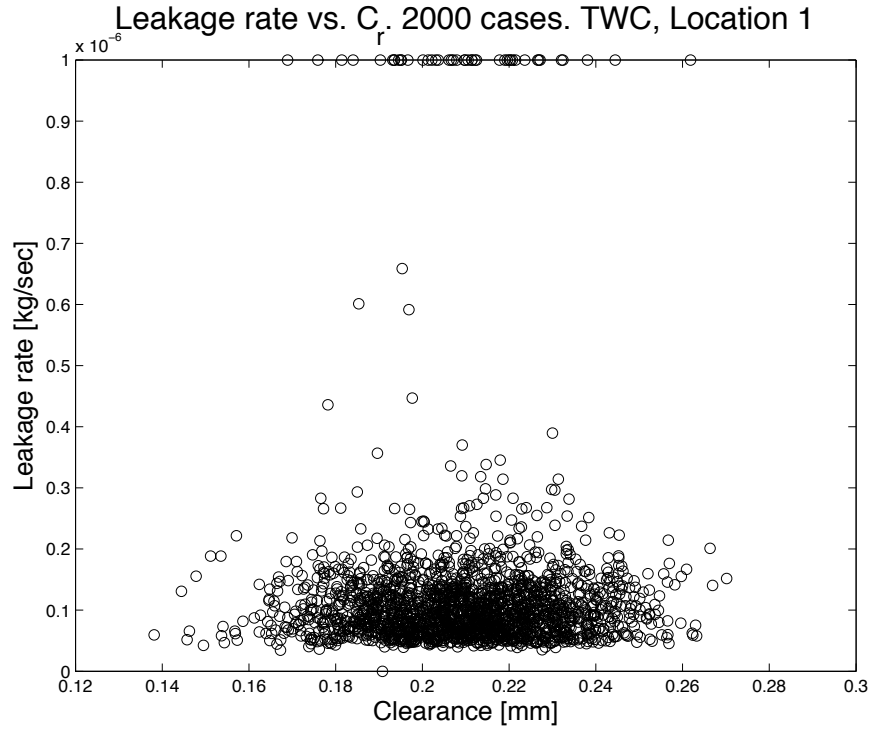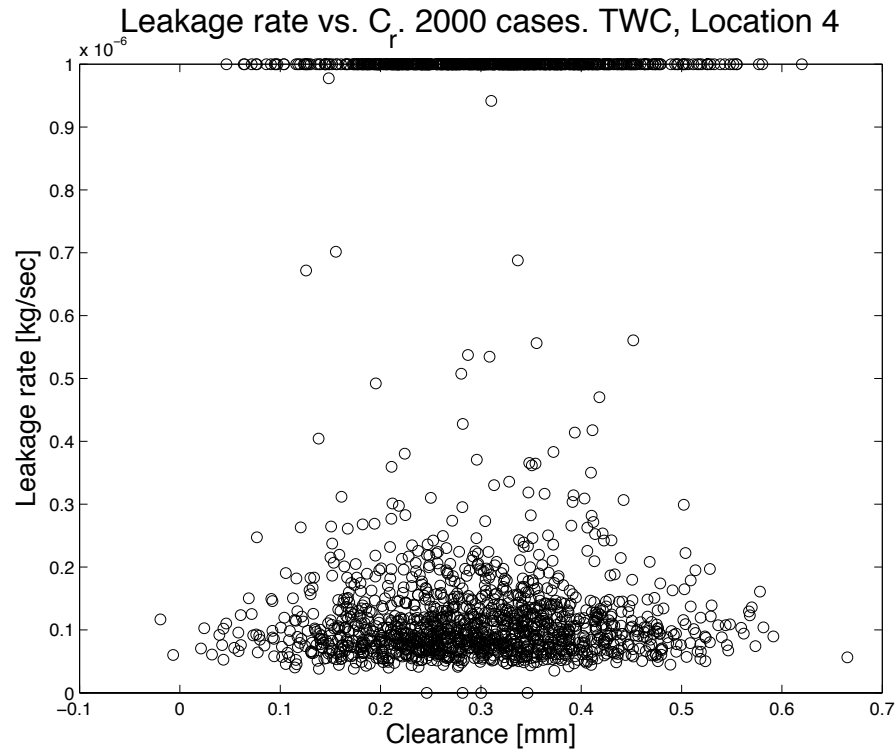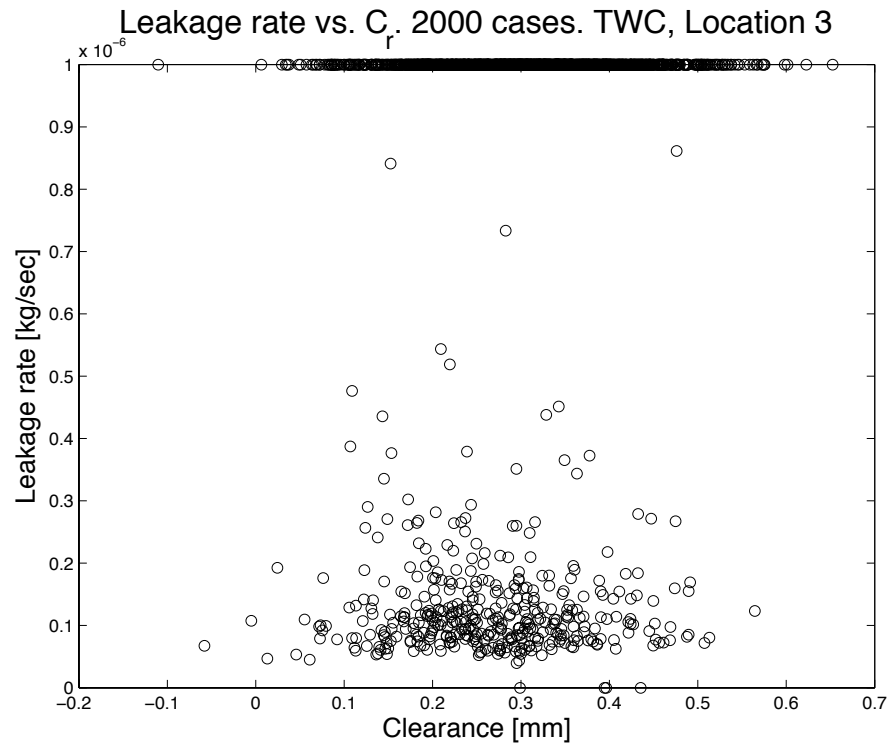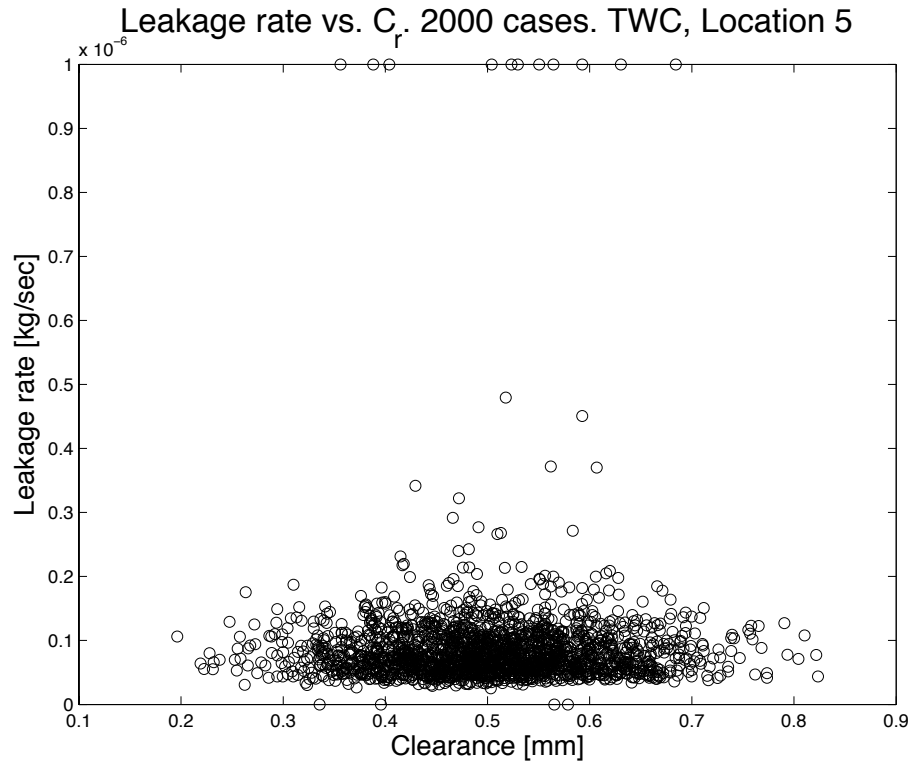
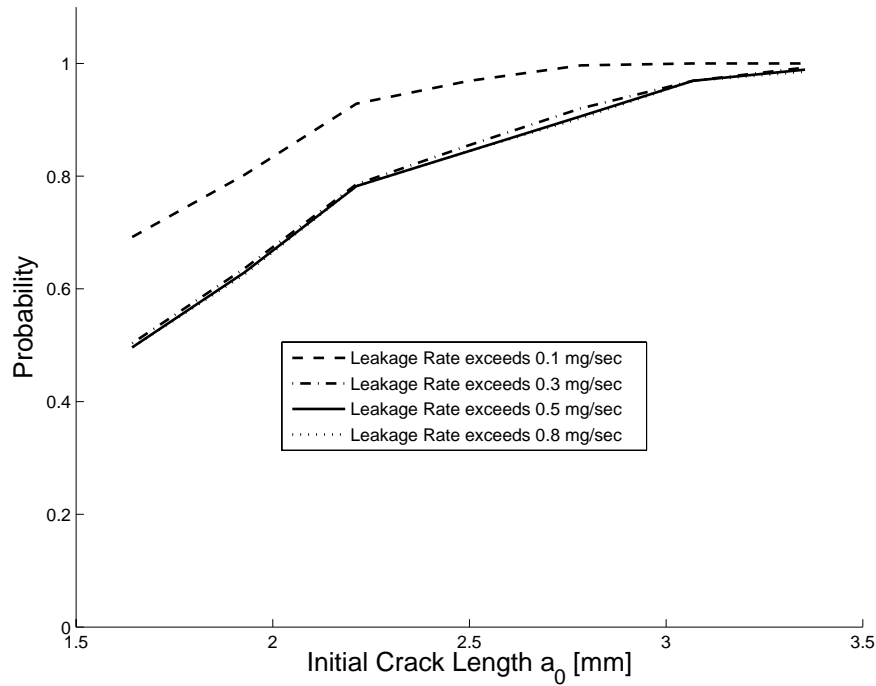# Appendix R: Probability of Leakage vs. Support Clearances

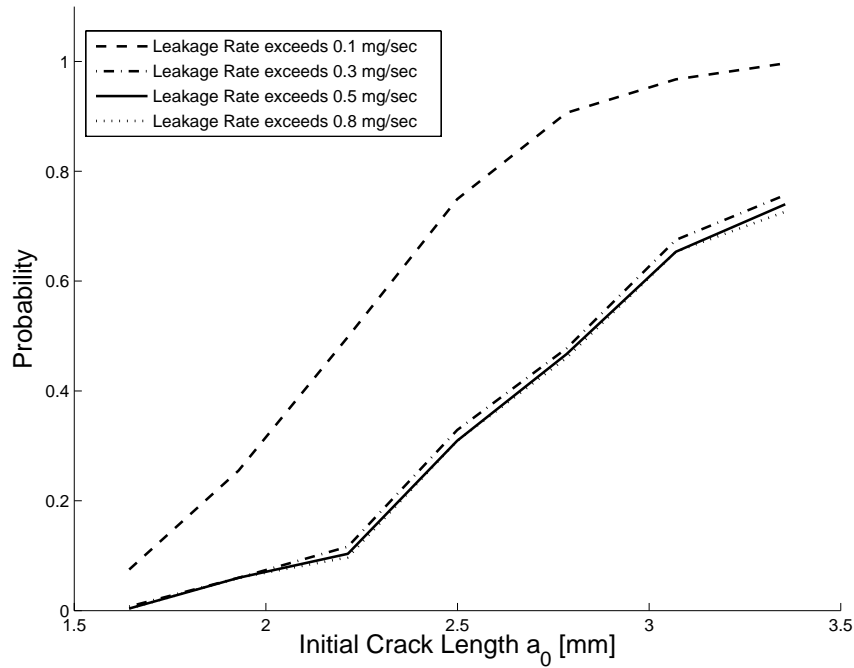Probability of leakage rate exceeding thresholds. TWC, Location 1



Probability of leakage rate exceeding thresholds. TWC, Location 2

Probability of leakage rate exceeding thresholds. TWC, Location 3



Probability of leakage rate exceeding thresholds. TWC, Location 4

Probability of leakage rate exceeding thresholds. TWC, Location 5